



LIGNIN CONVERSION

INTO HIGH ADDED-VALUE

PRODUCTS



Lignin conversion into high added-value products

A dissertation presented by

Amaia Morales Matías

In fulfilment of the requirements for the degree

Doctor of Philosophy by the University of the Basque Country

in the program Renewable Materials Engineering

Under the supervision of

Dr. Jalel Labidi & Dr. Patricia Gullón

Chemical and Environmental Engineering Department

DONOSTIA – SAN SEBASTIÁN

2022

✧ ✧ ✧
✧ ✧ ✧ *“Science is magic that works.”*

Kurt Vonnegut

Agradecimientos

Se me hace difícil pensar que ya han pasado 5 años desde la primera vez que pisé el laboratorio. La verdad es que nunca me había planteado hacer un doctorado hasta que empecé a hacer el Trabajo Fin de Máster y descubrí mi pasión por la ciencia y la investigación. El simple hecho de levantarme motivada los lunes para ir a trabajar me hizo apostar por este camino, y tras estos años llenos de subidas y bajadas, de mejores y peores momentos, de risas y llantos, por fin llego a la meta. Por ello, quisiera agradecer a todas esas personas que han sido partícipes de esta etapa tan importante de mi vida.

En primer lugar, me gustaría agradecer a mi director, el Dr. Jalel Labidi, por haberme animado y haber confiado en mí al blindarme la oportunidad de realizar esta tesis. Quisiera agradecer también a la Universidad del País Vasco/Euskal Herriko Unibertsitatea por concederme esta oportunidad mediante su ayuda a la Formación de Personal Investigador.

En segundo lugar, agradecer a la Prof. Margit Schulze por haberme dado la oportunidad de unirme a su grupo de investigación en Bonn, aunque solo fuese por dos semanas. Asimismo, quisiera darle las gracias a la Prof. Ebru Toksoy, por aparecer en un momento clave de mi tesis y poder colaborar con su grupo de investigación para así poder ponerle el broche final a mi trabajo. Muchísimas gracias a la Dra. Merve Erginer y a la doctoranda Selay Tornaci por haber dedicado su tiempo a mis experimentos.

Quisiera agradecer a todos los compañeros del grupo BioRP por su ayuda y apoyo, y también a Loli, tanto por su apoyo tanto científico como moral durante estos años. Gracias también a compañeros de otros grupos como Joseba, Mireia e Iratxe, que han hecho que el día a día sea más llevadero.

Me gustaría agradecer a mis *Morenitos* por haber sido uno de mis pilares más importantes durante este tiempo, por haberme ayudado a construir la base de esta torre que, como buena arquitecta frustrada, estoy a punto de terminar. Gracias en especial a Julen por su apoyo en mis momentos de crisis científicas y

personales, por rescatar a esta *drama queen* de sus momentos de ahogo en un vaso de agua. Y gracias también a Fabio, que aunque nos costó caernos bien, hemos sido fieles compañeros de viaje y nos hemos apoyado mutuamente cuando más lo hemos necesitado. Porque al mal tiempo, buena cara, y a un mal día (martes normalmente), un buen café.

Me gustaría, como no, dar las gracias a mis queridísimos *Rebujitos*, que me acogieron con los brazos abiertos en este loco mundo y me han ayudado a crecer tanto personal como científicamente. Gracias a Fabio, Rut, Leyre, Izas, Xabi y Jonatan por todos los momentos de locuras, por las risas, por hacerme descubrir mi pasión por las *escape rooms*, por hacer de los congresos viajes inolvidables, por hacer que los *Skypotes* sean ya una nueva tradición y por mimarme tanto por ser la más jovencita (aunque ya no tanto, pero lo seguiré siendo siempre). Que aunque nos vayamos desperdigando, siempre es un placer volver a juntarnos y seguir haciendo maldades y locuras. Nada hubiera sido lo mismo sin vosotros.

Quisiera también dar las gracias a mi cuadrilla, a esas personas que *finde* tras *finde*, han estado ahí escuchando mis aventuras de las no-estancias, las que han intentado entender qué hago en mi día a día, para qué sirven esos *bichos* que se hinchan, etc. Sé que no os lo digo mucho, pero gracias de corazón.

Gracias también a mis compañeros de *Amets Bide*, que han hecho de cada ensayo una vía de escape. Eskerririk asko en especial a Enara y a Beñat por aguantarme tanto, y también por aportar aire fresco de creatividad a esta tesis.

Me gustaría agradecer a mis padres por su apoyo incondicional, por escucharme y aconsejarme, por dejarme elegir mi camino en todo momento sin separarse ni un segundo de mi lado. Gracias a mi familia, en especial a mis abuelos, a los que tanto admiro y se preocupan siempre tanto por mí.

Quisiera agradecer a mi codirectora, la Dra. Patricia Gullón, por su infinita paciencia y su tiempo dedicado a mi trabajo. Gracias a Patri, por estar ahí siempre, por ser una amiga, por confiar en mí, por su profesionalidad. Todo lo

que he conseguido desde el primer día que pisé el laboratorio ha sido en gran parte gracias ella, y esta tesis es un claro reflejo de ello.

Por último, quisiera agradecer a Ander, que en todo este tiempo me ha ayudado a levantarme cada vez que me he tropezado, que me ha dado un abrazo cuando más lo he necesitado, que me ha aguantado día tras día, que me ha escuchado y apoyado siempre. Por ponerle un poco de cordura a mi locura y por seguir consiguiendo más retos personales y profesionales juntos. “*Questions of science, science and progress do not speak as loud as my heart*”. Eskerrik asko, bihotzez.

A todos los que de alguna manera habéis dejado huella en esta tesis,

Mila esker!

Abstract

Due to the multiple advantages that they offer, polymeric commodities have stirred up our daily lives and they have turned into indispensable materials in almost every sector. However, these materials usually come from fossil resources, which are not limitless and, thus, their depletion together with their price fluctuation has become a worrying concern for the current society. Moreover, plastics or polymeric materials usually lack of biodegradability, which makes their inadequate disposal and mismanagement harmful for the environment and dangerous for living species, including humans.

In this context, the abovementioned concerns have promoted the urgent need of searching for sustainable and more eco-friendly resources such as biopolymers. Herein, biorefineries have emerged as potential solutions, since they are able of processing biomass into a portfolio of marketable biopolymers and bio-based products. Lignocellulosic biomass has gained great attention owing to the multiple applications that its main constituents (cellulose, hemicelluloses and lignin) offer after being isolated. Among them, lignin appears to be a promising candidate for the replacement of fossil resources in the manufacturing of carbon-based compounds such as chemicals and materials. Nevertheless, this biopolymer seems to be under-exploited, which might be related to its highly recalcitrant behaviour and complex chemical structure. However, the valorisation of lignin into value-added product is essential in order to make biorefinery plants cost-competitive.

In this regard, this thesis focuses on the valorisation of lignin for its conversion into high added-value compounds such as hydrogels. The present manuscript has been divided into 5 chapters: 1. Introduction, 2. Objectives and challenges, 3. Methodology, 4. Results and discussion and 5. Conclusions and Future works. Chapter 4 has also been divided into 4 sections: in the first one,

the characterisation of the lignins employed in this thesis is described; in the second one, the optimisation of the synthesis of hydrogels based on poly (vinyl alcohol) and commercial alkaline lignin is developed; in the third one, the effect of multiple factors on the final properties of the hydrogels is discussed, and in the fourth one, the results for the applicability of the synthesized materials in many fields are explained.

The results showed that physically crosslinked lignin hydrogels can be successfully obtained by blending lignin with an environmentally friendly matrix polymer such as poly (vinyl alcohol) (PVA), and that the characteristics of these materials can be tailored by varying many synthesis and formulation parameters. In addition, lignin-hydrogels have demonstrated to be potential materials to be applied in many application fields such as water remediation, packaging or biomedicine.

List of appended publications

This thesis is constituted by the combination and summary of the following publications:

Publication I: A. Morales, J. Labidi, P. Gullón, G. Astray, *Synthesis of advanced biobased green materials from renewable biopolymers*, *Curr. Opin. Green Sustain. Chem.* 29 (2021) 100436. DOI: 10.1016/j.cogsc.2020.100436.

Publication II: A. Morales, J. Labidi, P. Gullón, *Assessment of green approaches for the synthesis of physically crosslinked lignin hydrogels*, *J. Ind. Eng. Chem.* 81 (2020) 475-487. DOI: 10.1016/j.jiec.2019.09.037.

Publication III: A. Morales, J. Labidi, P. Gullón, *Effect of the formulation parameters on the absorption capacity of smart lignin-hydrogels*, *Eur. Polym. J.* 129 (2020) 109631. DOI: 10.1016/j.eurpolymj.2020.109631.

Publication IV: A. Morales, J. Labidi, P. Gullón, *Impact of the lignin type and source on the characteristics of physical lignin hydrogels*, *Sustain. Mater. Technol.* 31 (2021) e00369. DOI: 10.1016/j.susmat.2021.e00369.

Publication V: A. Morales, J. Labidi, P. Gullón, *Influence of lignin modifications on physically crosslinked lignin hydrogels for drug delivery applications*, *Ind. Crops. Prod.* (under review).

Contributions not included in the thesis

📖 A. Morales, F. Hernández-Ramos, L. Sillero, R. Fernández-Marín, I. Dávila, P. Gullón, X. Erdocia, J. Labidi, *Multiproduct biorefinery based on almond shells: Impact of the delignification stage on the manufacture of valuable products*, Bioresour. Technol. 315 (2020). DOI: 10.1016/j.biortech.2020.123896.

📖 A. Morales, J. Labidi, P. Gullón, *Hydrothermal treatments of walnut shells: A potential pretreatment for subsequent product obtaining*, Sci. Total Environ. 764 (2021) 142800. DOI: 10.1016/j.scitotenv.2020.142800.

📖 L. Sillero, A. Morales, R. Fernández-Marín, F. Hernández-Ramos, I. Dávila, X. Erdocia, J. Labidi, *Life Cycle Assessment of various biorefinery approaches for the valorisation of almond shells*, Sustain. Prod. Consum. 28 (2021) 749–759. DOI: 10.1016/j.spc.2021.07.004.

📖 A. Morales, J. Labidi, P. Gullón, *Integral valorisation of walnut shells based on a three-step sequential delignification*, J. Environ. Manage. (under review).

Contributions to conferences

🌀 BIOPOL 2019 (June 17-19, Stockholm - Sweden): A. Morales, J. Labidi, P. Gullón; *Influence of the molecular weight of poly (vinyl alcohol) in physically crosslinked lignin-based green hydrogels* (Oral Communication)

🌀 BIORESTEC 2021 (May 17-19, Garda - Italy): A. Morales, P. Gullón, J. Labidi; *Effect of differently extracted shell lignins on the synthesis of smart materials* (Poster)

🌀 MZT 2021 (November 29-30, Bilbao – Spain): A. Morales, P. Gullón, J. Labidi; *Fruitu lehorren azaletatik isolaturiko lignina eraldatuek hidrogelen ezaugarrietan duten eragina* (Oral Communication)

Nomenclature

Abbreviation Description

AS	Almond shells
ASL	Acid soluble lignin
ATR-FTIR	Attenuated Total Reflection-Fourier Transformed Infrared Spectroscopy
CQE	Commercial quercetin
DMSO	Dimethyl sulphoxide
DSC	Differential Scanning Calorimetry
FGI	Fungal growth inhibition
G units	Guaiacyl units in lignin
GAE	Gallic acid equivalents
GI	Growth inhibition
H units	4-hydroxyl phenyl units in lignin
H/M/LM _w	High/Medium/Low molecular weight
HPLC	High Performance Liquid Chromatography
HPSEC	High Performance Size Exclusion Chromatography
LSR	Liquid to solid ratio
MAE	Microwave assisted extraction
MB	Methylene blue
M _n	Number average molecular weight
M _w	Weight average molecular weight
M _w /M _n	Polydispersity index
PBS	Phosphate buffer saline
³¹ P NMR	Phosphorous-31 Nuclear magnetic resonance
PDA	Potato dextrose agar
PVA	Poly (vinyl alcohol)
Py-GC/MS	Pyrolysis-Gas chromatography/Mass spectrometry
QAH	Quantitative acid hydrolysis
QE	Quercetin extract
RSM	Response Surface Methodology
S units	Syringil units in lignin
S/G ratio	Syringil to guaiacyl ratio
SEM	Scanning Electron Microscopy
TFC	Total flavonoid content
T _g	Glass transition temperature

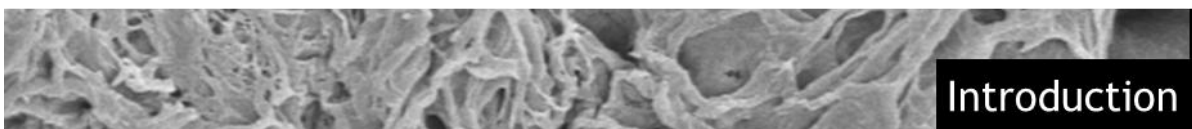
TGA Thermogravimetric analyses
TPC Total phenolic content
UV-Vis Ultraviolet-visible spectroscopy
WNS Walnut shells
 XL Crosslinking
XRD X-Ray Diffraction

Table of Contents

1	Introduction	1
1.1	Global environmental crisis	1
1.2	Biorefineries & biomass	3
1.2.1	Types of biorefineries	4
1.2.2	Types of biomass	5
1.3	Lignocellulosic biomass	7
1.3.1	Non-structural compounds	8
1.3.2	Cellulose	8
1.3.3	Hemicelluloses	9
1.3.4	Lignin.....	10
1.4	Hydrogels.....	14
1.4.1	Definition & general properties	14
1.4.2	Synthesis & classification.....	15
1.4.3	From synthetic to bio-based hydrogels	16
1.4.4	Lignin-based hydrogels	17
1.4.5	Applications of lignin-based hydrogels	17
1.5	Research gap.....	20
2	Objectives and challenges of the thesis	23
2.1	Specific objectives	23
2.2	Main challenges	24
3	Methodology	27
3.1	Raw materials.....	27
3.2	Characterisation of raw materials	27
3.3	Procedures for lignin extraction and modification	28
3.3.1	Lignin extraction from AS and WNS	28
3.3.2	Modification of extracted AS and WNS lignins	30
3.4	Procedures for hydrogel synthesis	30

3.5	Characterisation methods	33
3.5.1	Lignin characterisation methods	34
3.5.2	Hydrogel characterisation	36
3.5.3	General methods.....	38
3.6	Specific methods for hydrogel applications.....	40
3.6.1	Methylene blue adsorption tests.....	40
3.6.2	Antifungal tests.....	41
3.6.3	Quercetin extraction and characterisation.....	42
3.6.4	Quercetin loading and release tests.....	44
3.6.5	<i>In-vitro</i> biocompatibility tests.....	45
4	Results & Discussion.....	51
4.1	Characterisation of the lignins	53
4.1.1	Commercial and self-extracted lignins	53
4.1.2	Modified lignins	61
4.1.3	Conclusions.....	66
4.2	Optimization of the synthesis of lignin-based hydrogels.....	67
4.2.1	Modelling and optimization of hydrogel composition.....	68
4.2.2	Influence of the input variables on the swelling capacity.....	69
4.2.3	Influence of the input variables on the lignin waste	74
4.2.4	Optimization of the synthesis conditions and validation of the model	74
4.2.5	Conclusions.....	75
4.3	Influence of different formulation parameters on the properties of the hydrogels.....	76
4.3.1	Curing type	76
4.3.2	Molecular weight of PVA and number of freeze-thawing cycles ..	80
4.3.3	Lignin type.....	86
4.3.4	Duration of the freeze-thawing cycles.....	91
4.3.5	Type of lignin modification.....	95

4.3.6	Conclusions	99
4.4	Applications of the synthesized lignin-based hydrogels	101
4.4.1	Dye adsorption.....	101
4.4.2	Antifungal properties	102
4.4.3	Drug delivery.....	105
4.4.4	<i>In-vitro</i> Biocompatibility studies	108
4.4.5	Conclusions	114
5	Conclusions & Future works	117
5.1	General and specific conclusions	117
5.2	Future works	118
	References	121
	Appended publications	138



1 Introduction

1.1 Global environmental crisis

Since the dawn of time, mankind has been constantly challenged to change its primary resources in order to cover its energetic requirements. In the same way that the industrial revolution drove the use of coal as a primary resource, during the 20th century, society became highly dependent on petroleum [1]. Nevertheless, fossil resources are not limitless and, thus, their depletion together with their price fluctuation has become a worrying concern for the current society. Despite the multiple predictions about the end of these resources, their global consumption is still very high (98,272 thousand barrels per day) [2], and it is estimated that by 2030 this demand will continue to increase [1]. Moreover, the environmental impact that the exploitation and consumption of fossil resources cause is huge, especially in terms of greenhouse gas emissions [1]. In 2019, 34,169 million tonnes (Mt) of carbon dioxide were emitted concerning oil, gas and coal combustion related activities [3].

In addition to energy production, polymer industry has completely relied on petroleum-derived chemistry, refinery and engineering processes since the mid-20th century [4]. Polymeric commodities have stirred up our daily lives and they have turned into indispensable materials in almost every sector, reaching a global production of around 350 million tonnes per year [5]. In spite of their multiple benefits, plastics or polymeric materials usually lack of biodegradability. Therefore, their inadequate disposal and mismanagement have made plastic debris abundant pollutants of the environment, especially in estuarine and marine environments [6,7]. In fact, up to 90% of marine litter is comprised by plastic wastes such as food and beverage packaging, cigarette butts and bags [8]. This can be translated as an annual discharge of 8 Mt of plastic into the oceans, which is equates to a full truckload per minute [8]. In

addition, this risk is enhanced when these materials break down into smaller particles, the so called “micro- and nanoplastics”, since they can be ingested as food by fish or animals, entering, in this way, trophic chains and, consequently, the human body [5]. Furthermore, these persistent particles can be transported by the wind and breathed into humans lungs [9].

Thus, the abovementioned insatiable demand for energy and the worrying consequences of plastic pollution has promoted the urgent need of searching for alternative sustainable and more eco-friendly resources. Sustainable development is necessary to keep a balance between current and future human well-being, coupled with the conservation of natural resources and ecosystems [1]. On the other hand, circular economy is understood as a concept of sustainability that aims to limit or hinder the consumption of virgin resources providing a sustainable alternative to the linear “take, make, and dispose” economic model by enhancing the “resource, recovery and recycle” economic model by enhancing the “resource, recovery and recycle” [10], as depicted in Figure 1.1.

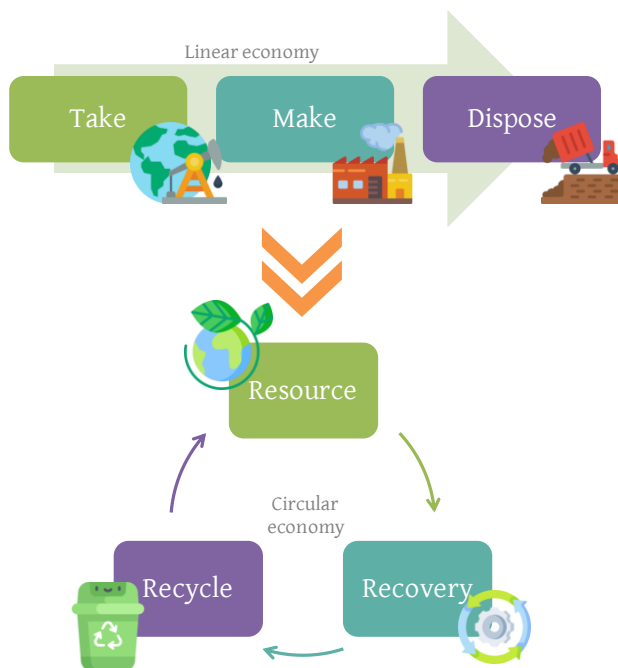


Figure 1.1. Graphical description of linear and circular economy.

In this context, renewable sources for the production of energy, chemicals and materials have arisen as promising alternatives for the shift from the fossil-based economy to a bio-based one [11]. Renewable sources for energy can be wind, solar, hydraulic, geothermal, tidal energy and biomass [1,12]. Among these, biomass has emerged as a promising resource because of its sustainability [4]. Biomass has been defined as any biological material excluding those that have undergone a mineralization process [1]. These include organic matter of vegetal origin and the resulting materials from their natural or artificial transformation (wastes and by-products) [1]. Despite being the oldest energy source, as it has been used for direct combustion since ancient times, it is still unusual to employ biomass for the obtaining of chemical building blocks and fuels [4].

In this context, biorefineries were developed to maximize the utilization of biomass and minimize the waste and emissions, converting biomass into a wide spectrum of products and energy in a sustainable manner [10,13]. Thus, biorefineries have loomed as a revolutionary approach to fulfil the current and future energetic and material needs of humankind.

1.2 Biorefineries & biomass

According to the International Energy Agency (IEA) biorefining is the “sustainable processing of biomass into a portfolio of marketable bio-based products (food and feed ingredients, chemicals, materials, fuels, energy, minerals and CO₂) and bioenergy (fuels, power and heat)” [14]. In other words, biorefineries are industrial plants in which several conversion processes such as thermochemical, biological, physical and chemicals are integrated to produce sustainable bio-based product streams [10,15]. Biomass is, therefore, the feedstock for biorefineries as oil is for refineries.

1.2.1 Types of biorefineries

As biorefineries can transform various types of biomass, the required processes depend on the input feedstock and the desired outputs [16]. Therefore, the wide possibility of combining inputs and outputs makes it difficult to classify biorefineries in a single way. In fact, the IEA sorts them depending on the degree of technological development, on the type of biomass used and on the type of prevailing conversion process [16]. However, they can also be classified depending on the aimed products, being energy- or product-driven biorefineries. Whereas the formers aim to produce fuels, gas, heat or power, the later aim to obtain chemicals or materials [14].

According to the technological implementation status, there are four generations of biorefineries (see Figure 1.2) [17].

1 st generation	2 nd generation	3 rd generation	4 th generation
<ul style="list-style-type: none"> • Single feedstock • Foodstuff 	<ul style="list-style-type: none"> • Single feedstock • Non-food 	<ul style="list-style-type: none"> • Multiple feedstock 	<ul style="list-style-type: none"> • Self-cultivated marine feedstock • Microalgae
<ul style="list-style-type: none"> • Limited technology and products 	<ul style="list-style-type: none"> • Limited technology 	<ul style="list-style-type: none"> • Advanced technology 	<ul style="list-style-type: none"> • Advanced technology
<ul style="list-style-type: none"> • Competition with food, price increase 	<ul style="list-style-type: none"> • Multiple products 	<ul style="list-style-type: none"> • Multiple products 	<ul style="list-style-type: none"> • Multiple products

Figure 1.2. Types of biorefineries according to the technological implementation status [17].

As shown in Figure 1.2, first generation biorefineries employ unique feedstock and technology to obtain limited products. High-sugar or oil-containing crops, maize stovers, or sunflower are the main input in this type of biorefineries. Despite being useful for the production of biofuels, substantial quantities of cereals are needed for the process and, thus, this can create competition with food prices, which is not desirable. Second generation biorefineries also employ single biomass and technology but are able to generate multiple

products. In this case, the feedstock is not limited to food crops; in fact, lignocellulosic biomass is also employed. Third generation biorefineries present an important improvement over the previous two generations since several products can be obtained from multiple inputs and technologies. This generation maximises the use of all the constituents of the raw materials but aims to improve the production efficiency while minimising the environmental impact. In addition, these biorefineries try to generate high added-value compounds. Based on the third generation, fourth-generation biorefineries focus on large-scale growing of microalgae and work towards the reduction of economic cost whilst incrementing environmental benefit.

1.2.2 Types of biomass

As aforementioned, a wide variety of biomass can be utilised as input feedstock in biorefineries, either in liquid, solid or gaseous state. These include agricultural crops and residues, industrial residues, municipal waste, aquatic organisms, woody residues and herbs, among others [17].

- ♣ Agricultural crops and residues: herbaceous or woody species produced through the activities of cultivation on agricultural land, harvesting and processing of harvested raw materials [16]. Tea, tobacco and tomato seeds, crop wastes, rice straw, wood chips and fruits waste are some examples of this biomass [15]. Algae can also be included in this group.
- ♣ Industrial wastes: by-products and wastes generated in agricultural, forestry and food industries. These include residues from olive oil production, citrus processing, wine and brewing industries as well as wastes from forestry industries (bark, sawmills, carpentry, etc.), by-products of the cellulose industry (black liquors) and from the recovery of lignocellulosic materials (pallets, building materials, old furniture, etc.) [16].

- ♣ Municipal wastes: biodegradable fraction of the urban waste generated in daily lives. This category includes sewage sludge, wastewater and food waste [16].
- ♣ Aquatic organisms: these mainly include macro and micro-algae, which are a sustainable source of bio-compounds that can be converted to food and high-value products [10].
- ♣ Woody residues and herbs: these usually are generated in forestry activities. They are the most abundant biomass, since they comprise around 89.3% of the total standing biomass and 42.9% of the total biomass production every year worldwide [15].

Figure 1.3 shows the location of different types of biorefineries in Europe in the year 2017 according to the employed input biomass. Altogether, 234 plants were accounted, a figure that has probably increased since then.

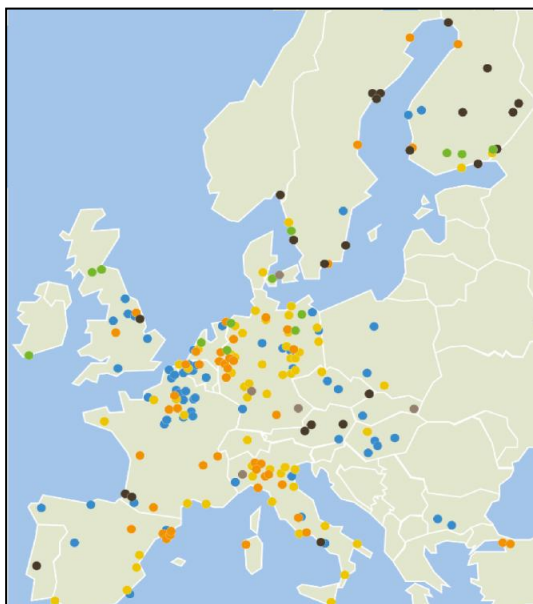


Figure 1.3. Map of the European biorefineries based on different feedstock: biowaste-based (green), lignocellulosic biomass-based (light brown), oil/fat for biodiesel (yellow), oil/fat for oleochemistry (orange), sugar/starch-based (blue) and wood-based (dark brown) (Adapted from [18]).

1.3 Lignocellulosic biomass

Lignocellulosic or plant biomass has emerged as an attractive source of bioenergy and bio-based chemicals [19]. It is the most abundant renewable biomass on earth, with an annual production of around 200 billion tonnes [20]. It includes woody plants (i.e. softwoods and hardwoods), sawdust (wood chips, slashes and sawmills) and bark thinning residues, and non-woody plants such as herbaceous vegetation, agricultural residues and food and non-food crops [21]. Apart from the abundance of lignocellulosic biomass, it is an extensively available, carbon-neutral and inedible bioresource coming from plant cell walls [21,22].

Lignocellulose is a complex natural composite with three main structural components (cellulose, hemicelluloses and lignin) together with other non-structural compounds (e.g. pectin, protein, extractives and ash). As shown in Table 1.1 the composition of this biomass can vary significantly depending on the source of the biomass feedstock, as well as on the growing conditions of the plant [23].

Table 1.1. Illustrative composition of lignocellulosic biomass (Adapted from [24]).

Feedstock	Cellulose (%)	Hemicelluloses (%)	Lignin (%)
Softwood	45–50	25–35	25–35
Hardwood	45–55	24–40	18–25
Grass	25–40	25–50	10–30

Among the various lignocellulosic feedstock, nut shells are produced worldwide in huge amounts annually. The global production of some nuts in 2019 is presented in Figure 1.4.

In fact, around 3.5 and 4.5 Mt of almonds and walnuts were produced in the world. However, the low percentage of edible kernel in these nuts leads to an enormous production of shells with low added-value industrial or commercial applications. However, these shells belong to the lignocellulosic biomass and they could be further valorised through a biorefinery strategy so as to use them as input feedstock for the production of high added-value materials.

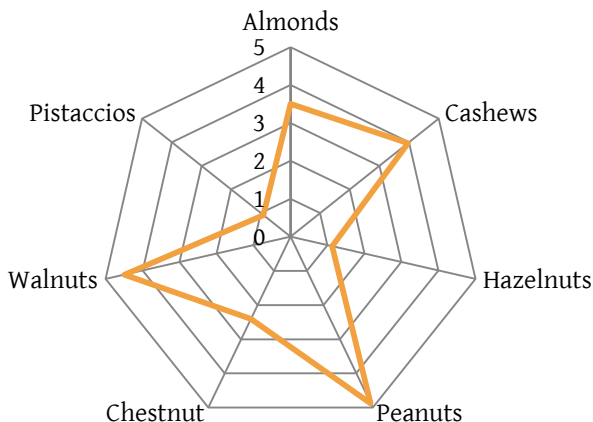


Figure 1.4. Global production of nuts in 2019 (in million tonnes, Mt) [25].

1.3.1 Non-structural compounds

Non-structural components are usually low molecular weight compounds and their presence in lignocellulosic biomass is scarce (5–10%). In spite of not being part of the cell wall structure, these compounds provide the plants with indispensable physiological properties such as elasticity or permeability and protection against root, fungi or insect attack. Phenolic compounds, fatty acids, terpenes, lignans, flavonoids, tannins and waxes are some of these compounds, and some of them are bioactive, which means they are beneficial not only for health related applications but also for food preservation among others [23].

1.3.2 Cellulose

Cellulose is the main constituent of the cell walls of plants and it gives them mechanical strength and chemical stability [22,26]. It is the most abundant biopolymer on Earth and it can be found in plants, bacteria, marine algae and other biomass [26]. Cellulose is a linear carbohydrate polymer constituted by D-glucose units linked with each other via β -1,4 bonds [27]. Owing to their strong inter- and intra-chain hydrogen and Van der Waals bonding, compact

fibrils of cellulose are formed, which can be differently oriented leading to different levels of crystallinity [21]. Cellulose microfibrils pack together with other structural components to form the macrofibrils that make up cell walls (see Figure 1.5). Due to the physicochemical features, biodegradability, biocompatibility and renewability of this biopolymer, it has been used for multiple applications and continues to gain interest because of the potential shown after adequate treatments and surface modifications [21].

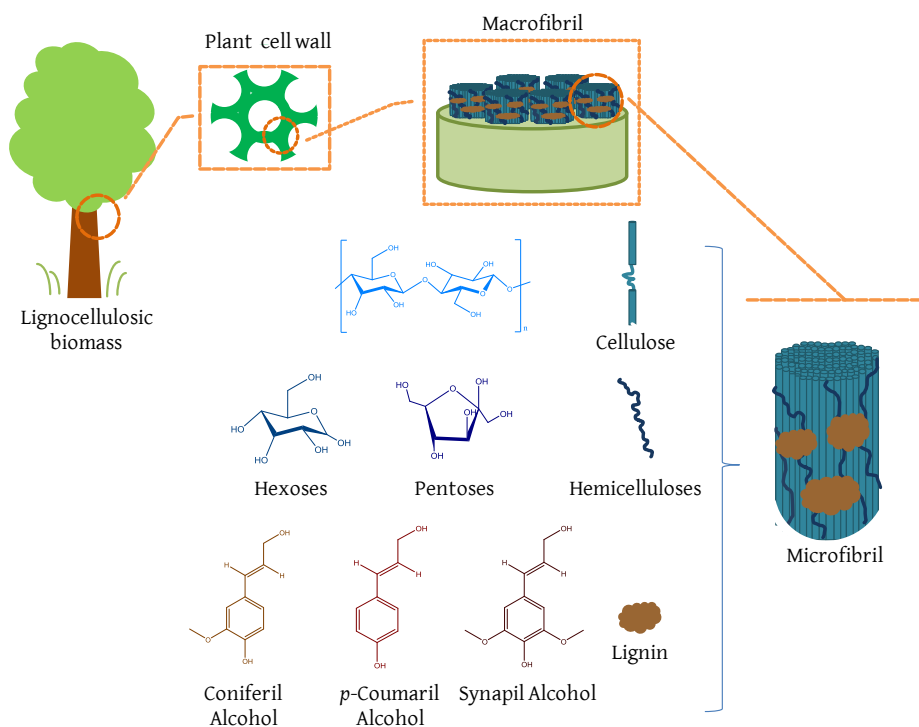


Figure 1.5. Representation of the structural compounds forming the plant cell wall and the chemical structures of their units.

1.3.3 Hemicelluloses

Unlike cellulose, hemicelluloses are more branched, amorphous and random short-chain heteropolymers [21]. They are constituted of five- and six-carbon sugars (pentoses and hexoses, respectively) linked together via β -1,4 glycosidic linkages [20]. Pentoses such as xylose and arabinose, hexoses such as

glucose, galactose, mannose and arabinose, together with other saccharides such as rhamnose and fructose usually combine to form hemicelluloses, although uronic acids (methylgalacturonic, galacturonic and glucuronic acids) and acetyl groups can also sometimes be found [21]. Hemicelluloses are responsible for packaging cellulose fibrils into microfibrils by forming a complex network of linkages through hydrogen bonds and Van der Waals interactions and crosslinking with lignin [21]. Thus, these heteropolymers give rigidity to the biomass matrix [20].

1.3.4 Lignin

Lignin is the most abundant phenolic biopolymer on Earth. It can comprise up to 40% of the dry matter of woody biomass [26,28,29] and it confers rigidity and hydrophobicity to the structure of the plant. Lignin also adds resistance against microbial and fungal attack, oxidative stress, UV radiation and flames [24,28]. It is estimated that around 100 billion tonnes of lignin are renewed annually in the biosphere, and this leads to an industrial production of 1.5–1.8 billion tonnes [30]. From this amount, up to 70 million tonnes of lignin derive from the pulp and paper industry, which are employed for internal energy recovery [30]. Nevertheless, this biopolymer is believed to be under-exploited, since it could be a potential candidate for the replacement of fossil resources in the manufacturing of carbon-based compounds such as chemicals and materials [30].

Lignin has a complex and highly branched structure formed by three different phenylpropanoid units: syringyl alcohol (syringil, S unit), coniferyl alcohol (guaiacyl, G unit), and *p*-coumaryl alcohol (4-hydroxyl phenyl, H unit) [26,28,29]. These units have a great amount of polar functional groups and they are randomly crosslinked via ether bonds, generating a three-dimensional amorphous structure. Carbon–carbon (C–C) and carbon–oxygen (C–O) bonds are the common linkages between the lignin monomers [28]. Nevertheless, the

most typical one is the β -O-4, a C-O link between an H unit and the β -end of the propenyl group [28], which is also one of the most labile bonds and is easily cleaved by most lignin extraction methods [31]. Figure 1.6 shows a proposed chemical structure for lignin.

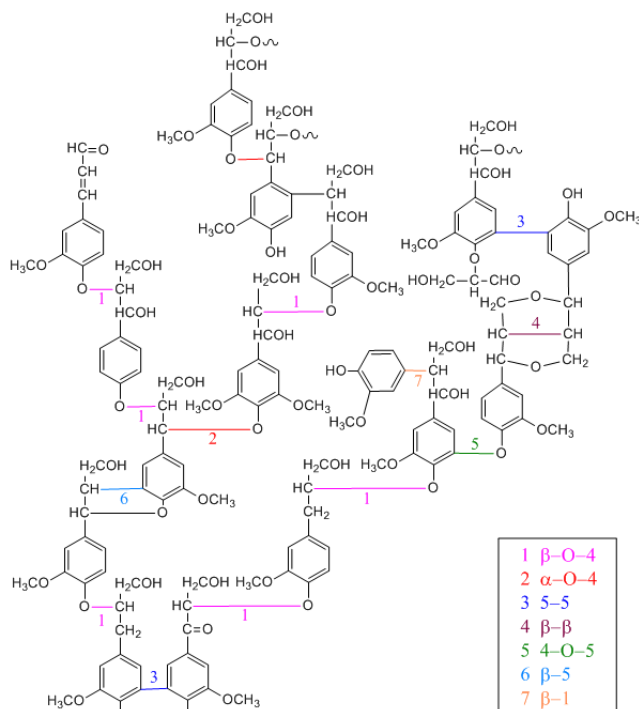


Figure 1.6. A possible chemical structure of lignin (Adapted from [32]).

Depending on the type and amounts of the present G, S and H units, the composition of lignin varies between plants [24]. Moreover, although molecular weights of 1,000–20,000 g/mol have been reported in literature, it is difficult to know the real degree of polymerisation of lignin in nature, since it is fragmented during the extraction process [28]. It is known that the G units are predominant in softwoods, whereas a combination of S and G units is usually presented in hardwood lignins. H units are commonly found in higher amounts in grass lignins [28]. These units, together with the existence of the multiple functional groups and their inter β -O-4 linkages, are responsible for the high recalcitrant behaviour of lignin to chemical and biochemical

depolymerisation [33]. This factor coupled with its complex structure and the condensation reactions that degraded fractions with high reactivity tend to undergo make the valorisation of lignin challenging. However, the valorisation of lignin into value-added product is believed to be essential in order to make biorefinery plants cost-competitive [34].

1.3.4.1 *Lignin extraction methods*

As aforementioned, many features of lignin suffer significant changes depending on the utilised extraction process. In fact, its composition, molecular structure, molecular weight and physical properties such as solubility, hydrophobicity or hydrophilicity can be affected by these processes [35], which strongly limits its chemical upgrading into value-added chemicals [36].

An effective isolation process should allow a high-yield extraction of high purity lignin, retaining the largest amount of β -O-4 ether bonds that would favour the consecutive valorisation routes [34]. Currently, several delignification methods can be found, which are summarised in Figure 1.7. The main differences between them can be usually found in the involved reagents, the applied temperatures and the employed times, among other parameters. Lignin forms lignin-carbohydrate complexes due to covalent bondages with hemicelluloses [30,34]. In any delignification or extraction process these bonds must be cleaved [30], and partial depolymerisation of lignin is also inevitable so as to extract it from biomass [34].

From the presented methods, Kraft and sulphite ones have been used worldwide in pulp and paper industry since late 19th century. However, in these processes lignin has been obtained as a by-product and, thus, in the last years, alternative biorefinery processes in which lignin is a target-product have gained significant attention. Nevertheless, all these methods present some drawbacks (i.e. complexity, high solvent and chemical consumption, long

processing times...) and they can also be demanding in terms of energy, owing to the harsh required conditions. In this context, novel methods have emerged with the aim of achieving higher extraction efficiency and promoting the scale up [37].

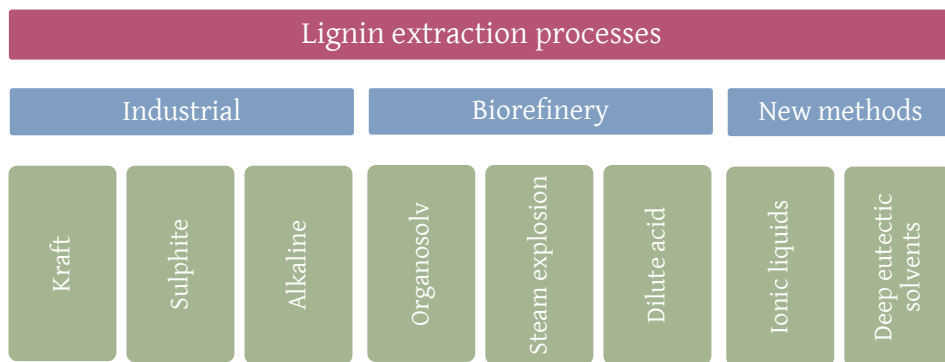


Figure 1.7. Summary of the most popular lignin extraction methods in literature.

1.3.4.2 Lignin modification routes

Although the lignin structure is highly branched and has multiple functional groups that directly affect its reactivity [30,38], the reactivity of lignin is usually not high enough for some applications. This can be ascribed to its high molecular weight, steric hindrance and few reactive sites on its structure [13,39]. Hence, it is sometimes crucial to perform a chemical modification of its structure if an enhancement on its reactivity is desired [40]. For this aim, there are four main ways (see Figure 1.8): the first one involves its depolymerisation or fragmentation, the second one focuses on the synthesis of new chemically active sites, the third one is related to the modification of the hydroxyl groups in its structure, and the last one would be through the production of graft copolymers [41]. These modifications highly rely on the reactivity of the functional groups and structural features of the lignin that is used.

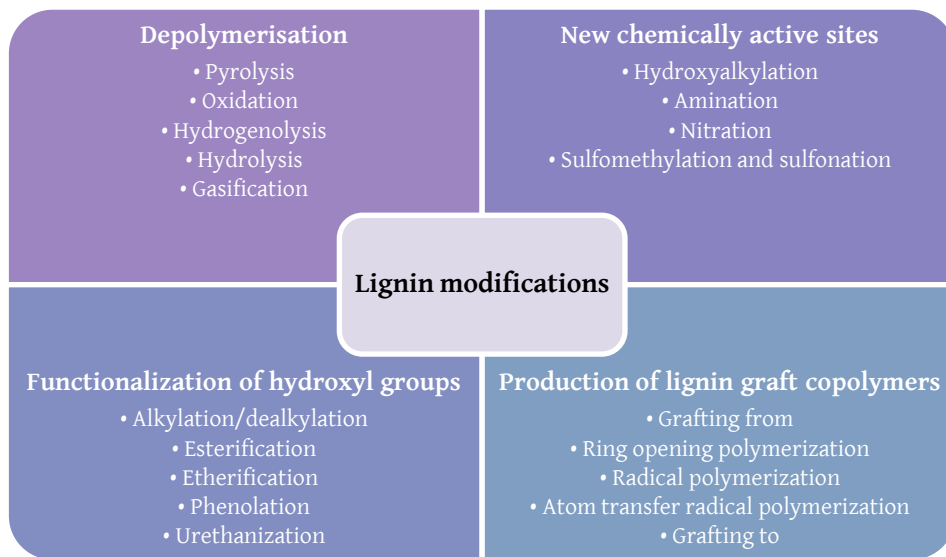


Figure 1.8. Chemical modifications of lignin (Adapted from [41]).

1.4 Hydrogels

1.4.1 Definition & general properties

Hydrogels are three-dimensional polymeric structures with great water absorption capacity. This property is related to their net structure, where the gaps between the physically or chemically entangled polymeric chains permit aqueous and other biological fluid retention [42,43]. Their water content is usually higher than 90%, which, together with their elastic properties, makes them alike native soft human tissues, and thus, also adequate for biomedical applications such as wound dressing [44,45]. Other applications have also been reported in this field (e.g. cell encapsulation [44], biosensors, bone tissue engineering [43], artificial muscle design, contact lenses, etc.) as well as in food industry, pharmacy, controlled drug delivery and super-absorbent materials [46]. Many of these functions are achieved thanks to the responsiveness of these materials to external stimuli such as temperature, pH, ionic concentration, magnetic and electric fields. These hydrogels are known as smart systems and have become interesting for advanced technological applications [47].

1.4.2 Synthesis & classification

In general, three main elements are needed for the synthesis of a hydrogel: a monomer, an initiator and crosslinker. Water or aqueous solutions may also be useful in order to control the reaction heat and the final properties of the resulting material [48]. Nevertheless, the final characteristics completely depend on the preparation techniques.

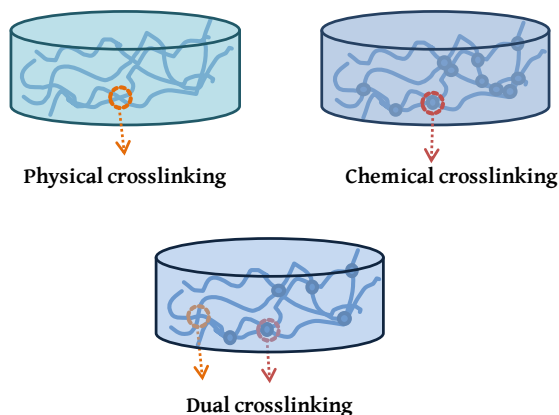


Figure 1.9. Schematic representation of physically, chemically and dually crosslinked hydrogels.

Although hydrogels can be classified according to several criteria, the most common one is the type of crosslinking. Based on the latter, physical and chemical crosslinking can occur between the polymeric chains, which can be achieved by several preparation methods. For physical entanglement, for instance, freeze-thawing, irradiation, solvent-casting or phase separation may be used, which at the same time provoke several physical interactions such as ionic, hydrogen bonding, hydrophobic or host-guest. Besides, for chemical ones, other methods including solution polymerisation or irradiation can be employed, which implicate free radical polymerization, condensation and addition reactions, for example [46]. Sometimes, hydrogels can contain both types of crosslinking simultaneously, which is known as dual crosslinking (see Figure 1.9), and possess different properties to sole chemically or physically crosslinked ones [49].

1.4.3 From synthetic to bio-based hydrogels

Wichterle and Lim in 1960 were pioneers in the synthesis of crosslinked hydrogels compatible with the human tissues and since then the attention on hydrogels has increased exponentially due to the interest on the development of the so called “smart hydrogels” [47].

It is said that the history of hydrogels is divided into three main periods [47]. The first hydrogel generation consisted of a wide range of crosslinking methods with the aim of creating materials with high swelling abilities, good mechanical properties and a simple theoretical background [47]. The second generation, which begun in the seventies, was focused on the obtaining of materials capable of responding to specific external stimuli (i.e. temperature, pH, etc.). The third generation consisted on the research and development of stereo complex materials and hydrogels crosslinked by other physical interactions [47].

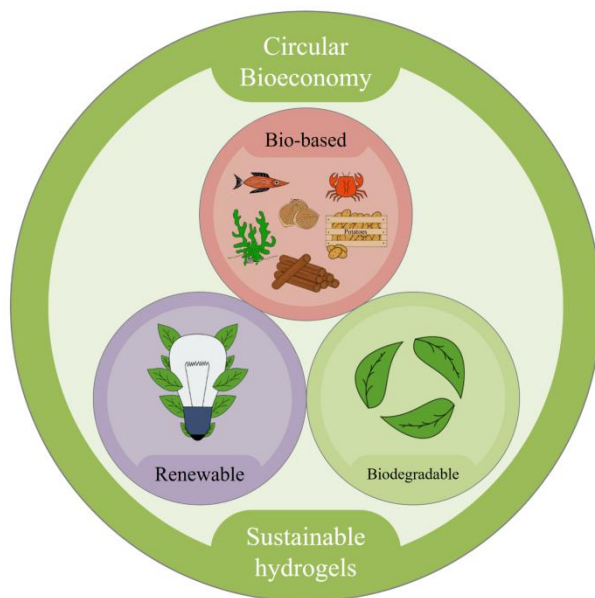


Figure 1.10. Graphical definition of sustainable hydrogels.

Natural polymers such as collagen and shark cartilages started to be used in hydrogels in the late 1980s [47]. Since then, biopolymer-based hydrogels have become very popular owing to their applicability in the fields of food, cosmetics, pharmaceuticals and biomedical implants [50]. Limited oil reserves, the environmental problems caused by the toxic compounds from the degradation of this type of materials together with the expanding hydrogel market generate an urgent need for the development of environmentally friendly and safe alternative hydrogels from renewable materials, which would also expand the life cycle opportunities for reusing and recycling biomass and would contribute to circular bioeconomy (see Figure 1.10) [11].

1.4.4 Lignin-based hydrogels

Among the available and abundant biopolymers, lignin is the only aromatic one, which makes it interesting for its application on functional hydrogels [50]. Many studies have recently demonstrated that it can be successfully used for the formulation of lignin-derived composites used for tissue scaffolding and drug release or as UV absorbents [51]. Thus, a clear increasing trend on the publications about lignin and lignin applications has been noticed in the last years [30,52,53]. Lignin is usually combined with other biosynthetic or synthetic polymers owing to the lack of self gel-forming properties. For this reason, it has been included in different polymeric networks through physical interactions or chemical reactions that promote hydrogel structure [54].

1.4.5 Applications of lignin-based hydrogels

A big part of the synthesized lignin-based hydrogels has been used to remove heavy metals and cationic compounds presented in aqueous solutions [55]. Nonetheless, many authors have also reported their use on fields such as biomedicine for drug delivery and tissue engineering [55].

The controlled release of water is a commonly used term in agriculture. In climates where the rain is scarce, soils need to be irrigated frequently. Nevertheless, equipping soils with small and smart hydrogels, such as lignin-hydrogels, have proven to absorb significant amounts of water and retain it until the crops require it [50]. The water content of hydrogels can vary according to their degree of crosslinking, which can be controlled during their synthesis.

The functional groups of lignin (phenolic hydroxyl, alcohol hydroxyl, methoxy and carboxyl groups) can act as adsorption sites for dye molecules and heavy metals [56]. These structures are capable of attracting positive molecules through the negatively charged functional groups and aromatic organics via π - π reactions [50]. For this reason, they have been used for the absorption of both inorganic ions and organic compounds in soils and water [50]. Table 1.2 summarises some works in this field.

Hydrogels can also be an attractive alternative for their application in food packaging systems as absorbent pads [57]. Apart from water absorption properties, these materials must increase the stored food products shelf-life and avoid microbial growth on food surface [57]. Therefore, the antimicrobial activity of the polymers constituting the hydrogel network is crucial. In this context, lignin and its derivatives, and lignin-hydrogel coatings have demonstrated to present antimicrobial behaviour [58–60], so they could be employed in food packaging.

Antimicrobial, antioxidant and low cytotoxicity features are also important for the synthesis of biocompatible materials. In this sense, hydrogels can provide effective removal of undesirable metabolites from wounds due to their high absorption capacity, and the addition of lignin may help to protect the wound from future problems such as further injury or contamination thanks to its

good mechanical properties [53]. Hence, lignin has also gained interest in wound dressing [61] and tissue engineering [62].

Table 1.2. Literature review of hydrogels as pollutant removers.

Lignin type in hydrogels	Pollutant	Medium	Removal	Reference
Sodium lignosulfonate	Cadmium ions (Cd^{2+})	Soil	$< 61.77 \pm 1.09$ mg/g	[63]
Lignin	Methylene blue (MB) and lead ions (Pb^{2+})	Aqueous	201.7 mg/g MB and 753.5 mg/g Pb^{2+}	[64]
Alkali, Kraft and organosolv lignins	Toluene	Aqueous	164–170 mg/g	[65]
Aminated alkali lignin	Heavy metal cations (Pb^{2+} , Hg^{2+} and Ni^{2+}) and dyes (Methylene blue, methyl, orange and malachite green)	Aqueous	2.1–55 mg/g for heavy metal cations and 2–155 mg/g for dyes	[66]
Alkali, Kraft and enzymatic hydrolysis lignin	Rhodamine 6G, crystal violet, methylene blue and methyl orange	Aqueous	10–196 mg/g	[56]
Soda, Kraft and organosolv lignins	Methylene blue	Aqueous	69 to 629 mg/g	[67]
Pine Kraft lignin Indulin AT	Prednisolone drug and 3,4-dichloroaniline	Aqueous	1.35 mg/g for Prednisolone and 4 mg/g for 3,4-dichloroaniline	[68]
Alkali lignin	Hexavalent chromium Cr(VI)	Aqueous	599.9 mg/g	[69]
Acid-pretreated alkali lignin	Pb^{2+} , Cu^{2+} and Cd^{2+} ions	Aqueous	1.076 mmol/g for Pb^{2+} , 0.3233 mmol/g for Cu^{2+} and 0.059 mmol/g for Cd^{2+}	[70]

Lignin-hydrogels have also demonstrated to be useful in another important part of the biomedical field: the controlled release of both hydrophobic [59] or hydrophilic drugs. Stimuli-responsive hydrogels can be created by combining other (bio)polymers and lignin. These hydrogels are of great interest in drug delivery since they are able to alter their volume in response to environmental stimuli [71] such as pH, temperature, or light [54].

The use of lignin-based materials applied to energy devices has proven to be promising [72]. Among other applications, these materials have gained attention as electrode materials for super capacitors as a result of their high

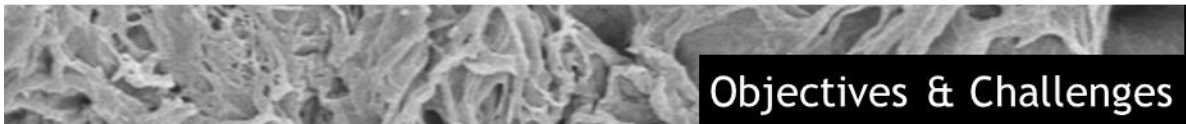
surface areas and chemical stability, and superior electrical conductivity [72,73].

Taking the previous into account, it can be concluded that, although lignin has been underused in the past, it presents multiple advantages not only from the economical (e.g. high availability and low cost) perspective but also from the environmental (i.e. renewable and biodegradable) and technological (i.e. excellent physicochemical features) points of view, making it very useful for many applications.

1.5 Research gap

In spite of the increase on the scientific interest related to lignin-hydrogels in the last years, most of the studied systems present chemically crosslinked structures, which often involve the use of highly toxic reagents. Moreover, the amounts of lignin with whom the matrix polymer is loaded are usually very low, which limits the valorisation of this biopolymer. In addition, many studies just analyse the effect of one type of lignin on the final properties of the synthesized hydrogels, which also restricts its extrapolation when other kind of lignins are needed to be used.

Taking the abovementioned into account, this work focuses on the optimisation of the synthesis and characterisation of lignin-based hydrogels, starting from a combination between commercial alkaline lignin and a poly (vinyl alcohol) (PVA) matrix. The optimal conditions have been extrapolated to the synthesis of hydrogels from self-extracted and modified lignins coming from different agroalimentary lignocellulosic wastes (almond and walnut shells). The synthesized materials have been characterised and evaluated for several advanced applications such as water remediation, active packaging or drug delivery, giving lignin an added-value.



2 Objectives and challenges of the thesis

The general objective of this thesis was the valorisation of different types of lignin by the synthesis of advanced hydrogels, which were characterised in order to define their most suitable applications. To this aim, several parameters of the hydrogel synthesis were firstly optimised and then the optimal conditions were applied for the obtaining of hydrogels from other types of lignins.

2.1 Specific objectives

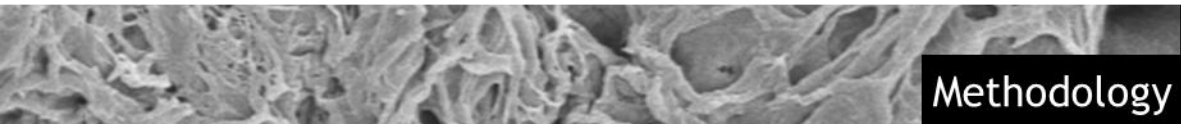
To achieve the main objective, and after a first step of literature review (**Publication I**), the following specific objectives were proposed:

- ✧ **Objective 1 (Publication II):** Optimisation of the synthesis route of lignin-based hydrogels by means of experimental designs for the maximisation of the swelling capacity and minimisation of lignin waste.
- ✧ **Objective 2 (Publication III):** Study of the effect of the molecular weight of the matrix polymer on the final properties of lignin-hydrogels by synthesizing hydrogels from the optimal conditions deduced previously.
- ✧ **Objective 3 (Publication IV):** Extraction and characterization of lignins using different processes and lignocellulosic materials and use of these lignins for the synthesis of hydrogels.
- ✧ **Objective 4 (Publication V):** Modification and characterisation of the extracted and commercial lignins for the synthesis of lignin-hydrogels with improved properties.
- ✧ **Objective 5 (Publications III, IV and V):** Assessment of the use of the synthesized hydrogels for various applications: water remediation (pollutant removal), active packaging (as antifungal materials) and biomedicine (drug delivery and biocompatibility).

2.2 Main challenges

The main challenges of this thesis derived principally from the uncertain structure of lignin and its variability according to its source and extraction method. Moreover, its recalcitrant character, high molecular weight and steric hindrance make working with it laborious and challenging. Apart from that, it is known that the synthesis of materials usually involves the influence of many external parameters, which are sometimes uncontrollable but can highly affect the obtaining and the features of the products. Thus, the identification and the detection of the influence of these parameters is also a challenging task.

In the light of the above, the synthesis of new materials becomes even more complicated when using lignin. Therefore, this thesis is presented as a bumpy path that will have to be carefully crossed.



3 Methodology

For all publications the commercial reagents were used as supplied. For detailed information see **Appended Publications**.

3.1 Raw materials

For **Publications IV and V**, almond shells (AS) were given by local farmers (Marcona variety) and walnut shells (WNS) were kindly supplied by Olagi cider house (Altzaga, Gipuzkoa).

3.2 Characterisation of raw materials

Almond and walnut shells were analysed according to the methods described previously [74]. TAPPI standards were employed for the determination of moisture (TAPPI T264-om-88), ashes (TAPPI T211-om-02) and ethanol-toluene extractives (TAPPI T204-cm-97). Klason lignin and carbohydrate content were determined by the protocol TP-510-42618 of the National Renewable Energy Laboratory (NREL), which consisted on a quantitative acid hydrolysis (QAH) first with 72% (w/w) H_2SO_4 for 1 h and 30 °C, and then with 4% (w/w) H_2SO_4 for 1 h and 121 °C. The solid phase that was recovered after the QAH was gravimetrically measured and considered as Klason lignin, while the liquid phase was analysed for the quantification of sugars (glucose, xylose and arabinose), galacturonic and acetic acid by High Performance Liquid Chromatography (HPLC). Acid soluble lignin was determined spectrophotometrically (TAPPI UM250-um-83). All the analyses were done by triplicate.

3.3 Procedures for lignin extraction and modification

The lignins employed in each **Appended Publication** of this thesis are described in the following scheme:

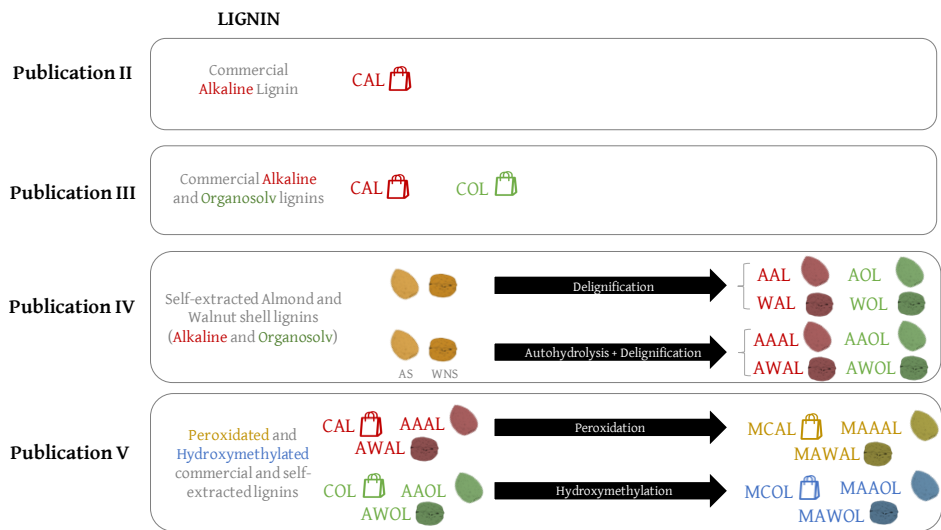


Figure 3.1. Schematic overview of all the lignin samples employed in the present thesis.

3.3.1 Lignin extraction from AS and WNS

For **Publications IV and V**, AS and WNS were milled and sieved to a particle size between 2 and 1 mm. Then, the shells were subjected to two different processes: the first one, contained a single delignification step, and the second one was composed of a pre-treatment step (autohydrolysis) and a subsequent delignification stage (see Figure 3.2).

The autohydrolysis of both raw materials was performed according to previous studies [74,75]. AS with a liquid to solid ratio (LSR) of 8 (g H₂O/g in oven-dried basis) were heated to 179 °C in a 1.5 L stainless steel 5100 Parr reactor with a 4848 Parr controller operating in isothermal regime for 23 minutes. WNS with the same LSR were heated up to 200 °C in non-isothermal regime, which means they were immediately cooled down after the set temperature was achieved.

After the treatments, the solid phases were washed with water and dried at 50 °C.

The delignification of both raw materials was also performed according to prior research. The shells were subjected to two different extraction methods. On the one hand, an alkaline treatment was performed by introducing untreated and pre-treated shells into an autoclave at 121 °C for 90 min with a sodium hydroxide (NaOH) solution (7.5 w.%) and a LSR of 6 (g solvent/g in oven-dried basis). On the other hand, an organosolv treatment was carried out by introducing untreated and pre-treated shells into the aforementioned stainless steel Parr reactor at 200 °C for 90 min with an ethanol/H₂O solution of 70/30 (v/v) and a of LSR 6 (g solvent/g in oven-dried basis).

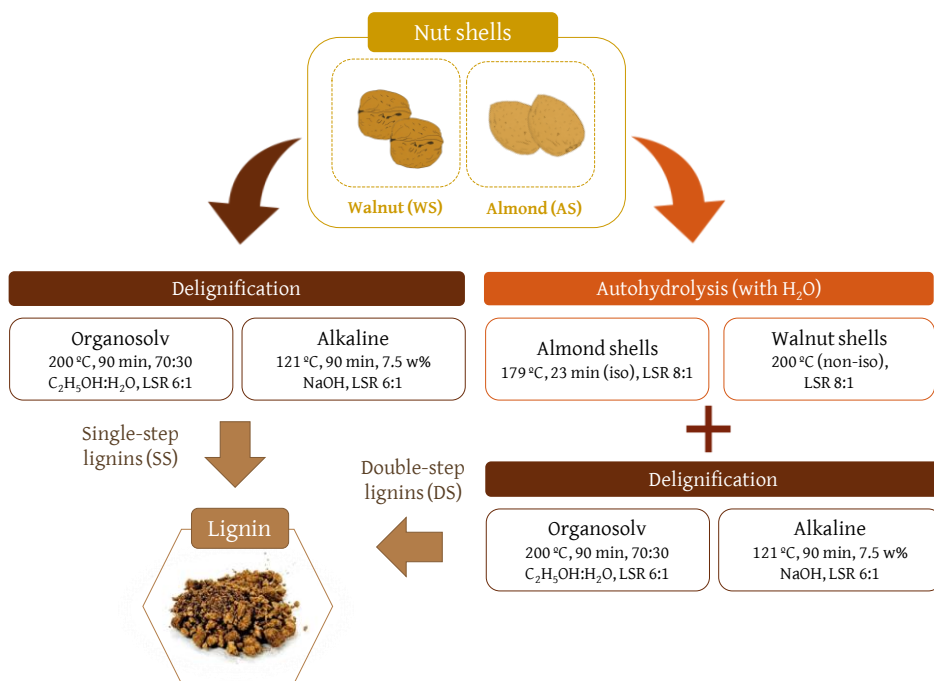


Figure 3.2. Schematic explanation of the experimental procedure for nut shell lignin extraction.

After the delignification processes, the suspensions were filtered and the lignin contained in the black liquors was precipitated by adding two volumes

of acidified water (pH 2) in the case of organosolv liquors and by acidification with H_2SO_4 until pH 2 in the case of alkaline liquors. The precipitates were then filtered and neutralised with distilled water, and finally, lignins were dried at 50 °C for 24-48 h.

3.3.2 Modification of extracted AS and WNS lignins

For **Publication V**, alkaline double-step lignins from AS and WNS as well as the commercial one were subjected to a microwave assisted (flexiWAVE, Milestone Srl) peroxidation reaction with hydrogen peroxide (H_2O_2) as described by Infante *et al.* (2007) [76]. Briefly, lignin and hydrogen peroxide were introduced into a high-pressure vessel keeping a LSR of 10 (mL H_2O_2 /g lignin). After sealing the vessel, it was subjected to three irradiation cycles of 10 seconds at 1100 W with a 30 second suspension period between them. Afterwards, the vessel was cleaned with distilled water and the collected mixture was left to dry over an oven.

Organosolv lignins (from AS, WNS and the commercial one) were exposed to a hydroxymethylation reaction with formaldehyde following the method described by Chen *et al.* (2020) with slight modifications [39]. Concisely, 0.6 g of lignin were dissolved in an aqueous NaOH solution (140 mL). Then, 0.495 mL of formaldehyde were added and the solution was heated up to 80 °C under magnetic stirring and refrigeration. The reaction was left for 3.5 hours. Afterwards, the modified lignin was precipitated with 2% hydrochloric acid, filtered, neutralized and dried.

3.4 Procedures for hydrogel synthesis

The first step of the synthesis of all hydrogels was the same (see Figure 3.3). Firstly, the corresponding amount of poly (vinyl alcohol) (PVA) was added to a 2% NaOH aqueous solution, which was magnetically stirred and heated to 80–90 °C simultaneously. When the PVA pellets were dissolved, the corresponding

amount of lignin was incorporated under agitation until it was completely dissolved. Defined amounts of the blends were poured into silicon moulds and, the bubbles trapped in the solution were eliminated by introducing the moulds into an ultrasound bath while the ones on the surface were poked manually with a needle.

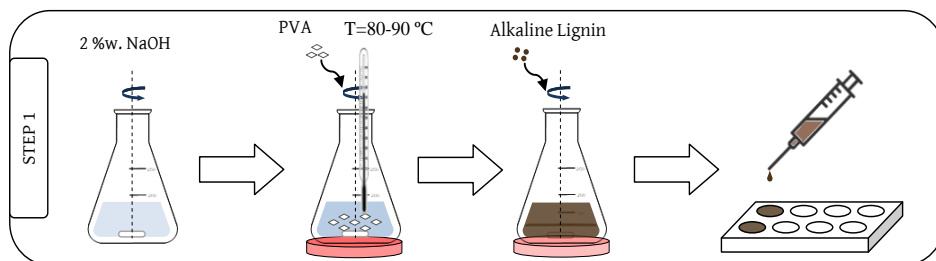


Figure 3.3. Diagram of the experimental procedure of the 1st step of the hydrogel synthesis.

The second part of the synthesis, the crosslinking (see Figure 3.4), was optimised according to **Publication II**, and the optimal conditions were then employed in the following works. In brief, 3 different crosslinking methods were studied: 3 freeze-thawing cycles, 5 freeze-thawing cycles and vacuum drying at 50 °C. After the crosslinking stage, all the samples were washed separately into 50 mL of distilled water and rinsed at certain times during 27-48 hours so as to eliminate the non-reacted lignin and the residual NaOH. Then, the curing (or drying) stage was performed, in which two different ways were studied: air drying and vacuum drying. After the corresponding optimisation analyses, the optimal route was selected, which consisted of 5 cycles of freezing and thawing and air drying.

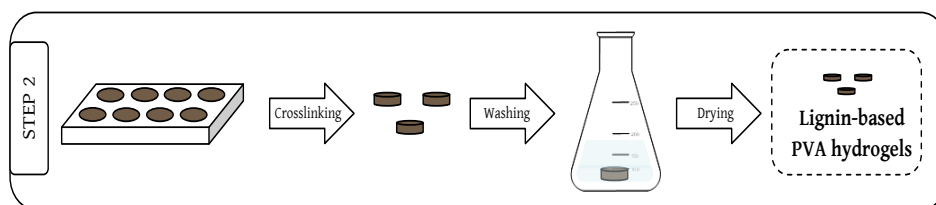


Figure 3.4. Diagram of the experimental procedure of the 2nd step of the hydrogel synthesis.

In **Publication III**, the time of the optimal route selected from **Publication II** was shortened in order to reduce the duration of the synthesis. Each cycle in **Publication III** consisted of a freezing step during 16 h and a thawing step for 8 h. Here, this time was reduced to 2 h and 1.5 h for each freezing and thawing step, subsequently. This method was then followed in **Publications IV and V**.

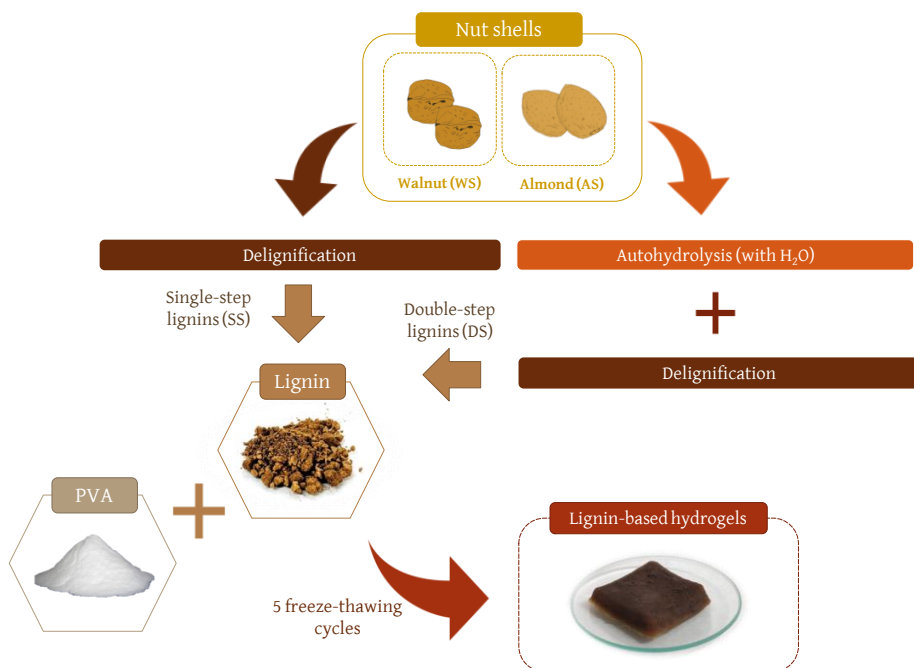


Figure 3.5. Schematic explanation of the experimental procedure.

For **Publication IV**, the lignins involved in the synthesis of the hydrogels were extracted from nut shells as indicated in Section 3.3.1 and Figure 3.5. In this case, apart from the abovementioned shorter freeze-thawing cycles, the influence of the duration of the last thawing stage was studied by lengthening it 24 h.

In **Publication V**, the employed lignins (commercial and double step alkaline and organosolv lignins) were the ones modified as aforementioned in Section 3.3.2. Otherwise, the synthesis procedure consisted of short (2 h + 1.5 h) freeze-thawing cycles, as in **Publications III and IV**.

3.5 Characterisation methods

Table 3.1. Characterisation methods employed in each publication.

Analysis	Publication			
	II	III	IV	V
Purity	-	-	L	L
Acid soluble lignin (ASL)	-	-	L	L
Composition (Py-GC/MS)	-	-	L	-
Molecular weight (HPSEC)	-	-	L	L
Total phenolic content (TPC)	-	-	L	L
Thermal degradation (TGA)	HG, L	HG	L	L
Crystallinity (XRD)	HG, L	HG	L	L
Chemical structure (ATR-FTIR)	HG, L	HG	L	L
Lignin Waste	HG	HG	HG	HG
Swelling	HG	HG	HG	HG
Morphology (SEM)	HG	HG	HG	HG
Thermal properties (DSC)	HG, L	HG	HG	HG
Compression tests	HG	HG	HG	HG

L: Lignin; HG: Hydrogels

3.5.1 Lignin characterisation methods

3.5.1.1 Purity

The purity of the lignins was determined by the procedure described by Dávila *et al.* (2017), taking both Klason lignin and acid soluble lignin (ASL) into account [77]. The lignins were subjected to a quantitative acid hydrolysis (QAH) with 72% w/w H₂SO₄ for 1 h at 30 °C followed by a second acid hydrolysis after diluting the samples to 12% (w/w) H₂SO₄ and autoclaving them for 1 h at 121 °C. Afterwards, the samples were filtered and the remaining solid phase was considered as Klason lignin. The liquid phases obtained were analysed by HPLC for determination of monosaccharides (glucose, xylose and arabinose), galacturonic acid, acetic acid and degradation products (hydroxymethyl furfural and furfural).

ASL content was determined by spectrophotometry using a Jasco UV-Vis 730 spectrophotometer. The filtrates from the acid hydrolysis of the lignins were diluted with 1 M H₂SO₄ until the absorption measured at 205 nm was between 0.1 and 0.8 (TAPPI UM250 um-83). The calculation of the ASL content was carried out using Eq. 3.1.

$$ASL (\%) = \frac{Abs_{250nm} \cdot DF \cdot VF}{\epsilon \cdot DM_i} \cdot 100 \quad (\text{Eq. 3.1})$$

where Abs_{250nm} is the absorption of the sample (taking the absorbance of 1 M H₂SO₄ at 205 nm as the reference), DF is the dilution factor, VF is the volume of filtrate, ϵ is the extinction coefficient of the lignin at 205 nm (110 L·cm/g) and DM_i is the weight of the sample before acid hydrolysis (g as 100% dry matter).

3.5.1.2 Determination of the molecular weight

The weight average (M_w) and number-average (M_n) molecular weights, together with the polydispersity indexes (M_w/M_n) of the lignin samples were analysed by High Performance Size Exclusion Chromatography (HPSEC). The

used chromatograph was a Jasco LC Net II/ADC equipped with a refractive index detector and it provided with two Varian Polymer Laboratories PolarGel-M columns in series (300 mm × 7.5 mm). The mobile phase in which the lignins were dissolved consisted in dimethylformamide with 0.1% of lithium bromide. The operational conditions were: injection volume 20 µL, flow of 0.7 mL/min and temperature of 40 °C. The calibration curve was carried out using polystyrene standards with different molecular weights (between 62,500 and 266 g/mol) provided by Sigma Aldrich.

3.5.1.3 *Composition analyses*

Pyrolysis-Gas chromatography-Mass spectrometry analyses (Py-GC/MS) were performed to the lignin samples using a 5150 a Pyroprobe pyrolyzer (CDS Analytical Inc.) connected to an Agilent 6890 gas chromatograph coupled to an Agilent 5973 (Agilent Technologies Inc.) mass spectrometer, as reported by Dávila *et al.* (2017) [77]. The GC was equipped with a 30 m × 0.25 mm × 0.25 µm film thickness HP-5MS ((5% phenyl)-methylpolysiloxane) column and helium was used as the carrier gas. The pyrolysis was performed at 600 °C (15 s) reached at a heating speed of 20 °C/ms, being the interface kept at 260 °C. The GC oven was programmed from 50 °C (2 min) to 120 °C (5 min) at 10 °C/min, then to 280 °C (8 min) at 10 °C/min and finally to 300 °C (10 min) at 10 °C/min. The compounds were identified by comparing their mass spectra with the National Institute of Standards Library (NIST) and with compounds reported in the literature.

3.5.1.4 *Total Phenolic Content (TPC)*

The lignin samples were dissolved in dimethyl sulfoxide (DMSO) for TPC analyses, which were carried out according to the Folin-Ciocalteu spectrophotometric method [75]. In brief, firstly, a calibration curve was designed in order to relate the absorbance measurements to the total phenolic content, expressed as gallic acid (GA) equivalents (C_{GAE} , mg/L). The calibration

curve was constructed using several solutions of gallic acid with concentrations between 0 and 200 ppm. For the measurements, 300 μL of the samples/GA solutions were introduced in test tubes and 2.5 mL of a 1/10 (v/v) aqueous solution of Folin-Ciocalteu were added and stirred. Then, 2 mL of a 7.5 % (w/v) sodium carbonate (Na_2CO_3) solution were incorporated to each tube and also stirred before incubating them during 5 minutes at 50 $^\circ\text{C}$. Lastly, the samples were cooled down to room temperature and their absorbance was measured at 760 nm using a Jasco UV-Vis 730 spectrophotometer.

3.5.1.5 ^{31}P Nuclear Magnetic Resonance (^{31}P NMR)

For the verification of the hydroxymetylation of lignin in **Publication V**, ^{31}P NMR was carried out according to the methods described by Chen *et al.* (2020) and Meng *et al.* (2019) [38,39]. In brief, a solution of deuterated chloroform (CDCl_3) and anhydrous pyridine at a volume ratio of 1:1.6 (v/v) was prepared. Then, the Internal Standard (IS) solution was prepared by adding chromium (III) 2, 4-pentanedionate ($\text{Cr}(\text{acac})_3$) to the previous solution at a concentration of around 5.0 mg/mL. Then, N-hydroxy-5-norbornene-2, 3-dicarboxylic acid imide (NHND) was added to the $\text{Cr}(\text{acac})_3$ solution at a concentration of around 18.0 mg/mL.

Around 30 mg of lignin were dissolved in 0.5 mL of the CDCl_3 /pyridine solution, to which 0.1 mL of the IS solution were added. Finally, 0.1 mL of 2-chloro-4,4,5,5-tetramethyl-1,3,2-dioxaphospholane (TMDP) were incorporated so as the hydroxyl groups were phosphitylated. The samples were stirred and then transferred into NMR tubes for the analyses.

3.5.2 Hydrogel characterisation

3.5.2.1 Lignin waste

In order to quantify the lignin that was removed from the hydrogels during the washing stage, aliquots of every washing solution were taken. For the

determination of the lignin concentration in these solutions, a calibration curve was firstly designed by employing several lignin solutions prepared in 2% (w/w) NaOH with known concentrations. Then, their absorbance was measured at the maximum absorbance wavelength using a Jasco UV-Vis 730 spectrophotometer. Thus, each absorbance measurement was related to the concentration of the prepared dissolutions. In this way, a calibration curve was obtained. Then, the absorbance of the taken aliquots was measured at the same wavelength, diluting the samples when needed. The concentrations of the aliquots were calculated with the calibration curve, and finally, taking the volume of each rinse into account, the total lignin loss was calculated.

3.5.2.2 Swelling capacity

The hydrogels were weighted in dry state and immersed in 40 mL of distilled water for 48 h. For the swelling kinetics, the hydrogels were weighted at certain times, removing the water remaining on the surface with filter paper. The swelling degree was calculated from the following Eq. 3.2:

$$\text{Swelling (\%)} = \frac{m_{\text{swollen}} - m_{\text{dry}}}{m_{\text{dry}}} \cdot 100 \quad (\text{Eq. 3.2})$$

where m_{swollen} and m_{dry} are the masses of swollen and dry hydrogels, respectively.

3.5.2.3 Scanning Electron Microscopy (SEM)

SEM analyses were carried out in order to study the morphology of the hydrogels. The samples were swollen in water for 48 h at room temperature and then frozen at -20 °C. Afterwards, they were freeze-dried in an Alpha 1-4 LD freeze drier. The images of secondary electrons were taken with a MEB JEOL 7000-F. The working conditions were 5 kV and an intensity of 0.1 nA. The samples were covered with 20 nm of Cr by sputtering.

3.5.2.4 *Compression studies*

Uniaxial compression tests were performed on the hydrogels in order to assess their mechanical strength. A compression gear was set up on an Instron 5967 machine using a 500 N load cell with a crosshead speed of 2 mm/min. Square samples of around 5 x 5 mm were cut from the initial hydrogels, which were left to swell during 48 h at room temperature. Then, the samples were compressed up to the 80% of their initial thickness. This strain was selected according to other works and the limitations of the compression test equipment caused by the thicknesses of the samples. The swollen modulus, G_e , of each sample was calculated automatically by employing Eq. 3.3.

$$\sigma = \frac{F}{A} = G_e \cdot \left(\lambda - \frac{1}{\lambda^2} \right) \quad (\text{Eq. 3.3})$$

where F is the force, A is the original cross-sectional area of the swollen hydrogel and $\lambda = L/L_0$ where L_0 and L are the thicknesses of the samples before and after compression, respectively.

3.5.3 **General methods**

3.5.3.1 *Attenuated Total Reflection-Fourier Transformed Infrared Spectroscopy (ATR-FTIR)*

In order to study the chemical structure of the samples, a PerkinElmer Spectrum Two FTIR Spectrometer equipped with a Universal Attenuated Total Reflectance accessory with internal reflection diamond crystal lens was used to collect Infrared spectra of the hydrogels. The studied range was from 600 to 4000 cm^{-1} and the resolution was 8 cm^{-1} . 20 scans were recorded for each sample [78].

3.5.3.2 *X-Ray Diffraction (XRD)*

X-Ray Powder Diffraction tests were carried out using a Phillips X'Pert PRO automatic diffractometer operating at 40 kV and 40 mA, in theta-theta

configuration. Monochromatic Cu-K α ($\lambda = 1.5418 \text{ \AA}$) radiation and a PIXcel solid-state detector (active length in 2θ 3.347°) were employed. The collected data ranged from 5 to 80° 2θ at room temperature, where θ is the incidence angle of the X-ray beam on the sample. The samples were subjected to XRD analysis grated and in dry state. The approximate size (D) of crystallites was calculated using the Scherrer equation (Eq. 3.4):

$$D = \frac{k \cdot \lambda}{\beta \cdot \cos \theta} \quad (\text{Eq. 3.4})$$

where D is the mean size of ordered domains (nm), k is the Scherrer constant (0.9), λ is the X-ray wavelength (0.154 nm) and β is the full-width at half-maximum of the reflection (FWHM) measured in 2θ of the corresponding Bragg angle [78].

3.5.3.3 Differential Scanning Calorimetry (DSC)

DSC analyses were done on a Mettler Toledo DSC 822. Between 3 and 5 mg of the samples were subjected to a heating ramp from -25°C to 225°C at a rate of $10^\circ\text{C}/\text{min}$ under a nitrogen atmosphere to avoid oxidative reactions inside aluminium pans. After the first heating step, cooling and second heating stages were also performed. The glass transition temperature (T_g), was considered as the inflection point of the specific heat increment during the second heating scan. The calibration was performed with indium standard. In the case of the hydrogels, the degree of crystallinity (χ_c) was obtained from the enthalpy evolved during crystallization using Eq. 3.5:

$$\chi_c = \frac{\Delta H}{\Delta H_0 \cdot (1 - m_{filler})} \cdot 100 \quad (\text{Eq. 3.5})$$

where ΔH is the apparent enthalpy for melting or crystallization, ΔH_0 is the melting enthalpy of 100% crystalline PVA (average value: 161.6 J/g) and $(1 - m_{filler})$ is the weight percent of PVA in the hydrogels [78].

3.5.3.4 Thermogravimetric Analysis (TGA)

TGA were performed using a TGA/SDTA RSI analyzer 851 Mettler Toledo. Between 3 and 5 mg of the lignins were weighed in aluminium pans and tested from 25 °C to 800 °C under a nitrogen atmosphere with a heating rate of 10 °C/min.

3.6 Specific methods for hydrogel applications

3.6.1 Methylene blue adsorption tests

For **Publications III and IV** methylene blue (MB) adsorption tests were carried out as follows [79]: a solution of MB was prepared at a concentration of 1 mg/L. Dry hydrogel samples (≈ 0.5 g) were immersed into 15 mL of this solution. These experiments were statically performed at room temperature for 24-48 h. Then, a calibration curve was designed by employing several solutions of known concentrations (0.25–5 mg/L) of MB and their absorbance measured at 665 nm by a UV-Vis 730 Jasco spectrophotometer. After the adsorption tests, the concentrations of the initial and final dissolutions were determined employing the calibration curve and the adsorption performances were calculated by Eq. 3.6.

$$Q_e \left(\frac{m.g_{MB}}{g_{HG}} \right) = \frac{C_0 - C_{eq}}{m \cdot V} \quad (\text{Eq. 3.6})$$

where C_0 is the initial dye concentration, C_{eq} is the dye concentration at equilibrium, V is the total volume of dye employed for each sample and m is the dry weight of the hydrogel.

The percentage of removal was also calculated by means of Eq. 3.7:

$$P(\%) = \frac{C_0 - C_{eq}}{C_0} \cdot 100 \quad (\text{Eq. 3.7})$$

where P is the equilibrium adsorption rate of the hydrogel and the rest of variables are the same as the ones defined for Eq. 3.6.

3.6.2 Antifungal tests

Antifungal tests for **Publication IV** were performed according to the methods reported by Salaberria *et al.* (2017) and da Silva *et al.* (2018) with slight modifications [80,81]. Briefly, after culturing the mould fungus *Aspergillus niger* (CBS 554.65) on Petri dishes covered with potato dextrose agar (PDA) for 7 days at $25\text{ }^\circ\text{C} \pm 1.5\text{ }^\circ\text{C}$ in a climatic chamber, some spores were diluted in a phosphate buffer saline (PBS) dissolution and its concentration was adjusted to around 1.21×10^6 spores/ml using an automatic cell counter for the measurements (Cellometer[®] Mini, Nexcelom Bioscience LLC). Then, the procedure was varied according to the type of sample.

The lignins were firstly dissolved in DMSO (around 75–100 mg/mL) and then, 40 μL of the sample dissolution was poured on a Petri dish covered with PDA and the fungal strain was sprayed around. The blank was performed with DMSO [81]. In the case of the hydrogels, square portions (approximately 1 cm x 1 cm) of each sample were introduced into the PDA covered Petri dishes after having inoculated them with fungal strain. The blank was performed using neat PVA hydrogel portions.

All the tests were done by duplicate. After 7 days of incubation at $25\text{ }^\circ\text{C} \pm 1.5\text{ }^\circ\text{C}$, the growth inhibition (GI) of lignins was evaluated visually using a numerical scale (Table 3.1) reported by da Silva *et al.* (2018) in accordance with ISO 846 [81], whereas the hydrogels were extracted from the agar and washed with 1 mL of PBS in order to collect the spore solution into an Eppendorf.

Table 3.2. Visual assessment of the antifungal studies according to ISO 846.

GI	Evaluation
0	No growth apparent under magnification
1	No visible growth but visible under magnification
2	Visible growth up to 25 % coverage
3	Visible growth up to 50 % coverage
4	Visible growth up to 75 % coverage
5	Heavy growth covering more than 75 % of the studied area

Afterwards, these solutions were tinged blue with 5 μ L trypan blue solution and after shaking them, their spore concentration was determined with the abovementioned cell counter [80]. The fungal growth inhibition (FGI) of the samples was calculated through Eq. 3.8 [80].

$$FGI(\%) = \frac{C_g - T_g}{C_g} \cdot 100 \quad (\text{Eq. 3.8})$$

where C_g is the average concentration in the control samples set (neat PVA hydrogels) and T_g is the average concentration in the treated sample, both expressed as concentration of spores/mL.

3.6.3 Quercetin extraction and characterisation



Figure 3.6. Red onion peels.

For quercetin (drug) extraction in **Publication V** the methods reported by George *et al.* (2019) and Jin *et al.* (2011) were combined [82,83]. Firstly, red onion peels were acquired from domestic wastes and they were cleaned and dried at 50 °C before being powdered. Then, quercetin, together with other compounds, was extracted by microwave assisted extraction (MAE) (flexiWAVE, Milestone Srl), which was based on previous experiments (data not shown) modifying the microwave power reported by Jin *et al.* (2011). The extraction was done with a 70% ethanol/water (v/v) solution, keeping a LSR of 40:1 (v/w) and the employed power for intermittent 10 second irradiations was fixed at 375 W. The total reaction time

was 2 minutes, leaving a 20 second interval between the irradiations. After the reaction, the solid was filtered and the liquid phase was rotary evaporated for the complete elimination of ethanol. The remaining aqueous solution was considered as quercetin extract (QE).

The concentration of the quercetin extract was determined by UV spectrophotometry. For this aim, a calibration curve was designed using several solutions of known concentrations of commercial quercetin (CQE) and measuring their absorbance at 375 nm [83]. QE was freeze-dried and analysed by ATR-FTIR and compared with the spectrum of CQE. The extraction yield was estimated from the solid content of the QE (non-volatile content). Briefly, 2 mL of QE were placed in dry recipients, weighted and left to dry at 105 °C for 24 h. Afterwards, the recipient was cooled down in a desiccator and weighted again. The solid content was calculated as follows (Eq. 3.9):

$$Yield(\%) = \frac{m_f - m_r}{m_i - m_r} \cdot 100 \quad (\text{Eq. 3.9})$$

where m_r is the mass of the dry recipient, m_i is the mass of the recipient and 2 mL of the QE and m_f is the weight of the recipient and the extract after 24 h, all of them expressed in grams.

Further characterisation of QE was performed by measuring its total phenolic and flavonoid contents (TPC and TFC, respectively). The TPC was measured as explained in Section 3.5.1.4 for lignin, replacing DMSO by methanol, as described by Sillero *et al.* (2019) [23].

In the case of TFC the aluminium chloride (AlCl_3) colorimetric assay was used, employing commercial quercetin as standard [82,84] and the method described by Sillero *et al.* (2019) [23]. In brief, 2 mL of a diluted aliquot of the extract was mixed with 0.3 mL of a 5% solution of sodium nitrite (NaNO_2). After 5 minutes, 0.3 mL of a 10% solution AlCl_3 was added, and after other 6 minutes, 2 mL of 1 N

NaOH was added to neutralize the mixture. After 5 minutes, the absorbance at 415 nm was measured. The results were expressed as mg of quercetin equivalents (CQE)/g of dry extract.

3.6.4 Quercetin loading and release tests

For **Publication V**, the quercetin loading tests were performed by introducing dry hydrogel samples (≈ 0.5 g) into diluted QE (1 mL QE into 250 mL distilled water) solutions for 24 hours. The absorbed QE amount was calculated by the difference on the concentrations of the initial and final solutions [82]. After the loaded hydrogels were dried, they were weighted and again immersed into PBS at 37 °C, simulating *in vitro* conditions, for 24 hours. The release kinetics was performed by measuring the concentration of QE in PBS at certain times. All release tests were performed in triplicates. The obtained data were applied in various kinetic models such as zero order, first order, Korsmeyer–Peppas and Higuchi (see Eqs. 3.10-3.13) so as to understand the release mechanism for QE [82,85,86].

$$F = k_0 \cdot t \quad (\text{Eq. 3.10})$$

$$\ln(1 - F) = -k_1 \cdot t \quad (\text{Eq. 3.11})$$

$$\frac{M_t}{M_\infty} = k_{kp} \cdot t^n \quad (\text{Eq. 3.12})$$

$$F = k_h \cdot t^{1/2} \quad (\text{Eq. 3.13})$$

where F is the fraction of drug released at time t and k_0 , k_1 , k_{kp} and k_h the rate constants of zero order, first order, Korsmeyer–Peppas and Higuchi kinetic release models, respectively, and n the diffusion exponent parameter.

3.6.5 *In-vitro* biocompatibility tests

In-vitro biocompatibility tests of hydrogels were performed in Marmara University, Department of Bioengineering, Industrial Biotechnology and Systems Biology Research Group Cell Culture Research Lab. All stages of experiments were performed in extreme sterile conditions with sterile media and equipment's to prevent any fungal, bacterial or yeast contamination.

3.6.5.1 *Sterilization of the samples*

Hydrogels were swollen in PBS for 48 hours and sterilized by 70% ethanol and UV for 1 hour and 2% Penicillin-streptomycin in PBS for 2 hours, washed with PBS and saturated with Dulbecco's Modified Eagle Medium (DMEM) complete media prior to experiment.

3.6.5.2 *Cell seed and cell proliferation test*

Human dermal fibroblast cells (PCS-201-012) were used for cell proliferation tests. Briefly, frozen cells were thawed immediately and centrifuged with DMEM complete media (10% Fetal Bovine Serum (FBS), 1% Penicillin-Streptomycin) and the cell pellet was seeded onto cell culture T25 flask to allow cellular attachment and growth at a 5% CO₂ incubator at 37 °C. When the cells reached confluence, a subculturing protocol was applied. For this aim, the media was removed and the cells were washed with PBS 2 times. 1 mL of Trypsin-EDTA was added onto the cells and incubated in an incubator for a couple of minutes. After cellular adhesion breakdown, DMEM complete media was added into the flasks and the cell media suspension was centrifuged at 2000 rpm for 5 minutes. Then, the cell pellet was resuspended and spread to T75 cell culture flasks (TPP) for cell growth. When adequate cell number was achieved, the cells were detached as previously described and counted after being dyed with Trypan blue for cell counting by using a microscope. Afterwards, as indicated in Figure 3.7, they were seeded on pre-sterilized and cell culture media saturated hydrogels in 96 well plate at the density of 15×10^4

cells/well and incubated for 24, 48 and 72 hours. At the end of incubation period, WST-1 ((4-[3-(4-iodophenyl)-2-(4-nitrophenyl)-2H-5-tetrazolio]-1,3-benzenedisulfonate) solution was added to the cells (1:10 v/v) and incubated for 2 more hours for their posterior absorbance measurement via a Biotek Cytation 3 microplate reader at 450 nm.

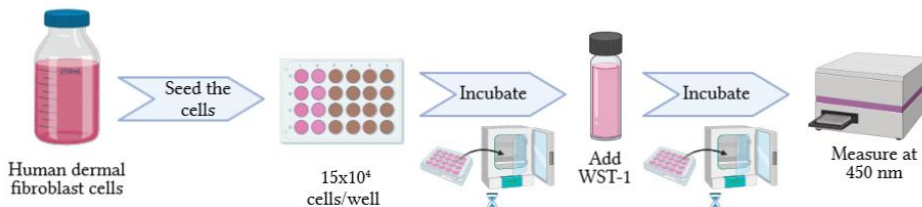


Figure 3.7. Schematic explanation of the cell seeding procedure.

3.6.5.3 Cell viability calculations

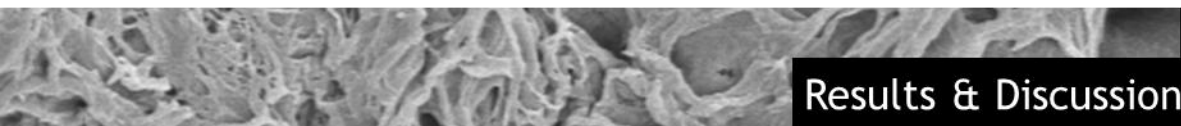
The viabilities of the samples were calculated as follows:

- a. After the absorbances of all samples were read, they were converted into viability percentages considering the absorbance of the control cell-well as a reference (100% viability).
- b. The outlier values were detected through Grubbs' test (see Eq. 3.14), which takes into consideration the mean value of each data series and its standard deviation.

$$Z = \frac{|x_{mean} - x|}{SD} \quad (\text{Eq. 3.14})$$

where x_{mean} is the mean value of the data series, x is the suspicious value and SD is the standard deviation of the data series. If this Z value is higher than the critical value tabulated for the tested number of observations, the selected x value is an outlier. If not, it should be considered for the calculations.

- c. For the experiments after 48 and 72 h, the viabilities were also calculated taking the absorbance of the control sample after 24 h as a reference.
- d. In the cases in which experiments were performed longer than for 24 h, a second viability approach was made similarly taking the absorbances of the blank samples (neat PVA hydrogels) as control.



4 Results & Discussion

In this thesis, lignin-based hydrogels were synthesized combining different materials and formulations. Firstly, the synthesis procedure was optimised using an experimental design and a Response Surface Methodology (RSM) for six different synthesis routes. The optimal conditions were then applied for the obtaining of hydrogels varying the molecular weight of the matrix polymer, PVA, in order to study its influence on the final properties of the hydrogels. The same conditions were also applied for the synthesis of self-extracted nut shell lignin-based hydrogels, as well as for the development of hydrogels from modified alkaline and organosolv lignins. Although all these results have been published separately, the summary of the main findings has been organised in the following sections:

- 4.1 Characterisation of the lignins
- 4.2 Optimisation of the synthesis of lignin-based hydrogels
- 4.3 Influence of different formulation parameters on the properties of the hydrogels
 - 4.3.1 Curing type
 - 4.3.2 Molecular weight of PVA and number of F-T cycles
 - 4.3.3 Lignin type
 - 4.3.4 Duration of the F-T cycles
 - 4.3.5 Type of lignin modification
- 4.4 Applications of the synthesized lignin-hydrogels
 - 4.4.1 Dye adsorption
 - 4.4.2 Antifungal properties
 - 4.4.3 Drug delivery
 - 4.4.4 *In-vitro* biocompatibility studies

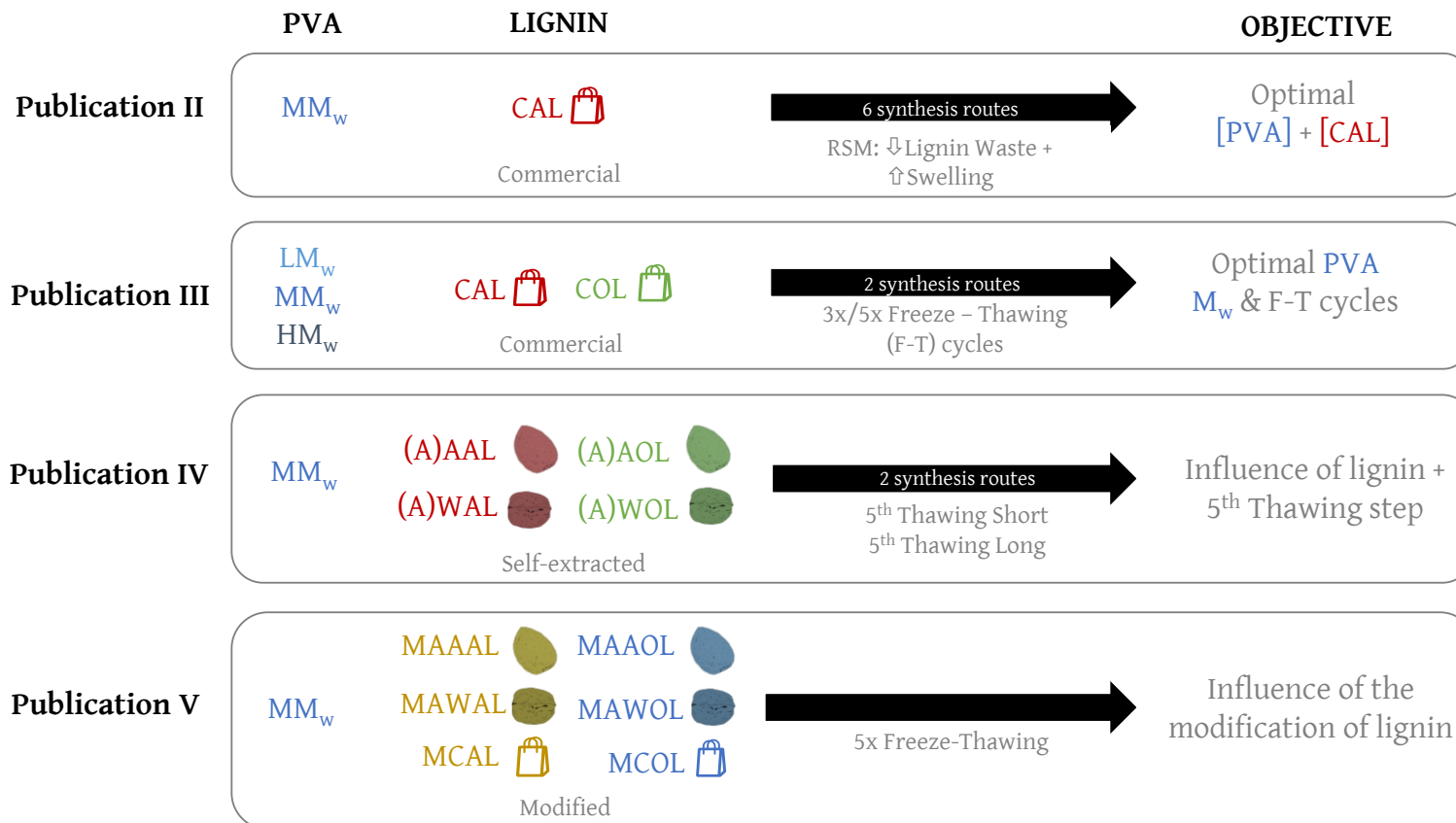


Figure 4.1. Schematic summary of the experiments carried out on the involved publications.

4.1 Characterisation of the lignins

4.1.1 Commercial and self-extracted lignins

4.1.1.1 Purity

As shown in Table 4.1, the purity results for native commercial and self-extracted lignins were, in general, higher for organosolv lignins than for alkaline ones due to the greater selectivity of this type of extractions [87]. Commercial lignins presented purities of around 92%. Self-extracted organosolv lignins without autohydrolysis (AOL and WOL) also had purities over 90%, whereas the ones for alkaline lignins were lower than 59%. After the autohydrolysis treatment of the feedstock, however, the purities for the alkaline lignins increased up to 88–95% while for the organosolv ones this increment was just of a 3–5%. Therefore, it can be said that autohydrolysis especially improves the purity of the alkaline lignins [77].

4.1.1.2 Molecular weight

From the HPSEC analyses, it was observed that the commercial alkaline lignin was much more homogeneous than the organosolv one, since the latest presented very high M_w , not typical for organosolv lignins (see Table 4.1). Nut shell organosolv lignins without autohydrolysis also presented higher M_w than the alkaline ones, whereas for the lignins coming from the double-step process (with autohydrolysis) the opposite behaviour was observed. A similar trend was perceived for the polydispersity indexes. It was also observed that the autohydrolysis treatment enhanced the weight and number average molecular weights of lignins. It should also be noticed that the M_w for all the organosolv lignins was very alike, whereas for the alkaline lignins this difference was huge. However, and looking at the purity percentages and previous works [88], it is possible that these results for the analysed lignin fractions for AAL and WAL were not representative of the whole lignin samples.

Table 4.1. Summary of the purity, HPSEC, TPC and TGA results for all the lignin samples.

Sample	Description	Purity (%)	M_w^a (g/mol)	M_n^b (g/mol)	M_w/M_n^c	TPC (% GAE ^d)	T_{max}^e (°C)
CAL	Commercial alkaline lignin	91.5	9333	1365	6.8	20.3	379
COL	Commercial organosolv lignin	92.5	32933	1123	29.3	19.3	343
AAL	AS alkaline lignin	58.2	4770	1109	4.3	13.8	307
AOL	AS organosolv lignin	90.4	8301	1072	7.8	15.6	389
WAL	WNS alkaline lignin	49.4	4761	1054	4.5	10.6	295
WOL	WNS organosolv lignin	92.7	6371	1246	5.1	16.5	388
AAAL	Autohydrolysed AS alkaline lignin	88.2	12793	1528	8.4	33.1	355
AAOL	Autohydrolysed AS organosolv lignin	95.2	9020	1520	5.9	26.2	357
AWAL	Autohydrolysed WNS alkaline lignin	95.7	16670	1604	10.4	33.8	354
AWOL	Autohydrolysed WNS organosolv lignin	95.2	7644	1359	5.6	27.2	365
MCAL	Modified CAL	91.9	12141	1718	7.1	25.8	396
MCOL	Modified COL	96.5	32997	968	34.07	21.5	390
MAAAL	Modified MAAAL	85.2	17675	1348	13.1	25.3	384
MAAOL	Modified MAAOL	92.3	9557	1636	5.8	20.4	383
MAWAL	Modified AWAL	84.0	19939	1369	14.6	27.6	384
MAWOL	Modified AWOL	83.6	8187	1420	5.8	23.6	383

^a M_w : weight average molecular weight; ^b M_n : number average molecular weight; ^c M_w/M_n : polydispersity index; ^d% GAE: percentage of gallic acid equivalents; ^e T_{max} : maximum degradation temperature from TG/DTGA curves.

4.1.1.3 Total Phenolic Content (TPC)

Looking at total phenolic content results (see Table 4.1), it was observed that the values for the native lignin samples coming from the direct delignification of nut shells (AAL, AOL, WAL and WOL) were considerably lower than those reported for the ones obtained from the double-step process (AAAL, AAOL, AWAL and AWOL) or commercial lignins, which could be related to their purities [89]. A comparable behaviour was reported by Dávila *et al.* (2019), suggesting that a prior hydrothermal treatment can be crucial to obtain high total phenolic contents in lignin [89].

4.1.1.4 Thermogravimetric Analysis (TGA)

The thermal degradation curves (see Figure 4.2) of the lignins permitted the detection of the maximum degradation temperatures displayed in Table 4.1. Besides, all the samples had a common initial degradation step below 100 °C, corresponding to moisture evaporation. Commercial alkaline lignin then presented a second degradation step, which was the maximum degradation stage, at around 379 °C. This step was also observed for self-extracted samples, but whereas the alkaline lignins obtained through the single-step processes (AAL and WAL) presented the maximum degradation temperature around 300 °C, this temperature was significantly higher for the organosolv lignins (≈ 390 °C). However, commercial organosolv lignin presented a degradation step before the maximum degradation stage, and the latest was detected around 343 °C, which was lower than that reported for the extracted organosolv lignins. The decrease on the thermal stability is usually ascribed to the high amount of impurities as well as to the fractions with low molecular weight [77,90].

The lignins coming from the double-step processes presented similar maximum degradation temperatures (354–365 °C), which were within the ones reported for single-step process lignins and were in accordance with previous

results [75]. In this temperature range, the scission of β -O-4 ether bondages tend to occur, followed by the division of C-C linkages and aromatic rings [90].

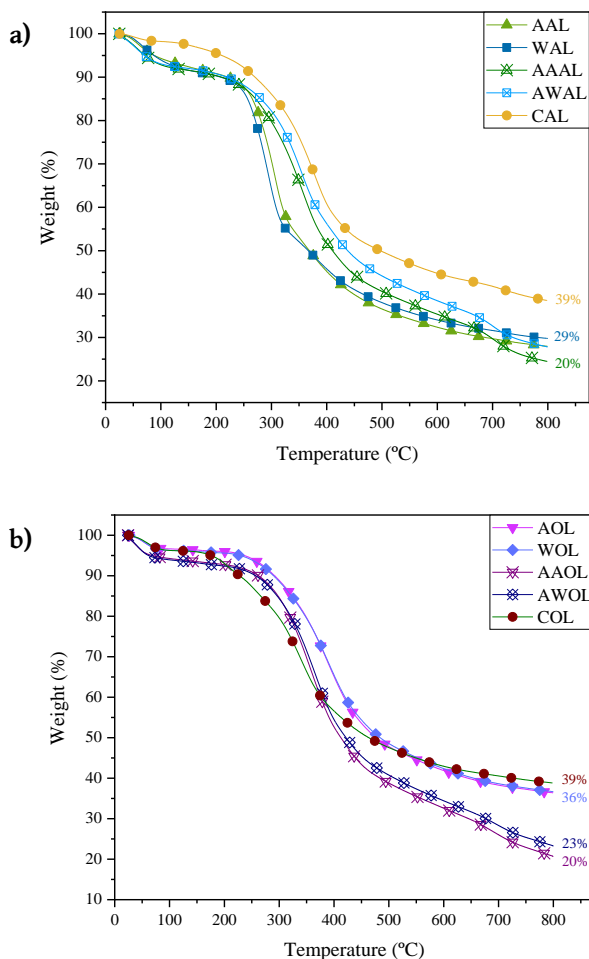


Figure 4.2. TGA curves of the native a) alkaline and b) organosolv lignin samples employed in the present thesis.

A third degradation stage was observed around 420 °C, although this temperature was again lower for AAL and WAL (\approx 390 °C) samples and higher for AOL and WOL samples (\approx 470 °C). The latest then presented a constant weight loss until 37% of their initial weight. The rest of the samples presented a fourth degradation step around 700 °C, leading to a final residue or *biochar* between 20 and 29% of their initial weight. This last stage could be related to

the demethoxylation or condensation reactions of the volatile products of lignin [90], and the amounts of residue were aligned with those reported previously [75].

4.1.1.5 Attenuated Total Reflection-Fourier Transformed Infrared Spectroscopy (ATR-FTIR)

The main functional groups of the employed lignins were determined by ATR-FTIR technique (Figures 4.3 and 4.4). Although all the recorded spectra presented the typical lignin bands (see Table 4.2) [74,89,91–94], the intensities of some of them changed from sample to sample.

Table 4.2. ATR-FTIR bands of lignins and their assignment.

Wavenumber (cm ⁻¹)	Assignment
3460-3215	-OH stretching vibration
2998-2947	Alkyl asymmetric vibration
2913-2827	Aromatic C-H stretching vibration
1710	C=O stretch vibration in unconjugated ketones
1679-1650	C=O ester bonds
1597	C=C stretching vibration
1513	C=C aromatic vibrations
1456	C-H bonds of the methyl groups
1429	Aromatic skeletal vibration
1330-1269	G and S units breathing + impurities
1215	Aromatic methyl ethers
1100	C-C bonds
1157-1030	C-O stretching vibration + impurities
975	-HC=CH out-of-plane vibrations
910-896	C-H deformation vibrations
865	C-C stretching vibration
832-317	Aromatic -CH out of plane vibration + β -glucosidic linkages

Among the commercial lignins, the main differences were detected around 1330, 1265 (α band in Figures 4.3 and 4.4) and 840 cm⁻¹, which could be attributed to the variation on S and G units and also their impurities. Between the self-extracted lignins, notable variations were observed in the range 2827–2998 cm⁻¹, which corresponded to the C–H stretching vibration of lignin and polysaccharides [91], and were more notable for alkaline lignin samples,

probably due to their higher sugar content. At 1650 cm^{-1} , a peak corresponding to conjugated C=O stretching vibration [91] was detected for the single-step lignins, but it disappeared after the autohydrolysis step. Although some authors have previously related this band to alkaline processes [95], it may be attributed to the presence of impurities in AAL, WAL, AOL and WOL lignins.

On the fingerprint range ($1500\text{--}600\text{ cm}^{-1}$) the main changes were seen on the intensity of the bands. AAL and WAL samples, for instance, presented a clear decrease on the intensity of the bands ascribed to the condensed syringil or guaiacyl unit breathing (1330 cm^{-1}) [92,96] and aromatic methyl ethers of lignin (1215 cm^{-1} , *b* band in Figures 4.3 and 4.4) [91]. Conversely, the peaks at 1157 , 1080 , 975 and 896 cm^{-1} (*c-f* bands in Figures 4.3 and 4.4, respectively), corresponding to C–O stretching vibration in ester groups [92,96], C–O deformation in secondary alcohol and aliphatic ethers, –HC=CH out-of-plane and C–H deformation vibrations [92], subsequently, got intensified in the aforementioned samples.

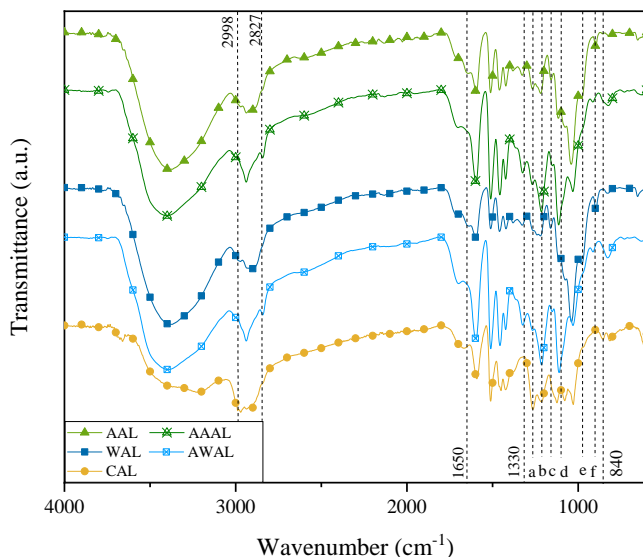


Figure 4.3. ATR-FTIR spectra of the native alkaline lignin samples employed in the present thesis.

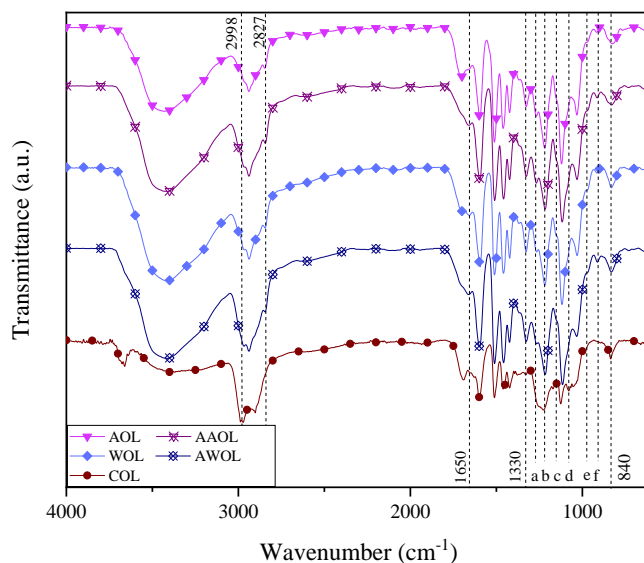


Figure 4.4. ATR-FTIR spectra of the native organosolv lignin samples employed in the present thesis.

4.1.1.6 Composition analyses (Py-GC/MS)

The compounds that were determined out of the Py-GC/MS analyses are shown in Table 4.3. The pyrograms of the self-extracted lignins showed peaks at early times (3–7 min) corresponding to degradation compounds such as furfural from impurities [75], which were especially visible in the less pure lignin samples (AAL and WAL). Thus, the identified compounds in the range of 7–23 minutes were grouped according to the origin of their aromatic structure (*p*-hydroxyphenyl (H), guaiacol (G) and syringol (S)) [74,75,92,94].

Among the identified compounds, guaiacol, 4-methylguaiacol, syringol and 4-methylsyringol were the most abundant ones in all the lignin samples, especially on CAL, where guaiacol was the principal compound. 4-ethylguaiacol and 4-vinylguaiacol were also present in large amounts in all the samples. The compounds coming from the *p*-hydroxyphenyl unit such as phenol, *p*-cresol and *p*-ethylphenol seemed to be more abundant in WNS lignins. Other compounds such as vanillin were only present in organosolv

Table 4.3. Identification and abundance (relative area, %) of the compounds detected by Py-GC/MS for native lignins.

Retention Time (min)	Compound	Origin	Lignin Sample									
			CAL	COL	AAL	AOL	WAL	WOL	AAAL	AAOL	AWAL	AWOL
7.5-7.7	Phenol	H	1.80	3.85	1.62	0.98	6.56	3.29	1.16	-	4.26	2.95
8.7-8.9	<i>o</i> -Cresol	H	1.60	0.79	1.53	1.04	2.42	1.22	1.80	1.14	1.66	1.21
9.0-9.2	<i>p</i> -Cresol	H	1.55	1.71	1.82	1.62	5.22	5.31	1.39	0.92	4.58	4.12
9.3-9.5	Guaiacol	G	38.40	9.65	13.62	11.80	9.30	8.91	17.14	7.40	11.72	7.56
10.4	Phenol, 2,6-dimethyl	H	-	-	1.68	1.38	1.45	1.53	1.95	1.77	1.44	1.52
10.7-10.8	<i>p</i> -Ethylphenol	H	-	-	0.74	-	2.40	1.66	0.54	-	1.71	1.43
11.0-11.1	3-Methylguaiacol	G	1.85	0.63	2.08	1.35	0.94	1.29	3.90	1.17	2.28	1.24
11.7-11.9	Catechol	S	2.70	1.27	0.64	-	0.35	-	-	-	0.40	-
11.4-11.6	4-Methylguaiacol	G	5.07	3.87	9.75	12.74	5.23	10.86	15.19	8.08	10.07	7.73
13.3-13.5	3-Methoxycatechol	S	-	3.06	0.19	3.29	0.95	4.22	2.56	3.67	4.39	4.33
13.8-14.0	4-Ethylguaiacol	G	4.02	4.58	7.78	5.67	3.80	5.15	8.82	3.63	7.09	3.79
15.0-15.2	4-Vinylguaiacol	G	8.15	18.74	6.94	7.16	3.76	5.77	4.52	3.00	3.51	3.10
16.1-16.2	Syringol	S	1.98	8.07	7.45	9.69	3.96	10.57	8.13	5.42	16.52	7.18
16.3	3,4-Dimethoxyphenol	S	-	0.90	1.69	1.87	0.64	2.55	1.82	0.88	-	2.13
16.3-16.4	4-Propylguaiacol	G	0.86	0.52	-	1.48	-	1.34	-	0.88	-	0.94
17.1-17.3	Vanillin	G	-	0.86	-	0.82	-	0.80	-	0.71	-	0.63
17.4	<i>cis</i> -Isoeugenol	G	4.83	1.18	1.12	1.70	0.34	1.60	1.19	0.85	1.35	0.84
18.3	4-Methylsyringol	S	-	-	4.75	12.03	2.69	13.66	5.94	6.80	9.23	7.54
18.8-19.0	Acetovanillone	G	4.22	-	-	0.85	-	1.23	0.26	0.97	0.49	-
19.6	4-Ethylsyringol	S	-	-	1.02	1.28	0.78	1.95	1.16	0.82	2.47	0.90
20.2-20.8	4-Vinylsyringol	S	-	-	0.23	1.92	0.24	1.72	0.62	0.73	0.87	0.96
21.6	Syringaldehyde	S	0.70	-	-	1.20	0.47	0.62	0.40	1.65	0.16	2.56
22.1	4-Allylsyringol	S	0.93	2.27	0.51	2.09	0.83	2.11	0.50	0.40	0.51	1.56
22.5	Acetosyringone	S	1.82	-	0.13	2.03	0.87	0.86	0.34	1.45	0.17	2.44
23	Homosyringic acid	S	0.89	-	-	1.07	-	0.42	0.15	0.64	-	1.30
	Total S		9.03	15.57	16.60	36.48	11.78	38.67	21.62	22.47	34.72	30.90
	Total G		67.40	40.02	41.29	43.59	23.37	36.96	51.04	26.70	36.51	25.83
	S/G ratio		0.13	0.39	0.40	0.84	0.50	1.05	0.42	0.84	0.95	1.20

lignins, and 4-propylguaiacol appeared in all organosolv lignins and CAL. Some S-derived compounds such as 4-methylsyringol, 4-ethylsyringol and 4-vinylsyringol were just present in self-extracted lignins, which might be related to the extraction process. Regarding the estimated S/G ratios, all the samples presented more G units except for WOL and AWOL samples. Thus, almost all the S/G ratios were below 1. Commercial lignins were the ones presenting the lowest S/G values, followed by alkaline AS lignins.

However, an increase of this ratio was observed for the samples from the single to the double-step process, which will be further studied so as to find a consistent explanation. Nevertheless, these values are quite different to the ones reported previously for AS and WNS lignins [74,75], which could be related to any possible modification on the composition of the feedstock or in the extraction process.

4.1.2 Modified lignins

4.1.2.1 Purity

As shown in Table 4.1, the purity of the modified commercial and self-extracted lignins, regardless of the modification method, was altered especially in the latter lignins, which might be due to the employed reagents.

4.1.2.2 Molecular weight

In comparison with native lignins, the weight average molecular weights of the modified lignins augmented in all cases, especially in alkaline lignins. The number average molecular weights got decreased for modified self-extracted alkaline lignins and for commercial organosolv lignin, leading to a more meaningful rise in their polydispersity index.

As for commercial organosolv lignin, its modified version (MCOL) was also the most heterogeneous modified lignin, whereas the self-extracted native and

modified organosolv lignins (AAOL, AWOL, MAAOL and MAWOL) were the most homogeneous ones.

Although the peroxidation reaction is supposed to depolymerise lignin, a high percentage of the chains seemed to undergo re-condensation reactions, which made the total weight average molecular weights of modified alkaline lignins increase.

On the other hand, the variation on the distributions (see Supplementary data in **Publication V**) and average molecular weights of hydroxymethylated organosolv lignins suggested that the modification occurred successfully [97]. Despite the fact that the change on the polydispersity of the lignins was not representative of having obtained more homogeneous modified lignins, their molecular weight distributions evoked a trend of homogenization of the highest molecular weight fractions towards the ones with lower molecular weights. This behaviour was also observed by other authors [98]. Moreover, the increase on the number and weight average molecular weights was observed for MAAOL and MAWOL samples, which was also reported by the same authors for grass lignins [98].

4.1.2.3 Total Phenolic Content (TPC)

For peroxidated alkaline lignins, the change on the total phenolic content suggested the degradation of aromatic rings in lignin [76,99]. However, MCAL presented the opposite trend, which could be related to the differences on the pH of the solutions. According to the results reported by Xinping *et al.* (2010) [99], the reaction might have yielded more degradation compounds under alkaline conditions [41], but as Infante *et al.* (2007) had demonstrated that this could also be achieved with the non presence of a catalyst, the present reaction was done according to the latter [76].

In the case of hydroxymethylated lignins, except for the commercial lignin, a slight drop was also observed on the TPC, which could be attributed to the oxidation of the aromatic rings.

4.1.2.4 Thermogravimetric Analysis (TGA)

The thermal stability of all the modified samples is shown in Figure 4.5.

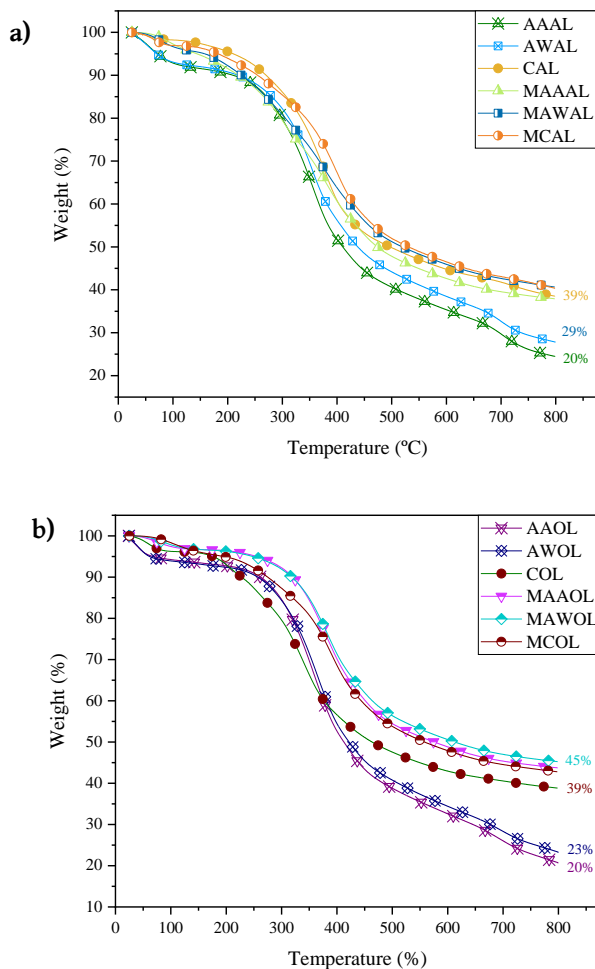


Figure 4.5. TGA curves of the modified a) alkaline and b) organosolv lignin samples.

It was observed that the thermal stability of these samples was altered through the modification reactions. In fact, the maximum degradation step was shifted to higher temperatures in all cases. However, in the case of alkaline lignins, another degradation step appeared between the stage corresponding to moisture evaporation (< 100 °C) and the maximum degradation stage. This peak was detected around 300 °C, and was attributed to the lower molecular weight fractions of lignin generated during the modification step [77,90].

It was also observed that organosolv lignins were more thermally stable and started to lose weight at higher temperatures than alkaline lignins, although their maximum degradation temperatures were slightly lower. Compared to native lignins, modified organosolv lignins presented higher thermal stability and final residue, which was also observed by other authors [39]. In addition, despite all the left *biochars* being of around the 40% of the initial sample weight, modified organosolv lignins left higher residues than alkaline ones, conversely to what happened for native lignins, which may be attributed to the modification and lignin precipitation stages.

4.1.2.5 Attenuated Total Reflection-Fourier Transformed Infrared Spectroscopy (ATR-FTIR)

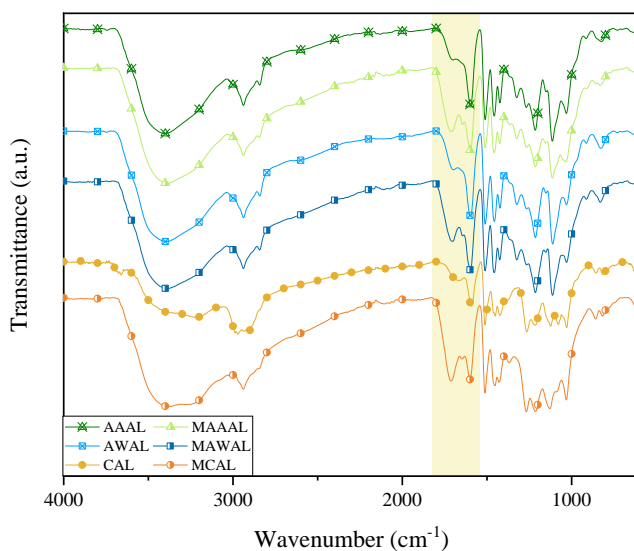


Figure 4.6. ATR-FTIR spectra of the modified alkaline lignin samples.

Modified lignins presented some variations in their spectra that suggested a change on their structure. In the case of peroxidated lignins, the differences on the range 1600-1730 cm⁻¹ on their ATR-FTIR spectra confirmed the reaction (see Figure 4.6). In fact, the band around 1710 cm⁻¹ moved to higher wavenumbers in all cases, which was attributed to the -OH oxidation of side

chains, together with the weakening of the peak at 1599 cm^{-1} corresponding to aromatic C=C stretching vibration. In addition, as reported by Infante *et al.* (2010), the appearance of the band around 1640 cm^{-1} was also representative of the degradation of aromatic rings [76].

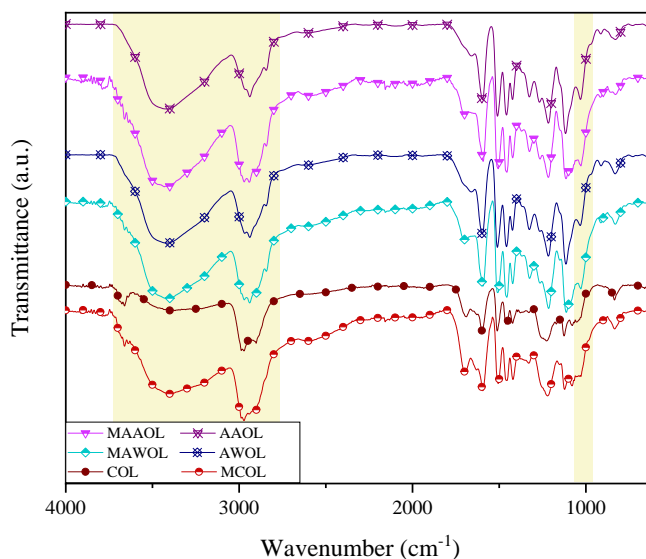


Figure 4.7. ATR-FTIR spectra of the modified organosolv lignin samples.

On the other hand, in the case of hydroxymethylated lignins (Figure 4.7), the intensification of the $-\text{OH}$ band (at 3400 cm^{-1}), the one corresponding to C-H (around 2930 cm^{-1}), the one attributed to methoxyl and hydroxymethyl groups (around 2850 cm^{-1}) and the one related to the C-O stretching vibration of aliphatic C-OH and hydroxymethyl C-OH (around 1030 cm^{-1}) were a clear evidence of the introduction of hydroxymethyl groups via the modification reaction [39,97]. The appearance of a shoulder at 3660 cm^{-1} suggested the presence of free $-\text{OH}$ groups within the modified lignin structures [100]. Thus, the spectra confirmed the success of the reaction. These results were in agreement with those obtained from ^{31}P NMR analyses, in which an increase on the aliphatic hydroxyl signal between 150 and 145.4 ppm was observed for all

the samples after the hydroxymethylation reaction [39] (see Supplementary data in **Publication V**).

4.1.3 Conclusions

In this section, commercial, self-extracted and modified alkaline and organosolv lignins were characterised. Self-extracted lignins were isolated from almond and walnut shells through two different biorefinery strategies: via a single delignification process and a double-step process composed by an autohydrolysis and a delignification stage. The characterisation of the lignins showed significant differences between the samples, especially on their composition, average molecular weights and total phenolic contents. As expected, the autohydrolysis enhanced the purity of the lignins, especially in the case of alkaline ones, and it also promoted the extraction of lignins with higher average molecular weights. The modification of the lignins was confirmed via the employed characterisation techniques and it led to higher weight average molecular weights and, thus, also to more thermally stable lignins.

4.2 Optimization of the synthesis of lignin-based hydrogels

As shown in **Publication II**, in order to optimize the synthesis of lignin-based hydrogels, commercial alkaline lignin (CAL) and poly (vinyl alcohol) (PVA, $M_w = 83,000\text{--}124,000$ g/mol, 99+ % hydrolyzed) were blended in the concentrations indicated by a three-level-two-factorial experimental design with three replicates in the central point. A Response Surface Methodology (RSM) was then employed to perform the modelling and the optimization of the conditions of the lignin-hydrogel synthesis.

All the hydrogels were prepared as described in Section 3.4, and the blends were subjected to three different crosslinking (XL) methods: 3 and 5 cycles of freezing and thawing (16 h at -20 °C and 8 h at 28 °C) and inside a vacuum hood at 37 °C (-60 cm Hg) for a week. After the crosslinking stage, the hydrogels were separately washed and afterwards, half of them were left to dry at room temperature while the other half were dried under vacuum (-60 cm Hg) at 27 °C. The hydrogels with the optimal compositions were prepared similarly employing the corresponding amounts of lignin and PVA. The six synthesis routes depicted in Figure 4.8 represent the following used pathways:

- (1) Vacuum XL + Air Drying (Vac-Air)
- (2) Vacuum XL + Vacuum Drying (Vac-Vac)
- (3) 5 Cycles of Freeze-Thawing XL + Air Drying (F-T x5-Air)
- (4) 5 Cycles of Freeze-Thawing XL + Vacuum Drying (F-T x5-Vac)
- (5) 3 Cycles of Freeze-Thawing XL + Air Drying (F-T x3-Air)
- (6) 3 Cycles of Freeze-Thawing XL + Vacuum Drying (F-T x3-Vac)

As aforementioned, the selected independent variables were both the alkaline lignin (x_1) and the PVA concentrations (x_2), which ranged from 5 to 25% (w/w) and from 5 to 11% (w/w), respectively. Conversely, the response variables were the swelling capacity of the hydrogels (% , y_1) and the lignin waste during the washing stage (% , y_2). Eleven experiments were designed for each pathway considering the selected parameters' values and the triplicate central point, so

sixty six experiments were carried out in total. The optimization was carried out so as to obtain hydrogels with the minimum lignin waste and the maximum swelling capacity. The models were validated by carrying out the experiments at the optimal points and comparing the results obtained experimentally with the predicted data.

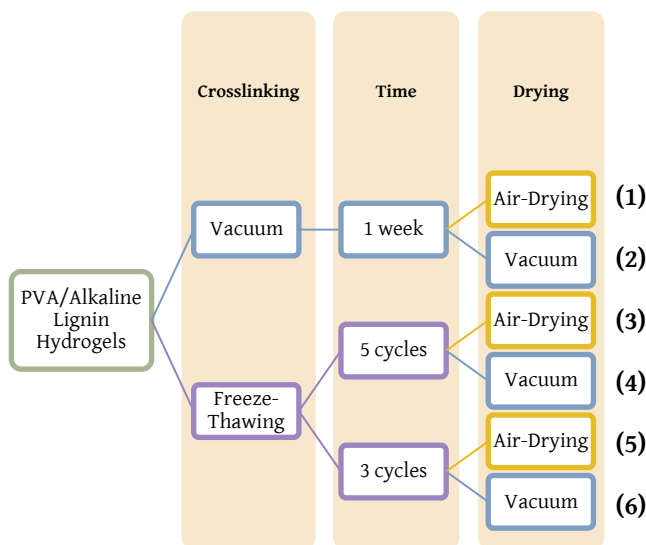


Figure 4.8. Scheme of the six hydrogel synthesis pathways.

4.2.1 Modelling and optimization of hydrogel composition

After measuring the swelling capacities and lignin wastes of the synthesized hydrogels, the six optimal concentrations for the maximum swelling and the minimum lignin waste were calculated by Statgraphics Centurion XV software, which are shown in Table 4.4 together with the predicted values of the response variables. The optimal conditions of the six pathways were verified by the triplicate synthesis of the hydrogels. Table 4.5 shows the regression coefficients obtained for each model according to a second-degree polynomial equation, their statistical significance (based on a Student’s t-test), the parameters measuring the correlation (R^2) and statistical significance (Fisher’s F test) of the models.

As shown in Table 4.5, the R^2 determined for most of the variables was higher than 0.86, which indicated that the model was adequate to represent the real relationships among the selected variables [101], but in some other cases this value was lower than 0.82. Moreover, the estimated significance levels confirm the regular fit of the data. The values for each equation term were calculated in order to assess the contribution of their linear interaction, and quadratic effects of the independent variables. Employing the calculated significant regression coefficients at the 90% confidential level, two quadratic regression equations were set up, one for each output variable (y_1 -Swelling and y_2 -Lignin waste), for the six models. Hence, twelve equations were obtained in total, which are described in **Publication II**.

4.2.2 Influence of the input variables on the swelling capacity

The swelling capacities ranged between 314 and 1647%, which corresponded to experiments 4 of the routes (1) and (2), respectively. According to the regression coefficients (Table 4.5), it was seen that the two input variables had an influence on the swelling capacity. Specifically, x_2 had a significant influence on this output variable, as well as the quadratic effect of x_1 (x_1^2). The interaction between both input variables was also important in the case of the routes (5) and (6). The quadratic effect of x_2 (x_2^2) presented a high influence on route (4). Ciolacu *et al.* (2018) and Yang *et al.* (2018) did also report that the swelling capacity depends on the composition of the hydrogels [60,102].

The surface plots for synthesis routes (1), (2) and (3) (see Figure 4.9-a,b and c) showed that for a fixed concentration of PVA, as the lignin content augmented, the swelling capacity of the hydrogel tended to increase. However, after a certain concentration of lignin (15%), the swelling capacity decreased, setting the maximum point in between the extreme concentrations of lignin. It is also worth to mention that the swelling ability was displayed to be higher for lower PVA concentrations, but the response variable was much more influenced by the lignin content than by the PVA one.

Table 4.4. Optimal conditions and predicted/experimental values for the response variables.

Synthesis Route	Alkaline Lignin (%, w/w)	PVA (%, w/w)	Predicted Value		Experimental Average Value		Error (%)	
			Swelling (%)	Lignin Waste (%)	Swelling (%)	Lignin Waste (%)	Swelling (%)	Lignin Waste (%)
(1)	23.02	5	710.29	69.17	345.30	81.16	51.39	-17.34
(2)	22.26	5	1083.59	70.88	199.26	82.75	81.61	-16.74
(3)	9.12	9.87	770.14	58.11	789.89	51.94	-2.57	10.63
(4)	5	10.39	587.82	49.09	567.06	41.06	3.53	16.35
(5)	25	11	719.77	46.71	659.67	45.77	8.35	2.02
(6)	25	11	729.51	46.71	547.93	44.12	24.90	5.55

Table 4.5. Regression coefficients and statistical parameters measuring the correlation and significance of the models.

	(1) Vac-Air		(2) Vac-Vac		(3) F-T x5-Air		(4) F-T x5-Vac		(5) F-T x3-Air		(6) F-T x3-Vac	
	y_1	y_2	y_1	y_2	y_1	y_2	y_1	y_2	y_1	y_2	y_1	y_2
β_0	778.78	80.99	1144.76	80.99	902.17	69.08	468.74	69.08	552.83	68.70	557.40	68.70
β_1	40.67 ^b	-0.93	46.89	-0.93	-56.45	-1.83	-47.17	-1.83	-37.92	-0.87	-66.98	-0.87
β_2	-64.45 ^a	-3.34	-146.12	-3.34	-98.37 ^b	-10.58 ^a	60.89 ^c	-10.58 ^a	-112.85 ^b	-7.15 ^c	-0.96	-7.15 ^c
β_{11}	-344.30 ^a	-10.18 ^a	-686.08 ^a	-10.18 ^a	-241.29 ^a	-14.26 ^a	95.02 ^c	-14.26 ^a	55.44	-18.08 ^b	105.88	-18.08 ^b
β_{22}	42.65	-2.91	100.40	-2.91	-49.67	0.03	-105.90 ^c	0.03	43.03	1.91	-52.12	1.91
β_{12}	-16.27	6.19 ^b	-26.17	6.19 ^b	4.41	1.49	5.72	1.49	219.24 ^a	2.20	186.30 ^b	2.20
R^2	0.98	0.92	0.86	0.92	0.93	0.90	0.76	0.90	0.89	0.82	0.77	0.82
F-exp	50.93	11.12	5.96	11.12	13.53	9.22	3.24	9.22	8.467	4.44	3.32	4.44
S.L.* (%)	99.97	99.03	96.39	99.03	99.37	98.54	88.87	98.54	98.24	93.61	89.29	93.61

^a Significant coefficients at the 99 % confidence level; ^b Significant coefficients at the 95 % confidence level; ^c Significant coefficients at the 90 % confidence level; * Significance Level

This behaviour could be explained by the high influence of the quadratic term of lignin on the swelling equations [101].

The surface plots for the synthesis routes (4), (5) and (6) showed that for a fixed concentration of PVA, as lignin content augmented, the swelling capacity of the hydrogel tended to decrease (see Figure 4.9-d, e and f). Nevertheless, after a certain concentration of lignin (15%), the swelling capacity started to increase again. Therefore, the surfaces presented a minimum in between the extreme contents of lignin and, the highest swelling capacities were found on the upper and lower concentration limits. In these three surfaces, however, no clear dominant variable was observed, since the quadratic terms did not have such a high significance level.

The optimal values for each synthesis route are shown in Table 4.4. It was clearly seen that the addition of lignin did, in all cases, have a positive effect on the swelling properties of the PVA hydrogels. This fact was confirmed by the synthesis and characterization of the blank hydrogels, i.e., neat PVA hydrogels with concentrations of 5, 8 and 11% PVA and the same crosslinking and drying pathways than the ones with lignin. In fact, the swelling ratio of these materials did not almost overpass the 350%. This behaviour may be attributed to the size of the attached lignin molecules, since they are high molecular weight chains and they can lead to the creation of bigger pores, which can permit an easier penetration and diffusion of water molecules [102,103]. Ciolacu *et al.* (2018) also reported the same behaviour for their PVA-lignin chemically crosslinked hydrogels [102]. Yang *et al.* (2018) also confirmed that lignin improved the swelling ability of chitosan- PVA hydrogels [60].

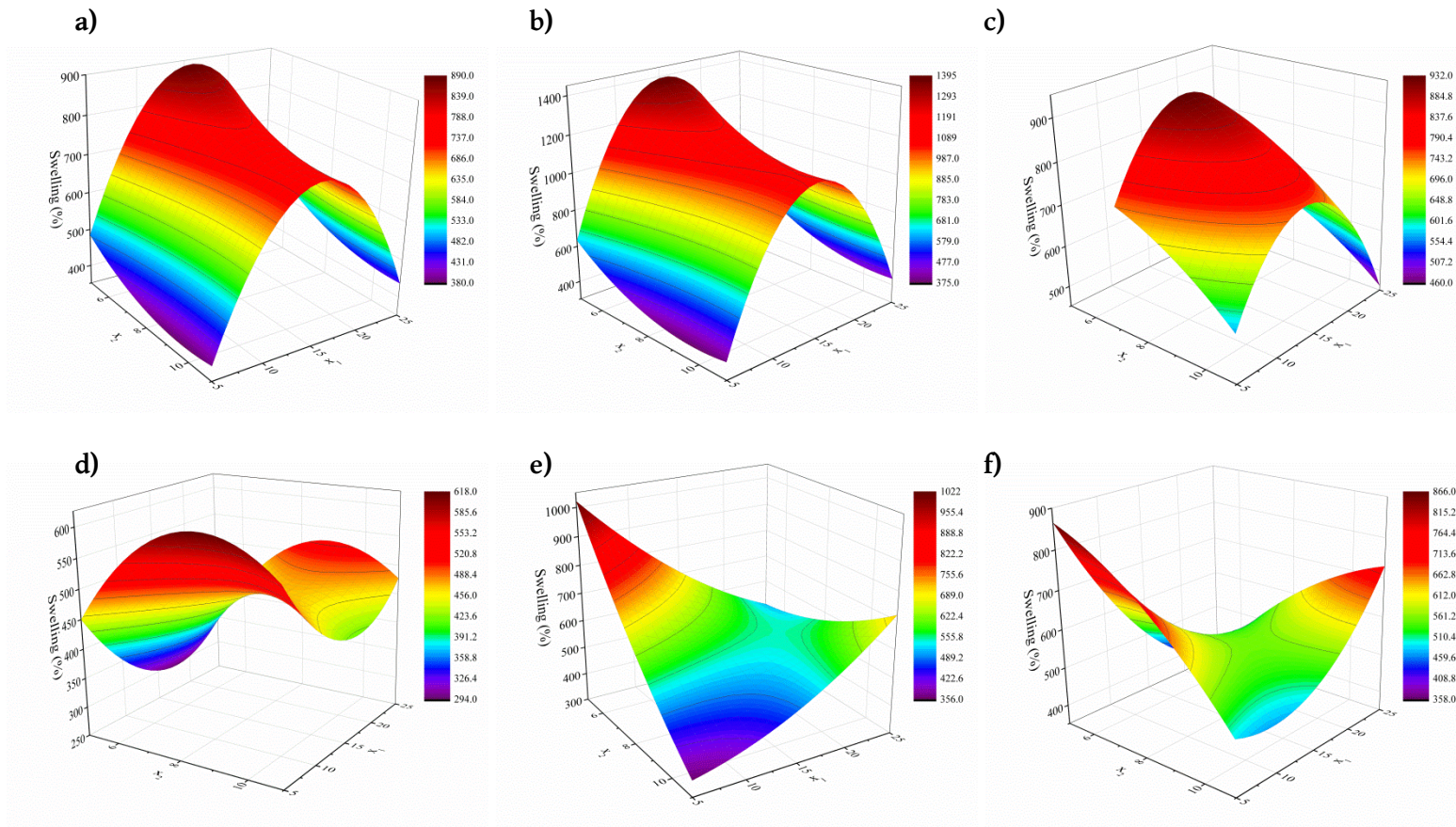


Figure 4.9. Response surface plots for the swelling capacity for 1-6 (a-f) synthesis routes.

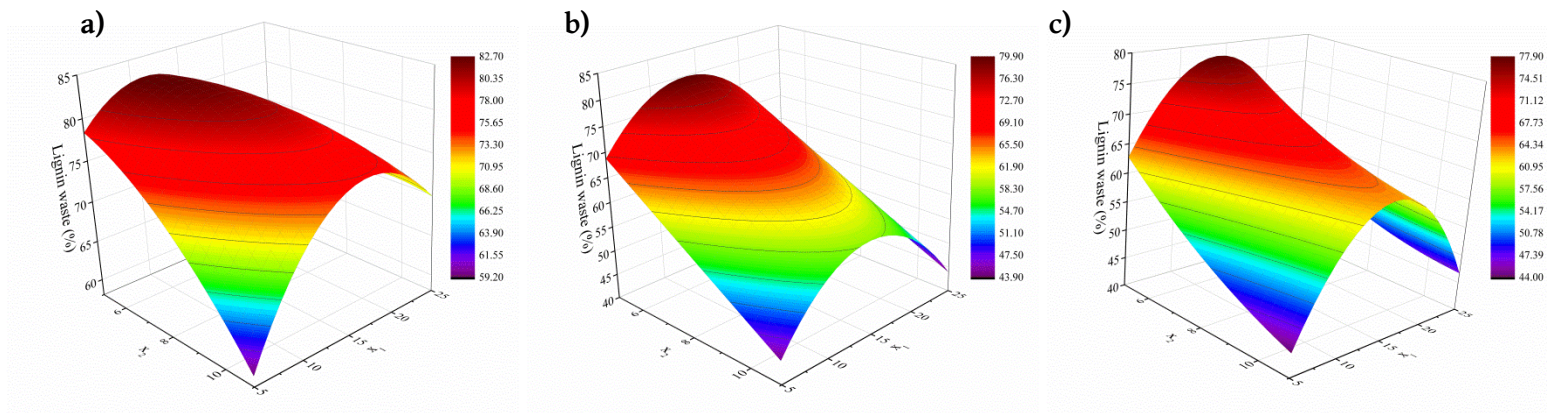


Figure 4.10. Response surface plots for the lignin waste for a) 1 and 2, b) 3 and 4 and c) 5 and 6 synthesis routes.

4.2.3 Influence of the input variables on the lignin waste

The lignin waste of the hydrogels synthesized from the six routes ranged between 44.5 and 85%, which corresponded to experiment 3 of the routes (5) and (6), and to experiment 5 of the routes (1) and (2), respectively. It was observed that the freeze–thawing method permitted the retention of more lignin inside the matrix than the vacuum crosslinking.

For routes (1) and (2) the most influencing regression coefficients on the lignin waste were the quadratic effect of x_1 (x_1^2) and the interaction between both input variables x_1x_2 . In the other four synthesis pathways, the most significant regression coefficients were the quadratic effect of x_1 (x_1^2) and x_2 itself. Therefore, it can be concluded that the PVA content directly affects the lignin waste. To the best of our knowledge, no data has been collected within the literature about the lignin waste during the washing stage into account when characterizing hydrogels. Hence, this statement cannot be contrasted with any other work.

The surface plots for all the synthesis routes (see Figure 4.10) showed that for a fixed concentration of PVA, as lignin content augmented, the lignin waste during the washing stage of the hydrogels tended to increase. This behaviour could be related to the addition of reactive sites and a higher crosslinking rate between both components. However, after a certain concentration of lignin, the lignin waste decreased. For the six routes, the optimal concentrations for the minimum lignin wastes are shown in Table 4.4.

4.2.4 Optimization of the synthesis conditions and validation of the model

The objective of the optimization was to determine the formulations that would provide simultaneously the greatest swelling capacity and the lowest lignin waste during the washing stage via the six synthesis routes. For this aim, the values of the response variables were converted using a desirability function. This function was considered to disclose the combination of the

synthesis variables that maximise the swelling capacity and minimise the lignin waste at the same time. The predicted and experimental results for the response variables after the synthesis of the hydrogels under the optimal conditions are displayed in Table 4.4.

The suitability of the RSM model for quantitative predictions could only be verified by the agreement of the predicted and experimental values in two of the six synthesis routes. The errors in the output swelling variable were higher than a 4% in all the cases except for routes (3) and (4). However, the lowest errors in lignin waste were observed for the routes (5) and (6). Nevertheless, as the accuracy on swelling was considered more important than lignin waste and, as one of the aims of the optimisation was to obtain the best synthesis route, routes (3) and (4) were selected as the optimal pathways.

4.2.5 Conclusions

In this section, the optimization of the synthesis conditions of lignin-based PVA hydrogels was successfully carried out employing a three-level-two-factorial design. The statistical analysis showed that the PVA and lignin concentrations had great impact on the lignin waste during the washing stage and on the swelling capacity of the synthesized hydrogels. The selected optimal synthesis routes based on 5 freeze-thawing cycles enabled the obtaining of physically crosslinked hydrogels with up to 800% water absorption ability and a lignin waste between 40–50%.

4.3 Influence of different formulation parameters on the properties of the hydrogels

In this section, the effect that several formulation parameters have on the final properties on the synthesized hydrogels was studied. For this aim, a combination of the results obtained in different publications has been performed. The analysed parameters and the publications involved in each discussion section are displayed in Table 4.6:

Table 4.6. Summary of the studied parameters and the publications involved in each discussion section.

Parameter	Publication			
	II	III	IV	V
Curing type	✓			
PVA M_w /number of F-T cycles		✓		
Lignin type		✓	✓	
Duration of the last thawing step	✓	✓	✓	
Lignin modification			✓	✓

4.3.1 Curing type

The samples obtained in **Publication II** via the two optimal routes namely, 3 and 4 samples (as indicated in Section 4.2), together with their equivalent neat PVA hydrogels (namely, 3.0 and 4.0) were further characterised in order to see the impact of the curing type on their properties. The swelling kinetics of these four samples is shown in Figure 4.11. It can be clearly seen that the lignin-hydrogels obtained through route (3) presented much higher swelling capacities than the ones shown by neat PVA hydrogels. Moreover, the lignin-hydrogels obtained through route (4) almost presented half of the swelling degree of sample 3.

SEM micrographs of the freeze-dried neat PVA and PVA-lignin hydrogels at two magnifications (250x and 2500x) are shown in Figure 4.12. For all the analysed samples highly porous structures and different pore size distributions could be observed. However, for the neat PVA hydrogels (Figure 4.12-a-d) the morphology was more homogeneous than that for the lignin-

PVA hydrogel (Figure 4.12-e and f). In addition, some large pores did also appear on the sample without lignin that was vacuum-dried (sample 4.0, Figures 4.12-c and d), indicating that apart from the crosslinking method [104] the curing method also affected the morphology.

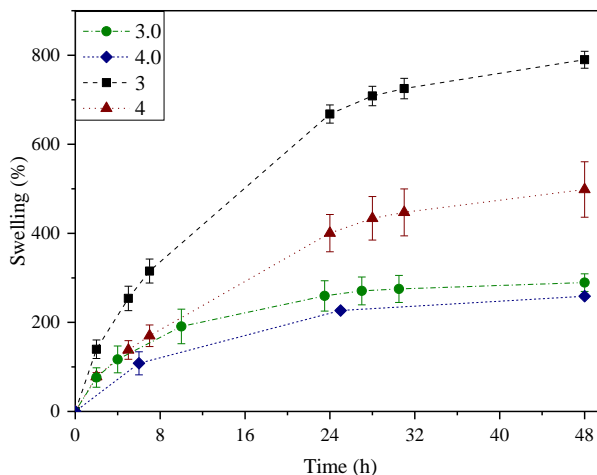


Figure 4.11. Swelling performance of the hydrogels during the first 48 h.

Although macro-pores often allow a facile penetration of water into the polymeric network causing a rapid initial swelling ability [103], this observation was not done here; in fact, lignin hydrogels presented a higher water swelling capacity in all cases. Moreover, the majority of the pores presented by neat PVA hydrogels were smaller than $1\ \mu\text{m}$, while the ones presented by lignin-based hydrogels were larger. This fact would confirm the previous statement about the size of the pores created due to the high molecular weight of lignin and its repercussion on the swelling capacity [102]. Furthermore, no lignin agglomerates were found in the SEM images, which confirmed the good miscibility between the components [105].

The onset and maximum degradation temperatures obtained from the TG and DTG curves of the samples, as well as the char residue at the end of the test are summarized in Table 4.7. For neat PVA hydrogels (3.0 and 4.0), four weight loss stages were observed around 150, 250, 375 and 440 °C attributed to the

evaporation of the adsorbed bound water, the initial degradation of the polymer, the depolymerisation of the acetylated and deacetylated units of the polymer and the thermal degradation of some by-products generated by PVA, subsequently [60], being the one at 375 °C the maximum degradation stage.

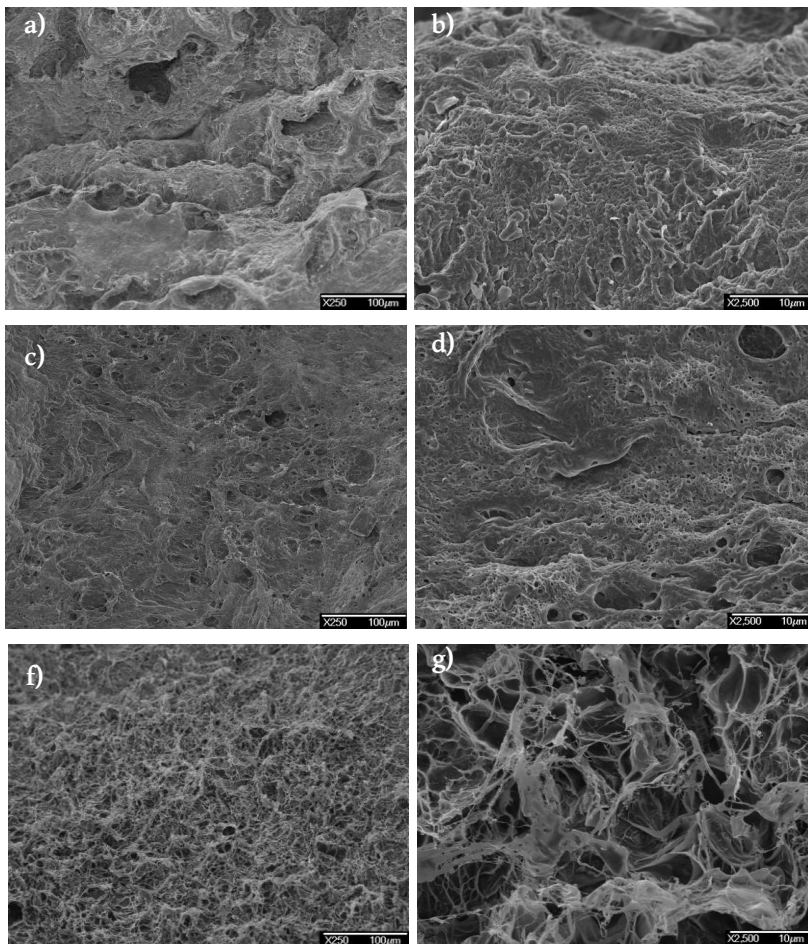


Figure 4.12. SEM micrographs of the samples 3.0, 4.0 and 4 at 250x (a, c and e) and 2500x (b, d and f) magnifications.

Commercial alkaline lignin presented a constant weight loss; however, the temperature of the maximum degradation was registered at 380 °C, and the final residue left was almost of 40%. When lignin was incorporated, the hydrogels presented three main weight loss stages (at 120, 280 and 430 °C), but there was a fourth stage which overlapped with the second one. The main

degradation stage appeared around 330 °C, but it overlapped with the one at 280 °C. This loss might have shifted to higher temperatures comparing to neat PVA because of the enhancement of the thermal stability due to the introduction of aromatic structures of lignin into PVA chains [106]. Although there was no evident change on the maximum degradation temperature for neat PVA hydrogels, for the lignin-based hydrogels there was a shift of around 15 °C on in when changing the curing method.

Table 4.7. Onset and maximum degradation temperatures and residue after TGA and compression moduli for the hydrogels.

Sample ID	T _{onset} (°C)	T _{max} (°C)	Residue (%)	Compression Modulus (MPa)
CAL	172.0	380.0	39.0	-
3.0	225.0	372.5	2.7	77.57 ± 8.40
4.0	230.5	374.0	2.6	41.64 ± 3.42
3	217.0	323.0	19.5	18.75 ± 0.53
4	223.0	334.5	14.7	29.21 ± 6.18

The results for the compression tests of the samples are shown in Table 4.7. At the maximum deformation, all the samples had an excellent ability of integrity and recovery. This could be due to the accommodation of the stress by the rearrangement of the polymeric chains and the retractable elastic forces developed consequently [107].

The estimated moduli for the blank hydrogels (3.0 and 4.0) were of around 77.6 and 41.7 MPa, respectively. When lignin was added to the samples, the moduli decreased to around 18.8 and 29.2 MPa for samples 3 and 4, subsequently. Therefore, as lignin was incorporated, the moduli of the hydrogels were reduced, which could be related to the pore-size of the samples and would confirm what was concluded for the swelling capacity; in other words, when lignin was blended with PVA, greater pores were generated due to the reduction of interactions within PVA which, at the same time, enhanced the adsorption of water and made the hydrogel less compact and rigid [60]. Moreover, as abovementioned, the curing method altered the morphology of

the samples and led to a change in their compression moduli. Nonetheless, the obtained moduli for the PVA-lignin samples would be high enough to support the weight of soil layers if the final application was agricultural, for instance.

As shown in **Publication II**, the rest of the employed characterisation techniques (ATR-FTIR, XRD and DSC) did not provide additional relevant information regarding the different curing methods.

4.3.2 Molecular weight of PVA and number of freeze-thawing cycles

In order to study the effect of the molecular weight of PVA on the final properties of the synthesized hydrogels, commercial alkaline lignin and 3 different poly (vinyl alcohol) (PVA, $M_w = 13,000\text{--}23,000$ g/mol, 87–89% hydrolyzed; $M_w = 83,000\text{--}124,000$ g/mol, 99+% hydrolyzed and $M_w = 130,000$ g/mol, 99+% hydrolyzed) were blended in **Publication III**. The hydrogels were synthesized according to the optimal pathway (3) and route (5) studied in **Publication II**.

The selected composition of the reagents enabled a successful crosslinking between alkaline lignin and medium and high molecular weight PVA (MM_w PVA and HM_w PVA, respectively) via 3 and 5 cycles of freeze-thawing. Conversely, the samples containing low molecular weight PVA (LM_w PVA) did not result in a proper crosslinking. This might have happened due to the scarce reactive sites in PVA for such amount of lignin [56] or to the hydrolysis degree of the PVA. The latter is related to the number of acetate groups in the PVA molecule, since PVA is synthesized from the hydrolysis of pre-polymerized polyvinyl acetate [60,108]. Thus, a high hydrolysis degree means there will be a lower number of acetate groups in the PVA, and these groups can interfere on its chemical properties, solubility and the capacity of crystallization [108]. Moreover, the presence of acetate groups weakens both intra- and intermolecular hydrogen bonding interactions between nearby

hydroxyl groups. In solution, as the degree of hydrolysis increases, the PVA interchain separation distance decreases [108]. Therefore, the unsuccessful crosslinking could be attributed to the lower degree of hydrolysis that LM_w PVA had (87–89%) in comparison to MM_w and HM_w PVA (99+%). For this reason, LM_w PVA samples were discarded for further studies. A possible scheme of the interactions through the hydrogel matrix is proposed in Figure 4.13.

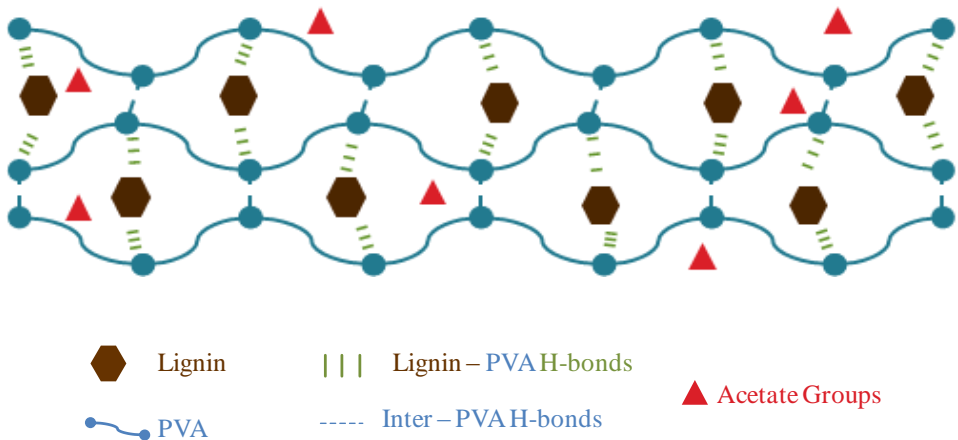


Figure 4.13. Possible crosslinking scheme between PVA and lignin.

For the samples with HM_w PVA the lignin waste during the washing stage (69.5 and 49.5% for samples 3HL and 5HL, subsequently) was lower than the one for MM_w PVA samples (77.8 and 57% for the samples 3ML and 5ML, subsequently). The former could be related to the number of reactive sites in the PVA, i.e. longer polymer chains had more entanglements with lignin. According to Hennink *et al.* (2012), the molecular weight of PVA affects the properties of the gel formed [109]. In addition, the number of cycles also affected the lignin waste, since the hydrogels formed via 3 freeze-thawing cycles had a higher lignin waste than the ones formed via 5 cycles. This fact could mean that as the number of cycles was increased, more entanglements were formed between the elements in the blend [46,109].

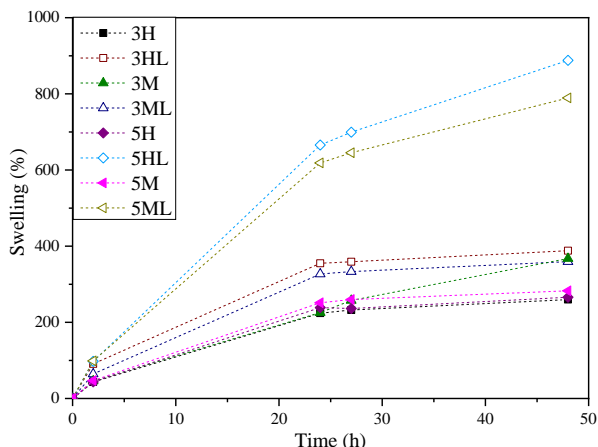


Figure 4.14. Swelling performance of the hydrogels during the first 48 h in water.

As displayed in Figure 4.14, the swelling capacity was significantly higher for the hydrogels synthesized via 5 freeze-thawing cycles (890 and 790% for HM_w and MM_w PVA, subsequently) than for the ones made via 3 cycles (380 and 360% for HM_w and MM_w PVA, respectively). Moreover, for the hydrogels with HM_w PVA, the swelling capacity was also the highest ($\approx 900\%$). This would again enhance the previous statement about the influence of parameters such as the molecular weight of the employed PVA and the number of cycles [109]. Hence, as the number of cycles and the molecular weight of PVA are increased, the increment on the entanglements with lignin may permit the creation of more pores and, thus, higher water absorption ability. Wu *et al.* (2019) also considered that an optimal amount of lignin would maintain the PVA network more relaxed [56], which would lead to higher water absorption. It is also worth to mention that neat PVA hydrogels presented a very low swelling ability (200–300%), so this would confirm the fact that lignin enhances the pore size and, therefore, the water retention inside the network [56,102,103].

The SEM images of the samples at 2500x magnification are presented in Figure 4.15. The microstructures of the hydrogels exhibited three dimensionally interconnected porous networks. The freeze-thawing process is responsible for these porous structures as the ice crystals formed inside the hydrogels

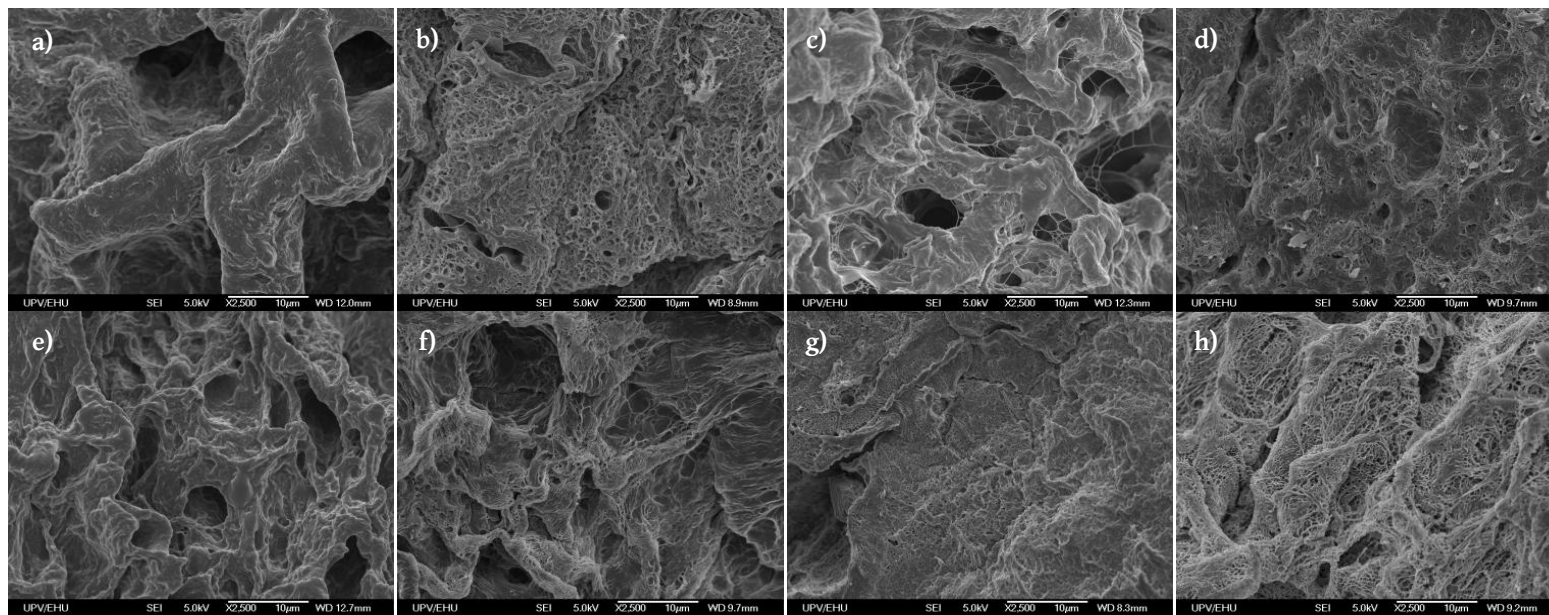


Figure 4.15. SEM micrographs of the samples 3H, 3HL, 3M, 3ML, 5H, 5HL, 5M and 5ML (a-h) at 2500x magnification.

during the freezing stage melt during the thawing, leaving the porous structure in the samples and high crosslinking degrees [110]. The neat PVA samples presented a more homogeneously distributed porous structure, with bigger pores as the molecular weight of the polymer was higher and the number of cycles lower. When lignin was added, the pore size distribution was more heterogeneous, leading to the creation of many macropores, since it is believed to act as a nucleation agent [60] or spacers [111]. The behavior of the incorporated lignin as a spacer could explain the formation of thinner walls between the micro voids, which were significantly helpful to the water-retention ability of the hydrogels due to the higher contact surface with it and, thus, its diffusion [103,111].

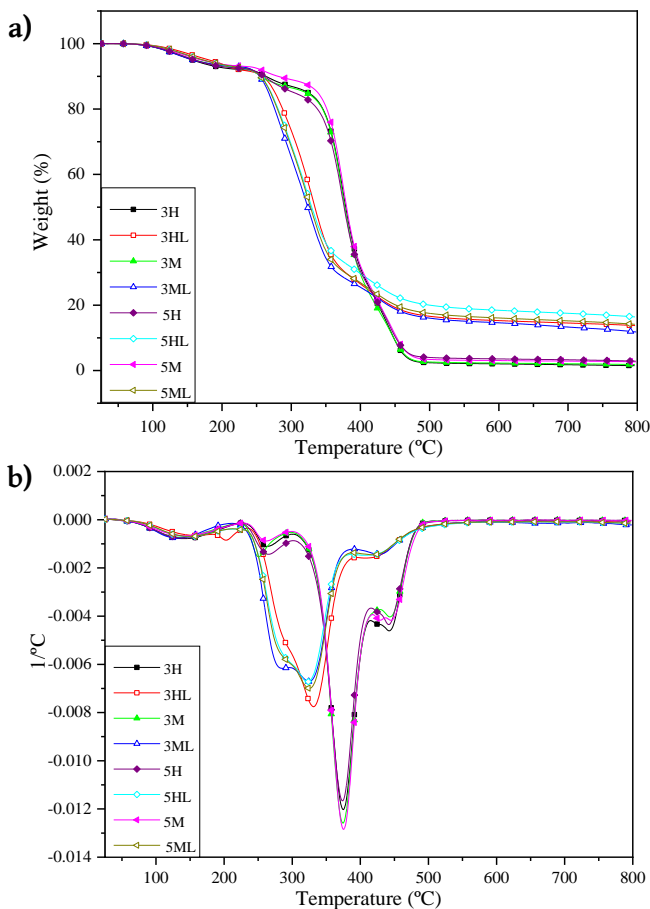


Figure 4.16. a) TG and b) DTG curves of the hydrogels.

Alike in **Publication II**, TG and DTG results showed similar degradation profiles for neat PVA samples (see Figure 4.16). As before, four main weight loss stages were observed at 150, 250, 375 and 440 °C, leading to a final residue below 3% in all the samples. When lignin was added, four main degradation steps were also observed. The first one, which was detected around 150 °C, was attributed to moisture evaporation and, as in the case of neat PVA hydrogels, no difference was noticed as the molecular weight of the polymer matrix varied. The second one was detected at around 280 °C for the samples with MM_w PVA and close to 290 °C for the samples with HM_w PVA, which in comparison with neat PVA hydrogels, was higher probably due to the thermal stability of lignin [112]. The third and main degradation step was found at 330 °C and the fourth one at 425 °C, in which no clear variation was detected as the molecular weight of the PVA changed. However, there was a significant increase on the residue with the addition of lignin, being the sample with the highest molecular weight and greater number of cycles (5HL) the one leaving the highest residual content (17%), and the one with the lowest molecular weight and fewer cycles (3ML) the one leaving the least residue (12.5%). Thus, the addition of lignin as well as the increase on the number of cycles and on the molecular weight of the employed matrix polymer led to a higher final residue.

Table 4.8. Results for the compression tests of the samples.

Sample	Compression Modulus (MPa)
3M	18.13 ± 4.23
3ML	8.77 ± 2.27
3H	28.13 ± 4.4
5M	19.85 ± 2.53
5ML	9.64 ± 4.56
5H	22.06 ± 3.29
5HL	10.32 ± 3.05

The compression tests of the samples showed that all the samples presented good ability of recovery, since none of them was broken and kept a total integrity. The calculated data is displayed in Table 4.8. For the samples without lignin, the compression moduli ranged from 18 to 28 MPa, from which the

lowest values corresponded to the samples with MM_w PVA (18.13 and 19.85 MPa for 3 and 5 cycles, successively) and the highest values to the ones with HM_w PVA (28.13 and 22.06 MPa for 3 and 5 cycles, respectively). A fall was observed in the moduli for HM_w PVA hydrogels from 3 to 5 cycles, but in the case of MM_w PVA, the opposite behaviour was seen.

As in Section 4.3.1, when lignin was added, a clear decrease of the moduli was observed in all cases (> 50%), which was directly related to its great swelling capacity. In addition, a slight increase on the moduli was observed when the number of cycles was augmented, which would be in agreement with the reported trend for neat MM_w PVA hydrogels. Other authors have also reported similar behaviours for their samples [56,113].

4.3.3 Lignin type

In this section, hydrogels obtained in **Publications III and IV** have been involved. Hydrogels in **Publication IV** were synthesized from self-extracted lignins, which were isolated from AS and WNS as described in Section 3.3.1. Then, lignin-hydrogels were synthesized according to **Publication III**, keeping the concentrations of the blends and the duration of the freeze-thawing cycles the same.

Table 4.9. Lignin waste of the synthesized hydrogels from nut shell lignins.

Sample	Lignin Waste (%)
AA	66.5 ± 2.9
AO	56.2 ± 2.4
WA	68.5 ± 0.7
WO	60.0 ± 1.8
AAA	59.6 ± 2.8
AAO	71.1 ± 3.0
AWA	44.2 ± 1.6
AWO	59.9 ± 4.0

The lignin waste results are shown in Table 4.9. For the samples made from alkaline lignin, the ones containing lignins from the single-step processes (AA

and WA) presented higher lignin wastes than the ones containing lignins coming from double-step processes (AAA and AWA). A similar trend was observed for organosolv lignins from WNS (WO and AWO), whereas the behaviour reported by the ones coming from AS (AO and AAO) was the opposite. Moreover, lower waste percentages were accounted for AS lignins than for WNS lignins in the case of the single-step lignins (56.2–66.5% vs. 60.0–68.5%), while for the double-step lignins the contrary was appreciated (44.2–59.9% vs. 59.6–71.1%). It should also be noted that among the single-step lignin containing samples the ones with alkaline lignin showed greater lignin wastes than the ones containing organosolv lignin, whereas the samples with double-step lignins exhibited the inverse trend.

The swelling capacity of the synthesized hydrogels is shown in Figure 4.17. The samples presented swelling values between 336 and 505%, which corresponded to AWO and WA samples, respectively. Moreover, the samples containing alkaline lignin showed in all cases higher swelling capacities, which is in accordance with the data reported previously [79].

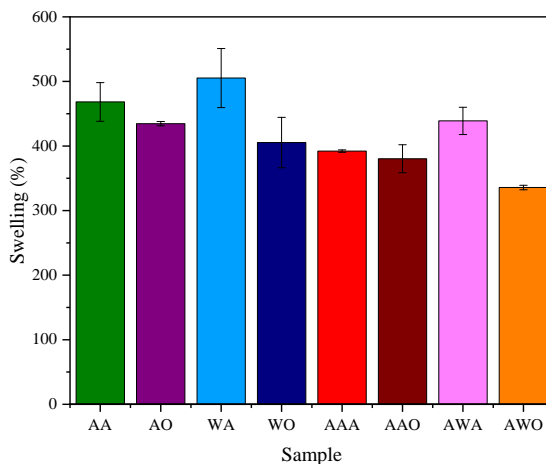


Figure 4.17. Swelling capacity of the synthesized hydrogels from nut shell lignins.

It should be mentioned that the samples containing lignins coming from single-step processes, presented higher swelling capacities than the ones coming from double-step processes, probably due to the interactions of their

impurities with the polymeric matrix. Although Wu *et al.* (2019) related the swelling properties to the content of phenolic hydroxyl groups and to the molecular weight of the employed lignins, their hypothesis would not explain the behaviour of the hydrogels in this case [56]. In fact, the samples containing lignins with the lowest total phenolic contents and lowest average molecular weights (AA and WA) presented the highest swelling capacities. However, this might support the previous statement about the non-representative average molecular weights determined for these lignins and also the one about the interactions with non-lignin components, since these samples presented high lignin wastes.

The morphology of the synthesized hydrogels studied by Scanning Electron Microscopy (SEM) is shown in Figure 4.18. At first sight, it was seen that although all the samples presented porous structures at different levels, their distribution, size and density was distinct. In fact, all the samples that corresponded to hydrogels containing lignins from single-step processes were quite similar and presented a highly porous honeycomb structure, as expected for lignin-PVA hydrogels [79,114–116]. Their pore sizes and distributions were quite homogeneous, but the walls between the micro voids were smoother and more brittle in the case of AA and WA samples than in AO and WO samples, which presented thicker walls. These structures were responsible for their high water absorption capacities [78].

When lignins from the double-step processes were employed, the synthesized hydrogels displayed much denser and continuous structures with hardly recognisable pores, which may be related to a higher crosslinking density with these lignins due to their higher contents in phenolic hydroxyl groups [56]. Raschip *et al.* (2013) also reported variable hydrogel morphologies according to the -OH and -COOH groups in lignin [117]. These microstructures would explain the drop on the swelling ability of the present samples compared to the aforementioned ones.

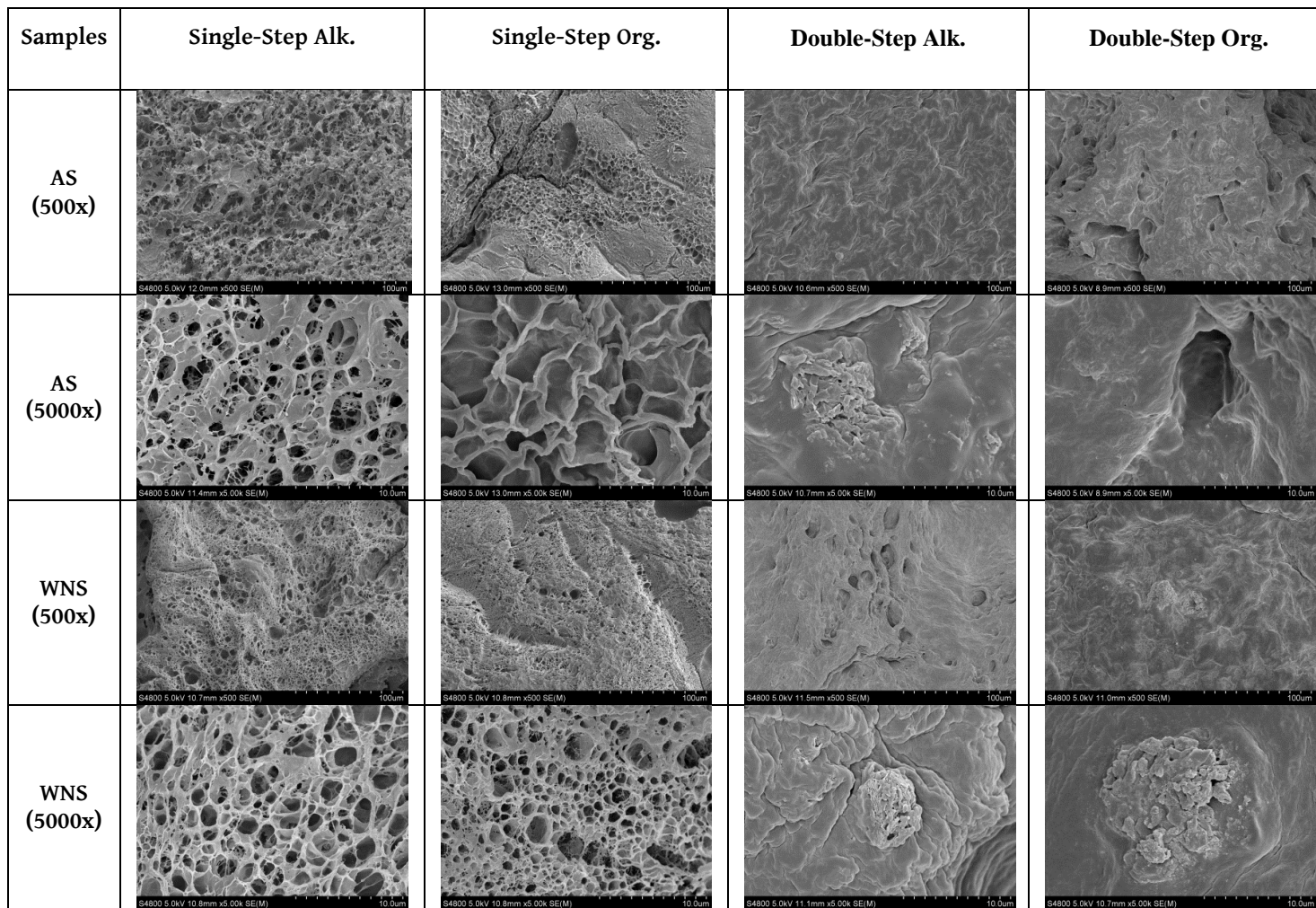


Figure 4.18. SEM micrographs of the hydrogels at 500x and 5000x magnifications.

From the compression stress-strain diagrams, the compression moduli were calculated, as displayed in Table 4.10. At the end of the tests none of the tested hydrogels was fractured and all of them showed excellent recoverability. Nevertheless, the samples containing alkaline lignin from the single-step processes were slightly damaged due to their heterogeneous appearance.

Table 4.10. Compression moduli of the synthesized hydrogels from nut shell lignins

Sample	Compression Modulus (MPa)
AA	16.3 ± 1.8
AO	5.0 ± 1.9
WA	14.9 ± 1.9
WO	6.0 ± 1.0
AAA	13.1 ± 0.8
AAO	2.1 ± 1.0
AWA	6.6 ± 2.9
AWO	5.4 ± 2.8

The aforementioned AA and WA samples were the ones presenting the highest compression moduli (14.8 and 16.3 MPa, respectively) although they were also the ones with the highest swelling ability, which might be related to the formed honeycomb structures due to the interactions of the matrix with lignin and its impurities, as shown in the SEM micrographs. In spite of their analogous morphology, the samples containing single-step organosolv lignins (AO and WO) presented much lower compression moduli (4.95 and 6.01 MPa, respectively). A similar behaviour was observed for the samples composed of double-step lignins: the ones with alkaline lignin presented higher compression moduli (6.63–13.07 MPa) than the organosolv ones (2.05–5.4 MPa). All the estimated moduli were in great accordance with previous results [79], and were higher than those reported by other authors for lignin-based hydrogels [113,118].

When comparing these results with the ones in **Publication III**, great differences were observed, especially on the swelling capacity of the

hydrogels. Nevertheless, as the synthesis procedure was carried out similarly, such differences did not seem to be in line with expectations. Thus, 5ML hydrogels in **Publication III** were repeated with commercial organosolv and alkaline lignins. The results were now more similar to the ones reported lately. In fact, alkaline hydrogels showed 450% of swelling ability whereas the organosolv ones presented a 360%, which was also reported in **Publication III** and ascribed to the type of lignin. These data led us to believe that something was overlooked in the synthesis of the previous hydrogels, and having a deep look at the followed procedure the answer was found on the duration of the last thawing cycle: some of the hydrogels were left at 28 °C for almost 24 h due to logistical issues. Thus, the hydrogels in **Publication IV** were repeated lengthening their last thawing step and the results are presented in the following section.

4.3.4 Duration of the freeze-thawing cycles

In **Publications III and IV** the duration of the freeze-thawing cycles was reduced comparing to the ones in the synthesis process reported in **Publication II**. The effect of this reduction was slightly appreciated in **Publication III** since these hydrogels presented hardly lower swelling values (970% vs. 890–790% samples in **Publications II and III**, respectively). However, although no significant differences were appreciated in SEM micrographs, the compression moduli were highly influenced, since they decreased up to 50%. When the swelling verification was performed, the impact of the reduction on the duration of the freezing and thawing cycles was much more evident.

As abovementioned, based on previous experiments, it was thought that the duration of the last thawing step could alter the features of the synthesized hydrogels. Therefore, in **Publication IV** hydrogels with a longer 5th thawing stage (24 h inside the heater at 28 °C) were prepared. These samples were tagged as LC samples (long cycle), and in general, they presented lower lignin waste values than the hydrogels with short 5th thawing step, suggesting that

the lengthening of the last cycle may have enhanced the interactions between the PVA and the lignin (see Table 4.11). Furthermore, the samples with single-step alkaline WNS lignin (WA) showed a significant reduction on their lignin waste. On the contrary, the samples with double-step alkaline WNS lignin (AWA) presented much greater lignin waste values than those reported before. It can also be said that, except for AWA sample, all the alkaline lignin containing hydrogels lost less lignin than the ones containing organosolv lignin.

Table 4.11. Lignin waste of the synthesized hydrogels with long 5th cycle (LC).

Sample	Lignin Waste (%)
AA	48.5 ± 3.0
AO	53.9 ± 3.4
WA	26.0 ± 6.4
WO	53.9 ± 2.1
AAA	36.3 ± 2.0
AAO	48.1 ± 3.3
AWA	74.3 ± 3.7
AWO	51.7 ± 2.2

Comparing these samples with the ones with a short last thawing stage, a huge enhancement of their swelling capacity was clearly seen (see Figure 4.19). The most significant improvement (80% more regarding its prior swelling ability) was seen on AWO sample, which was the one that had previously presented the lowest swelling capacity. On the contrary, the sample that exhibited the slightest enhancement was AWA, whose swelling ability was just improved about 22%. Agudelo *et al.* (2018) reported that the excessive lengthening of the thawing cycles leads to the dissolution of the formed crystallites, which reduces of their quantity and size and, hence, also the crosslinking density and the swelling capacity of the hydrogel [119]. Nevertheless, as in the present section the lengthened thawing step was the last one, the molten crystallites might have evaporated and this could have enhanced the water absorption ability of the samples.

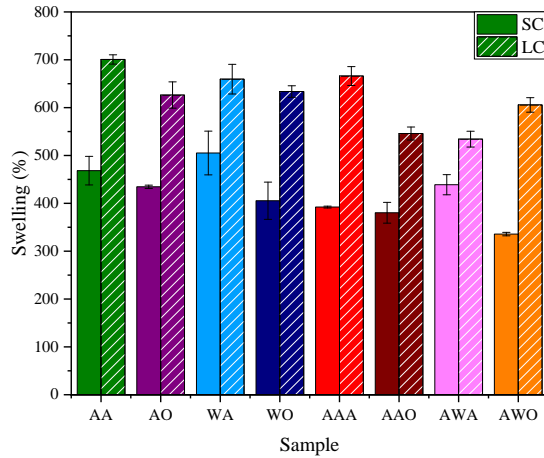


Figure 4.19. Swelling capacity of the synthesized hydrogels with short (SC) and long (LC) last thawing steps.

These results were validated by the SEM images displayed in Figure 4.20. It was appreciated that when the last thawing step was lengthened, there was an evident creation of macro pores in all cases. As aforementioned, this might be ascribed to the evaporation of molten crystallites during the last step of the synthesis, which permitted the formation of these structures and improved the swelling performance of all the hydrogels, regardless of the origin or extraction type of the involved lignin.

Table 4.12. Compression moduli of the synthesized hydrogels via short (SC) and long (LC) 5th thawing step.

Sample	Compression Modulus (MPa)	
	SC	LC
AA	16.3 ± 1.8	10.8 ± 3.2
AO	5.0 ± 1.9	2.1 ± 0.7
WA	14.9 ± 1.9	13.6 ± 0.8
WO	6.0 ± 1.0	2.0 ± 0.8
AAA	13.1 ± 0.8	7.5 ± 2.7
AAO	2.1 ± 1.0	2.0 ± 0.8
AWA	6.6 ± 2.9	6.4 ± 1.3
AWO	5.4 ± 2.8	2.88 ± 1.2

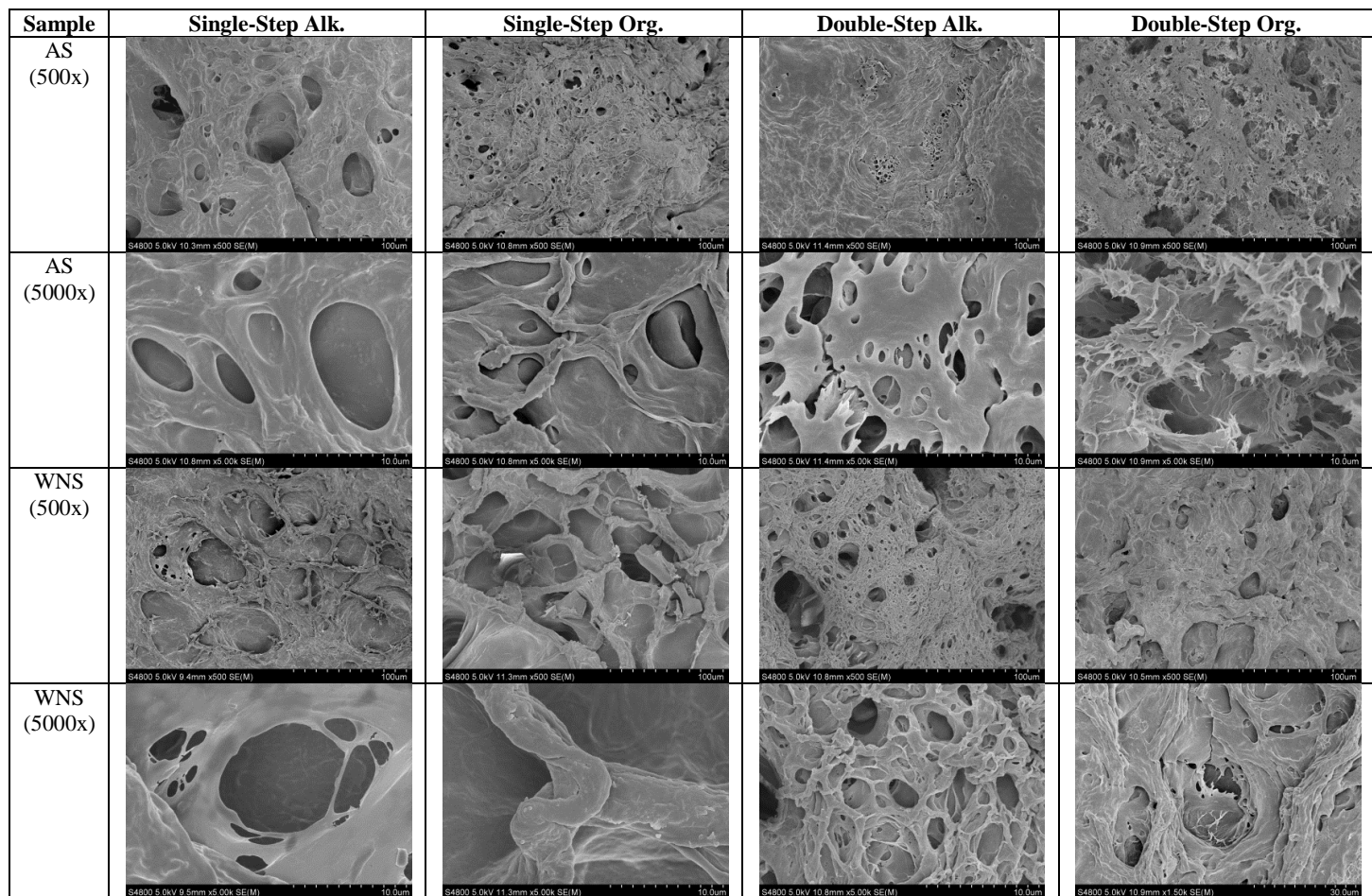


Figure 4.20. SEM micrographs of the hydrogels with long 5th thawing cycle at 500x and 5000x magnifications.

As shown in Table 4.12, the compression moduli of all the samples presented a slight drop when increasing the duration of the last thawing step, probably due to the creation of the macro pores, as aforementioned. This trend was also aligned to the one observed for T_g values in **Publication IV**, which suggested that a less compact structure was obtained. Nevertheless, all the estimated moduli were in great accordance with previous results [79].

4.3.5 Type of lignin modification

In **Publication V** hydrogels were synthesized from modified alkaline and organosolv commercial and self-extracted lignins. These lignins were characterised as detailed in Section 4.1. Then hydrogels following the synthesis route described in **Publication IV** with short 5th thawing stage were produced.

It was expected that modified lignin containing hydrogels would have lower lignin wastes than previous samples due to the higher reactivity of the modified lignins. Nevertheless, the results proved that the hypothesis was incorrect, since the lignin waste determined for all the samples resulted to be higher than those reported previously. All these results are shown in Table 4.13. This change was significantly greater for the samples containing MCAL and MCOL, which presented a loss of almost 89 and 97% of their initial amount of lignin, respectively. The samples containing MAWA did also show a huge increase. The rest of the samples exhibited lower lignin waste raises, ranging from 12–14%.

Table 4.13. Lignin waste (%) of native and modified lignin-containing hydrogels.

Sample	Native (%)	Modified (%)
AAA	59.6 ± 2.8	73.5 ± 0.5
AAO	71.1 ± 3.0	83.4 ± 4.6
AWA	44.2 ± 1.6	71.6 ± 0.5
AWO	59.9 ± 4.0	74.0 ± 4.8
CA	67.8 ± 2.0	88.7 ± 3.4
CO	77.4 ± 1.7	96.5 ± 0.3

As the observed lignin wastes were so unexpected, these lignins were precipitated so as to study their molecular weights. From these results it was observed that in all cases the lost lignins had a lower weight average molecular weight than the native ones, and they were also more homogeneous, which suggested that the polymeric matrix could have reacted with the highest molecular weight fractions.

In order to determine the effect that the lignin modifications had on the properties of the synthesized hydrogels, their swelling capacity was studied. The results are depicted in Figure 4.21.

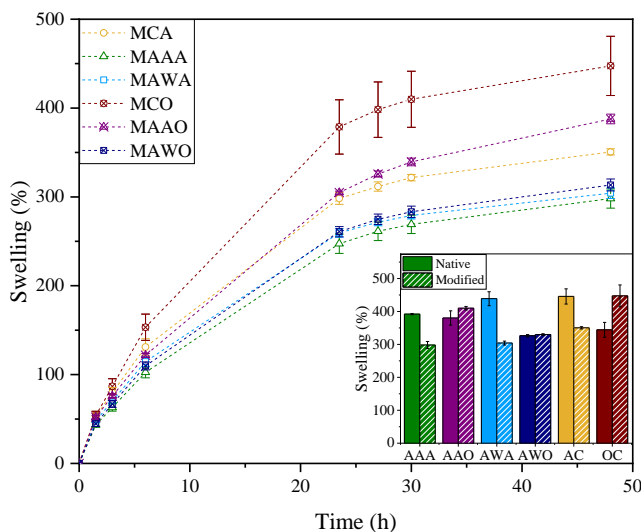


Figure 4.21. Swelling performance of modified lignin-based hydrogels during the first 48 h and their comparison with native lignin containing hydrogels.

Comparing to previous results, it was observed that in the case of the alkaline lignin-containing samples, the swelling capacity got significantly reduced when modified lignins were employed for their synthesis. These results suggest that the peroxidation of lignin performed in the present section was not an appropriate modification to obtain hydrogels with a high swelling capacity. On the other hand, when modified organosolv lignins were used, their swelling capacity was enhanced, especially in the case of the samples

with MCOL (450%), which had also presented the highest lignin waste. Moreover, MAAO samples were the second ones with improved swelling capacity (410%), which also coincided with the second highest lignin waste. Similarly, MAWO samples exhibited the lightest enhancement on their swelling degree and had displayed the lowest lignin waste among the samples containing modified organosolv lignins. Thus, it could be concluded that hydroxymethylation could be a good method to enhance the swelling ability of organosolv lignin-based hydrogels.

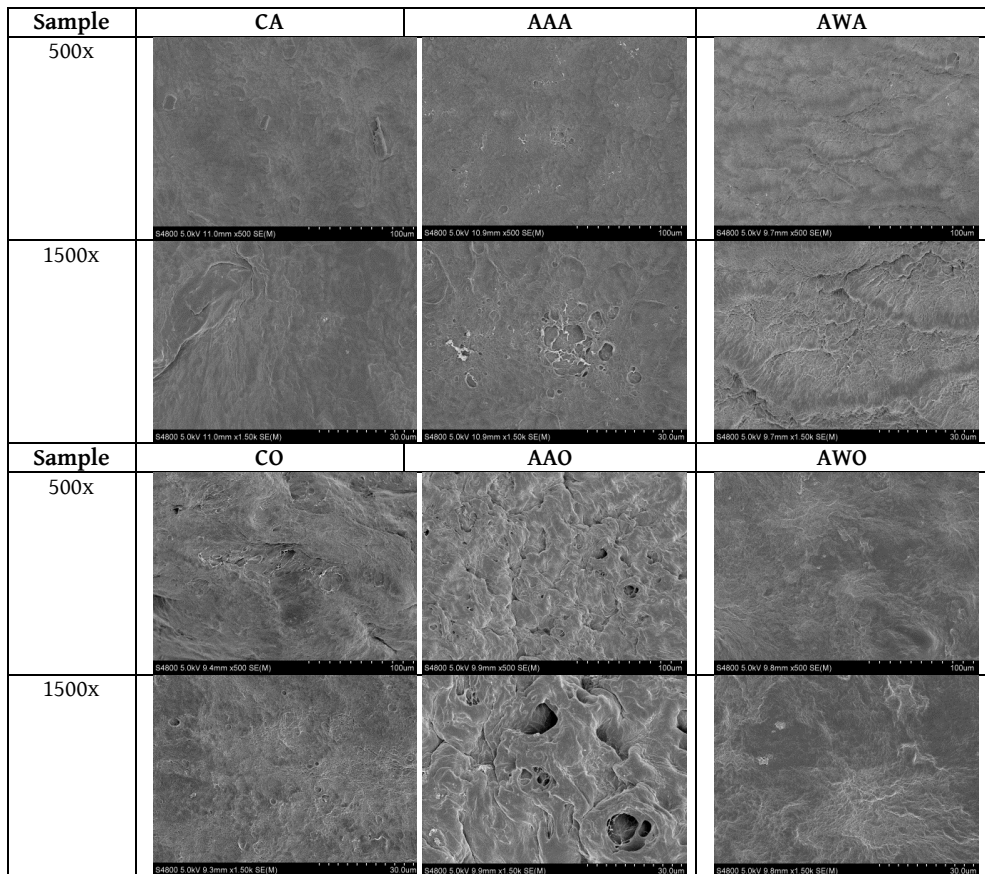


Figure 4.22. SEM micrographs for modified lignin-based hydrogels at 500x and 1500x magnifications.

Looking at the present results and comparing them with previous ones, it should be mentioned that although hydroxymethylation demonstrated to be effective for improving the swelling capacity of lignin-hydrogels, other variations during the synthesis process (lengthening the last thawing step, for instance) led to higher improvements on this property, without needing to modify the native lignins.

The images obtained by SEM technique (Figure 4.22) did not reveal highly porous structures; indeed they showed quite dense and continuous morphologies with scarcely detectable voids. This fact was more evident in the samples containing alkaline lignins, which may be attributed to a greater crosslinking density, which would also clarify the decline on their swelling ability. For the samples containing organosolv lignins, especially for MAAO samples, the created voids were more obvious, which were probably responsible for the augment on their water absorption capacity. However, as the swelling study was performed at the same conditions as before, the obtained microstructures might have just hindered the water diffusion through the matrix, and after leaving them longer times immersed, they may present higher swelling capacities.

As for their thermal properties, all the determined T_g values were in the range of 77–103 °C. These values were higher than those reported previously, suggesting that lignin modifications led to more compact structures in which the movement of the amorphous polymeric chains was hindered, which was also in agreement with the obtained SEM micrographs.

The compression tests of the samples showed once again that all the tested hydrogels were able to keep total integrity and good recoverability thanks to their elastic behaviour. From the results in Table 4.14 it was concluded that hydrogels containing alkaline lignins had greater compression moduli than those containing organosolv lignins, which is consistent with the results

obtained for thermal analysis. In fact, all the compression modulus values for the samples with alkaline lignin were in the range of 10-12 MPa, whereas the ones for hydrogels with organosolv lignin were between 4.5 and 6 MPa. Comparing to the previous publications, an enhancement of the compression modulus was observed for alkaline lignin containing samples, especially for MCA sample, and a decrease for organosolv containing samples, although MAAO also got slightly higher.

Table 4.14. Compression moduli of native and modified lignin-containing hydrogels.

Sample	Compression Modulus (MPa)	
	Native	Modified
CA	2.3 ± 0.8	12.0 ± 3.6
AAA	13.1 ± 0.8	11.4 ± 3.7
AWA	6.6 ± 2.9	10.1 ± 2.5
CO	8.1 ± 0.7	5.9 ± 3.9
AAO	2.1 ± 1.0	4.5 ± 1.8
AWO	5.4 ± 2.8	5.0 ± 0.8

4.3.6 Conclusions

In this section, the influence that several synthesis parameters had on the properties of the prepared lignin-hydrogels was studied. All the studied parameters resulted to have great impact on the morphology of the hydrogels, which especially led to the variation on their swelling capacities and mechanical properties. The air-drying curing method enabled the obtaining of hydrogels with higher swelling capacities, and the employment of HM_w PVA and the increase on the number of freeze-thawing cycles together with their duration led to similar results. When different lignins were used, among the same type of lignins, the observed differences were not so significant. However, from alkaline to organosolv lignins the properties of the hydrogels were greatly modified, and it was seen that the purity of the lignins had a strong impact on their final characteristics. It was also concluded that depending on the selected lignin modification reaction, the properties of the

hydrogels can greatly vary. In fact, the hydroxymethylation of organosolv lignins led to hydrogels with higher swelling capacities than the same hydrogels with native lignins, and on the contrary, peroxidated lignins reduced the swelling capacity of the synthesized lignin-hydrogels, at least for the tested time-period. Therefore, it can be concluded that there are multiple parameters affecting the final properties of these materials, and that although some of them are uncontrollable or dismissed, they should be further studied to take them into account.

4.4 Applications of the synthesized lignin-based hydrogels

4.4.1 Dye adsorption

Lignin-based hydrogels present large negative charges on their surface due to the numerous carboxylic acid groups and thanks to the π - π hydrophobic interactions, these hydrogels can trap positively charged dyes, i.e. cationic dyes [56]. Among them, methylene blue (MB) is one of the best known. This substance is commonly used for cotton, wood and silk dyeing and it has been proven to be very harmful for human and animals [67]. For this reason, the adsorption of MB was evaluated during 24 h for the hydrogels that were synthesized in **Publications III and IV**.

Although the values obtained for the yield were not as high as the ones reported by other authors [56,67], the removal values were even higher than the ones reported by them. Among the samples in **Publication III**, it was observed that the tested lignin-hydrogels (5HL and 3ML) presented high removal percentages (71.6% for 5HL and 69.1% for 3ML) whereas the blank hydrogel (5H) was able to remove only 34.8% of MB.

The samples in **Publication IV** also demonstrated great potential for MB adsorption, being the lowest removal value 75% and the highest 93% of the pollutant, as shown in Figure 4.23, which exceeded the results in **Publication III**. In general, the samples containing double-step lignins were able to trap larger quantities of dye, and the alkaline lignin-based hydrogels removed slightly lower values of MB than the organosolv-based ones, which is also in line with the trend reported for the TPC of the lignins. Other authors also reported lower MB adsorption values for their samples containing soda lignin than for the ones with organosolv lignin, which could be related with the values they reported for the phenolic hydroxyl groups in these lignins [67]. In contrast, when the last thawing cycle was lengthened, the MB adsorption capacity of the samples containing alkaline lignins was enhanced whereas the

MB removal of organosolv lignin-based hydrogels got slightly reduced. This fact suggested that although the last thawing cycle intensified the porosity of the samples, the availability of the negative charges on the surface was altered; nevertheless, this statement cannot be demonstrated.

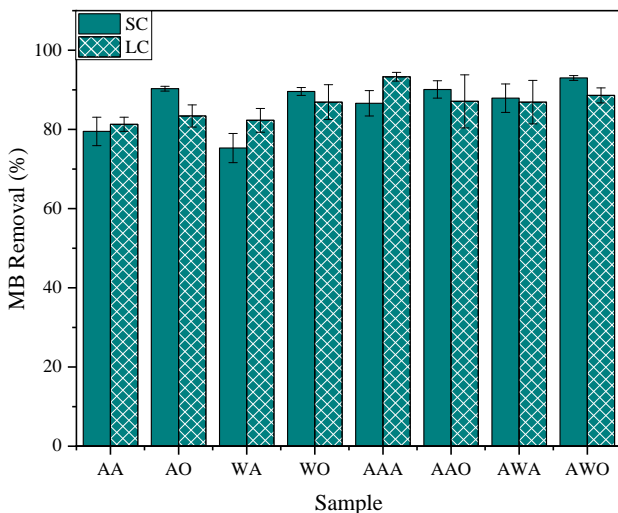


Figure 4.23. MB adsorption comparison between samples with short (SC) and long (LC) 5th thawing step.

4.4.2 Antifungal properties

The urgent need of searching for alternative eco-friendly materials has also swayed the food-packaging sector. In this context, bio-based hydrogels have emerged as potential absorbents for these systems [57]. However, these materials should extend the shelf-life of the packaged products, which involves hindering the growth of microorganisms and fungi on them [57,120]. Thus, the antifungal properties of the lignins and lignin-hydrogels in **Publication IV** against *Aspergillus niger* (brown-rot fungi), one of the most common fungi in food spoilage, were studied for all the synthesized hydrogels.

First of all, a visual evaluation of lignin’s antifungal capacity was performed. Although mainly white-rot fungi are able to depolymerise lignin [121], some authors have also seen that brown-rot fungi are also capable to be lignin

degraders. Nevertheless, in this case the tested fungi did not seem to have such ability (see Figure 4.24). In spite of the growth of fungi on the agar surface of all the samples, the deposited lignin drops could be clearly observed after the period of the test. This showed the antifungal ability of lignin, as also demonstrated by other authors before. Among the studied samples, the alkaline ones seemed to be able to inhibit more effectively the fungal growth than the organosolv ones, leading to a growth intensity of 3 ($GI = 3$), whereas most of the rest of the samples presented greater intensities ($GI \approx 4$), according to ISO 846 [81].

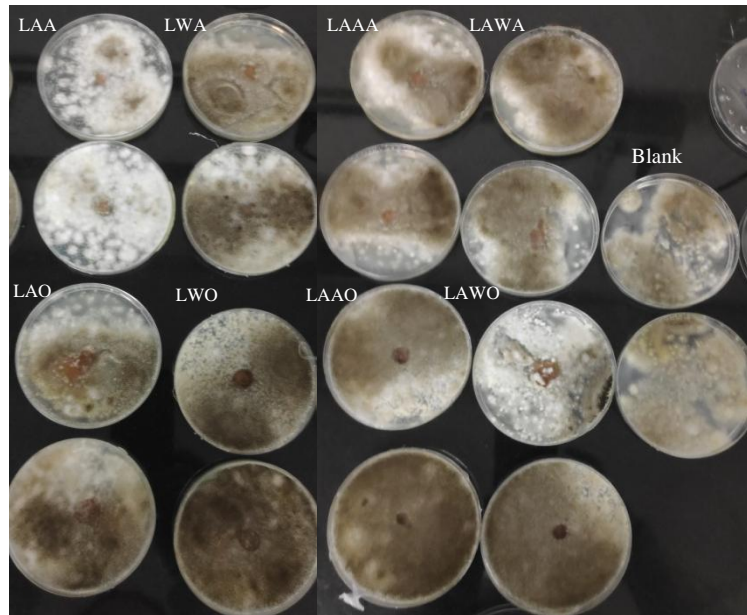


Figure 4.24. Images of the antifungal tests of lignins.

On the other hand, the same test was performed to the hydrogels (see Figure 4.25). In all cases, the whole hydrogel portion was visible after the test. At first sight, the samples with alkaline WNS lignins (WA and AWA) as well as the samples containing organosolv AS lignins (AO and AWO) seemed to hinder the fungal development more than the samples containing other lignins. Moreover, there was almost no appreciable fungal growth on the top surface of

the samples. In this case, the growth intensity would be between 3 and 4 for every sample [81].

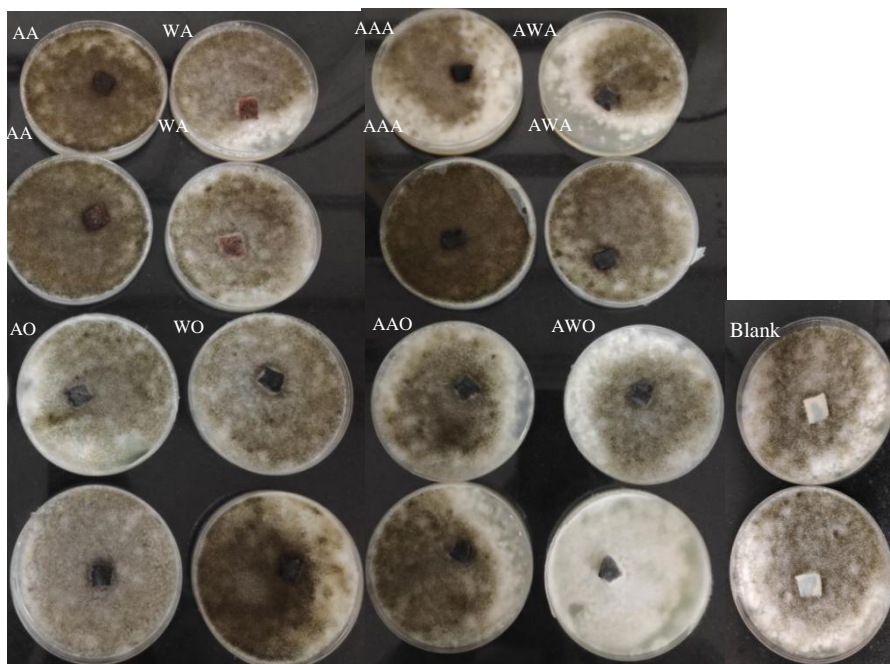


Figure 4.25. Images of the antifungal tests of hydrogels.

The samples were washed with PBS and the surrounding spores were quantified as aforementioned in Section 3.6.2. From the estimated FGI values (Figure 4.26), it was seen that among the studied samples, the ones presenting the lowest fungal activity were WO and AAO (with highest FGI), and the one presenting the highest growth was surprisingly AWA. Moreover, it was observed that the samples containing single-step AS lignins presented lower FGI values than the ones with double-step AS lignins. Conversely, the samples containing double-step WNS lignins presented worse antifungal activity than the ones with single-step WNS lignins. Although the estimated values were approximate, these results helped making an idea of the antifungal properties that the synthesized samples presented. It is also worth to mention that none

of the studied samples lost weight during the antifungal test, which supports their effectiveness against *A. niger*.

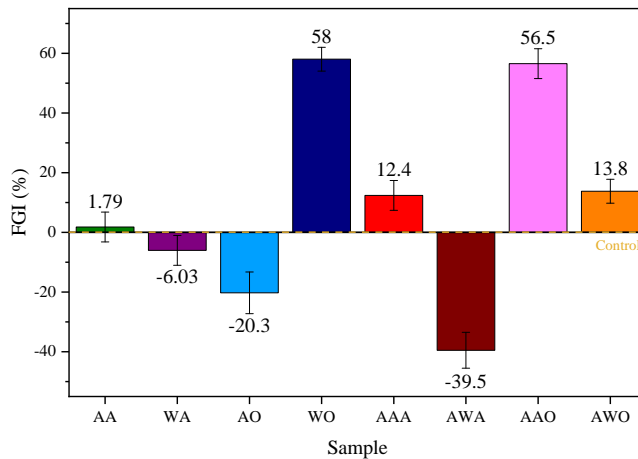


Figure 4.26. Fungal growth inhibition (FGI, %) of the samples with respect to the control hydrogels ($y = 0$).

Several authors reported similar FGI values for other materials for food packaging applications. For instance, Salaberria *et al.* (2017) reported 52–62% of inhibition for PLA films containing functionalized chitin nanocrystals [80]. In the study of Fernández-Marín *et al.* (2021), these values were between 72 and 86% for their chitosan/ β -chitin nanofibers nanocomposites due to the incorporation of deterpenated *Origanum majorana* L. essential oil [122]. Conversely, Dey *et al.* (2021) reported values between 51 and 56% for neat PVA films, which were negatively affected by the addition of cellulose nanocrystals and chitosan nanoparticles [123]. Thus, taking these data into account, it can be concluded that the results reported for WO and AAO hydrogels were in total agreement with the ones reported by other authors and could be employed in food packaging.

4.4.3 Drug delivery

Quercetin (QE) is a bioflavonoid present in fruits and vegetables with interesting anti-inflammatory, antioxidant, anti-carcinogenic and anti-obesity

properties [82,83,124]. Due to the aforementioned characteristics and the current trend of preferring natural compounds rather than synthesized drugs, quercetin has recently gained great attention. Thus, in **Publication V**, this compound was extracted through a green process (microwave assisted extraction) from red onion peels, which are an abundant waste all over the world, giving them an added-value. The hydrogels synthesized in the same publication were then loaded with QE and their release kinetics was studied.

After the hydrogels were loaded and dried as indicated in **Publication V**, they were immersed in PBS at 37 °C for drug release, simulating *in vitro* conditions. The absorbance of the release medium was performed at several times during the first 6.5 h. As the hydrogels contained lignin, and this lignin presented an absorbance peak at 330 nm, at high concentrations this peak sagged the results of the peak corresponding to QE at 375 nm. Thus, the release kinetics was performed during the first 6.5 h, while the released lignin was negligible.

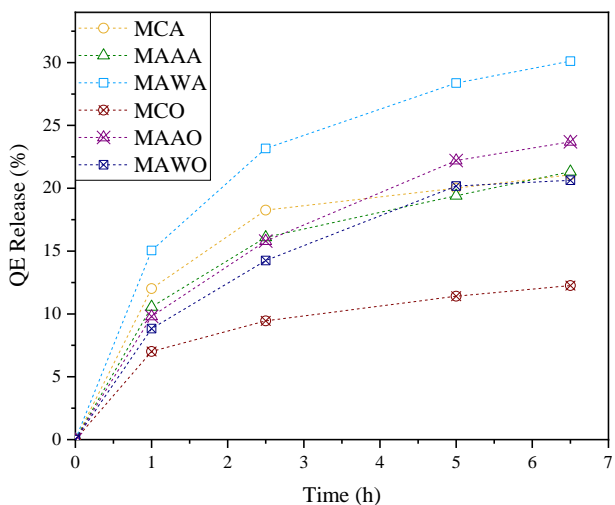


Figure 4.27. QE release profiles of modified lignin-based hydrogels.

From the release profiles shown in Figure 4.27 it was concluded that although all the samples were able to be loaded with similar drug amounts, the release capacity was completely different for each sample. In fact, with respect to the

loaded amounts of drug, the released drug percentages ranged from 12 to 30%. The samples displaying the highest release drug percentage were MAWA, followed by MAAO and MAAA. The lowest release was observed for MCO samples, suggesting that despite having higher drug loading abilities, the interactions with the drug made its release difficult. Nevertheless, it should be noted that these profiles were just for the first 6.5 h, and cannot be extrapolated to longer times.

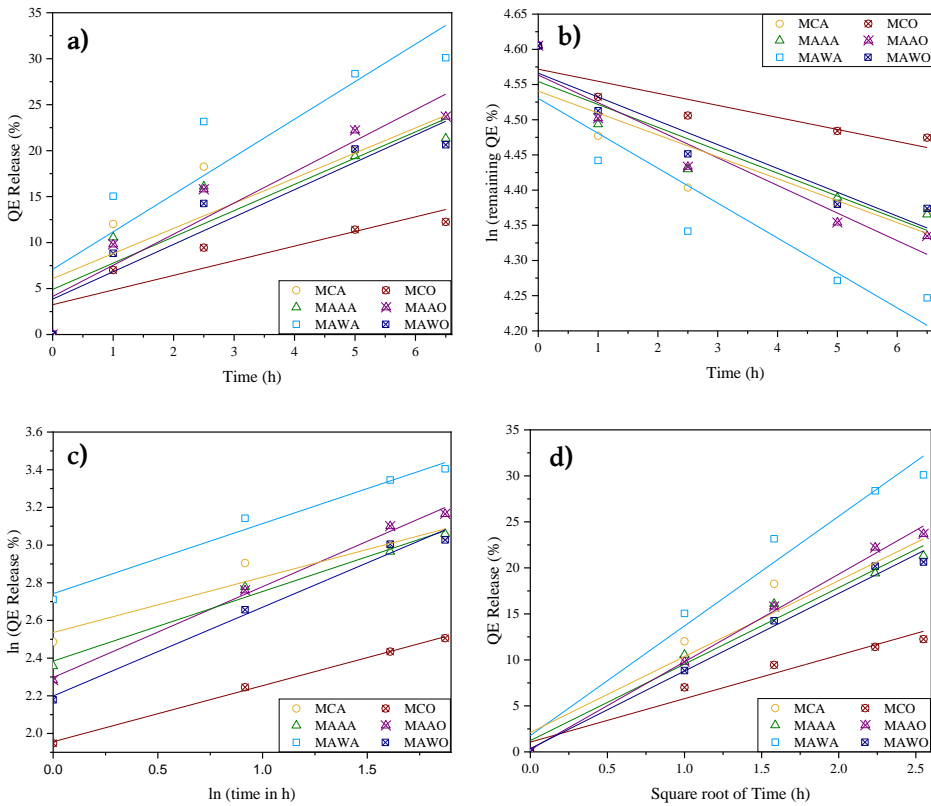


Figure 4.28. QE release kinetic models of a) zero order, b) first order, c) Korsmeyer-Peppas and d) Higuchi models.

So as to determine the release kinetics, several models were applied (i.e. zero order, first order, Korsmeyer-Peppas and Higuchi) [82,85,86]. The graphical representations of the four kinetic models are displayed in Figure 4.28 and the estimated kinetic parameters for each of them in Table 4.15. From the original

release profiles, it was inferred that the release kinetics would not fit correctly to a zero order model, which was confirmed by the determination coefficients (R^2). Among the rest of the models, Korsmeyer–Peppas model was the one fitting the best, except for MCA sample, whose fitting did not improve either with Higuchi model.

Table 4.15. Kinetic parameters estimated from models for QE release from hydrogels.

Sample	Loading (%)	Zero order	First order	Korsmeyer–Peppas		Higuchi	
		R^2	R^2	R^2	n	k_{kp}	R^2
MAAA	29.0	0.8194	0.8438	0.9852	0.37	10.85	0.9764
MAAO	31.8	0.8946	0.9165	0.9947	0.48	9.94	0.9962
MAWA	30.4	0.8134	0.849	0.9809	0.37	15.52	0.9741
MAWO	32.0	0.8781	0.8968	0.9868	0.47	9.01	0.9904
MCA	26.0	0.7248	0.7473	0.9284	0.29	12.63	0.9294
MCO	34.5	0.7725	0.7872	0.9978	0.30	7.07	0.9562

As indicated by Saidi *et al.* (2020) [86], the release exponents (n) and the rate constants (k_{kp}) were determined from the slopes and intercepts of the plots ($\ln(QE \%)$ versus $\ln t$) of the experimental data. As shown in Table 4.15, all the estimated values for n were below 0.5. Although Fickian diffusion is usually considered when $n=0.5$ [82,85], in this case it could also be said that the QE release followed a Fickian diffusion [82]. Thus, it could be said that the synthesized hydrogels could be used as controlled drug delivery systems.

4.4.4 *In-vitro* Biocompatibility studies

The viability results of PCS-201-012 fibroblast cells after 24, 48 and 72 hours were reported for control, B1 and B2 blank samples and AWA, AAA, AAO, AWO samples. At the end of the first 24 hours, the viability results of the lignin-hydrogels were (as shown in Figure 4.29 and Table 4.16) below 70%, whereas the ones for neat PVA hydrogels were higher than 80%. After 48 hours, the viability of the samples dropped below 66%, and just one of the blank samples

showed higher viability than 70%. At the end of 3rd day (72 hours), all the samples except for Blank 2 showed lower viability values than 60%.

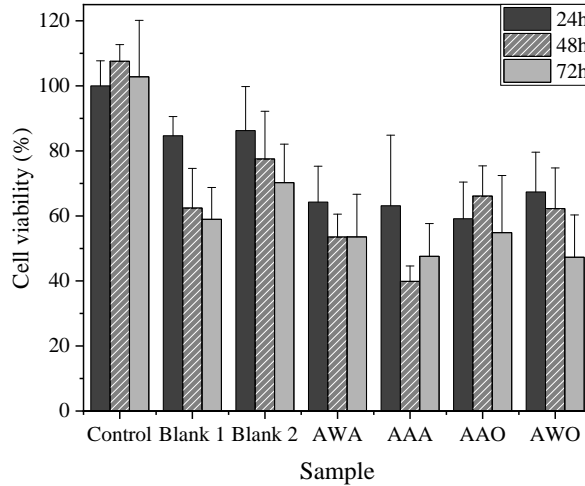


Figure 4.29. Cell viability results of PCS-201-012 (Human Dermal Fibroblast Cell line) cells after being cultivated with hydrogels for 24, 48 and 72 hours.

Table 4.16. Cell viability results of PCS-201-012 cells after being cultivated with hydrogels for 24, 48 and 72 hours.

Sample	Cell viability (%)		
	24 h	48 h	72 h
Control	100±7.7	107.6±5.1	102.8 ± 17.4
Blank 1	84.7±5.9	62.4±12.2	59.0±9.8
Blank 2	86.3±13.5	77.5±14.7	70.2±11.9
AWA	64.3±11.0	53.5±7.0	53.5±13.1
AAA	63.2±21.7	39.9±4.7	47.6±10.1
AAO	59.2±11.3	66.1±9.3	54.85±17.6
AWO	67.4±12.2	62.3±12.5	47.3±13.0

When Blank 1 and Blank 2 blank samples were considered as control (see Figure 4.30), the viability of AWA, AAA, AAO and AWO samples was recalculated and displayed in Tables 4.17 and 4.18. On the one hand, when the cell viability was calculated considering Blank 1 as the control group (see Figure 4.30-a), the estimated viability for all the samples after the first 24 hours was above 70%. When the incubation period was extended to 48 hours,

only organosolv lignin-containing hydrogels presented higher viability values than 70%. At the end of the 72 h, the viability percentages were between 55 and 64% for all the lignin-containing samples. It should be mentioned that the control sample presented a significant drop on its viability, since it showed less than 70% at the end of the test.

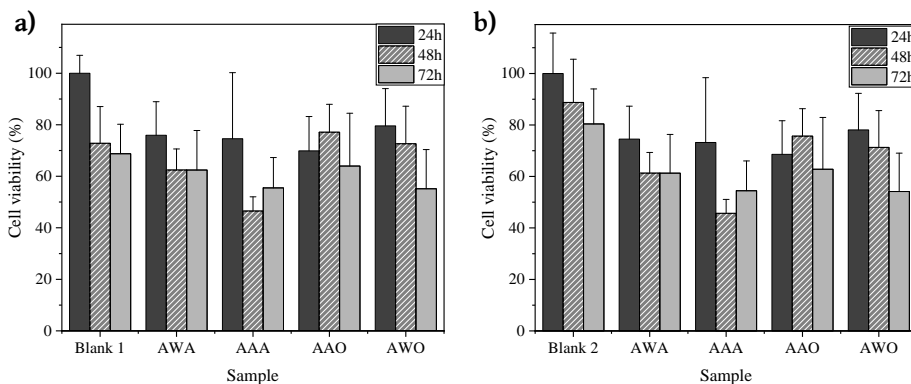


Figure 4.30. Cell viability results of PCS-201-012 (Human Dermal Fibroblast Cell line) cells after being cultivated with hydrogels for 24, 48 and 72 hours taking a) Blank 1 and b) Blank 2 as control.

Table 4.17. Cell viability results of PCS-201-012 cells after being cultivated with hydrogels for 24, 48 and 72 hours taking Blank 1 sample as control.

Sample	Cell viability (%)		
	24 h	48 h	72 h
Blank 1	100.0±6.7	72.8±14.2	68.8±11.4
AWA	75.9±13.0	62.4±8.2	62.4±15.3
AAA	74.6±25.6	46.5±5.5	55.5±11.8
AAO	69.9±13.3	77.1±10.9	64.0±20.5
AWO	79.6±14.5	72.7±14.6	55.2±15.2

On the other hand, when Blank 2 was accepted as control (see Figure 4.30-b), for the first 24 hours, the recorded viabilities were kept above 70% for all the samples. During the following 24 hours, these values decreased significantly for the samples containing alkaline lignin. In the case of the samples containing organosolv lignin, these values were still higher than 70%. At the end of the 72 hour incubation period, the viability results for organosolv

lignin-containing samples suffered a remarkable drop, while alkaline lignin-containing samples presented a slight increase on their viability. It should be noticed that, in this case, the decrease presented by the blank sample was lower than the one shown by Blank 1 sample.

Table 4.18. Cell viability results of PCS-201-012 cells after being cultivated with hydrogels for 24, 48 and 72 hours taking Blank 2 sample as control.

Sample	Cell viability (%)		
	24 h	48 h	72 h
Blank 2	100.0±15.7	88.8±16.8	80.4±13.6
AWA	74.5±12.8	61.3±8.1	61.3±15.0
AAA	73.2±25.2	45.7±5.4	54.5±11.6
AAO	68.6±13.1	75.7±10.7	62.8±20.1
AWO	78.1±14.2	71.3±14.3	54.1±14.9

When all samples were evaluated together, after the first 24 hours, AWA, AAA and AWO samples seemed to be the ones with the highest viability. Nevertheless, during the following 48 hours of assay, these values fell and, at the end of the test, sample AAO showed the highest viability. This sample also showed the highest cell proliferation after the three days when compared with both blank hydrogels. In fact, this sample was the only that permitted cell proliferation from the 24 to 48 hours of test.

Since according to the the ISO standard 10993-5, the viability of the materials is usually required to be higher than 70% so as to consider them non-cytotoxic [125,126], it could be said that in this case none of the tested lignin-hydrogels would be totally biocompatible. Despite PVA being considered a biocompatible material [125,127], the blank hydrogels did also decrease the cell viability during the test, which would not help the biocompatibility of the lignin-hydrogels either.

These samples were fixed and nuclei of cells on surface were stained with DAPI and examined under fluorescence microscope and cells found on surface of the

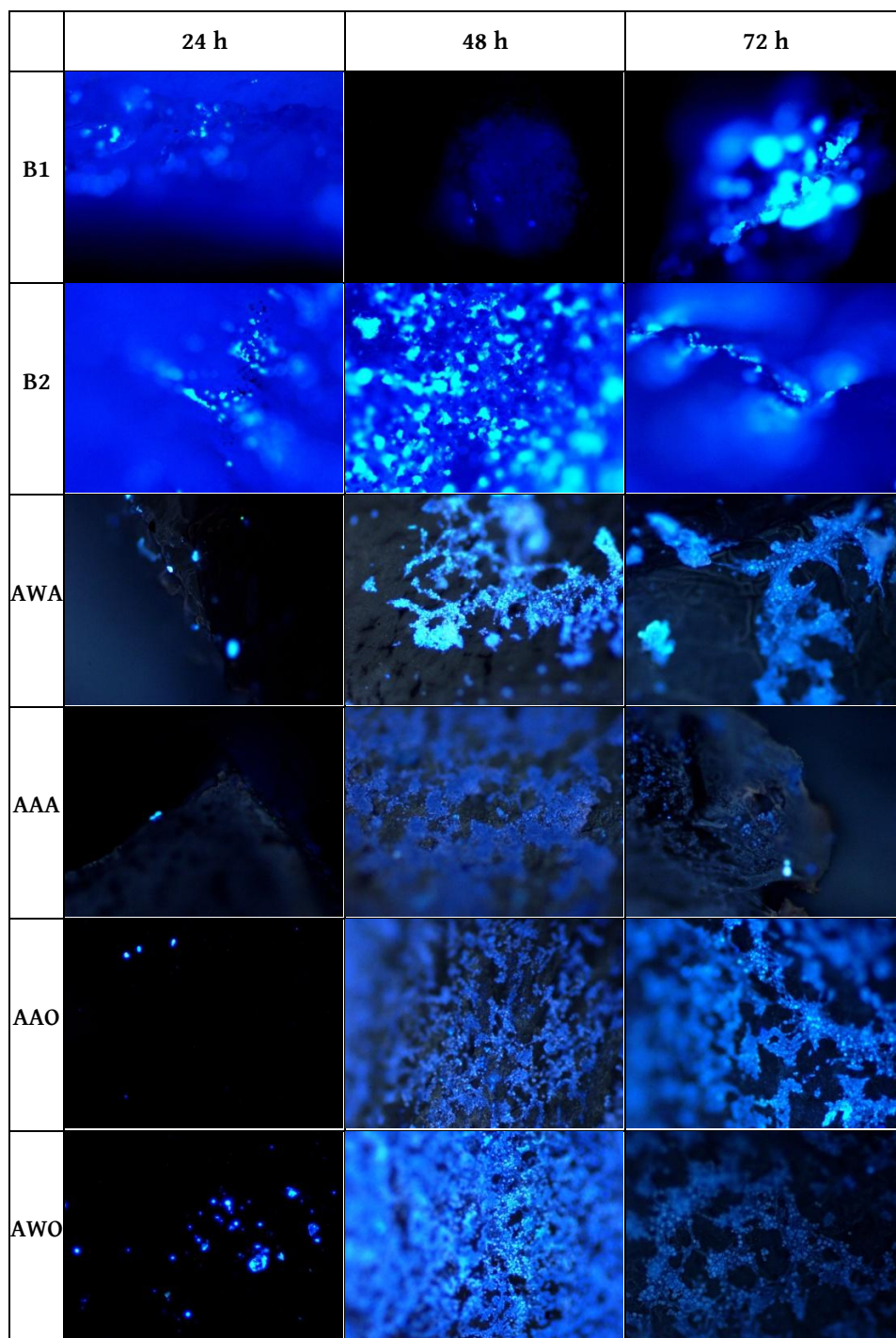


Figure 4.31. Fluorescent microscopy images of PCS-201-012 cells after cultivation with B1, B2, AWA, AAA, AAO and AWO samples for 24, 48 and 72 h.

hydrogels, but low viability concluded that cells died after attachment thus viability values dropped on graphs (see Figure 4.31).

Some authors have previously reported that the porosity of the tested material can be crucial for cell proliferation [128]. Thus, looking at the porosity of the previous samples, a second assay was performed employing more porous samples, as well as the ones that were synthesized from commercial alkaline lignin, in case the problem was in self-extracted lignins. In this second trial, the hydrogel samples were washed with PBS in an orbital shaker for 48 hours after swelling, and then, the abovementioned sterilization and cell seeding procedure was also applied. The viability results of the samples were obtained after testing them for 24 hours (see Figure 4.32).

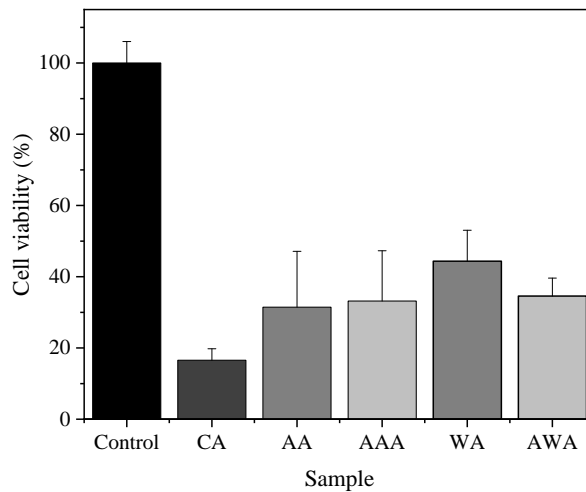


Figure 4.32. Viability results of PCS-201-012 (Human Dermal Fibroblast Cell line) cells after being cultivated with hydrogels for 24 hours.

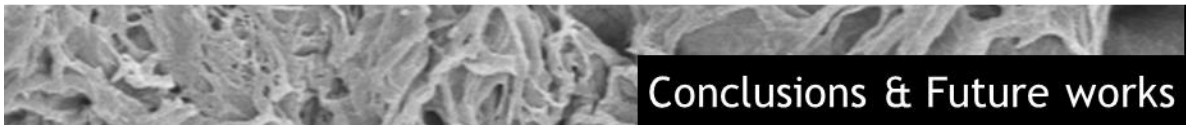
The recorded viability for the control and CA, AAA, AA, WA and AWA samples were 100.0, 16.56, 33.16, 31.46, 44.35 and 34.58%, respectively. In the hydrogels with improved porosity (AA and WA), the enhancement of the cell viability was more evident for WA comparing it with AWA. AA and AAA presented similar viability results, although the deviations of the measurements were

quite high. CA sample containing commercial alkaline lignin was the one presenting the worst results. This fact might be related to the sulphur content that has previously been detected through ATR-FTIR analyses of this lignin [78], which may be harmful for living cells.

Although the porosity of the samples has demonstrated to be an influencing parameter, the differences on the swelling characteristics of the hydrogels could have also affected the cell proliferation. In fact, some hydrogels released their pre-swollen amount of media, and this, together with their lignin amount might have led to cell death that resulted in reduced viability on hydrogels. Although some authors have previously stated that lignin addition to PVA-containing hydrogels can result in an enhancement of their biocompatibility [129], other authors have reported that the cytotoxicity of the lignins is usually concentration-dependent [130,131]. Thus, in this situation two possible alternatives should be considered: the first one, to study the cell-viability of native lignins alone; and the second one, to reduce the lignin content in the hydrogels so as to improve their biocompatibility.

4.4.5 Conclusions

In this section, the applicability of the hydrogels synthesized through this thesis was evaluated. From the obtained results it can be concluded that these materials can be very useful as water remediation systems, especially for cationic dye adsorption. In addition, the synthesized hydrogels could also be employed in active packaging due to the presented antifungal behaviour. Moreover, these materials showed the ability of being loaded with a natural drug and releasing it following a Fickian diffusion model. Thus, although the improvement of their biocompatibility should still be further explored, the produced hydrogels have demonstrated to be potential and versatile materials for multidisciplinary applications.



5 Conclusions & Future works

5.1 General and specific conclusions

As a general conclusion of this thesis, it can be said that physically crosslinked lignin hydrogels can be successfully obtained by blending lignin with an environmentally friendly matrix polymer such as poly (vinyl alcohol) (PVA). Moreover, it has been demonstrated that the properties of these materials can be tailored by varying many synthesis and formulation parameters. In addition, lignin-hydrogels have demonstrated to be potential materials to be applied in many application fields such as water remediation, packaging or drug delivery. Although the biocompatibility of these materials can be improved, the obtained results have shown that they may also have a future in the biomedical field. The specific conclusions obtained through this thesis are the following ones:

- ✓ The optimization of the synthesis of hydrogels based on commercial alkaline lignin and MM_w PVA resulted in materials with high swelling capacities, which could be modified according to the crosslinking and curing method.
- ✓ The molecular weight of PVA had great influence on the crosslinking and final properties of the synthesized hydrogels, leading to a higher swelling capacity as the molecular weight increased.
- ✓ The employment of self-extracted nut shell alkaline and organosolv lignins showed that their properties directly affect the final features of the synthesized hydrogels, being the purity of the lignins a highly influencing factor.
- ✓ The reduction of the duration of the freeze-thawing cycles led to a decrease on the swelling capacity of the hydrogels. Conversely, the

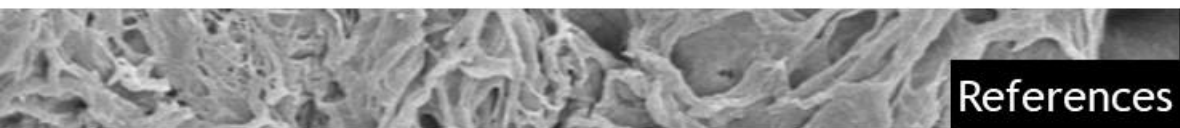
increase on the duration of the last thawing stage enhanced this property significantly.

- ✓ The chemical modification of the employed lignins can be useful for tailoring the characteristics of the hydrogels.
- ✓ The synthesized hydrogels showed promising results for the tested applications: dye adsorption, antifungal materials for food-packaging and drug delivery.
- ✓ Although the results of the biocompatibility tests were not as good as expected, they have opened the way for these materials to have a future in this field as well.

5.2 Future works

Although many influencing parameters and potential application fields have been studied throughout the present dissertation, there is still much to learn about lignin-hydrogels. For this reason, the following aspects should be further investigated in the future:

- The up-scaling possibility of the proposed hydrogel synthesis procedure
- A Life Cycle Analysis (LCA) of the hydrogels in this thesis
- The improvement of the biocompatibility of the synthesized hydrogels so as to employ them in the biomedical field
- The employment of other environmentally friendly matrixes for the development of alternative physical lignin-hydrogels
- The use of lignins from different sources such as grass, hardwood and softwood
- The employment of different lignin modification reactions and their influence on the properties of the hydrogels



References

R

References

- [1] D. Londoño-Pulgarin, G. Cardona-montoya, J.C. Restrepo, F. Muñoz-Leiva, Fossil or bioenergy? *Global fuel market trends*, 143 (2021). doi:10.1016/j.rser.2021.110905.
- [2] BP, *Statistical Review of World Energy (Oil)*, (2020).
- [3] BP, *Statistical Review of World Energy (CO₂)*, (2020).
- [4] H. Nakajima, P. Dijkstra, K. Loos, The recent developments in biobased polymers toward general and engineering applications: Polymers that are upgraded from biodegradable polymers, analogous to petroleum-derived polymers, and newly developed, *Polymers (Basel)*. 9 (2017) 1–26. doi:10.3390/polym9100523.
- [5] S. Walker, R. Rothman, Life cycle assessment of bio-based and fossil-based plastic: A review, *J. Clean. Prod.* 261 (2020) 121158. doi:10.1016/j.jclepro.2020.121158.
- [6] J. Soares, I. Miguel, C. Venâncio, I. Lopes, M. Oliveira, Public views on plastic pollution: Knowledge, perceived impacts, and pro-environmental behaviours, 412 (2021) 125227. doi:10.1016/j.jhazmat.2021.125227.
- [7] J.R. Jambeck, R. Geyer, C. Wilcox, T.R. Siegler, M. Perryman, A. Andrady, R. Narayan, K.L. Law, Plastic waste inputs from land into the ocean, *Science*, 347 (2015) 768–771. doi:10.1126/science.1260352.
- [8] A. Pellis, M. Malinconico, A. Guarneri, L. Gardossi, Renewable polymers and plastics: Performance beyond the green, *N. Biotechnol.* 60 (2021) 146–158. doi:10.1016/j.nbt.2020.10.003.
- [9] S.N. Akanyange, X. Lyu, X. Zhao, X. Li, Y. Zhang, J.C. Crittenden, C. Anning, T. Chen, T. Jiang, H. Zhao, Does microplastic really represent a threat? A review of the atmospheric contamination sources and potential impacts, *Sci. Total Environ.* 777 (2021) 146020. doi:10.1016/j.scitotenv.2021.146020.
- [10] A.T. Ubando, C.B. Felix, W.H. Chen, Biorefineries in circular bioeconomy: A comprehensive review, *Bioresour. Technol.* 299 (2020)

122585. doi:10.1016/j.biortech.2019.122585.
- [11] A. Morales, J. Labidi, P. Gullón, G. Astray, Synthesis of advanced biobased green materials from renewable biopolymers, *Curr. Opin. Green Sustain. Chem.* 29 (2021) 100436. doi:10.1016/j.cogsc.2020.100436.
- [12] S. Bilgen, Structure and environmental impact of global energy consumption, *Renew. Sustain. Energy Rev.* 38 (2014) 890–902. doi:10.1016/j.rser.2014.07.004.
- [13] G. Dragone, A.A.J. Kerssemakers, J.L.S.P. Driessen, C.K. Yamakawa, L.P. Brumano, S.I. Mussatto, Innovation and strategic orientations for the development of advanced biorefineries, *Bioresour. Technol.* 302 (2020) 122847. doi:10.1016/j.biortech.2020.122847.
- [14] R. van Ree, *The Role of Biorefining and Bioenergy in the Circular Economy*, (2017).
- [15] A.S. Nizami, M. Rehan, M. Waqas, M. Naqvi, O.K.M. Ouda, K. Shahzad, R. Miandad, M.Z. Khan, M. Syamsiro, I.M.I. Ismail, D. Pant, Waste biorefineries: Enabling circular economies in developing countries, *Bioresour. Technol.* 241 (2017) 1101–1117. doi:10.1016/j.biortech.2017.05.097.
- [16] BioPlat., SusChem., Ministerio de Economía, I. y Competitividad, *Manual sobre Biorrefinerías en España*, Minist. Econ. Ind. Y Compet. (2017) 1–92.
- [17] Y. Liu, Y. Lyu, J. Tian, J. Zhao, N. Ye, Y. Zhang, L. Chen, Review of waste biorefinery development towards a circular economy: From the perspective of a life cycle assessment, *Renew. Sustain. Energy Rev.* 139 (2021) 110716. doi:10.1016/j.rser.2021.110716.
- [18] Bio-based Industries Consortium, Nova Institute, *Biorefineries in Europe 2017*, (2017).
- [19] L.A. Zevallos Torres, A. Lorenci Woiciechowski, V.O. de Andrade Tanobe, S.G. Karp, L.C. Guimarães Lorenci, C. Faulds, C.R. Soccol, Lignin as a potential source of high-added value compounds: A review, *J. Clean. Prod.* 263 (2020) 121499. doi:10.1016/j.jclepro.2020.121499.

- [20] A.R. Mankar, A. Pandey, A. Modak, K.K. Pant, Pretreatment of lignocellulosic biomass: A review on recent advances, *Bioresour. Technol.* 334 (2021) 125235. doi:10.1016/j.biortech.2021.125235.
- [21] J.J. Liao, N.H.A. Latif, D. Trache, N. Brosse, M.H. Hussin, Current advancement on the isolation, characterization and application of lignin, *Int. J. Biol. Macromol.* 162 (2020) 985–1024. doi:10.1016/j.ijbiomac.2020.06.168.
- [22] R. Singh, A. Shukla, S. Tiwari, M. Srivastava, A review on delignification of lignocellulosic biomass for enhancement of ethanol production potential, *Renew. Sustain. Energy Rev.* 32 (2014) 713–728. doi:10.1016/j.rser.2014.01.051.
- [23] L. Sillero, R. Prado, M.A. Andrés, J. Labidi, Characterisation of bark of six species from mixed Atlantic forest, *Ind. Crops Prod.* 137 (2019) 276–284. doi:10.1016/j.indcrop.2019.05.033.
- [24] S.L. Mathews, J. Pawlak, A.M. Grunden, Bacterial biodegradation and bioconversion of industrial lignocellulosic streams, *Appl. Microbiol. Biotechnol.* 99 (2015) 2939–2954. doi:10.1007/s00253-015-6471-y.
- [25] FAOSTAT, Crops and livestock products, (2019). <https://www.fao.org/faostat/en/#data/QCL> (accessed June 30, 2021).
- [26] H. Chen, Chemical Composition and Structure of Natural Lignocellulose, in: *Biotechnology of Lignocellulose*, Springer, 2014: pp. 25–71. doi:10.1007/978-94-007-6898-7.
- [27] A. Satlewal, R. Agrawal, S. Bhagia, P. Das, A.J. Ragauskas, Rice straw as a feedstock for biofuels: Availability, recalcitrance, and chemical properties, *Biofuels, Bioprod. Biorefining.* 12 (2018) 83–107. doi:10.1002/bbb.1818.
- [28] W.O.S. Doherty, P. Mousavioun, C.M. Fellows, Value-adding to cellulosic ethanol: Lignin polymers, *Ind. Crops Prod.* 33 (2011) 259–276. doi:10.1016/j.indcrop.2010.10.022.
- [29] C.G. Yoo, X. Meng, Y. Pu, A.J. Ragauskas, The critical role of lignin in lignocellulosic biomass conversion and recent pretreatment strategies: A comprehensive review, *Bioresour. Technol.* 301 (2020) 122784. doi:10.1016/j.biortech.2020.122784.

- [30] A. Tribot, G. Amer, M. Abdou Alio, H. de Baynast, C. Delattre, A. Pons, J.D. Mathias, J.M. Callois, C. Vial, P. Michaud, C.G. Dussap, Wood-lignin: Supply, extraction processes and use as bio-based material, *Eur. Polym. J.* 112 (2019) 228–240. doi:10.1016/j.eurpolymj.2019.01.007.
- [31] S. Constant, H.L.J. Wienk, A.E. Frissen, P. de Peinder, R. Boelens, D.S. van Es, R.J.H. Grisel, B.M. Weckhuysen, W.J.J. Huijgen, R.J.A. Gosselink, P.C.A. Bruijninx, New insights into the structure and composition of technical lignins: a comparative characterisation study, *Green Chem.* 18 (2016) 2651–2665. doi:10.1039/C5GC03043A.
- [32] V. Hemmilä, S. Adamopoulos, O. Karlsson, A. Kumar, Development of sustainable bio-adhesives for engineered wood panels-A Review, *RSC Adv.* 7 (2017) 38604–38630. doi:10.1039/c7ra06598a.
- [33] V.K. Ponnusamy, D.D. Nguyen, J. Dharmaraja, S. Shobana, J.R. Banu, R.G. Saratale, S.W. Chang, G. Kumar, A review on lignin structure, pretreatments, fermentation reactions and biorefinery potential, *Bioresour. Technol.* 271 (2019) 462–472. doi:10.1016/j.biortech.2018.09.070.
- [34] H. Wang, Y. Pu, A. Ragauskas, B. Yang, From lignin to valuable products—strategies, challenges, and prospects, *Bioresour. Technol.* 271 (2019) 449–461. doi:10.1016/j.biortech.2018.09.072.
- [35] A. Kumar, Anushree, J. Kumar, T. Bhaskar, Utilization of lignin: A sustainable and eco-friendly approach, *J. Energy Inst.* 93 (2020) 235–271. doi:10.1016/j.joei.2019.03.005.
- [36] E. Paone, T. Tabanelli, F. Mauriello, The rise of lignin biorefinery, *Curr. Opin. Green Sustain. Chem.* 24 (2020) 1–6. doi:10.1016/j.cogsc.2019.11.004.
- [37] X. Erdocia, F. Hernández-ramos, A. Morales, N. Izaguirre, P.L. De Hoyos-martínez, J. Labidi, Lignin extraction and isolation methods, in: H. Santos, P. Figueiredo (Eds.), *Lignin-Based Mater. Biomed. Appl.*, Elsevier Inc., 2021; pp. 61–104. doi:10.1016/c2019-0-01345-3.
- [38] X. Meng, C. Crestini, H. Ben, N. Hao, Y. Pu, A.J. Ragauskas, D.S. Argyropoulos, Determination of hydroxyl groups in biorefinery resources via quantitative ³¹P NMR spectroscopy, *Nat. Protoc.* 14 (2019) 2627–2647. doi:10.1038/s41596-019-0191-1.

- [39] Y. Chen, H. Zhang, Z. Zhu, S. Fu, High-value utilization of hydroxymethylated lignin in polyurethane adhesives, *Int. J. Biol. Macromol.* 152 (2020) 775–785. doi:10.1016/j.ijbiomac.2020.02.321.
- [40] M. Goliszek, D. Kołodyńska, I. V. Pylypchuk, O. Sevastyanova, B. Podkościelna, Synthesis of lignin-containing polymer hydrogels with tunable properties and their application in sorption of nickel(II) ions, *Ind. Crops Prod.* 164 (2021) 20–31. doi:10.1016/j.indcrop.2021.113354.
- [41] P. Figueiredo, K. Lintinen, J.T. Hirvonen, M.A. Kostianen, H.A. Santos, Properties and chemical modifications of lignin: Towards lignin-based nanomaterials for biomedical applications, *Prog. Mater. Sci.* 93 (2018) 233–269. doi:10.1016/j.pmatsci.2017.12.001.
- [42] V. Maharana, D. Gaur, S.K. Nayak, V.K. Singh, S. Chakraborty, I. Banerjee, S.S. Ray, A. Anis, K. Pal, Reinforcing the inner phase of the filled hydrogels with CNTs alters drug release properties and human keratinocyte morphology: A study on the gelatin- tamarind gum filled hydrogels, *J. Mech. Behav. Biomed. Mater.* 75 (2017) 538–548. doi:10.1016/j.jmbbm.2017.08.026.
- [43] K. Lavanya, S.V. Chandran, K. Balagangadharan, N. Selvamurugan, Temperature- and pH-responsive chitosan-based injectable hydrogels for bone tissue engineering, *Mater. Sci. Eng. C.* 111 (2020) 110862. doi:10.1016/j.msec.2020.110862.
- [44] C. Echalié, L. Valot, J. Martinez, A. Mehdi, G. Subra, Chemical cross-linking methods for cell encapsulation in hydrogels, *Mater. Today Commun.* 20 (2019) 100536. doi:10.1016/j.mtcomm.2019.05.012.
- [45] J. Xiang, L. Shen, Y. Hong, Status and future scope of hydrogels in wound healing: Synthesis, materials and evaluation, *Eur. Polym. J.* 130 (2020) 109609. doi:10.1016/j.eurpolymj.2020.109609.
- [46] K. Varaprasad, G.M. Raghavendra, T. Jayaramudu, M.M. Yallapu, R. Sadiku, A mini review on hydrogels classification and recent developments in miscellaneous applications, *Mater. Sci. Eng. C.* 79 (2017) 958–971. doi:10.1016/j.msec.2017.05.096.
- [47] N. Chirani, L. Yahia, L. Gritsch, F.L. Motta, S. Chirani, S. Faré, History and Applications of Hydrogels, *J. Biomed. Sci.* 04 (2015) 1–23. doi:10.4172/2254-609x.100013.

- [48] E.M. Ahmed, Hydrogel: Preparation, characterization, and applications: A review, *J. Adv. Res.* 6 (2015) 105–121. doi:10.1016/j.jare.2013.07.006.
- [49] F. Ullah, M.B.H. Othman, F. Javed, Z. Ahmad, H.M. Akil, Classification, processing and application of hydrogels: A review, *Mater. Sci. Eng. C* 57 (2015) 414–433. doi:10.1016/j.msec.2015.07.053.
- [50] Y. Meng, J. Lu, Y. Cheng, Q. Li, H. Wang, Lignin-based hydrogels: A review of preparation, properties, and application, *Int. J. Biol. Macromol.* 135 (2019) 1006–1019. doi:10.1016/j.ijbiomac.2019.05.198.
- [51] S. Iravani, R.S. Varma, Greener synthesis of lignin nanoparticles and their applications, *Green Chem.* 22 (2020) 612–636. doi:10.1039/c9gc02835h.
- [52] D. Kun, B. Pukánszky, Polymer/lignin blends: Interactions, properties, applications, *Eur. Polym. J.* 93 (2017) 618–641. doi:10.1016/j.eurpolymj.2017.04.035.
- [53] O. Yu, K.H. Kim, Lignin to materials: A focused review on recent novel lignin applications, *Appl. Sci.* 10 (2020) 4626. doi:10.3390/app10134626.
- [54] D. Rico-García, L. Ruiz-Rubio, L. Pérez-Álvarez, S.L. Hernández-Olmos, G.L. Guerrero-Ramírez, J.L. Vilas-Vilela, Lignin-Based Hydrogels: Synthesis and Applications, *Polymers (Basel)*. 12 (2020) 1–23. doi:10.3390/polym12010081.
- [55] R. Mohammadinejad, H. Maleki, E. Larrañeta, A.R. Fajardo, A.B. Nik, A. Shavandi, A. Sheikhi, M. Ghorbanpour, M. Farokhi, P. Govindh, E. Cabane, S. Azizi, A.R. Aref, M. Mozafari, M. Mehrali, S. Thomas, J.F. Mano, Y.K. Mishra, V.K. Thakur, Status and future scope of plant-based green hydrogels in biomedical engineering, *Appl. Mater. Today*. 16 (2019) 213–246. doi:10.1016/j.apmt.2019.04.010.
- [56] L. Wu, S. Huang, J. Zheng, Z. Qiu, X. Lin, Y. Qin, Synthesis and characterization of biomass lignin-based PVA super-absorbent hydrogel, *Int. J. Biol. Macromol.* 140 (2019) 538–545. doi:10.1016/j.ijbiomac.2019.08.142.
- [57] R.A. Batista, P.J.P. Espitia, J. de S.S. Quintans, M.M. Freitas, M.Â. Cerqueira, J.A. Teixeira, J.C. Cardoso, Hydrogel as an alternative structure for food packaging systems, *Carbohydr. Polym.* 205 (2019)

- 106–116. doi:10.1016/j.carbpol.2018.10.006.
- [58] I. Spiridon, Biological and pharmaceutical applications of lignin and its derivatives: A mini-review, *Cellul. Chem. Technol.* 52 (2018) 543–550.
- [59] E. Larrañeta, M. Imízcoz, J.X. Toh, N.J. Irwin, A. Ripolin, A. Perminova, J. Domínguez-Robles, A. Rodríguez, R.F. Donnelly, Synthesis and Characterization of Lignin Hydrogels for Potential Applications as Drug Eluting Antimicrobial Coatings for Medical Materials, *ACS Sustain. Chem. Eng.* 6 (2018) 9037–9046. doi:10.1021/acssuschemeng.8b01371.
- [60] W. Yang, E. Fortunati, F. Bertoglio, J.S. Owczarek, G. Bruni, M. Kozanecki, J.M. Kenny, L. Torre, L. Visai, D. Puglia, Polyvinyl alcohol/chitosan hydrogels with enhanced antioxidant and antibacterial properties induced by lignin nanoparticles, *Carbohydr. Polym.* 181 (2018) 275–284. doi:10.1016/j.carbpol.2017.10.084.
- [61] Y. Zhang, B. Yuan, Y. Zhang, Q. Cao, C. Yang, Y. Li, J. Zhou, Biomimetic lignin/poly(ionic liquids) composite hydrogel dressing with excellent mechanical strength, self-healing properties, and reusability, *Chem. Eng. J.* 400 (2020) 125984. doi:10.1016/j.ccej.2020.125984.
- [62] L. Musilová, A. Mráček, A. Kovalcik, P. Smolka, A. Minařík, P. Humpolíček, R. Vícha, P. Ponížil, Hyaluronan hydrogels modified by glycinated Kraft lignin: Morphology, swelling, viscoelastic properties and biocompatibility, *Carbohydr. Polym.* 181 (2018) 394–403. doi:10.1016/j.carbpol.2017.10.048.
- [63] Y. Liu, Y. Huang, C. Zhang, W. Li, C. Chen, Z. Zhang, H. Chen, J. Wang, Y. Li, Y. Zhang, Nano-FeS incorporated into stable lignin hydrogel: A novel strategy for cadmium removal from soil, *Environ. Pollut.* 264 (2020) 114739. doi:10.1016/j.envpol.2020.114739.
- [64] H. Qian, J. Wang, L. Yan, Synthesis of lignin-poly(N-methylaniline)-reduced graphene oxide hydrogel for organic dye and lead ions removal, *J. Bioresour. Bioprod.* 5 (2020) 204–210. doi:10.1016/j.jobab.2020.07.006.
- [65] N. Tahari, P.L. de Hoyos-Martinez, M. Abderrabba, S. Ayadi, J. Labidi, Lignin - montmorillonite hydrogels as toluene adsorbent, *Colloids Surfaces A Physicochem. Eng. Asp.* 602 (2020) 125108. doi:10.1016/j.colsurfa.2020.125108.

- [66] Y. Meng, C. Li, X. Liu, J. Lu, Y. Cheng, L.P. Xiao, H. Wang, Preparation of magnetic hydrogel microspheres of lignin derivate for application in water, *Sci. Total Environ.* 685 (2019) 847–855. doi:10.1016/j.scitotenv.2019.06.278.
- [67] J. Domínguez-Robles, M.S. Peresin, T. Tamminen, A. Rodríguez, E. Larrañeta, A.S. Jääskeläinen, Lignin-based hydrogels with “super-swelling” capacities for dye removal, *Int. J. Biol. Macromol.* 115 (2018) 1249–1259. doi:10.1016/j.ijbiomac.2018.04.044.
- [68] F. Flores-Céspedes, M. Villafranca-Sánchez, M. Fernández-Pérez, Alginate-based hydrogels modified with olive pomace and lignin to removal organic pollutants from aqueous solutions, *Int. J. Biol. Macromol.* 153 (2020) 883–891. doi:10.1016/j.ijbiomac.2020.03.081.
- [69] H. Yuan, J. Peng, T. Ren, Q. Luo, Y. Luo, N. Zhang, Y. Huang, X. Guo, Y. Wu, Novel fluorescent lignin-based hydrogel with cellulose nanofibers and carbon dots for highly efficient adsorption and detection of Cr(VI), *Sci. Total Environ.* 760 (2021) 143395. doi:10.1016/j.scitotenv.2020.143395.
- [70] M. Liu, Y. Liu, J. Shen, S. Zhang, X. Liu, X. Chen, Y. Ma, S. Ren, G. Fang, S. Li, C. Tong Li, T. Sun, Simultaneous removal of Pb²⁺, Cu²⁺ and Cd²⁺ ions from wastewater using hierarchical porous polyacrylic acid grafted with lignin, *J. Hazard. Mater.* 392 (2020) 122208. doi:10.1016/j.jhazmat.2020.122208.
- [71] W. Farhat, R. Venditti, N. Mignard, M. Taha, F. Becquart, A. Ayoub, Polysaccharides and lignin based hydrogels with potential pharmaceutical use as a drug delivery system produced by a reactive extrusion process, *Int. J. Biol. Macromol.* 104 (2017) 564–575. doi:10.1016/j.ijbiomac.2017.06.037.
- [72] D. Wang, S.H. Lee, J. Kim, C.B. Park, “Waste to Wealth”: Lignin as a Renewable Building Block for Energy Harvesting/Storage and Environmental Remediation, *ChemSusChem.* 13 (2020) 2807–2827. doi:10.1002/cssc.202000394.
- [73] T. Liu, X. Ren, J. Zhang, J. Liu, R. Ou, C. Guo, X. Yu, Q. Wang, Z. Liu, Highly compressible lignin hydrogel electrolytes via double-crosslinked strategy for superior foldable supercapacitors, *J. Power Sources.* 449 (2020) 227532. doi:10.1016/j.jpowsour.2019.227532.

- [74] A. Morales, J. Labidi, P. Gullón, Hydrothermal treatments of walnut shells: A potential pretreatment for subsequent product obtaining, *Sci. Total Environ.* 764 (2021) 142800. doi:10.1016/j.scitotenv.2020.142800.
- [75] A. Morales, F. Hernández-Ramos, L. Sillero, R. Fernández-Marín, I. Dávila, P. Gullón, X. Erdocia, J. Labidi, Multiproduct biorefinery based on almond shells: Impact of the delignification stage on the manufacture of valuable products, *Bioresour. Technol.* 315 (2020) 123896. doi:10.1016/j.biortech.2020.123896.
- [76] M. Infante, F. Ysambertt, M. Hernández, B. Martínez, N. Delgado, B. Bravo, A. Cáceres, G. Chávez, J. Bullón, Microwave assisted oxidative degradation of lignin with hydrogen peroxide and its tensoactive properties, *Rev. Tec. La Fac. Ing. Univ. Del Zulia.* 30 (2007) 108–117.
- [77] I. Dávila, P. Gullón, M.A. Andrés, J. Labidi, Coproduction of lignin and glucose from vine shoots by eco-friendly strategies: Toward the development of an integrated biorefinery, *Bioresour. Technol.* 244 (2017) 328–337. doi:10.1016/j.biortech.2017.07.104.
- [78] A. Morales, J. Labidi, P. Gullón, Assessment of green approaches for the synthesis of physically crosslinked lignin hydrogels, *J. Ind. Eng. Chem.* 81 (2020) 475–487. doi:10.1016/j.jiec.2019.09.037.
- [79] A. Morales, J. Labidi, P. Gullón, Effect of the formulation parameters on the absorption capacity of smart lignin-hydrogels, *Eur. Polym. J.* 129 (2020) 109631. doi:10.1016/j.eurpolymj.2020.109631.
- [80] A.M. Salaberria, R.H. Diaz, M.A. Andrés, S.C.M. Fernandes, J. Labidi, The antifungal activity of functionalized chitin nanocrystals in poly (Lactid Acid) films, *Materials (Basel).* 10 (2017) 1–16. doi:10.3390/ma10050546.
- [81] D.T. Da Silva, R. Herrera, B.M. Heinzmann, J. Calvo, J. Labidi, *Nectandra grandiflora* by-products obtained by alternative extraction methods as a source of phytochemicals with antioxidant and antifungal properties, *Molecules.* 23 (2018) 1–16. doi:10.3390/molecules23020372.
- [82] D. George, P.U. Maheswari, K.M.M.S. Begum, Synergic formulation of onion peel quercetin loaded chitosan-cellulose hydrogel with green zinc oxide nanoparticles towards controlled release, biocompatibility, antimicrobial and anticancer activity, *Int. J. Biol. Macromol.* 132 (2019) 784–794. doi:10.1016/j.ijbiomac.2019.04.008.

- [83] E.Y. Jin, S. Lim, S. oh Kim, Y.S. Park, J.K. Jang, M.S. Chung, H. Park, K.S. Shim, Y.J. Choi, Optimization of various extraction methods for quercetin from onion skin using response surface methodology, *Food Sci. Biotechnol.* 20 (2011) 1727–1733. doi:10.1007/s10068-011-0238-8.
- [84] K. Pallab, B. Tapan K, P. Tapas K, K. Ramen, Estimation of Total Flavonoids Content (TFC) and Anti Oxidant Activities of Methanolic Whole Plant Extract of *Biophytum Sensitivum* Linn, *J. Drug Deliv. Ther.* 3 (2013) 33–37. doi:10.22270/jddt.v3i4.546.
- [85] D. George, K.M.M.S. Begum, P.U. Maheswari, Sugarcane Bagasse (SCB) Based Pristine Cellulose Hydrogel for Delivery of Grape Pomace Polyphenol Drug, *Waste and Biomass Valorization.* 11 (2020) 851–860. doi:10.1007/s12649-018-0487-3.
- [86] M. Saidi, A. Dabbaghi, S. Rahmani, Swelling and drug delivery kinetics of click-synthesized hydrogels based on various combinations of PEG and star-shaped PCL: influence of network parameters on swelling and release behavior, *Polym. Bull.* 77 (2020) 3989–4010. doi:10.1007/s00289-019-02948-z.
- [87] J. Fernández-Rodríguez, X. Erdocia, C. Sánchez, M. González Alriols, J. Labidi, Lignin depolymerization for phenolic monomers production by sustainable processes, *J. Energy Chem.* 26 (2017) 622–631. doi:10.1016/j.jechem.2017.02.007.
- [88] A. Morales, B. Gullón, I. Dávila, G. Eibes, J. Labidi, P. Gullón, Optimization of alkaline pretreatment for the co-production of biopolymer lignin and bioethanol from chestnut shells following a biorefinery approach, *Ind. Crops Prod.* 124 (2018) 582–592. doi:10.1016/j.indcrop.2018.08.032.
- [89] I. Dávila, B. Gullón, J. Labidi, P. Gullón, Multiproduct biorefinery from vine shoots: Bio-ethanol and lignin production, 142 (2019) 612–623.
- [90] C. Xu, F. Liu, M.A. Alam, H. Chen, Y. Zhang, C. Liang, H. Xu, S. Huang, J. Xu, Z. Wang, Comparative study on the properties of lignin isolated from different pretreated sugarcane bagasse and its inhibitory effects on enzymatic hydrolysis, *Int. J. Biol. Macromol.* 146 (2020) 132–140. doi:10.1016/j.ijbiomac.2019.12.270.
- [91] J. Li, P. Feng, H. Xiu, J. Li, X. Yang, F. Ma, X. Li, X. Zhang, E. Kozliak, Y. Ji, Morphological changes of lignin during separation of wheat straw

- components by the hydrothermal-ethanol method, *Bioresour. Technol.* 294 (2019) 122157. doi:10.1016/j.biortech.2019.122157.
- [92] L. Chen, X. Wang, H. Yang, Q. Lu, D. Li, Q. Yang, H. Chen, Study on pyrolysis behaviors of non-woody lignins with TG-FTIR and Py-GC/MS, *J. Anal. Appl. Pyrolysis.* 113 (2015) 499–507. doi:10.1016/j.jaap.2015.03.018.
- [93] S. De, S. Mishra, E. Poonguzhali, M. Rajesh, K. Tamilarasan, Fractionation and characterization of lignin from waste rice straw: Biomass surface chemical composition analysis, *Int. J. Biol. Macromol.* 145 (2020) 795–803. doi:10.1016/j.ijbiomac.2019.10.068.
- [94] A. Sequeiros, J. Labidi, Characterization and determination of the S/G ratio via Py-GC/MS of agricultural and industrial residues, *Ind. Crops Prod.* 97 (2017) 469–476. doi:10.1016/j.indcrop.2016.12.056.
- [95] M. Brahim, N. Boussetta, N. Grimi, E. Vorobiev, I. Zieger-Devin, N. Brosse, Pretreatment optimization from rapeseed straw and lignin characterization, *Ind. Crops Prod.* 95 (2017) 643–650. doi:10.1016/j.indcrop.2016.11.033.
- [96] X. Yang, Y. Zhao, H. Mussana, M. Tessema, L. Liu, Characteristics of cotton fabric modified with chitosan (CS)/cellulose nanocrystal (CNC) nanocomposites, *Mater. Lett.* 211 (2018) 300–303. doi:10.1016/j.matlet.2017.09.075.
- [97] I.A. Gilca, R.E. Ghitescu, A.C. Puitel, V.I. Popa, Preparation of lignin nanoparticles by chemical modification, *Iran. Polym. J.* 23 (2014) 355–363. doi:10.1007/s13726-014-0232-0.
- [98] A.M. Căpraru, E. Ungureanu, L.C. Trincă, Ț. Mălutan, V.I. Popa, Chemical and spectral characteristics of annual plant lignins modified by hydroxymethylation reaction, *Cellul. Chem. Technol.* 46 (2012) 589–597.
- [99] X. Ouyang, Z. Lin, Y. Deng, D. Yang, X. Qiu, Oxidative Degradation of Soda Lignin Assisted by Microwave Irradiation, *Chinese J. Chem. Eng.* 18 (2010) 695–702. doi:10.1016/S1004-9541(10)60277-7.
- [100] D. Zang, F. Liu, M. Zhang, Z. Gao, C. Wang, Novel superhydrophobic and superoleophilic sawdust as a selective oil sorbent for oil spill cleanup, *Chem. Eng. Res. Des.* 102 (2015) 34–41. doi:10.1016/j.cherd.2015.06.014.

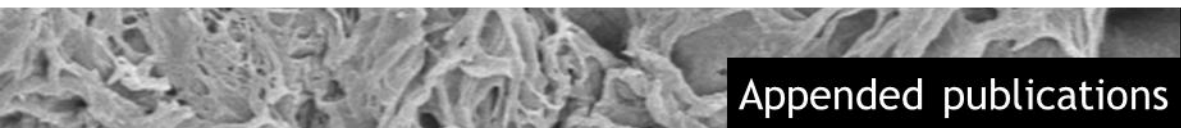
- [101] B. Gullón, P. Gullón, T.A. Lú-Chau, M.T. Moreira, J.M. Lema, G. Eibes, Optimization of solvent extraction of antioxidants from *Eucalyptus globulus* leaves by response surface methodology: Characterization and assessment of their bioactive properties, *Ind. Crops Prod.* 108 (2017) 649–659. doi:10.1016/j.indcrop.2017.07.014.
- [102] D. Ciolacu, G. Cazacu, New Green Hydrogels Based on Lignin, *J. Nanosci. Nanotechnol.* 18 (2018) 2811–2822. doi:10.1166/jnn.2018.14290.
- [103] N. Thombare, S. Mishra, M.Z. Siddiqui, U. Jha, D. Singh, G.R. Mahajan, Design and development of guar gum based novel, superabsorbent and moisture retaining hydrogels for agricultural applications, *Carbohydr. Polym.* 185 (2018) 169–178. doi:10.1016/j.carbpol.2018.01.018.
- [104] A. Kumar, S.S. Han, PVA-based hydrogels for tissue engineering: A review, *Int. J. Polym. Mater. Polym. Biomater.* 66 (2017) 159–182. doi:10.1080/00914037.2016.1190930.
- [105] K.J. Lee, J. Lee, J.Y. Hong, J. Jang, Influence of amorphous polymer nanoparticles on the crystallization behavior of Poly(vinyl alcohol) nanocomposites, *Macromol. Res.* 17 (2009) 476–482. doi:10.1007/BF03218895.
- [106] X.-Q. Hu, D.-Z. Ye, J.-B. Tang, L.-J. Zhang, X. Zhang, From waste to functional additives: thermal stabilization and toughening of PVA with lignin, *RSC Adv.* 6 (2016) 13797–13802. doi:10.1039/C5RA26385A.
- [107] M.R. Guilherme, F.A. Aouada, A.R. Fajardo, A.F. Martins, A.T. Paulino, M.F.T. Davi, A.F. Rubira, E.C. Muniz, Superabsorbent hydrogels based on polysaccharides for application in agriculture as soil conditioner and nutrient carrier: A review, *Eur. Polym. J.* 72 (2015) 365–385. doi:10.1016/j.eurpolymj.2015.04.017.
- [108] H.S. Mansur, C.M. Sadahira, A.N. Souza, A.A.P. Mansur, FTIR spectroscopy characterization of poly (vinyl alcohol) hydrogel with different hydrolysis degree and chemically crosslinked with glutaraldehyde, *Mater. Sci. Eng. C.* 28 (2008) 539–548. doi:10.1016/j.msec.2007.10.088.
- [109] W.E. Hennink, C.F. van Nostrum, Novel crosslinking methods to design hydrogels, *Adv. Drug Deliv. Rev.* 64 (2012) 223–236. doi:10.1016/j.addr.2012.09.009.

- [110] L.Y. Wang, M.J. Wang, Removal of Heavy Metal Ions by Poly(vinyl alcohol) and Carboxymethyl Cellulose Composite Hydrogels Prepared by a Freeze-Thaw Method, *ACS Sustain. Chem. Eng.* 4 (2016) 2830–2837. doi:10.1021/acssuschemeng.6b00336.
- [111] H. Bian, L. Wei, C. Lin, Q. Ma, H. Dai, J.Y. Zhu, Lignin-Containing Cellulose Nanofibril-Reinforced Polyvinyl Alcohol Hydrogels, *ACS Sustain. Chem. Eng.* 6 (2018) 4821–4828. doi:10.1021/acssuschemeng.7b04172.
- [112] H. Bian, L. Jiao, R. Wang, X. Wang, W. Zhu, H. Dai, Lignin nanoparticles as nano-spacers for tuning the viscoelasticity of cellulose nanofibril reinforced polyvinyl alcohol-borax hydrogel, *Eur. Polym. J.* 107 (2018) 267–274. doi:10.1016/j.eurpolymj.2018.08.028.
- [113] Y. Chen, K. Zheng, L. Niu, Y. Zhang, Y. Liu, C. Wang, F. Chu, Highly mechanical properties nanocomposite hydrogels with biorenewable lignin nanoparticles, *Int. J. Biol. Macromol.* 128 (2019) 414–420. doi:10.1016/j.ijbiomac.2019.01.099.
- [114] X. Han, Z. Lv, F. Ran, L. Dai, C. Li, C. Si, Green and stable piezoresistive pressure sensor based on lignin-silver hybrid nanoparticles/polyvinyl alcohol hydrogel, *Int. J. Biol. Macromol.* 176 (2021) 78–86. doi:10.1016/j.ijbiomac.2021.02.055.
- [115] L. Sun, Z. Mo, Q. Li, D. Zheng, X. Qiu, X. Pan, Facile synthesis and performance of pH/temperature dual-response hydrogel containing lignin-based carbon dots, *Int. J. Biol. Macromol.* 175 (2021) 516–525. doi:10.1016/j.ijbiomac.2021.02.049.
- [116] Q. Wang, J. Guo, X. Lu, X. Ma, S. Cao, X. Pan, Y. Ni, Wearable lignin-based hydrogel electronics: A mini-review, *Int. J. Biol. Macromol.* 181 (2021) 45–50. doi:10.1016/j.ijbiomac.2021.03.079.
- [117] I.E. Raschip, G.E. Hitruc, C. Vasile, M.C. Popescu, Effect of the lignin type on the morphology and thermal properties of the xanthan/lignin hydrogels, *Int. J. Biol. Macromol.* 54 (2013) 230–237. doi:10.1016/j.ijbiomac.2012.12.036.
- [118] R.M. Kalinoski, J. Shi, Hydrogels derived from lignocellulosic compounds: Evaluation of the compositional, structural, mechanical and antimicrobial properties, *Ind. Crops Prod.* 128 (2019) 323–330.

doi:10.1016/j.indcrop.2018.11.002.

- [119] J.I. Daza Agudelo, J.M. Badano, I. Rintoul, Kinetics and thermodynamics of swelling and dissolution of PVA gels obtained by freeze-thaw technique, *Mater. Chem. Phys.* 216 (2018) 14–21. doi:10.1016/j.matchemphys.2018.05.038.
- [120] N. Nguyen Van Long, C. Joly, P. Dantigny, Active packaging with antifungal activities, *Int. J. Food Microbiol.* 220 (2016) 73–90. doi:10.1016/j.ijfoodmicro.2016.01.001.
- [121] O.Y. Abdelaziz, D.P. Brink, J. Prothmann, K. Ravi, M. Sun, J. García-Hidalgo, M. Sandahl, C.P. Hulteberg, C. Turner, G. Lidén, M.F. Gorwa-Grauslund, Biological valorization of low molecular weight lignin, *Biotechnol. Adv.* 34 (2016) 1318–1346. doi:10.1016/j.biotechadv.2016.10.001.
- [122] R. Fernández-Marín, M. Mujtaba, D. Cansaran-Duman, G. Ben Salha, M.Á.A. Sánchez, J. Labidi, S.C.M. Fernandes, Effect of deterpenated organum majorana l. Essential oil on the physicochemical and biological properties of chitosan/ β -chitin nanofibers nanocomposite films, *Polymers (Basel)*. 13 (2021) 1507. doi:10.3390/polym13091507.
- [123] D. Dey, V. Dharini, S.P. Selvam, E.R. Sadiku, M.M. Kumar, J. Jayaramudu, U.N. Gupta, Physical, antifungal, and biodegradable properties of cellulose nanocrystals and chitosan nanoparticles for food packaging application, *Mater. Today Proc.* 38 (2021) 860–869. doi:10.1016/j.matpr.2020.04.885.
- [124] S.G. Lee, J.S. Parks, H.W. Kang, Quercetin, a functional compound of onion peel, remodels white adipocytes to brown-like adipocytes, *J. Nutr. Biochem.* 42 (2017) 62–71. doi:10.1016/j.jnutbio.2016.12.018.
- [125] M.S. Kim, G.W. Oh, Y.M. Jang, S.C. Ko, W.S. Park, I.W. Choi, Y.M. Kim, W.K. Jung, Antimicrobial hydrogels based on PVA and diphloretrohydroxycarmalol (DPHC) derived from brown alga *Ishige okamurae*: An in vitro and in vivo study for wound dressing application, *Mater. Sci. Eng. C*. 107 (2020) 110352. doi:10.1016/j.msec.2019.110352.
- [126] T. Demirci, M.E. Hasköylü, M.S. Eroğlu, J. Hemberger, E. Toksoy Öner, Levam-based hydrogels for controlled release of Amphotericin B for dermal local antifungal therapy of Candidiasis, *Eur. J. Pharm. Sci.* 145

- (2020) 105255. doi:10.1016/j.ejps.2020.105255.
- [127] C. Luo, A. Guo, Y. Zhao, J. Sun, Z. Li, Facile fabrication of nonswellable and biocompatible hydrogels with cartilage-comparable performances, *Mater. Today Commun.* 27 (2021) 102375. doi:10.1016/j.mtcomm.2021.102375.
- [128] A. Shamloo, Z. Aghababaie, H. Afjoul, M. Jami, M.R. Bidgoli, M. Vossoughi, A. Ramazani, K. Kamyabhesari, Fabrication and evaluation of chitosan/gelatin/PVA hydrogel incorporating honey for wound healing applications: An in vitro, in vivo study, *Int. J. Pharm.* 592 (2021) 120068. doi:10.1016/j.ijpharm.2020.120068.
- [129] Y. Zhang, M. Jiang, Y. Zhang, Q. Cao, X. Wang, Y. Han, Novel lignin – chitosan – PVA composite hydrogel for wound dressing, *Mater. Sci. Eng. C.* 104 (2019) 110002. <https://doi.org/10.1016/j.msec.2019.110002>.
- [130] O. Gordobil, A. Oberemko, G. Saulis, V. Baublys, J. Labidi, In vitro cytotoxicity studies of industrial Eucalyptus kraft lignins on mouse hepatoma, melanoma and Chinese hamster ovary cells, *Int. J. Biol. Macromol.* 135 (2019) 353–361. doi:10.1016/j.ijbiomac.2019.05.111.
- [131] O. Gordobil, P. Olaizola, J.M. Banales, J. Labidi, Lignins from agroindustrial by-products as natural ingredients for cosmetics: Chemical structure and in vitro sunscreen and cytotoxic activities, *Molecules.* 25 (2020) 1131. doi:10.3390/molecules25051131.



Appended publications

A

Synthesis of advanced biobased green materials from
renewable biopolymers

A. Morales, J. Labidi, P. Gullón, G. Astray

Permission is not required for this non-commercial use.

<http://10.1016/j.cogsc.2020.100436>

2452-2236/© 2021 Elsevier B.V. All rights reserved.

Curr. Opin. Green Sustain. Chem. 29 (2021) 100436



Synthesis of advanced biobased green materials from renewable biopolymers

Amaia Morales¹, Jalel Labidi¹, Patricia Gullón² and Gonzalo Astray^{3,4}

Polymeric materials such as hydrogels have become necessary in our daily lives. Hydrogels are three-dimensionally cross-linked polymeric networks that can absorb large amounts of water. Thanks to their properties, hydrogels are very useful in multiple application fields. However, they have usually been obtained from petroleum-derived polymers, contributing to plastic pollution and global warming. In this context, biomass has emerged as an appropriate alternative for production of chemicals, building blocks and biopolymers. Lignin is the second most ample and disposable biopolymer in the world. This biopolymer has been underused until recent decades, but as it has been demonstrated to provide composite materials such as hydrogels with excellent features, its valorization would mean a step forward in sustainability and circular economy. Hence, this review focuses on the state of the art of hydrogels and lignin-based hydrogels, as well as on their current applications.

Addresses

¹ Chemical and Environmental Engineering Department, University of the Basque Country UPV/EHU, Plaza Europa 1, 20018, San Sebastian, Spain

² Nutrition and Bromatology Group, Department of Analytical and Food Chemistry, Faculty of Food Science and Technology, University of Vigo, Ourense Campus, 32004, Ourense, Spain

³ Physical Chemistry Department, Faculty of Sciences, University of Vigo, Ourense Campus, 32004, Ourense, Spain

⁴ CITACA, Agri-Food Research and Transfer Cluster, University of Vigo, Campus Auga, 32004, Ourense, Spain

Corresponding author: Gullón, Patricia (patricia.gullon@ehu.es)

Current Opinion in Green and Sustainable Chemistry 2021, 29:100436

This review comes from a themed issue on **Sustainable solutions for renewable wastes**

Edited by Sara González García and Beatriz Gullón

<https://doi.org/10.1016/j.cogsc.2020.100436>

2452-2236/© 2021 Elsevier B.V. All rights reserved.

Introduction

Currently, synthetic polymer-based materials such as hydrogels have become indispensable for our everyday lives. These materials are usually obtained by polymerizing low-molecular-weight organic compounds that derive from fossil resources. Hydrogels are considered three-dimensionally cross-linked polymeric networks that contain many hydrophilic groups that allow huge

absorption of water molecules within their porous structure without being dissolved [1]. Apart from their excellent swelling properties, these materials stand out for their morphology and for their resistance to compression [2]. Different properties (control diffusion process, response to different factors — ionic strength changes, pH and/or temperature — and capacity to trap chemical species) [2] have made that hydrogels grow in popularity in the last decades. Owing to their outstanding features and the wide variety of substrates and forms they can be presented in, hydrogels have been applied in multiple fields such as personal hygiene, agriculture (water retention), environmental remediation (CO₂ capture) and biomedicine (drug delivery, among others) [1]. In fact, their global market represented in 2016 a total of \$15.6 billion, and the market should total \$22.3 billion in 2022 [3]. However, the high cost related to the complex production process of hydrogels, coupled with environmental hazards from disposable synthetic hydrogel products, is some of the major drawbacks restraining the growth of the market globally.

Since the middle years of the 20th century, the petroleum-derived chemistry, refinery and engineering processes have been the basis of the polymer industry [4]. The first decades of the 21st century have led to a big economic growth together with an irrecoverable environmental concern in which plastic pollution has been remarked as a global crisis. The latest involves plastic's whole life cycle, that is, from its production to its disposal and incineration. In this context, the development of biodegradable polymers has become one of the most suitable alternatives in this industry to face ecological problems [4], contributing at the same time both to sustainability and circular economy [5]. Therefore, the urgent transition from a petroleum-based to a biobased economy has marked the beginning of the current century, shifting the type of carbon resources from fossil to natural and renewable ones [6].

In the search of an appropriate solution to the exposed problem, biomass has resulted to be an alternative to petrochemicals for the production of chemicals, sugars and biopolymers [6]. Biopolymers are classified as natural polymers produced by plants, animals and microorganisms, which present biodegradability [4] as their main advantage. More specifically, lignocellulosic feedstock has emerged as a promising, renewable and vast

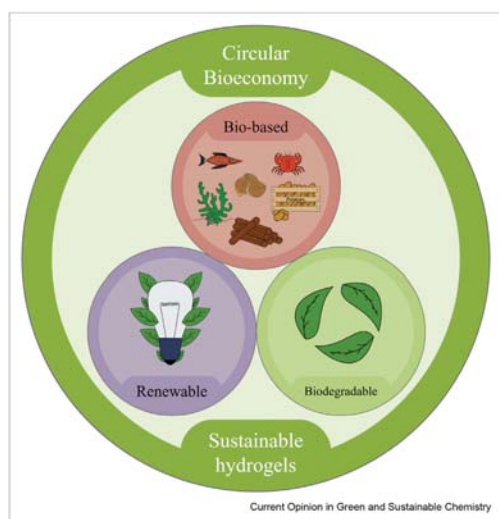
source for chemicals. This biomass is mainly constituted by carbohydrate polymers (cellulose and hemicelluloses) and by aromatic polymers (lignin and tannins), which can be isolated and used to form hydrogels without competing with other biopolymers with food applications such as starch. Although biopolymer-based hydrogels can sometimes exhibit poorer mechanical properties than synthetic ones, many strategies have recently been explored to overcome this drawback [7], and for this reason, renewable polymers are showing the tremendous potential to replace traditional polymers owing to their capacity for reducing energy consumption and pollution.

Among the aforementioned biopolymers, lignin, just after cellulose, is the second most plenty and fascinating terrestrial biopolymer [8]. In fact, about 150 billion tons of lignin is annually synthesized by Earth plants [9]. This intricate aromatic macromolecule is mostly constituted by three different types of phenyl propane monomers (p-coumaryl, coniferyl and sinapyl alcohols) that are cross-linked through different stable bondage types [8]. Lignin can be obtained by several isolation methods using different raw materials such as agricultural residues, dedicated crops or wood [8]. Owing to this, it is widely available as an important by-product from different industries, such as pulp and paper industry, among others, and it can be specifically produced in treatments of the new biorefinery schemes.

In the last ten years, the development of biorefinery approaches for biomass revalorization has increased the academic and industrial research about lignins. In this sense, renewable lignin as a new feedstock for biomaterial synthesis is being investigated for its positive effect on the thermal behaviour, hydrophilicity, biocompatibility and biodegradability of these systems [10]. Furthermore, its three-dimensional structure makes lignin suitable as a new potential cross-linking component for the development of hydrogels. Thus, the formulation of these materials has experimented a rapid shift from synthetic polymers to biopolymers [11].

Because less than 2% of the total amount of lignin generated by year in pulp and paper industry has an added value [8], the development of new green materials from lignin has attracted great attention from an environmental and economic point of view. Limited oil reserves, the environmental problems caused by the toxic compounds from the degradation of this type of materials and the expanding hydrogel market generate an urgent need for the development of environmentally friendly and safe alternative hydrogels from renewable materials, which would also expand the life cycle opportunities for reuse and recycling of lignocellulosic biomass and contribute to circular bioeconomy (see Figure 1). Hence, the novelty and potentiality of this review are focused on the use of this biopolymer for the synthesis of hydrogels and their applications in several fields to promote sustainable development.

Figure 1



Graphical definition of sustainable hydrogels.

Hydrogels and lignin

Over the last few years, studies on biopolymer-based hydrogels have become very popular owing to their applicability in the fields of food, cosmetics, pharmaceuticals and biomedical implants [12]. Besides, the integration of biopolymers together with other molecules can improve the functionality of the resultant hydrogels, making possible to formulate hydrogels capable of imitating the interrelated nature of human tissue [13]. Among these biopolymers, lignin is the only aromatic one, which makes it interesting for its application on functional hydrogels [12]. Although there is no defined structure for lignin [2], many studies have recently demonstrated that it can be successfully used for the formulation of lignin-derived composites used for tissue scaffolding and drug release or as UV absorbents [14]. Thus, if adequate routes for improving handling of lignin and development of technologies to process it were further investigated, this natural polymer would undoubtedly play an important role in the synthesis of new materials [15]. A clear increasing trend of the publications about lignin and lignin applications in the last years has been reported [9,15,16].

The lignin extraction method determines the type and features of the resultant lignin, which can be more or

less reactive depending on the used technique. The typical types of lignin used for hydrogel synthesis are kraft, lignosulfonate, alkaline and organosolv [2,12]. In any case, there are usually two pathways to valorize this biopolymer: the first one uses lignin as a macropolymer (to obtain valuable materials), whereas the second one implicates lignin depolymerization (to obtain low-molecular-weight monomers) [16]. In case of hydrogels, lignin is usually combined with other biosynthetic or synthetic polymers owing to the lack of self-gel-forming properties. For this reason, it has been included in different polymeric networks through physical interactions or chemical reactions that promote hydrogel structure [2].

Applications of lignin-based hydrogels

A big part of the synthesized lignin-based hydrogels has been used to remove heavy metal and cationic compounds present in aqueous solutions [17]. Nonetheless, Mohammadinejad et al. [17] also report their use in fields such as biomedicine for drug delivery and tissue engineering. Some hydrogel applications studied to date are described in the following paragraphs.

The controlled release of water is a commonly used term in agriculture. In climates wherein rain is scarce, soils need to be irrigated frequently. Nevertheless, equipping soils with small and smart hydrogels, such as lignin-based hydrogels, has proven to absorb significant amounts of water and retain it until the crops require it [12]. The water content of hydrogels can vary based on their degree of cross-linking, which can be controlled during their synthesis. Mazloom et al. [18,19], for instance, synthesized a lignin-based hydrogel (lignin alkali polymers—poly(ethylene glycol) diglycidyl ether) and then tested them as controlled water releasers in agricultural soils, which resulted in promising findings.

Meng et al. [20] also prepared some lignin-based hydrogels from copolymerization of acrylic acid and spent sulfite cooking solution (or red liquor) directly obtained from the paper industry. The materials developed by Meng et al. [20] exhibited superswelling and slow-release behaviours in water. Song et al. [21] combined lignin, sodium alginate and konjaku flour for synthesis of hydrogels with excellent soil conditioning properties tested with tobacco plants.

Lignin has functional groups (phenolic hydroxyl, alcohol hydroxyl, methoxy and carboxyl groups) that can act as adsorption sites for dye molecules and heavy metals [22]. According to Meng et al. [12], these structures are therefore capable of attracting positive molecules through negatively charged functional groups and aromatic organics via π - π reactions. For this reason, they have been used for adsorption of both inorganic ions and organic compounds in soils and water [12]. Table 1 summarizes some works in this field.

Thus, according to Andrade Batista et al. [31], hydrogels would be an attractive alternative for their application in food packaging systems as absorbent pads. Apart from water absorption properties, these materials should increase stored food products' shelf life and avoid microbial growth on food surface [31]. Therefore, the antimicrobial activity of the polymers constituting the hydrogel network is crucial. In this context, lignin and its derivatives and lignin-based hydrogel coatings have been shown to present antimicrobial behaviour [32–34]. For this reason, Yang et al. [35] proposed that their lignin-based hydrogels with antioxidant and antimicrobial properties could be used in food packaging.

Antimicrobial, antioxidant and low cytotoxicity features are also important for synthesis of biocompatible

Table 1

Literature review of hydrogels as pollutant removers.

Lignin type in hydrogels	Pollutant	Medium	Removal	Reference
Sodium lignosulfonate	Cadmium ions (Cd^{2+})	Soil	$<61.77 \pm 1.09$ mg/g	[23]
Lignin	Methylene blue (MB) and lead ions (Pb^{2+})	Aqueous	201.7 mg/g MB and 753.5 mg/g Pb^{2+}	[24]
Alkali, kraft and organosolv lignins	Toluene	Aqueous	164–170 mg/g	[25]
Aminated alkali lignin	Heavy metal cations (Pb^{2+} , Hg^{2+} and Ni^{2+}) and dyes (MB, methyl orange and malachite green)	Aqueous	2.1–55 mg/g for heavy metal cations and 2–155 mg/g for dyes	[26]
Alkali, kraft and enzymatic hydrolysis lignin	Rhodamine 6G, crystal violet, MB and methyl orange	Aqueous	10–196 mg/g	[22]
Soda, kraft and organosolv lignins	MB	Aqueous	69–629 mg/g	[27]
Pine kraft lignin Indulin AT	Prednisolone drug and 3,4-dichloroaniline	Aqueous	1.35 mg/g for prednisolone and 4 mg/g for 3,4-dichloroaniline	[28]
Alkali lignin	Hexavalent chromium $\text{Cr}(\text{VI})$	Aqueous	599.9 mg/g	[29]
Acid-pretreated alkali lignin	Pb^{2+} , Cu^{2+} and Cd^{2+} ions	Aqueous	1.076 mmol/g for Pb^{2+} , 0.3233 mmol/g for Cu^{2+} and 0.059 mmol/g for Cd^{2+}	[30]

materials. In this sense, hydrogels can provide effective removal of undesirable metabolites from wounds owing to their high absorption capacity, and the addition of lignin may help to protect the wound from future problems such as further injury or contamination, thanks to its good mechanical properties [16]. Hence, lignin has also gained interest in wound dressing [35] and tissue engineering [36].

Lignin-based hydrogels have also been shown to be useful in another important part of the biomedical field: the controlled release of both hydrophobic [33] and hydrophilic drugs. Stimulus-responsive hydrogels can be created by combining other (bio)polymers and lignin. These hydrogels are of great interest in drug delivery because they are able to alter their volume in response to environmental stimuli [37] such as pH, temperature or light [2]. Some authors, for instance, have studied the release kinetics of curcumin-loaded hydrogels at simulated human body conditions [33]. They concluded that as the lignin content was higher, the hydrogels were loaded with higher amounts of the drug, promoting a higher release of it [33].

Finally, the use of lignin-based materials applied to energy devices has proven to be promising [38]. Among other applications, these materials have gained attention as electrode materials for supercapacitors as a result of their high surface areas and chemical stability and superior electrical conductivity [38]. Liu et al. [39], for instance, created hybrid double-cross-linked lignin-based hydrogels by combining corn cob lignin media with poly(ethylene glycol) diglycidyl ether in alkaline media and immersing them in sulfuric acid afterwards. These authors reported not only excellent electrochemical performance for their supercapacitors but also improved mechanical properties [39].

Conclusions

Taking all the aforementioned information into account, it can be concluded that, although lignin has been underused in the past, it presents multiple advantages not only from the economical (e.g. high availability and low cost) perspective but also from the environmental (i.e. renewable and biodegradable) and technological (i.e. excellent physicochemical features) points of view, making it greatly potential for many applications. Although lignin-based materials are still at early stages in the global market, many spin-offs, start-ups and companies have placed their bet on them, producing lignin aerogels (Aerogel UG., Hamburg, Germany), for instance. A deeper understanding of the chemical structure and physicochemical properties of lignin would make it even more interesting and useful for the synthesis of globally used commodities in the near future. Thus, standardization of lignin manufacturing processes would lead to synthesis of bountiful

sustainable products such as thermoplastic and elastomeric materials for automotive or building applications, for instance, as well as to production of materials for packaging and electronic applications. Therefore, it is important that research continues in this field to create green and sustainable materials for substitution of conventional ones.

Acknowledgements

AM would like to thank the University of the Basque Country (Training of Researcher Staff, PIF17/207). GA thanks the University of Vigo for his contract supported by 'Programa de retención de talento investigador da Universidade de Vigo para o 2018'.

Author contributions

Amaia Morales: Conceptualization, Writing- Original draft preparation. **Jalel Labidi, Patricia Gullón and Gonzalo Astray:** Supervision, Writing- Reviewing and Editing.

Declaration of competing interest

The authors declare that they have no known competing financial interests or personal relationships that could have appeared to influence the work reported in this paper.

References

Papers of particular interest, published within the period of review, have been highlighted as:

- * of special interest
- 1. Kalinoski RM, Shi J: **Hydrogels derived from lignocellulosic compounds: evaluation of the compositional, structural, mechanical and antimicrobial properties.** *Ind Crop Prod* 2019, **128**:323–330.
- 2. Rico-García D, Ruiz-Rubio L, Pérez-Álvarez L, Hernández-Olmos SL, Guerrero-Ramírez GL, Vilas-Vilela JL: **Lignin-based hydrogels: synthesis and applications.** *Polymers* 2020, **12**:81. This work provides an interesting review about lignin-based hydrogels. For this aim, these authors explain the basic chemistry of lignin as well as its typical extraction methods. In addition, the main preparation routes of lignin-hydrogels reported in the last years are included and the current applications of lignin hydrogels as stimuli-responsive materials, flexible supercapacitors and wearable electronics for biomedical and water remediation applications are presented.
- 3. Singh V: **Hydrogels: applications and global markets to 2022.** *Bccresearch.com*; 2017. . [Accessed August 2020].
- 4. Nakajima H, Dijkstra P, Loos K: **The recent developments in biobased polymers toward general and engineering applications: polymers that are upgraded from biodegradable polymers, analogous to petroleum-derived polymers, and newly developed.** *Polymers* 2017, **9**:523.
- 5. RameshKumar S, Shaiju P, O'Connor KE, Babu R: **Bio-based and biodegradable polymers - state-of-the-art, challenges and emerging trends.** *Curr. Opin. Green Sustain. Chem.* 2020, **21**:75–81.
- 6. Liao JJ, Latif NHA, Trache D, Brosse N, Hussin MH: **Current advancement on the isolation, characterization and application of lignin.** *Int J Biol Macromol* 2020, **162**:985–1024.
- 7. Bao Z, Xian C, Yuan Q, Liu G, Wu J: **Natural polymer-based hydrogels with enhanced mechanical performances: preparation, structure, and property.** *Adv Healthcare Mater* 2019, **8**: 1900670.
- 8. Dragone G, Kerssemakers AAJ, Driessen JLSP, Yamakawa CK, Brumano LP, Mussatto SI: **Innovation and strategic**

- orientations for the development of advanced biorefineries. *Bioresour Technol* 2020, **302**:122847.
9. Tribot A, Amer G, Alio MA, de Baynast H, Delattre C, Pons A, *et al.*: **Wood-lignin: supply, extraction processes and use as bio-based material.** *Eur Polym J* 2019, **112**:228–240.
 10. Morales A, Labidi J, Gullón P: **Assessment of green approaches for the synthesis of physically crosslinked lignin hydrogels.** *J Ind Eng Chem* 2020, **81**:475–487.
 11. Thakur VK, Thakur MK: **Recent advances in green hydrogels from lignin: a review.** *Int J Biol Macromol* 2015, **72**:834–847.
 12. Meng Y, Lu J, Cheng Y, Li Q, Wang H: **Lignin-based hydrogels: a review of preparation, properties, and application.** *Int J Biol Macromol* 2019, **135**:1006–1019.
 13. Ilomuanya MO: **Hydrogels as biodegradable biopolymer formulations.** In *Biopolymer-based formulations – biomedical and food applications*. Edited by Pal K, Banerjee I, Sarkar P, Kim D, Deng WP, Dubey NK, *et al.*, Eds, Elsevier; 2020:561–585.
 14. Iravani S, Varma RS: **Greener synthesis of lignin nanoparticles and their applications.** *Green Chem* 2020, **22**: 612–636.
 15. Kun D, Pukánszky B: **Polymer/lignin blends: interactions, properties, applications.** *Eur Polym J* 2017, **93**:618–641.
 16. Yu Q, Kim KH: **Lignin to materials: a focused review on recent novel lignin applications.** *Appl Sci* 2020, **10**:4626.
- This publication reviews the recent research progress in lignin valorization, specifically focusing on medical, electrochemical, and 3D printing applications. The techno-economic assessment of lignin application is also discussed
17. Mohammadinejad R, Malekib H, Larrañeta E, Fajardo AR, Nik AB, Shavandif A, *et al.*: **Review Status and future scope of plant-based green hydrogels in biomedical engineering.** *Appl Mater. Today* 2019, **16**:213–246.
 18. Mazloom N, Khorassani R, Zohuri GH, Emami H, Whalen J: **Development and characterization of lignin-based hydrogel for use in agricultural soils: preliminary evidence, clean- soil, air, water.** 2019:1900101.
 19. Mazloom N, Khorassani R, Zohuri GH, Emami H, Whalen J: **Lignin-based hydrogel alleviates drought stress in maize.** *Environ Exp Bot* 2020, **175**:104055.
 20. Meng Y, Liu X, Li C, Liu H, Cheng Y, Lu J, Zhang K, Wang H: **Super-swelling lignin-based biopolymer hydrogels for soil water retention from paper industry waste.** *Int J Biol Macromol* 2019, **135**:815–820.
- This interesting work proposes a novel method for the valorization of the waste generated by pulp and paper industry by fabricating super-swelling biopolymer hydrogels from it. This study reports the first time that hydrogels are prepared by combining non-purified red liquor with acrylic acid, obtaining materials with super-swelling capacities and slow release behaviors in water.
21. Song B, Liang H, Sun R, Peng P, Jiang Y, She D: **Hydrogel synthesis based on lignin/sodium alginate and application in agriculture.** *Int J Biol Macromol* 2020, **144**:219–230.
 22. Wu L, Huang S, Zheng J, Qiu Z, Lin X, Qin Y: **Synthesis and characterization of biomass lignin-based PVA super-absorbent hydrogel.** *Int J Biol Macromol* 2019, **140**:538–545.
 23. Liu Y, Huang Y, Zhang C, Li W, Chen C, Zhang Z, *et al.*: **Nano-FeS incorporated into stable lignin hydrogel: a novel strategy for cadmium removal from soil.** *Environ Pollut* 2020, **264**: 114739.
 24. Qian H, Wang J, Yan L: **Synthesis of lignin-poly(N-methylaniline)-reduced graphene oxide hydrogel for organic dye and lead ions removal.** *J. Bioresour. Bioprod.* 2020, **5**: 204–210.
 25. Tahari N, de Hoyos-Martinez PL, Abderrabba M, Ayadi S, Labidi J: **Lignin - montmorillonite hydrogels as toluene adsorbent.** *Colloids Surf. A Physicochem. Eng. Asp.* 2020, **602**: 125108.
 26. Meng Y, Li C, Liu X, Lu J, Cheng Y, Xiao L-P, *et al.*: **Preparation of magnetic hydrogel microspheres of lignin derivate for application in water.** *Sci Total Environ* 2019, **685**:847–855.
 27. Domínguez-Robles J, Peresin MS, Tamminen T, Rodríguez A, Larrañeta E, Jääskeläinen A-S: **Lignin-based hydrogels with “super-swelling” capacities for dye removal.** *Int J Biol Macromol* 2018, **115**:1249–1259.
 28. Flores-Céspedes F, Villafranca-Sánchez M, Fernández-Pérez M: **Alginate-based hydrogels modified with olive pomace and lignin to remove organic pollutants from aqueous solutions.** *Int J Biol Macromol* 2020, **153**:883–891.
 29. H. Yuan, J. Peng, T. Ren, Q. Luo, Y. Luo, N. Zhang, *et al.*, Novel fluorescent lignin-based hydrogel with cellulose nanofibers and carbon dots for highly efficient adsorption and detection of Cr(VI), *Sci Total Environ* <https://doi.org/10.1016/j.scitotenv.2020.143395> (in press).
 30. Liu M, Liu Y, Shen J, Zhang S, Liu X, Chen X, *et al.*: **Simultaneous removal of Pb²⁺, Cu²⁺ and Cd²⁺ ions from wastewater using hierarchical porous polyacrylic acid grafted with lignin.** *J Hazard Mater* 2020, **392**:122208.
 31. Andrade Batista R, Perez Espitia PJ, de Souza Siqueira Quintans J, Machado Freitas M, Cerqueira MA, Teixeira JA, *et al.*: **Hydrogel as an alternative structure for food packaging systems.** *Carbohydr Polym* 2019, **205**:106–116.
 32. Spiridon I: **Biological and pharmaceutical applications of lignin and its derivatives: a mini-review.** *Cellul Chem Technol* 2018, **52**:543–550.
 33. Larrañeta E, Imízcoz M, Toh JX, Irwin NJ, Ripolin A, Perminova A, *et al.*: **Synthesis and characterization of lignin hydrogels for potential applications as drug eluting antimicrobial coatings for medical materials.** *ACS Sustain Chem Eng* 2018, **6**: 9037–9046.
 34. Yang W, Fortunati E, Bertoglio F, Owczarek JS, Bruni G, Kozanecki M, *et al.*: **Polyvinyl alcohol/chitosan hydrogels with enhanced antioxidant and antibacterial properties induced by lignin nanoparticles.** *Carbohydr Polym* 2018, **181**:275–284.
 35. Zhang Y, Yuan B, Zhang Y, Cao Q, Yang C, Li Y, *et al.*: **Bio-mimetic lignin/poly(ionic liquids) composite hydrogel dressing with excellent mechanical strength, self-healing properties, and reusability.** *Chem Eng J* 2020, **400**:125984.
- This work provides the design and synthesis of novel lignin/poly(ionic liquids) composite hydrogels with excellent mechanical strength, self-healing properties, bactericidal activity and antioxidant activity. It is stated that the supramolecular interactions between the lignin/poly(ionic liquids) compounds enhance the self-healing ability of the materials, and the introduction of lignin produces an improvement on their mechanical properties of the hydrogel dressing.
36. Musilová L, Mráček A, Kovalčík A, Smolka P, Minařík A, Humpolíček P, *et al.*: **Hyaluronan hydrogels modified by glycinated Kraft lignin: morphology, swelling, viscoelastic properties and biocompatibility.** *Carbohydr Polym* 2018, **181**: 394–403.
 37. Farhat W, Venditti R, Mignard N, Taha M, Becquart F, Ayoub A: **Polysaccharides and lignin based hydrogels with potential pharmaceutical use as a drug delivery system produced by a reactive extrusion process.** *Int J Biol Macromol* 2017, **104**: 564–575.
 38. Wang D, Lee SH, Kim J, Park CB: **“Waste to wealth”: lignin as a renewable building block for energy harvesting/storage and environmental remediation.** *ChemSusChem* 2020, **13**: 2807–2827.
- This work highlights the most recent advances in the development of lignin-based materials for energy and environmental applications, apart from reviewing its physico-chemical properties and possible modifications. The exposed applications include lithium-ion batteries, super-capacitors, solar cells, triboelectric nanogenerators and adsorbents.
39. Liu T, Ren X, Zhang J, Liu J, Ou R, Guo C, *et al.*: **Highly compressible lignin hydrogel electrolytes via double-crosslinked strategy for superior foldable supercapacitors.** *J Power Sources* 2020, **449**:227532.

Publication II

Assessment of green approaches for the synthesis of
physically crosslinked lignin hydrogels

A. Morales, J. Labidi, P. Gullón



Permission is not required for this non-commercial use.

<http://10.1016/j.jiec.2019.09.037>

1226-086X/© 2019 Published by Elsevier B.V. All rights reserved.

J. Ind. Eng. Chem. 81 (2020) 475-487



Contents lists available at ScienceDirect

Journal of Industrial and Engineering Chemistry

journal homepage: www.elsevier.com/locate/jiec

Assessment of green approaches for the synthesis of physically crosslinked lignin hydrogels

Amaia Morales, Jalel Labidi*, Patricia Gullón

Chemical and Environmental Engineering Department, University of the Basque Country UPV/EHU, Plaza Europa 1, 20018 San Sebastián, Spain



ARTICLE INFO

Article history:

Received 2 August 2019

Received in revised form 25 August 2019

Accepted 21 September 2019

Available online 28 September 2019

Keywords:

Lignin

Poly(vinyl alcohol)

Physical crosslinking

Hydrogels

Swelling

Mechanical properties

ABSTRACT

Lignin is an excellent candidate to be used as a starting material for hydrogel synthesis due to its highly functional character. The exhaustible character of the fossil resources linked to the increase of plastic residues in the environment encourages an intensive research on biorenewable and biodegradable polymers to synthesize new materials. Taking into account this current scenario, this work searches for new green routes to elaborate physical hydrogels with excellent capacity of swelling and suitable consistency. To this end, lignin and poly(vinyl alcohol) were blended in different proportions following a three-level-two-factorial design and using six different routes of crosslinking and drying for each set of experiments. The hydrogels formed under the optimal conditions were characterized by FTIR, SEM, XRD, DSC and TGA and their mechanical properties were also evaluated by compression tests. The selected optimum synthesis routes enabled the obtaining of physically crosslinked hydrogels with up to 800% water retention ability. FTIR spectra confirmed the interactions between lignin and PVA showing shifts and modifications on the characteristic bands of the raw polymers. Compression tests showed that all the hydrogels kept complete integrity even compressing them up to an 80% of their initial thickness.

© 2019 The Korean Society of Industrial and Engineering Chemistry. Published by Elsevier B.V. All rights reserved.

Introduction

Lignocellulosic biomass is mainly composed of carbohydrate polymers (cellulose and hemicellulose), and aromatic polymers (lignin and tannin) [1]. In recent years, these biorenewable polymers have attracted a greater attention of the research community due to the advantages such as eco-friendliness, low cost, biodegradability, etc.

Among these biorenewable polymers, lignin is the second most abundant and fascinating natural polymer next to cellulose. Lignin is primarily composed of three different phenylpropane units, namely, *p*-coumaryl, coniferyl and sinapyl alcohols. Different types of carbon–carbon/and carbon–oxygen bonds are formed between different monomer units in lignin [2]. Lignin can be obtained as a byproduct of the pulp and paper industry, bio-ethanol production and can be specifically generated in new biorefinery schemes [3], however, it is often burnt to generate energy for the process. Nevertheless, if added-value applications were searched for lignin, an integral valorisation of the lignocellulosic feedstock would be enabled and, hence, biorefineries would contribute to a circular economy.

The impressive properties of lignin, such as its high abundance, antioxidant, antimicrobial, and biodegradable nature, along with its CO₂ neutrality and reinforcing capability, make it an excellent candidate for chemical modifications and reactions as well as for the development of new biobased materials [4]. Lignin is, therefore, a low cost environmentally friendly feedstock with a great potential to be used as a starting material for hydrogel synthesis due to its highly functional character (i.e., rich in phenolic and aliphatic hydroxyl groups).

Hydrogels are three-dimensionally crosslinked polymeric networks with high water retention capacity which have significantly gained attention over the last 20 years [5]. They have been employed in many fields such as biomedicine or agriculture and they have become very interesting materials due to their adequate physic-chemical characteristics for many applications [6]. According to the type of crosslinking, they can be classified as physical (with physical entanglements or secondary forces) or chemical (with covalent bondages) hydrogels [5]. Chemical crosslinking is the highly resourceful method for the formation of hydrogels having an excellent mechanical strength but the crosslinkers used in hydrogel preparation should be extracted from the hydrogels before use due to their reported toxicity, which is a considerable inconvenience. Physical crosslinking methods for the preparation of hydrogels are the alternative solution to crosslinkers' toxicity and cost. They are usually formed by hydrogen bondages and

* Corresponding author.

E-mail address: jalel.labidi@ehu.es (J. Labidi).

electrostatic, hydrophobic and host-guest interactions [7]. However, due to the weak nature of these forces, these hydrogels are also known as reversible hydrogels and sometimes disintegrate and dissolve in water [8] and they can also be thermally reversible [9]. Nevertheless, the weakness problem can be solved by supramolecular chemistry [7,10] and the reversibility can be an advantage when talking about self-healable hydrogels, which have gained great interest in the last years [11,12]. Therefore, it is clear that physically crosslinked hydrogels present several benefits that chemically crosslinked ones do not, enabling at the same time a greener and a more economical synthesis process [13].

The increase of concern about the environmental and health impacts caused by the use of non-biodegradable polymers produced from fossil resources requires an urgent shift to renewable carbon-resource. This is why the possibility of synthesizing bio-based hydrogels has been investigated recently. The abundance and the cheapness of lignin, as well as the need to valorize it, have made lignin attractive to employ as a backbone polymer for hydrogel synthesis. Some authors have already incorporated lignin into hydrogels [14,15], but as it has a complex structure, it is difficult to design precise synthesis and obtain materials with the desired properties. Nevertheless, in spite of their brownish colour, the applicability of the lignin-based hydrogels is considerably wide (see Table 1). However, in most of the cases, chemical crosslinking has been performed and, hence, toxic reagents have been employed [2].

According to the aforementioned, the aim of this work was to find the optimum synthesis route to produce physical hybrid hydrogels based on biodegradable polymers via a greener synthesis route, avoiding the use of toxic chemical reagents. To this end, lignin was blended with poly(vinyl alcohol) (PVA), which is a biodegradable and non-toxic synthetic polymer [16]. In this way, the interactions between both components in the blend would enable the generation of highly hydrophilic three-dimensional networks. An experimental design was employed as the basis of the hydrogel synthesis, with lignin and PVA concentrations as input variables and lignin waste and swelling rate as output dependent variables. Three levels of the input variables were studied, which led to a factorial design of 3 levels, 3², with a triplicate central point. Eleven experiments were designed and they were subjected to six different synthesis pathways, varying the crosslinking method and curing method, in order to obtain the optimal lignin and PVA concentrations as well as the better synthesis routes to minimize the lignin waste and maximize the swelling rate. The accuracy of the six models was then evaluated by statistical analysis and, after selecting the best models, the hydrogels formed under the optimal conditions were characterized by Attenuated Total Reflection-Fourier Transformed Infrared Radiation (FTIR), Scanning Electron Microscopy (SEM), X-Ray Diffraction (XRD), Differential Scanning Calorimetry (DSC)

and Thermogravimetric Analysis (TGA). Their mechanical properties were also evaluated by compression tests.

Materials and methods

Materials

Alkaline lignin and poly(vinyl alcohol) (PVA, $M_w = 83,000$ – $124,000$ g/mol, 99+ % hydrolyzed) were supplied by Sigma Aldrich. Sodium hydroxide (NaOH, analytical grade, $\geq 98\%$, pellets) was purchased from PanReac Química SLU. All reagents were employed as supplied.

Hydrogel synthesis

Different hydrogels were synthesized according to the combinations designed by an experimental model (see Section “Model description”), in which the input variables were both the lignin and the PVA concentrations. All the hydrogels were prepared by adding the corresponding PVA amount (5, 8 or 11% (w/w)), i.e. 0.5, 0.8 or 1.1 g of PVA to 10 mL of a 2% NaOH aqueous solution, which was magnetically stirred and heated to 80–90 °C simultaneously. When the PVA pellets were dissolved, the corresponding amount of lignin (5, 15 or 25% (w/w), i.e. 0.5, 1.5 or 2.5 g) was incorporated under agitation until it was completely dissolved. Defined amounts of the blends were poured into silicon moulds and the bubbles on the surface were poked manually with a needle, while the ones trapped in the solution were eliminated by introducing the moulds into an ultrasound bath.

In order to study the influence of the synthesis paths, the blends were subjected to three different crosslinking (XL) methods: 3 and 5 cycles of freeze-thawing (16 h at -20 °C and 8 h at 28 °C) and inside a vacuum hood at 37 °C (-60 cm Hg) for a week. After the crosslinking stage, the hydrogels were separately washed in 50 mL of distilled water with orbital shaking several times. The washing was performed so as to eliminate the non-reacted lignin and the residual NaOH. Afterwards, the hydrogels were dried in two different ways: half of them were left to dry at room temperature while the other half dried under vacuum (-60 cm Hg) at 27 °C. These two drying or curing methods were employed in order to observe the influence of this stage (Fig. 1).

The hydrogels with the optimal compositions were prepared similarly employing the corresponding amounts of lignin and PVA into 15 mL of a 2% NaOH solution.

The six synthesis routes depicted in Fig. 2 represent the following used paths:

- (1) Vacuum XL + Air Drying (Vac-Air)
- (2) Vacuum XL + Vacuum Drying (Vac-Vac)
- (3) 5 Cycles of Freeze-Thawing XL + Air Drying (F-T x5-Air)

Table 1
Literature overview about hydrogels with lignin and their applications.

Crosslinking type	Interactions	Type of hydrogel	Polymers	Applications	References
Chemical	Ester bondages	Synthetic polymer based	Poly(methyl vinyl ether <i>co</i> -maleic acid) and different technical lignins	Water purification	[15]
Chemical	Ester bondages	Synthetic polymer based	Lignin and poly(ethylene glycol)/ poly(methyl vinyl ether- <i>co</i> -maleic acid)	Drug delivery	[35]
Chemical	Chemical crosslinker	Polysaccharide-based	Glycinated Kraft lignin and Hyaluronan	Tissue engineering	[36]
Chemical	Chemical crosslinker	Synthetic polymer based	Poly(vinyl alcohol), cellulose nanofibrils and lignin	Pressure sensors	[37]
Chemical	Chemical crosslinker	Polysaccharide-based	Agarose and Kraft lignin	Non determined	[29]
Physical	Co-dissolution in 1-ethyl-3-methylimidazolium acetate beads	Polysaccharide- based	Cellulose and lignin	Lipase immobilizers	[14]
Physical	Electrostatic interactions	Polysaccharide-based	Chitosan and lignin	Scaffolds in tissue engineering	[38]

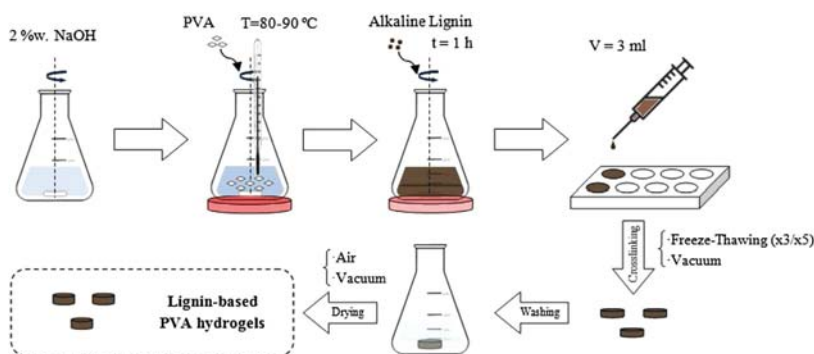


Fig. 1. Diagram of the experimental procedure of the hydrogel synthesis.

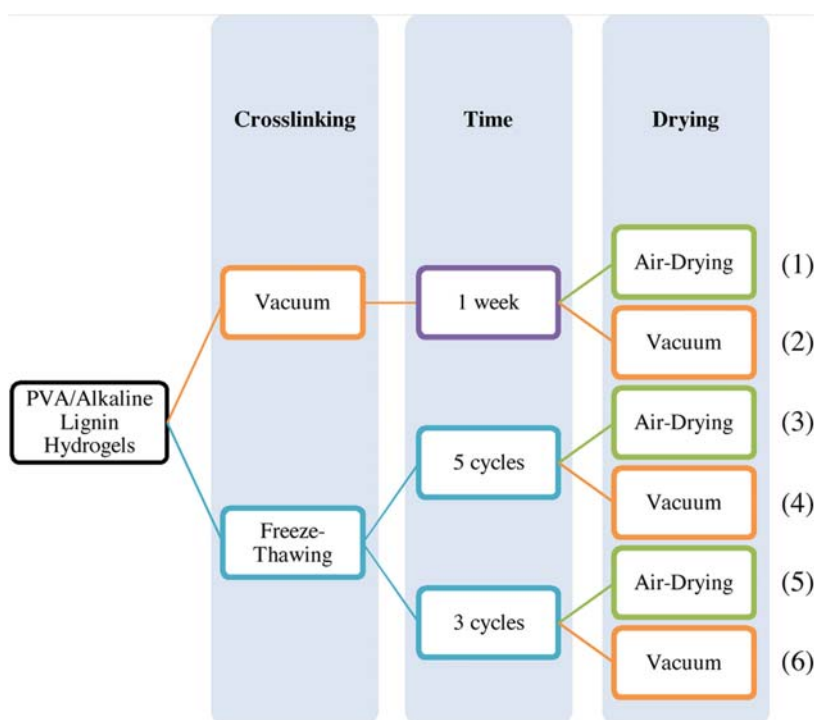


Fig. 2. Scheme of the six hydrogel synthesis pathways.

- (4) 5 Cycles of Freeze–Thawing XL + Vacuum Drying (F–T x5–Vac)
 (5) 3 Cycles of Freeze–Thawing XL + Air Drying (F–T x3–Air)
 (6) 3 Cycles of Freeze–Thawing XL + Vacuum Drying (F–T x3–Vac)

Model description

Three-level-two-factorial design with three replicates in the central point and a Response Surface Methodology (RSM) were employed to perform the optimization of the conditions of the lignin-hydrogel synthesis. The selected independent variables were both the alkaline lignin (x_1) and the PVA concentrations (x_2), which ranged from 5 to 25% (w/w) and from 5 to 11% (w/w), respectively. These ranges were chosen on the basis of previous

experiments (data not shown). The response variables were the swelling capacity of the hydrogels (% , y_1) and the lignin waste during the washing stage (% , y_2). Moreover, the accuracy of each of the models would also help to select the best synthesis route. Eleven experiments were designed for each pathway considering the selected parameter values and the triplicate central point (see Table 2), so sixty six experiments were carried out in total. Experimental data were fitted using a second-order polynomial described by Eq. (1):

$$y_j = \beta_0 + \beta_1 x_1 + \beta_2 x_2 + \beta_{11} x_1^2 + \beta_{22} x_2^2 + \beta_{12} x_1 x_2 \quad (1)$$

where y_j are the dependent variables ($j = 1-2$), β_0 , β_1 , β_2 , β_{11} , β_{22} and β_{12} are the regression coefficients calculated from the experimental results by the least-squares method, and x_1 and x_2 are the

Table 2
Experimental design.

Experiment #	x ₁	x ₂	Alkaline lignin (% w/w)	PVA (% w/w)
1	-1	-1	5	5
2	-1	0	5	8
3	-1	1	5	11
4	0	-1	15	5
5	0	0	15	8
6	0	0	15	8
7	0	0	15	8
8	0	1	15	11
9	1	-1	25	5
10	1	0	25	8
11	1	1	25	11

dimensionless, normalized independent variables, with variation ranges from -1 to 1. Experimental data were fitted using the regression analysis function of Microsoft Excel's Data Analysis Add-In, USA. The adequacy of the model was determined by evaluating the lack of fit, the coefficient of determination (R^2) and the F-test value obtained from the analysis of variance.

To generate the experimental design, the statistical analysis and the regression model, Statgraphics Centurion version XVI (Statpoint Technologies Inc., Warrenton, VA, USA) software was employed. The figures were reproduced using OriginPro®9 (OriginLab Corp., Northampton, MA, USA). The models were validated by carrying out the experiments at the optimal points and comparing the results obtained experimentally with the predicted data.

Hydrogel characterization

Lignin waste

First, a calibration curve was performed by employing five lignin solutions (10 mL) prepared in 2% (w/w) NaOH with known concentrations (0.25, 0.5, 1.5, 2.5 and 5.0 mg lignin/mL solution) and a V-630 UV-Jasco spectrophotometer. In order to fix the correct wavelength to measure the absorbance of the samples, a preliminary scan was performed from 760 to 250 nm. Thus, the measurements were done at 515 nm and each absorbance was related to the concentration of the prepared dissolutions. In this way, a calibration curve was obtained, which corresponded to Eq. (2):

$$A_{515nm} = 0.7643 \cdot [\text{Lignin}] \quad (2)$$

The hydrogels were washed in 50 mL of distilled water until the water was clear, for 24–30 h approximately. During the washing stage, aliquots were taken each time and the washing water was changed every 2–3 h. The concentrations of the aliquots were calculated from the measured absorbance at 515 nm. Finally, taking the volume of each rinse into account, the total lignin loss was calculated.

Swelling

The hydrogels were weighted in dry state and immersed in 40 mL of distilled water for 48 h. For the swelling kinetics, the hydrogels were weighted at certain times, removing the water remaining on the surface with filter paper. The swelling degree was calculated from the following Eq. (3) [6]:

$$\text{Swelling (\%)} = \frac{m_{\text{swollen}} - m_{\text{dry}}}{m_{\text{dry}}} \cdot 100 \quad (3)$$

in which m_{swollen} and m_{dry} are the masses of swollen and dry hydrogels, respectively.

Attenuated Total Reflection-Fourier Transformed Infrared Radiation (ATR-FTIR)

In order to study and verify the interactions between the polymers, a PerkinElmer Spectrum Two FT-IR Spectrometer

equipped with a Universal Attenuated Total Reflectance accessory with internal reflection diamond crystal lens was used to collect Infrared spectra of the hydrogels. The studied range was from 600 to 4000 cm^{-1} and the resolution was 8 cm^{-1} . 20 scans were recorded for each grated dry sample.

Scanning Electron Microscopy (SEM)

SEM analyses were carried out in order to study the morphology of the hydrogels. The samples were swollen in water for 48 h at room temperature and then frozen at -20°C . Afterwards, they were freeze-dried in an Alpha 1–4 LD freeze drier. The images of secondary electrons were taken with a MEB JEOL 7000-F. The working conditions were 5 kV and an intensity of 0.1 nA. The samples were covered with 20 nm of Cr by sputtering technique.

X-Ray Diffraction (XRD)

X-Ray Powder Diffraction tests were carried out using a Phillips X'Pert PRO automatic diffractometer operating at 40 kV and 40 mA, in theta-theta configuration. Monochromatic Cu-K α ($\lambda = 1.5418 \text{ \AA}$) radiation and a PIXcel solid-state detector (active length in 2θ 3.347°) were employed. The collected data ranged from 5 to 80° 2θ at room temperature. The step size was 0.026 and the time per step was 80 s. 0.04 rad soller slit and fixed 1° divergence slit giving a constant volume of sample illumination were employed. The samples were subjected to XRD analysis grated and in dry state.

The approximate size (D) of crystallites was calculated using the Scherrer equation (Eq. (4)):

$$D = \frac{k \cdot \lambda}{\beta \cdot \cos \theta} \quad (4)$$

where D is the mean size of ordered domains (nm), k is the Scherrer constant (0.9), λ is the X-ray wavelength (0.154 nm) and β is the full-width at half-maximum of the reflection (FWHM) measured in 2θ of the corresponding Bragg angle [17,18].

Differential Scanning Calorimetry (DSC)

DSC analyses were done on a Mettler Toledo DSC 822 (Mettler Toledo, Spain). Between 3–5 mg of dry grated samples were subjected to a heating ramp from -25°C to 225°C at a rate of $10^\circ\text{C}/\text{min}$ under a nitrogen atmosphere to avoid oxidative reactions inside aluminium pans. After the first heating step, cooling and second heating stages were also performed. The glass transition temperature (T_g), was considered as the inflection point of the specific heat increment during the second heating scan. The calibration was performed with indium standard. The degree of crystallinity (χ_c) was obtained from the enthalpy evolved during crystallization using Eq. (5) [19]:

$$\chi_c = \frac{\Delta H}{\Delta H_0 \cdot (1 - m_{\text{filler}})} \cdot 100 \quad (5)$$

where ΔH , is the apparent enthalpy for melting or crystallization, ΔH_0 is the melting enthalpy of 100% crystalline PVA (average value: 161.6 J/g) and $(1 - m_{\text{filler}})$ is the weight percent of PVA in the hydrogels [19].

Thermogravimetric Analysis (TGA)

TGA analyses were done on a TGA/SDTA 851 Mettler Toledo (Mettler Toledo, Spain) instrument. Around 7 mg of dry grated sample were subjected to a heating ramp of $25^\circ\text{C}/\text{min}$ from room temperature up to 800°C under a nitrogen atmosphere inside platinum pans.

Compression studies

Uniaxial compression tests were performed on the hydrogels in order to assess their mechanical strength. A compression gear was

set up on an Instron 5967 machine using a 500 N load cell with a crosshead speed of 2 mm/min. Square samples of around 5×5 mm were cut from the initial hydrogels, which were left to swell during 48 h at room temperature. Then, the samples were compressed up to the 80% of their initial thickness. This strain was selected according to other works and the limitations of the compression test equipment caused by the thicknesses of the samples. The swollen modulus, G_e , of each sample was calculated automatically by employing Eq. (6) [20,21]

$$\sigma = \frac{F}{A} = G_e \cdot \left(\lambda - \frac{1}{\lambda^2} \right) \quad (6)$$

where F is the force, A is the original cross sectional area of the swollen hydrogel, and $\lambda = L/L_0$ where L_0 and L are the thicknesses of the samples before and after compression, respectively.

Results and discussion

Modelling and optimization of hydrogel composition

In order to obtain the best hydrogel formulations and the best synthesis route, the optimization of the input variables was addressed using the three-level-two-factorial design combined with Response Surface Methodology for the six synthesis pathways. The results for the all the measured swelling capacities and lignin wastes are shown in Table 3. The six optimal concentrations for the maximum swelling and the minimum lignin waste calculated by the software, as well as the predicted values of the response variables, are shown in Table 4. The optimal conditions of the six paths were verified by the triplicate synthesis of the hydrogels.

Table 5 shows the regression coefficients obtained for each model according to a second-degree polynomial equation, their statistical significance (based on a Student's t-test), the parameters measuring the correlation (R^2) and statistical significance (Fisher's

F test) of the models. The value determined for R^2 for most of the variables was higher than 0.86, which would indicate that the model was adequate to represent the real relationships among the selected variables [22], but in some other cases this value was lower than 0.82. Moreover, the estimated significance levels confirm the regular fit of the data. The values for each equation term were calculated in order to assess the contribution of their linear interaction, and quadratic effects of the independent variables. Employing the calculated significant regression coefficients at the 90% confidential level, two quadratic regression equations were set up, one for each output variable (y_1 -Swelling and y_2 -Lignin waste), for the six models. Hence, twelve equations were obtained in total Eqs. (7)–(18):

(1) Vacuum XL + Air Drying (Vac-Air):

$$y_{1(\text{Swelling } \%)} = 778.78 + 40.67x_1 - 64.45x_2 - 344.30x_1^2 + 42.65x_2^2 - 16.27x_1x_2 \quad (7)$$

$$y_{2(\text{Lignin Waste } \%)} = 80.99 - 0.93x_1 - 3.34x_2 - 10.18x_1^2 - 2.91x_2^2 + 6.19x_1x_2 \quad (8)$$

(2) Vacuum XL + Vacuum Drying (Vac-Vac)

$$y_{1(\text{Swelling } \%)} = 1144.76 + 46.89x_1 - 146.12x_2 - 686.08x_1^2 + 100.40x_2^2 - 26.17x_1x_2 \quad (9)$$

$$y_{2(\text{Lignin Waste } \%)} = 80.99 - 0.93x_1 - 3.34x_2 - 10.18x_1^2 - 2.91x_2^2 + 6.19x_1x_2 \quad (10)$$

Table 3
Values of the response variables for the six synthesis paths.

	(1) Vac-Air		(2) Vac-Vac		(3) F-T x5-Air		(4) F-T x5-Vac		(5) F-T x3-Air		(6) F-T x3-Vac	
	Swelling (%)	Ligning waste (%)	Swelling (%)	Ligning waste (%)	Swelling (%)	Ligning waste (%)	Swelling (%)	Ligning waste (%)	Swelling (%)	Ligning waste (%)	Swelling (%)	Ligning waste (%)
E1	454.52	77.90	467.93	77.90	732.94	77.90	411.06	77.90	968.07	68.90	910.01	68.90
E2	435.68	72.43	512.54	72.43	757.72	72.43	656.48	72.43	659.40	44.89	712.96	44.89
E3	376.51	59.03	455.68	59.03	562.00	59.03	553.42	59.03	397.16	44.49	463.58	44.49
E4	909.86	79.82	1647.59	79.82	970.53	79.82	314.48	79.82	779.88	68.08	380.05	68.08
E5	754.12	85.15	1172.55	85.15	905.98	85.15	434.21	85.15	584.94	66.49	674.16	66.49
E6	764.04	80.53	947.88	80.53	965.14	80.53	473.91	80.53	532.82	71.26	627.44	71.26
E7	806.91	80.81	1256.51	80.81	865.27	80.81	537.01	80.81	584.92	76.28	479.17	76.28
E8	744.23	72.79	900.06	72.79	704.59	72.79	372.25	72.79	367.62	65.20	521.91	65.20
E9	604.65	66.15	686.14	66.15	666.55	66.15	370.30	66.15	489.03	60.14	440.44	60.14
E10	444.50	65.63	462.15	65.63	534.15	65.63	432.10	65.63	512.94	48.40	505.00	48.40
E11	461.56	72.02	569.20	72.02	513.25	72.02	535.53	72.02	795.10	44.52	739.20	44.52

Table 4
Optimal conditions and predicted/experimental values for the response variables.

Synthesis route	Alkaline lignin (% w/w)	PVA (% w/w)	Predicted value		Experimental average value		Error (%)	
			Swelling (%)	Ligning waste (%)	Swelling (%)	Ligning waste (%)	Swelling (%)	Ligning waste (%)
(1)	23.02	5	710.29	69.17	345.30	81.16	51.39	-17.34
(2)	22.26	5	1083.59	70.88	199.26	82.75	81.61	-16.74
(3)	9.12	9.87	770.14	58.11	789.89	51.94	-2.57	10.63
(4)	5	10.39	587.82	49.09	567.06	41.06	3.53	16.35
(5)	25	11	719.77	46.71	659.67	45.77	8.35	2.02
(6)	25	11	729.51	46.71	547.93	44.12	24.90	5.55

Table 5
Regression coefficients and statistical parameters measuring the correlation and significance of the models.

	(1) Vac–Air		(2) Vac–Vac		(3) F–T x5–Air		(4) F–T x5–Vac		(5) F–T x3–Air		(6) F–T x3–Vac	
	Y ₁	Y ₂	Y ₁	Y ₂	Y ₁	Y ₂	Y ₁	Y ₂	Y ₁	Y ₂	Y ₁	Y ₂
β ₀	778.78	80.99	1144.76	80.99	902.17	69.08	468.74	69.08	552.83	68.70	557.40	68.70
β ₁	40.67 ^b	−0.93	46.89	−0.93	−56.45	−1.83	−47.17	−1.83	−37.92	−0.87	−66.98	−0.87
β ₂	−64.45 ^a	−3.34	−146.12	−3.34	−98.37 ^b	−10.58 ^a	60.89 ^c	−10.58 ^a	−112.85 ^b	−7.15 ^c	−0.96	−7.15 ^c
β ₁₁	−344.30 ^a	−10.18 ^a	−686.08 ^a	−10.18 ^a	−241.29 ^a	−14.26 ^a	95.02 ^c	−14.26 ^a	55.44	−18.08 ^b	105.88	−18.08 ^b
β ₂₂	42.65	−2.91	100.40	−2.91	−49.67	0.03	−105.90 ^c	0.03	43.03	1.91	−52.12	1.91
β ₁₂	−16.27	6.19 ^b	−26.17	6.19 ^b	4.41	1.49	5.72	1.49	219.24 ^a	2.20	186.30 ^b	2.20
R ²	0.98	0.92	0.86	0.92	0.93	0.90	0.76	0.90	0.89	0.82	0.77	0.82
F-exp	50.93	11.12	5.96	11.12	13.53	9.22	3.24	9.22	8.467	4.44	3.32	4.44
S.L.* (%)	99.97	99.03	96.39	99.03	99.37	98.54	88.87	98.54	98.24	93.61	89.29	93.61

* Significance level.

^a Significant coefficients at the 99% confidence level.

^b Significant coefficients at the 95% confidence level.

^c Significant coefficients at the 90% confidence level.

(3) 5 cycles of Freeze–Thawing XL + Air Drying (F–T x5–Air)

$$Y_{1(\text{Swelling \%})} = 902.17 - 56.45x_1 - 98.37x_2 - 241.29x_1^2 - 49.67x_2^2 + 4.41x_1x_2 \quad (11)$$

$$Y_{2(\text{Lignin Waste \%})} = 69.08 - 1.83x_1 - 10.58x_2 - 14.26x_1^2 + 0.03x_2^2 + 1.49x_1x_2 \quad (12)$$

(4) 5 cycles of Freeze–Thawing XL + Vacuum Drying (F–T x5–Vac)

$$Y_{1(\text{Swelling \%})} = 468.74 - 47.17x_1 + 60.89x_2 + 95.02x_1^2 - 105.90x_2^2 + 5.72x_1x_2 \quad (13)$$

$$Y_{2(\text{Lignin Waste \%})} = 69.08 - 1.83x_1 - 10.58x_2 - 14.26x_1^2 + 0.03x_2^2 + 1.49x_1x_2 \quad (14)$$

(5) 3 cycles of Freeze–Thawing XL + Air Drying (F–T x3–Air)

$$Y_{1(\text{Swelling \%})} = 552.83 - 37.92x_1 - 112.85x_2 + 55.44x_1^2 + 43.03x_2^2 + 219.24x_1x_2 \quad (15)$$

$$Y_{2(\text{Lignin Waste \%})} = 68.70 - 0.87x_1 - 7.15x_2 - 18.08x_1^2 + 1.91x_2^2 + 2.20x_1x_2 \quad (16)$$

(6) 3 cycles of Freeze–Thawing XL + Vacuum Drying (F–T x3–Vac)

$$Y_{1(\text{Swelling \%})} = 557.40 - 66.98x_1 - 0.96x_2 + 105.88x_1^2 - 52.12x_2^2 + 186.30x_1x_2 \quad (17)$$

$$Y_{2(\text{Lignin Waste \%})} = 68.70 - 0.87x_1 - 7.15x_2 - 18.08x_1^2 + 1.91x_2^2 + 2.20x_1x_2 \quad (18)$$

Influence of the input variables on the swelling capacity

For the Vac–Air synthesis pathway, the minimum value (376%) was for experiment 3 while the maximum (909%) was registered for experiment 4 (see Table 3). For the Vac–Vac synthesis route, the minimum was also for experiment 3 (455%) whereas the maximum was for experiment 4 (1647%) too. Based on these results, it could be observed that despite being the minimum and maximum values for the same experiments, the type of drying has an effect on the swelling capacity, in fact, vacuum drying enhances it. It is worth to mention that experiment 4 had a film-like shape, so the contact surface with water was higher and this is why it was so swollen. However, for the other two vacuum dried routes, vacuum reduced the subsequent swelling rate of the hydrogels. In the case of F–T x5–Air synthesis, the minimum was found on experiment 11 (513%) and the maximum value was again for experiment 4 (970%). At the F–T x5–Vac synthesis, the minimum was observed for experiment 4 (314%) while the maximum value was for experiment 2 (656%). The swelling ability for the F–T x3–Air experiments ranged from 367 to 968%, being the minimum for the experiment 8 and the maximum for experiment 1. The values for F–T x3–Vac hydrogels were in the interval of 380–910 %, where the minimum value corresponded to experiment 4 whereas the maximum corresponded to experiment 1.

According to the regression coefficients (Table 5), it could be seen that the two input variables had an influence on the swelling capacity. Specifically, x₂ (PVA concentration) had a significant influence on this output variable, as well as the quadratic effect of x₁ (lignin concentration). The interaction between both input variables was also important in the case of the F–T x3–Air and F–T x3–Vac. The quadratic effect of x₂ presented a high influence on F–T x5–Vac synthesis. Ciolacu et al. (2017) and Yang et al. (2018) did also report that the swelling capacity depends on the composition of the hydrogels [18,23].

The surface plots for synthesis routes (1), (2) and (3) showed that for a fixed concentration of PVA, as lignin content was augmented, the swelling capacity of the hydrogel tended to increase (see Supplementary data). However, after a certain concentration of lignin, the swelling capacity decreased. So, it was found that the maximum point was in between the extreme concentrations of lignin. It is also worth to mention that the swelling ability was displayed to be higher for lower PVA concentrations, but the response variable was much more influenced by the lignin content than by PVA one. This behavior could be due to the high influence of the quadratic term of lignin on the swelling equations [22]. The optimal conditions for routes (1),

(2) and (3) were 15.8% lignin and 5% PVA, 15.5% lignin and 5% PVA and 13.7% lignin and 5.3% PVA, subsequently.

The surface plots for synthesis routes (4), (5) and (6) showed that for a fixed concentration of PVA, as lignin content was augmented, the swelling capacity of the hydrogel tended to decrease (see Supplementary data). Nevertheless, after a certain concentration of lignin, the swelling capacity started to increase again. Therefore, the surfaces presented a minimum in between the extreme contents of lignin and, therefore, the highest swelling capacities were found on the upper and lower concentration limits. Thus, the optimal conditions for the achievement of the highest swelling capacities following the routes (4), (5) and (6) were 5% lignin and 8.8% PVA, 5% lignin and 5% PVA and 5% lignin and 5% PVA, subsequently. In these three surfaces, however, no clear dominant variable was observed, since the quadratic terms did not have such a high significance level.

It was clearly seen that the addition of lignin did, in all cases, have a positive effect on the swelling properties of the PVA hydrogels. This fact was confirmed by the synthesis and characterization of the blank hydrogels, i.e., neat PVA hydrogels with concentrations of 5, 8 and 11% PVA and the same crosslinking and drying pathways than the ones with lignin. In fact, the swelling ratio of these materials did not almost overpass the 350%. This behaviour may be attributed to the size of the attached lignin molecules, since they are high molecular weight chains and they can lead to the creation of bigger pores, which can permit the penetration of more water molecules [18,24]. This fact would justify the incorporation of lignin into water absorbent polymeric materials. Ciolacu et al. also reported the same behaviour for their PVA-lignin chemically crosslinked hydrogels [18]. Yang et al. also confirmed that lignin improved the swelling ability of chitosan-PVA hydrogels [25].

Influence of the input variables on the lignin waste

The lignin waste of the 11 experiments in Vac–Air and Vac–Vac synthesis pathways were in the interval of 59–85%. The minimum value was found for experiment 3 while the maximum was registered for experiment 5 (see Table 3). For the F–T x3–Air and F–T x3–Vac synthesis routes, the minimum was for experiment 11 (42%) whereas the maximum was for experiment 7 (76%). In the case of F–T x5–Air synthesis, the minimum was found on experiment 3 (44%) and the maximum value was again experiment 7 (76%). It could be observed that the freeze–thawing method permits the retention of more lignin inside the matrix than the vacuum crosslinking. Moreover, the ranges in both freeze–thawing routes were very similar.

For the Vac–Air and Vac–Vac synthesis routes the most influencing regression coefficients on the lignin waste were the quadratic effect of x_1 and the interaction between both input variables x_1x_2 . In the other four synthesis pathways, the most significant regression coefficients were the quadratic effect of x_1 and x_2 (PVA concentration) itself. Therefore, it can be concluded that the PVA content directly affects lignin waste. To the best of our knowledge, no data has been collected within the literature about the lignin waste during the washing stage into account when characterizing hydrogels. Hence, this statement cannot be contrasted with any other work.

The surface plots for all synthesis routes showed that for a fixed concentration of PVA, as lignin content was augmented (see Supplementary data), the lignin waste during the washing stage of the hydrogels tended to increase. This behaviour could be related to the addition of reactive sites and a higher crosslinking rate between both components. However, after a certain concentration of lignin, the lignin waste decreased. So, it could also be said here that the maximum points were found in between the extreme concentrations of lignin. It is also worth to mention that the

swelling ability was tended to be higher for higher PVA concentrations; however, the response variable was much more influenced by the lignin content due to the significance level of its quadratic term. For the six routes, the optimal concentrations for the minimum lignin wastes were 5% lignin and 11% PVA (Vacuum XL, routes (1) and (2)), 25% lignin and 11% PVA (F–T x5 XL, routes (3) and (4)) and 5% lignin and 11% PVA (F–T x3 XL, routes (5) and (6)).

Optimization of the synthesis conditions and validation of the model

The objective of the optimization was to determine the formulations that would provide simultaneously the greatest swelling capacity and the lowest lignin waste during the washing stage via the six synthesis routes. Statgraphics Centurion XV software was used to carry out the optimization. For this aim, the values of the responses of each variable were converted using a desirability function. This function was considered to disclose the combination of the synthesis variables that maximize the swelling capacity and minimize the lignin waste at the same time. The optimum conditions for the independent variables as well as the predicted and experimental results for the response variables are displayed in Table 4.

The suitability of the response surface methodology model for quantitative predictions could only be verified by the agreement of the predicted and experimental values in two of the six synthesis routes. The errors in the output swelling variable were higher than a 4% in all the cases except for the two 5-times-freeze–thawed routes. However, the lowest errors in lignin waste were observed for the 3-times-freeze–thawed samples. The optimum formulations were repeated again in case the error was experimental, but similar results were obtained. Nevertheless, as the accuracy on swelling was considered more important than lignin waste and, as one of the aims of the optimization was to obtain the best synthesis route, the two via 5 freeze–thawing cycles were selected as the optimum pathways. Hence, the samples obtained via these two optimal routes were subjected to further characterization (namely 3 and 4 samples), together with their equivalent neat PVA hydrogels (namely 3.0 and 4.0). The swelling kinetics of these four samples are shown in Fig. 3.

Hydrogel characterization

Attenuated Total Reflection-Fourier Transformed Infrared Radiation (ATR-FTIR)

The two best optimal hydrogels (the ones obtained via the routes 3 and 4) were analyzed by FTIR technique. Fig. 4 represents the spectra of both of them (namely 3 and 4) along with the spectra of neat PVA hydrogels (namely 3.0 and 4.0), commercial PVA and alkaline lignin. As it can be seen, there was no significant difference between both hydrogels without lignin, since the employed PVA was the same and the only difference was the quantity used for their synthesis. These hydrogels showed the characteristic peaks of commercial PVA (see Table 6), and the peak around 2855 cm^{-1} , which was a small shoulder in the commercial PVA spectrum, got intensified. This band corresponds to the stretching C–H from alkyl groups, as reported by Mansur et al. [26]. A peak did also appear at around 1545 cm^{-1} , which was attributed to C–O bondages, probably created when dissolving it into water [27].

As for the hydrogels containing lignin, there was not any notable variation between their spectra due to the use of identical components for the blends. The lignin hydrogels presented similar peaks to these shown by the neat PVA hydrogels, but some bands appeared or were shifted due to the interactions with alkaline lignin (see Table 7). The band around 2920 cm^{-1} , for example, lost intensity, and was divided into two peaks at 2945 and 2916 cm^{-1} , probably due to the interactions with lignin, which presented two

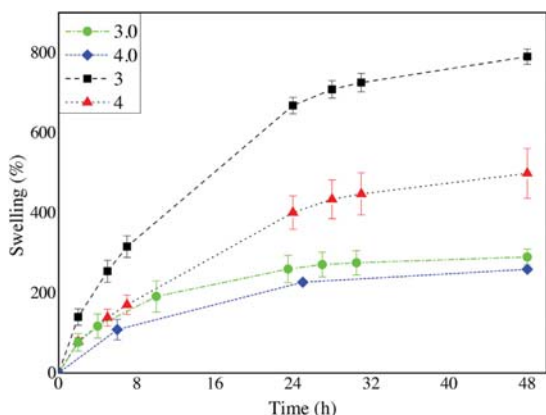


Fig. 3. Swelling performance of the hydrogels during the first 48 h.

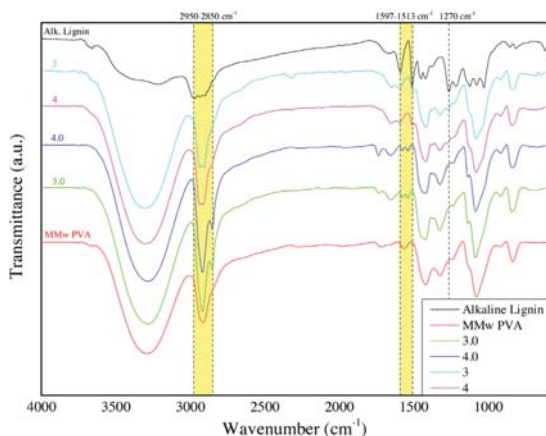


Fig. 4. FTIR of commercial PVA, commercial alkaline lignin and the selected hydrogels with (samples 3 and 4) and without lignin (samples 3.0 and 4.0).

bands at 2947 and 2913 cm^{-1} . These bands correspond to alkyl asymmetric and aromatic C—H stretch vibrations, and also to the intramolecular hydrogen bonds. Moreover, the peak corresponding to the ester C=O bonds (at 1720 cm^{-1}) lost intensity, and the one belonging to the C=C stretch vibration at around 1570 cm^{-1} shifted to higher wavenumbers due to the intense band presented by lignin at 1597 cm^{-1} . The band appearing around 1545 cm^{-1} shifted to lower wavenumbers, probably due to the interactions with

Table 6
Characteristic FTIR peaks of PVA.

Wavenumber (cm^{-1})	Assignment
3300	—OH stretch vibration
2920	Alkyl asymmetric C—H stretch vibration
2855	Symmetric C—H stretch vibration
1720	Ester C=O stretch vibration
1660	Residual C=O stretch vibration
1560	C=C stretch vibration
1425	CH_2 bending vibration
1325	O—H deformation vibration
1100	C—C stretching vibration
840	C—C and C—O stretching vibration

Table 7
Characteristic FTIR peaks of alkaline lignin.

Wavenumber (cm^{-1})	Assignment
3215	—OH stretch vibration
2947	Alkyl asymmetric vibration
2913	Aromatic C—H stretching vibration
1679	C=O ester bonds
1597	C=C stretch vibration
1513	C=C aromatic vibrations
1456	C—H bonds of the methyl groups
1429	C—H bonds of the methyl groups
1269	Guaiacyl units
1100	C—C bonds
1030	C—O stretching vibration
865	C—C stretching vibration
821	aromatic —CH out of plane vibration
618	C—S bonds

lignin, which presented a strong peak around 1513 cm^{-1} that corresponded to the C=C aromatic vibrations [28]. Around 1275 cm^{-1} , a shoulder did also appear, which could be related to the intense lignin peak at 1270 cm^{-1} and belonged to the guaiacyl units [29]. The band at 1100 cm^{-1} also got intensified, meaning that new C—C bonds might have been created and the peak at 840 cm^{-1} was enhanced too, which corresponded to C—O stretching vibrations.

The weak band at 618 cm^{-1} means that the commercial alkaline lignin contains carbon-sulphur bonds, which are characteristic of Kraft lignin [29].

Scanning Electron Microscopy (SEM)

SEM micrographs of the freeze-dried neat PVA and PVA-lignin hydrogels at two magnifications (250 \times and 2500 \times) are shown in Fig. 5. For all the analyzed samples highly porous structures and different pore size distributions could be observed. However, it seemed that for the neat PVA hydrogels (Fig. 5A–D) the morphology was more homogeneous than that for the lignin-PVA hydrogel (Fig. 5E and F). In addition, some macro-pores did also appear on the sample without lignin that was vacuum-dried (sample 4.0, Fig. 5C and D), indicating that apart from the crosslinking method [16], the curing method also affected the morphology. This behaviour was also reported by Dominguez-Robles et al. [15] for straw alkaline lignin solved in soda and crosslinked with poly(methyl vinyl ether co-maleic acid). Thombare et al. [24] explained that the macro-pores often allow a facile penetration of water into the polymeric network, which would be the cause of a rapid initial swelling ability. Once the macro-pores have been filled, water starts to diffuse gradually through micro-pores. This could have happened in the case of the blank hydrogels, since they presented considerably big pores. However, this observation was not done here; in fact, lignin hydrogels presented a higher water swelling capacity in all cases (see Fig. 3). Moreover, the walls that interconnect the micro voids amongst the sample with lignin are much smoother and more brittle than the ones presented by neat PVA in samples 3.0 and 4.0. This microstructure in PVA can be associated with its strong intra and inter-molecular hydrogen bonds [30]. Yang et al. also described a similar result on the SEM characterization of their PVA/Chitosan hydrogels [25].

As deduced from the micrographs, the majority of the pores presented by neat PVA hydrogels were smaller than 1 μm , while the ones presented by lignin-based hydrogels were larger. This fact would confirm the previous statement about the size of the pores created due to the high molecular weight of lignin and its repercussion on the swelling capacity (Section “Influence of the input variables on the swelling capacity”) [18]. Furthermore, unlike in the case of other authors [25], no lignin agglomerates were

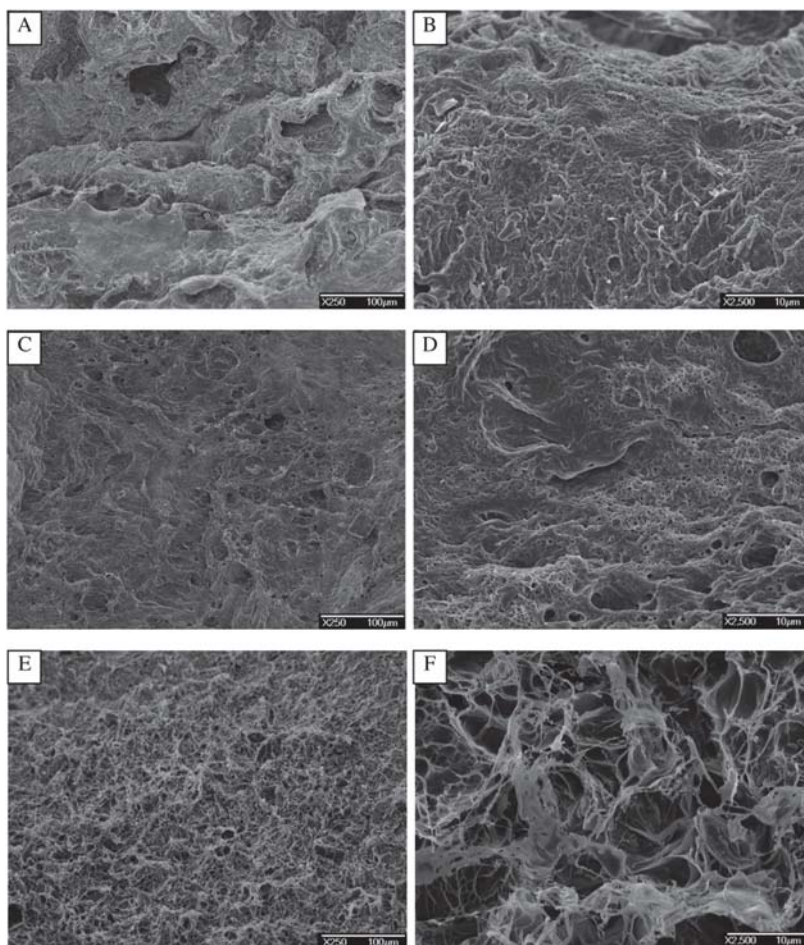


Fig. 5. SEM micrographs of the samples 3.0, 4.0 and 4 at 250 \times (A, C and E) and 2500 \times (B, D and F) magnifications.

found in the SEM images, which confirmed the good miscibility between the components [31].

X-Ray Diffraction (XRD)

The X-Ray Diffractograms for lignin, neat PVA hydrogels and lignin-PVA hydrogels are depicted in Fig. 6. Neat PVA hydrogels presented their characteristic crystalline peaks. As previously reported [18,32], a strong peak was observed at $2\theta = 19.77^\circ$, which corresponded to the (101) lattice plane, followed by a shoulder around 22.78° , corresponding to the (201) plane. Two weak peaks were also appreciated at 11.5° (attributed to the plane (100)) and 40.8° .

Lignin is an amorphous polymer and its diffractogram presented an intense broad peak at around 19° as shown in Fig. 6. Goudarzi et al. also reported a similar maximum diffraction angle for softwood Kraft lignin [17]. As lignin was incorporated to the hydrogels, the semicrystalline structure of PVA was slightly modified, although the main peaks did not disappear [18]. When lignin was added into the hydrogels, the strong signal at 19.77° was broadened, meaning that the crystalline regions of these hydrogels

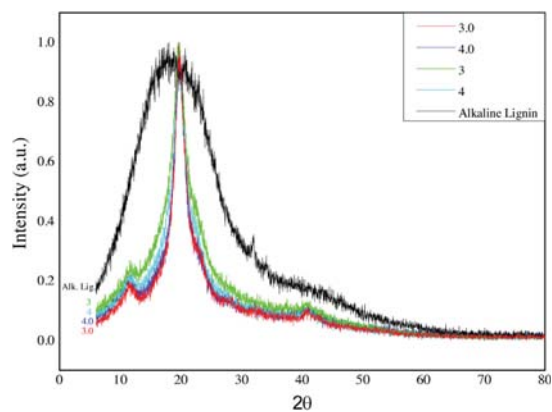


Fig. 6. XRD diffractograms of the hydrogels 3.0, 4.0, 3, 4 and commercial alkaline lignin.

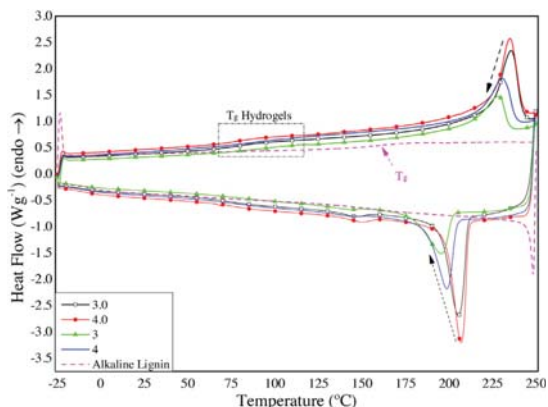


Fig. 7. DSC thermograms of the first cooling stage and second heating stage of hydrogels 3.0, 4.0, 3, 4 and commercial alkaline lignin.

were lessened and the degree of crystallinity was, therefore, decreased. This fact was also confirmed by DSC analyses.

In order to calculate the mean size of the crystallites, which are the ordered domains in a polymer, Scherrer's equation was employed (Eq. (4)). Measuring the width at half of the main crystalline peak, the estimated crystallite size for both blank and lignin-hydrogels was lower than 5 nm. In addition, the notably wide peak of the lignin would mean that the crystallite size was significantly smaller than the ones in the hydrogels, since lignin is an amorphous biopolymer and usually has few ordered domains. Thus, the only conclusion we could get from these results was that all the crystallites were smaller than 5 nm and that the values calculated by any crystallinity equation would not be representative for the samples [33], although some authors have published these results [17,18].

Differential Scanning Calorimetry (DSC)

DSC analyses were performed in order to analyze the thermal properties of the synthesized hydrogels. The results for the analyzed parameters during the cooling and the second heating stages (T_c , ΔH_c , T_g , T_m , ΔH_m and χ_c) are summarized in Table 8, and the DSC curves for these stages are also shown in Fig. 7.

After removing the thermal history of the samples with the first heating scan, the appearance of a single T_g indicated a good blend miscibility [25], as previously observed in the SEM micrographs. This fact was noticed in all the analysed hydrogels. For neat PVA hydrogels (samples 3.0 and 4.0), the T_g values were similar (73.10 and 68.24 °C, successively). When lignin was incorporated into the samples, for hydrogels 3 and 4, the T_g values increased up to around

85 °C. This could be a consequence of the interactions such as hydrogen bonds between PVA and lignin, which could have restricted the chain mobility [19].

The T_m also got modified with the addition of lignin. Neat PVA hydrogels melted at around 236 °C, while the hydrogels containing lignin presented the fusion peak at around 230 °C. This behaviour is also an evidence of the good miscibility of the components [19]. As for the crystallization temperature (T_c), the addition of lignin also caused a decrease on it. In fact, the T_c of the neat PVA samples was placed around 205 °C and the one for the hydrogels with lignin at around 195 °C. Moreover, the crystallization enthalpy was also diminished from around 55 and 58 J/g (for samples 3.0 and 4.0, subsequently) to 27 and 41 J/g for samples 3 and 4, subsequently. This was attributed to the diminution of the crystalline regions as lignin was incorporated, which was also confirmed by the reduction on the melting enthalpy at the second heating scan. Thus, the degree of crystallinity (χ_c) was calculated from the latest data and Eq. (5). The results confirm that χ_c decreased with lignin the addition [19], since the values for neat PVA samples (21.63 and 23.04% for samples 3.0 and 4.0, subsequently) were around 1.5% higher than the ones for the lignin samples (20.10 and 21.56% for samples 3 and 4, subsequently). Moreover, the crystallinity degrees of the samples 3 and 3.0 were below the ones reported for 4 and 4.0, probably due to a lower PVA content and higher lignin content in the case of sample 3. However, it is important to bear in mind that these values derive from the second heating scan, so the initial crystallinity would be slightly higher. These results were in accordance with the ones obtained from XRD analysis. As previously reported [31], it is known that when an amorphous polymer is blended with a semicrystalline polymer, the degree of its crystallinity decreases, and this statement was also confirmed in this case.

Thermogravimetric Analysis (TGA)

TG and DTG curves of lignin, neat PVA hydrogels and lignin-PVA hydrogels are shown in Fig. 8A and 8B. The onset and maximum degradation temperatures, as well as the char residue at the end of the test are summarized in Table 9. Thermogravimetric studies were done in order to investigate the effect of lignin on the degradation of the blended hydrogels. For neat PVA hydrogels (3.0 and 4.0), four weight loss stages were observed. The first one appeared at around 150 °C and it was attributed to the evaporation of the adsorbed bound water [25]. A second stage was detected at around 250 °C, which still left an 85% of residue and belonged to the initial degradation of the polymer. The maximum weight loss and, hence, the major degradation was viewed at around 375 °C, corresponding to the depolymerization of the acetylated and deacetylated units of the polymer [25]. This stage was followed by another weight loss at 440 °C, achieved to the thermal degradation of some by-products generated by PVA, and a final residue of around 2.6% was accounted [25].

Commercial alkaline lignin presented a constant weight loss; however, the temperature of the maximum degradation was

Table 8
Summarized results for the analyzed parameters by DSC and calculations.

Sample	Cooling scan			2 nd Heating scan					
	T_c (°C)	ΔH_c (W ^o C/g)	ΔH_c (J/g)	T_g (°C)	T_m (°C)	ΔH_m (W ^o C/g)	ΔH_m (J/g)	m_{filler} (%)	χ_c (%)
3.0	204.50	18.29	54.87	76.43	236.53	11.65	34.95	0	21.63
4.0	205.93	19.30	57.90	79.37	235.90	12.41	37.23	0	23.04
3	195.30	8.90	26.70	87.07	228.63	7.81	23.43	0.28	20.10
4	198.17	13.80	41.40	88.80	230.43	9.22	27.66	0.21	21.56

T_c : crystallization temperature; T_g : glass transition temperature; ΔH_m : melting enthalpy; χ_c : crystallinity degree; ΔH_c : crystallization enthalpy; T_m : melting temperature; m_{filler} : filler mass percentage.

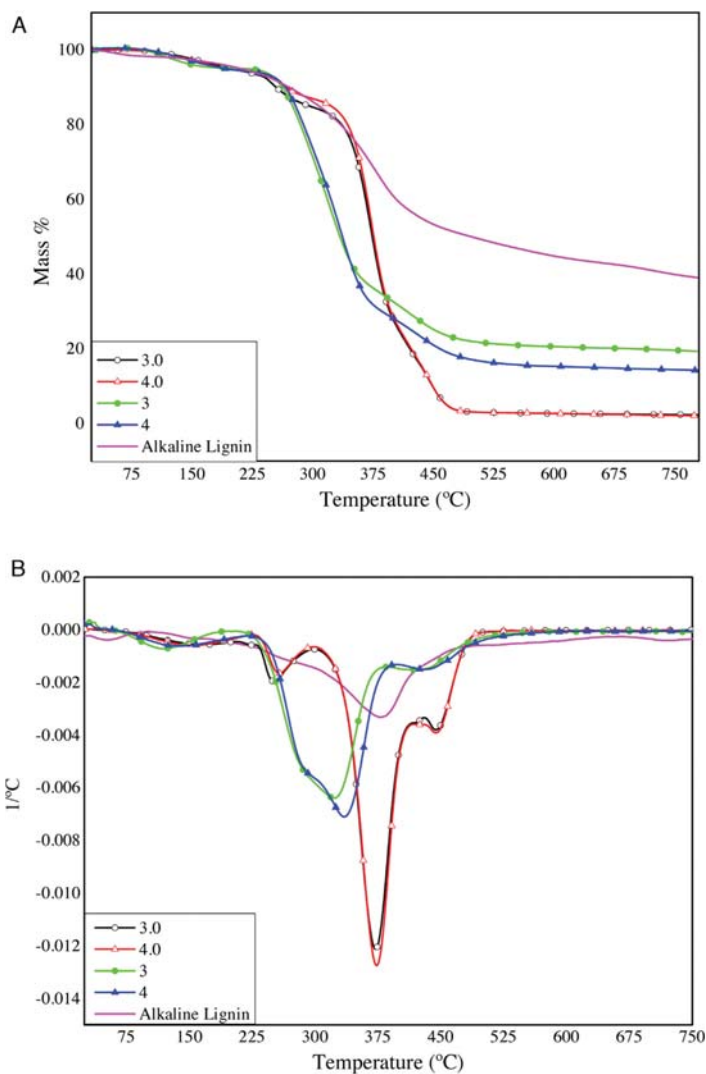


Fig. 8. (A) TG and (B) DTG curves of hydrogels 3.0, 4.0, 3, 4 and commercial alkaline lignin.

registered at 380 °C. No other significant degradation stages were detected and the final residue left was high, since it was almost of 40%. This implies that commercial alkaline lignin has many inorganic impurities, and would confirm the possibility of containing carbon-sulphur traces, as previously stated in Section “Attenuated Total Reflection-Fourier Transformed Infrared Radiation (ATR-FTIR)”.

Table 9

Onset and maximum degradation temperatures and residue after TGA.

Sample ID	T _{onset} (°C)	T _{max} (°C)	Residue (%)
AL	172.0	380.0	39.0
3.0	225.0	372.5	2.7
4.0	230.5	374.0	2.6
3	217.0	323.0	19.5
4	223.0	334.5	14.7

When lignin was incorporated, the hydrogels presented three main weight loss stages, but there was a fourth stage which overlapped with the second one, as shown in Fig. 8B. The first stage was observed at around 120 °C and it was as well attributed to moisture evaporation. The main degradation stage appeared around 330 °C, but it was overlapped with the one at 280 °C. This loss might have been the one appearing at 250 °C in the case of neat PVA, but as lignin was incorporated, the thermal stability was enhanced and, hence, it could have shifted to higher temperatures. Hu et al. [34] explained this behaviour as the possible introduction of aromatic structures of lignin into PVA chains via strong hydrogen bonds. After the main degradation step, another loss was detected around 430 °C, which was shifted to a lower temperature than in the previous case. The residue left for both lignin hydrogels was between 14–20 %, which was directly related to lignin.

Table 10
Results for the compression tests of the samples.

Sample	Young's compression modulus (MPa)	Standard deviation (MPa)
3.0	77.57	8.40
4.0	41.64	3.42
3	18.75	0.53
4	29.21	6.18

Compression tests

The compression tests of the samples were studied and the calculated data from the stress–strain curves for compression to 80% of the initial thickness are shown in Table 10. At the maximum deformation, none of the samples were broken; in fact, all the samples had an excellent ability of integrity and recovery. This could be due to the accommodation of the stress by the rearrangement of the polymeric chains and the retractable elastic forces developed consequently [6]. Nevertheless, there were some variations in the estimated modulus. For the blank hydrogels (3.0 and 4.0) the reported moduli were of around 77.6 and 41.7 MPa, respectively. When lignin was added to the samples, the modulus decreased to around 18.8 and 29.2 MPa for samples 3 and 4, subsequently. Therefore, as lignin was incorporated, the moduli of the hydrogels were reduced despite the different drying method, making the samples less rigid. This could be related to the pore-size of the samples and would confirm what was concluded for the swelling capacity; in other words, when lignin was blended with PVA, greater pores were generated due to the reduction of interactions within PVA which, at the same time, enhanced the adsorption of water and made the hydrogel less compact and rigid [25]. Nonetheless, the obtained modulus for the PVA-lignin samples would be high enough to support the weight of soil layers if the final application was agricultural, for instance.

Conclusions

The optimization of the synthesis conditions of lignin-based PVA hydrogels was successfully carried out employing a three-level-two-factorial design. The statistical analysis showed that the PVA and lignin concentrations had great impact on the lignin waste during the washing stage and on the swelling capacity of the synthesized hydrogels. The selected optimum synthesis routes enabled the obtaining of physically crosslinked hydrogels with up to 800% water retention ability and a lignin waste between 40–50%. The interactions between lignin and PVA were confirmed by the shifts and modifications on the FTIR bands. The SEM images permitted the observance of a different porous microstructure when lignin was added, which was responsible of the high swelling capacity. XRD analyses indicated the disappearance of some crystalline regions as amorphous lignin was incorporated, which was also confirmed by DSC and TGA techniques. Compression tests showed that, although Young's modulus was more than halved as lignin content increased, all the hydrogels kept complete integrity even compressing them up to an 80% of their initial thickness. In conclusion, physically crosslinked greener lignin hydrogels were synthesized via two methods, which had great water retention capacities as well as good thermal and mechanical properties, meaning they could be applied in many fields.

Acknowledgements

The authors would like to acknowledge the financial support of the Department of Education of the Basque Government (IT1008-16). A. Morales would like to thank the University of the Basque

Country (Training of Researcher Staff, PIF17/207). P. Gullón would like to express her gratitude to MINECO for financial support (Grant reference IJCI-2015-25304). The authors thank for technical and human support provided by SGIker (UPV/EHU/ ERDF, EU).

Appendix A. Supplementary data

Supplementary material related to this article can be found, in the online version, at doi:<https://doi.org/10.1016/j.jiec.2019.09.037>.

References

- [1] S. Laurichesse, L. Avérous, *Prog. Polym. Sci.* 39 (7) (2014) 1266, doi:<http://dx.doi.org/10.1016/j.progpolymsci.2013.11.004>.
- [2] V.K. Thakur, M.K. Thakur, *Int. J. Biol. Macromol.* 72 (2015) 834, doi:<http://dx.doi.org/10.1016/j.jbiomac.2014.09.044>.
- [3] M.H. Sipponen, H. Lange, C. Crestini, A. Henn, M. Österberg, *ChemSusChem* 12 (10) (2019) 2038, doi:<http://dx.doi.org/10.1002/cssc.201901218>.
- [4] V.K. Thakur, M.K. Thakur, P. Raghavan, M.R. Kessler, *ACS Sustain. Chem. Eng.* 2 (5) (2014) 1072, doi:<http://dx.doi.org/10.1021/sc500087z>.
- [5] M. Mahinroosta, Z. Jomeh Farsangi, A. Allahverdi, Z. Shakoori, *Mater. Today Chem.* 8 (2018) 42, doi:<http://dx.doi.org/10.1016/j.mtchem.2018.02.004>.
- [6] M.R. Guilherme, F.A. Aouada, A.R. Fajardo, A.F. Martins, A.T. Paulino, M.F.T. Davi, A.F. Rubira, E.C. Muniz, *Eur. Polym. J.* 72 (2015) 365, doi:<http://dx.doi.org/10.1016/j.eurpolymj.2015.04.017>.
- [7] L. Voorhaar, R. Hoogenboom, *Chem. Soc. Rev.* 45 (14) (2016) 4013, doi:<http://dx.doi.org/10.1039/c6cs00130k>.
- [8] P. Vashisth, V. Pruthi, *Mater. Sci. Eng. C* 67 (2016) 304, doi:<http://dx.doi.org/10.1016/j.msec.2016.05.049>.
- [9] M. Li, X. Jiang, D. Wang, Z. Xu, M. Yang, *Colloids Surf. B Biointerfaces* 177 (September 2018) (2019) 370, doi:<http://dx.doi.org/10.1016/j.colsurfb.2019.02.029>.
- [10] Y. Geng, X.Y. Lin, P. Pan, G. Shan, Y. Bao, Y. Song, Z.L. Wu, Q. Zheng, *Polymer (Guildf)* 100 (2016) 60, doi:<http://dx.doi.org/10.1016/j.polymer.2016.08.022>.
- [11] B. Gyarmati, B.Á. Szilágyi, A. Szilágyi, *Eur. Polym. J.* 93 (March) (2017) 642, doi:<http://dx.doi.org/10.1016/j.eurpolymj.2017.05.020>.
- [12] Z. Gao, L. Duan, Y. Yang, W. Hu, G. Gao, *Appl. Surf. Sci.* 427 (2018) 74, doi:<http://dx.doi.org/10.1016/j.apsusc.2017.08.157>.
- [13] A. Oryan, A. Kamali, A. Moshiri, H. Baharvand, H. Daemi, *Int. J. Biol. Macromol.* (2017), doi:<http://dx.doi.org/10.1016/j.jbiomac.2017.08.184>.
- [14] S. Park, S.H. Kim, J.H. Kim, H. Yu, H.J. Kim, Y.H. Yang, H. Kim, Y.H. Kim, S.H. Ha, S. H. Lee, *J. Mol. Catal. B Enzym.* 119 (2015) 33, doi:<http://dx.doi.org/10.1016/j.molcatb.2015.05.014>.
- [15] J. Domínguez-Robles, M.S. Peresin, T. Tamminen, A. Rodríguez, E. Larrañeta, A. S. Jääskeläinen, *Int. J. Biol. Macromol.* 115 (2018) 1249, doi:<http://dx.doi.org/10.1016/j.jbiomac.2018.04.044>.
- [16] A. Kumar, S.S. Han, *Int. J. Polym. Mater. Polym. Biomater.* 66 (4) (2017) 159, doi:<http://dx.doi.org/10.1080/00914037.2016.1190930>.
- [17] A. Goudarzi, L.-T. Lin, F.K. Ko, *J. Nanotechnol. Eng. Med.* 5 (2) (2014) 021006, doi:<http://dx.doi.org/10.1115/1.4028300>.
- [18] D. Ciolacu, G. Cazacu, *J. Nanosci. Nanotechnol.* 18 (4) (2018) 2811, doi:<http://dx.doi.org/10.1166/jnn.2018.14290>.
- [19] X. He, F. Luzi, X. Hao, W. Yang, L. Torre, Z. Xiao, Y. Xie, D. Puglia, *Int. J. Biol. Macromol.* 127 (2019) 665, doi:<http://dx.doi.org/10.1016/j.jbiomac.2019.01.202>.
- [20] S.A. Bencherif, A. Srinivasan, F. Horkay, J.O. Hollinger, K. Matyjaszewski, *N.R. Washburn, Biomaterials* 29 (12) (2008) 1739, doi:<http://dx.doi.org/10.1016/j.biomaterials.2007.11.047>.
- [21] M.N. Collins, C. Birkinshaw, *J. Mater. Sci. Mater. Med.* 19 (11) (2008) 3335, doi:<http://dx.doi.org/10.1007/s10856-008-3476-4>.
- [22] B. Gullón, P. Gullón, T.A. Lú-Chau, M.T. Moreira, J.M. Lema, G. Eibes, *Ind. Crops Prod* 108 (April) (2017) 649, doi:<http://dx.doi.org/10.1016/j.indcrop.2017.07.014>.
- [23] M. Yang, M.S.U. Rehman, T. Yan, A.U. Khan, P. Oleskowicz-Popiel, X. Xu, P. Cui, J. Xu, *Bioresour. Technol.* 249 (October 2017) (2018) 737, doi:<http://dx.doi.org/10.1016/j.biortech.2017.10.055>.
- [24] N. Thombare, S. Mishra, M.Z. Siddiqui, U. Jha, D. Singh, G.R. Mahajan, *Carbohydr. Polym.* 185 (October 2017) (2018) 169, doi:<http://dx.doi.org/10.1016/j.carbpol.2018.01.018>.
- [25] W. Yang, E. Fortunati, F. Bertoglio, J.S. Owczarek, G. Bruni, M. Kozanecki, J.M. Kenny, L. Torre, L. Visai, D. Puglia, *Carbohydr. Polym.* 181 (October 2017) (2018) 275, doi:<http://dx.doi.org/10.1016/j.carbpol.2017.10.084>.
- [26] H.S. Mansur, C.M. Sadahira, A.N. Souza, A.A.P. Mansur, *Mater. Sci. Eng. C* 28 (4) (2008) 539–548, doi:<http://dx.doi.org/10.1016/j.msec.2007.10.088>.
- [27] S. Karimi, J. Feizy, F. Mehrjo, M. Farrokhnia, *RSC Adv.* 6 (27) (2016) 23085–23093, doi:<http://dx.doi.org/10.1039/c5ra25983e>.
- [28] A. Morales, B. Gullón, I. Dávila, G. Eibes, J. Labidi, P. Gullón, *Ind. Crops Prod.* 124 (2018), doi:<http://dx.doi.org/10.1016/j.indcrop.2018.08.032>.
- [29] S. Sathawong, W. Sridach, K.A. Techato, *J. Environ. Chem. Eng.* 6 (5) (2018) 5879–5888, doi:<http://dx.doi.org/10.1016/j.jece.2018.05.008>.
- [30] L.Y. Wang, M.J. Wang, *ACS Sustain. Chem. Eng.* 4 (5) (2016) 2830, doi:<http://dx.doi.org/10.1021/acscuschemeng.6b00336>.
- [31] K.J. Lee, J. Lee, J.Y. Hong, *J. Jang, Macromol. Res.* 17 (7) (2009) 476, doi:<http://dx.doi.org/10.1007/BF03218895>.

- [32] H. Dai, H. Zhang, L. Ma, H. Zhou, Y. Yu, T. Guo, Y. Zhang, H. Huang, *Carbohydr. Polym.* 209 (381) (2019) 51, doi:<http://dx.doi.org/10.1016/j.carbpol.2019.01.014>.
- [33] A. Morales, M.Á. Andrés, J. Labidi, P. Gullón, *Ind. Crops Prod.* 131 (2019), doi:<http://dx.doi.org/10.1016/j.indcrop.2019.01.071>.
- [34] X.-Q. Hu, D.-Z. Ye, J.-B. Tang, L.-J. Zhang, X. Zhang, *RSC Adv.* 6 (17) (2016) 13797, doi:<http://dx.doi.org/10.1039/C5RA26385A>.
- [35] E. Larrañeta, M. Imízcoz, J.X. Toh, N.J. Irwin, A. Ripolin, A. Perminova, J. Domínguez-Robles, A. Rodríguez, R.F. Donnelly, *ACS Sustain. Chem. Eng.* 6 (7) (2018) 9037, doi:<http://dx.doi.org/10.1021/acssuschemeng.8b01371>.
- [36] L. Musilová, A. Mráček, A. Kovalčík, P. Smolka, A. Minařík, P. Humpolíček, R. Vícha, P. Ponižil, *Carbohydr. Polym.* 181 (October 2017) (2018) 394, doi:<http://dx.doi.org/10.1016/j.carbpol.2017.10.048>.
- [37] H. Bian, L. Jiao, R. Wang, X. Wang, W. Zhu, H. Dai, *Eur. Polym. J.* 107 (August) (2018) 267, doi:<http://dx.doi.org/10.1016/j.eurpolymj.2018.08.028>.
- [38] K. Ravishankar, M. Venkatesan, R.P. Desingh, A. Mahalingam, B. Sadhasivam, R. Subramaniam, R. Dhamodharan, *Mater. Sci. Eng. C* 102 (January) (2019) 447, doi:<http://dx.doi.org/10.1016/j.msec.2019.04.038>.

Assessment of green approaches for the synthesis of physically crosslinked lignin hydrogels

Amaia Morales, Jalel Labidi*, Patricia Gullón

Chemical and Environmental Engineering Department, University of the Basque Country UPV/EHU, Plaza Europa 1, 20018, San Sebastián, Spain

Supplementary Data

Figure S1: Response surfaces for the swelling capacity of paths 1, 2, 3, 4, 5 and 6 (A, B, C, D, E and F, subsequently).

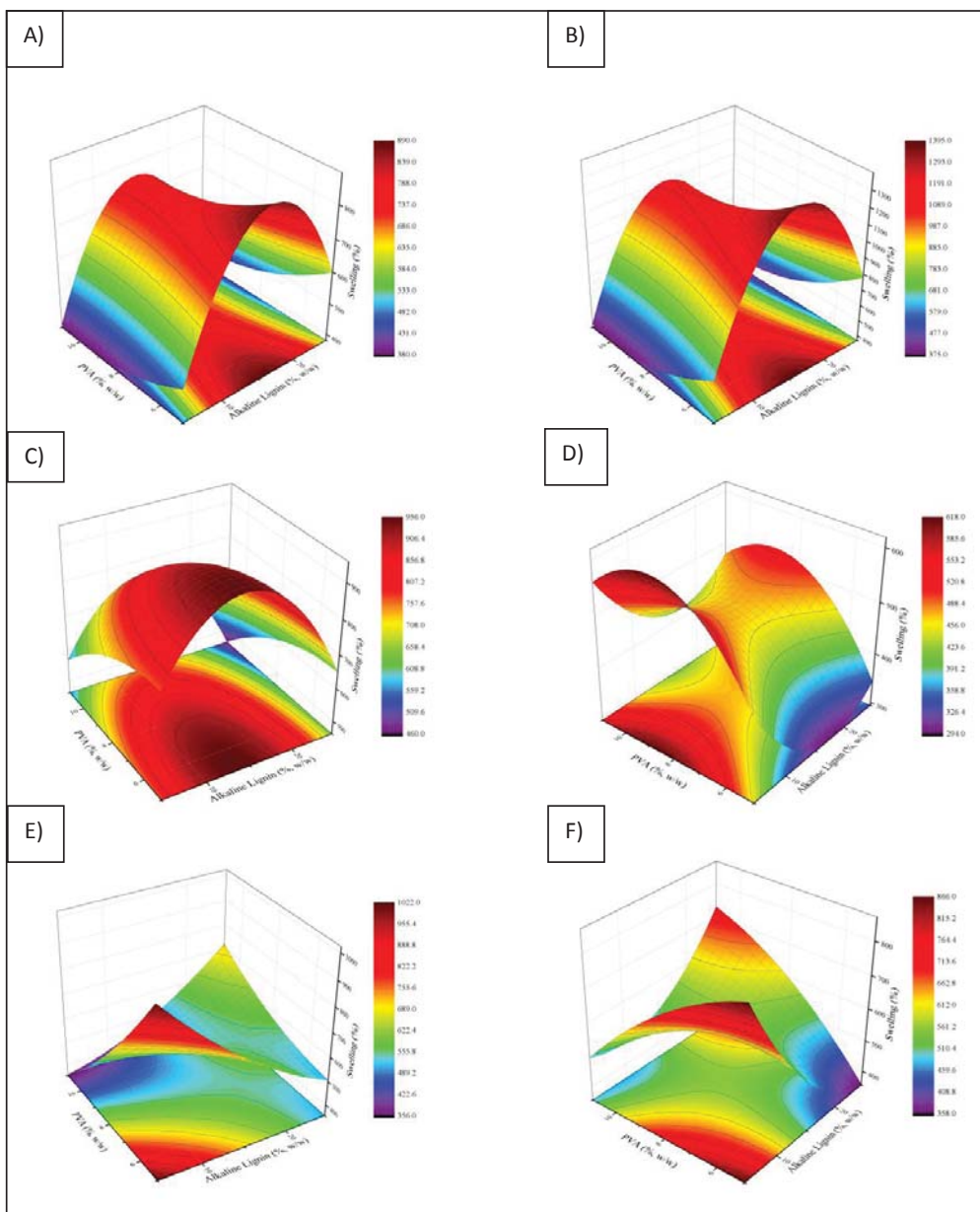
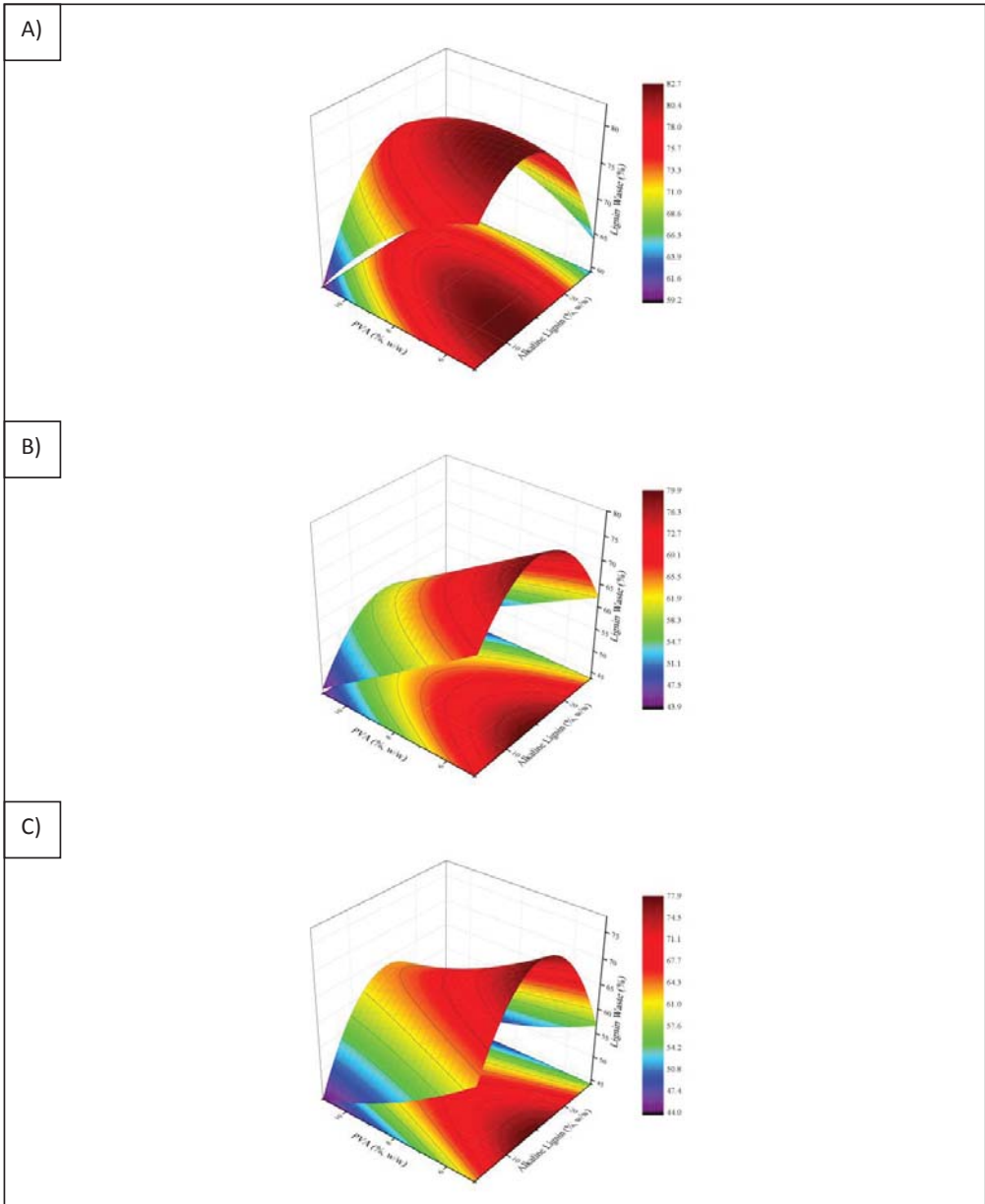


Figure S2: Response surfaces for the lignin waste of paths 1 and 2 (A), 3 and 4 (B) and 5 and 6 (C).



Publication III

Effect of the formulation parameters on the absorption capacity of smart lignin-hydrogels

A. Morales, J. Labidi, P. Gullón



Permission is not required for this non-commercial use.

<http://10.1016/j.eurpolymj.2020.109631>

0014-3057/© 2020 Elsevier Ltd. All rights reserved.

Eur. Polym. J. 129 (2020) 109631



Contents lists available at ScienceDirect

European Polymer Journal

journal homepage: www.elsevier.com/locate/europolj

Effect of the formulation parameters on the absorption capacity of smart lignin-hydrogels

Amaia Morales, Jalel Labidi*, Patricia Gullón

Chemical and Environmental Engineering Department, University of the Basque Country UPV/EHU, Plaza Europa 1, 20018 San Sebastian, Spain



ARTICLE INFO

Keywords:

Lignin
Poly (vinyl alcohol)
Molecular weight
Physical crosslinking
Hydrogels
Swelling

ABSTRACT

Hydrogels have become very popular in the last decades and they are widely employed in many application fields. Physically crosslinked hydrogels lack of toxic and expensive reagents and, thus, they enable a greener and a more economical synthesis process. Till date, many biopolymers have been explored for hydrogel synthesis, but lignin has promised to be a potential one for this aim. To this end, lignin and three different molecular weight PVA ($M_w = 13,000\text{--}23,000$ g/mol, 87–89% hydrolyzed; $M_w = 83,000\text{--}124,000$ g/mol, 99+ % hydrolyzed and $M_w = 130,000$ g/mol, 99+ % hydrolyzed) were blended in optimized concentrations via two routes of crosslinking. Only the two highest molecular weight PVAs enabled a successful crosslinking. The swelling capacity of the hydrogels in water as well as in four other mediums showed that lignin enhanced the water absorption capacity and the pH and temperature responsiveness. In addition, it was seen that the swelling rate and the lignin waste of the obtained hydrogels were directly influenced by the molecular weight of the employed PVA. Moreover, the re-swelling capacity of the hydrogels suggested that these materials could be re-used. The differences in pore size and morphology in SEM analyses were in accordance with the behaviour of the samples in compression tests. Additionally, lignin promoted dye adsorption capacity.

1. Introduction

The industrial development and the dizzying growth of the world population are provoking the depletion of fossil resources. This situation has led to the current environmental problems as consequence, among others, of the greenhouse gases derived from mankind activities and the presence of huge amounts of plastics in oceans with disastrous effects causing the deterioration of the different ecosystems of the planet. An attempt to change this current scenario is the transition from fossil fuels to the biorenewable biomass as a source of raw materials to obtaining chemical platforms, energy, and polymers as base of materials. For this, in the last decades, the efforts of researchers have been addressed towards the development of green and sustainable materials based on biorenewable polymers, what it is of prime interest from the environment, social, politician and economic point of view.

Among these polymers, lignin, one of the main components of lignocellulosic materials, is the most abundant aromatic biopolymer in the world. It is an amorphous copolymer [1], synthesized from random polymerization of trans-*p*-coumaryl, coniferyl and sinapyl alcohols, and it is obtained in huge amounts as a by-product in pulp and paper industry. Lignin is often burnt to produce energy or discarded as waste and, despite its abundance, only a minor proportion of the total volume

produced in the forest industry is recovered for added value applications. Its recalcitrant character makes the development of adequate technologies for its use a great challenge for the researchers. Additionally, lignin presents several advantages facing other bio-polymers such as low cost and biodegradability. Therefore, the use of lignin for the synthesis of added-value compounds would mean a significant step forward, especially in the context of the biorefinery processes as it would contribute to a circular economy.

Recently, many authors have reported the use of lignin as starting material for the synthesis of hydrogels. It is well known that hydrogels are three-dimensionally crosslinked polymeric networks with high water retention capacity. Due to this property and other physico-chemical characteristics, they have significantly gained attention during the last decades [2] and they have already been employed in many fields such as biomedicine or agriculture [3].

Most of the lignin-based hydrogels described in the literature are synthesized through chemical crosslinking [4–7], which usually involves many disadvantages such as toxicity, need of removing the residual crosslinker and more expensive reagents than the ones used for physical crosslinking [8]. Hence, the production of greener hydrogels from the physical crosslinking of lignin would be interesting in order to revalorize this abundant by-product.

* Corresponding author.

E-mail address: jalel.labidi@ehu.es (J. Labidi).<https://doi.org/10.1016/j.eurpolymj.2020.109631>

Received 18 February 2020; Received in revised form 17 March 2020; Accepted 18 March 2020

Available online 20 March 2020

0014-3057/ © 2020 Elsevier Ltd. All rights reserved.

Physically crosslinked hydrogels, compared to chemically cross-linked ones, lack of toxic and sometimes expensive crosslinking reagents, which is an advantageous fact. As a consequence, physical crosslinking enables a greener and a more economical synthesis process [8].

Due to the increasing concern about the environmental impact that synthetic plastics have caused, the possibility of producing bio-based and biodegradable materials such as hydrogels is currently being investigated. Bio-based hydrogels are environmentally friendly and biocompatible in comparison with the fossil-based hydrogels [9].

In this work, two of the previously studied synthesis routes [10] were employed combining commercial alkaline lignin with three different molecular weight poly (vinyl alcohol) via 3 and 5 cycles of freeze-thawing. This was done in order to study the influence of the molecular weight of the blending polymer and the time of the cycles on the properties of the final hydrogels, especially on the swelling capacity and the lignin waste.

The hydrogels that were successfully formed were characterized by FTIR, SEM, XRD, DSC and TGA. Their mechanical properties were also evaluated by compression tests and were compared with the results for the ones made via longer cycles. Their pH and temperature response was also studied. The swelling and re-swelling capacity of the hydrogels in water was assessed. Moreover, as the lignin waste during washing was rather meaningful, twin hydrogels were again synthesized using a reduced amount of lignin, subtracting the wasted one to the initially added lignin. Besides, organosolv lignin was also employed as substituent of the alkaline one in order to study the influence of the lignin type keeping the concentration of this component constant. Additionally, the adsorption capacity of the synthesized lignin-PVA hydrogels toward methylene blue was evaluated.

2. Materials and methods

2.1. Materials

Alkaline lignin and poly (vinyl alcohol) (PVA, Mw = 13,000–23,000 g/mol, 87–89% hydrolyzed; Mw = 83,000–124,000 g/mol, 99+% hydrolyzed and Mw = 130,000 g/mol, 99+% hydrolyzed) were supplied by Sigma Aldrich. Sodium hydroxide (NaOH, analysis grade, $\geq 98\%$, pellets), hydrochloric acid (HCl, 37% w/w) and methylene blue were purchased from PanReac Química SLU. Organosolv Lignin was supplied by Chemical Point. All reagents were employed as supplied.

2.2. Hydrogel synthesis

Hydrogels were synthesized according to two of the pathways

studied previously (see Fig. 1) [10]. All the hydrogels were prepared in the same way, except for the difference on the number of cycles at the crosslinking stage: half of them were subjected to 3 freeze-thawing cycles while the others were subjected to 5. The concentrations of the blends were also determined according to a previous study [10]. All the hydrogels were prepared by adding a 9.87% (w/w) i.e. 5.92 g of the corresponding weight averaged molecular weight (Mw) PVA to 60 mL of a 2% (w/w) NaOH aqueous solution, which was magnetically stirred and heated to 80–90 °C simultaneously. Once the PVA pellets were dissolved, the lignin (9.12% (w/w), i.e. 5.47 g) was incorporated under agitation until it was completely dissolved. The blends were introduced into 6 mL syringes and then poured into silicon moulds, poking the visible air bubbles at the surface and eliminating any remaining internal bubbles introducing them in an ultrasound bath for 10 min.

On the previous work [10], the blends had been frozen for 16 h at $-20\text{ }^{\circ}\text{C}$ in a freezer and then thawed during 8 h at $28\text{ }^{\circ}\text{C}$ in a heater, 3 and 5 times. In this work, the time of the cycles was optimized; in fact, when the blends were completely frozen (2.5 h approximately) they were taken out and put into the heater at $28\text{ }^{\circ}\text{C}$ until they were totally thawed (1.5 h approximately). In this way, the crosslinking time was significantly reduced, since this stage used to take between 3 and 5 days and in this way, it lasted less than 2 days. After this stage, the washing was performed as done in the previous work [10] so as to eliminate the non-reacted lignin and the residual NaOH. Afterwards, the hydrogels were left to dry at room temperature.

In order to analyze the influence of the lignin type, complementary swelling tests were performed, for which organosolv-lignin-based hydrogels were similarly synthesized. Briefly, the same initial amounts of both MMw and HMw PVA and organosolv lignin were taken, and the same abovementioned experimental method was followed.

2.3. Hydrogel characterization

2.3.1. Lignin waste

During the washing stage, aliquots were taken each time the hydrogels were rinsed. A calibration curve was designed as described in the previous work [10]. Briefly, by employing several solutions of known concentrations of lignin and their absorbance measured at 515 nm by a V-630 UV-Jasco spectrophotometer the calibration curve was designed. Then, the absorbance of all aliquots was registered and, finally, their concentrations and the total lignin loss were calculated taking the volume of each rinse into account.

2.3.2. Swelling

The swelling of the synthesized hydrogels was estimated as in the previous work [10]. Briefly, they were weighted in dry state before being immersed into 50 mL of distilled water for 48 h. Then, they were

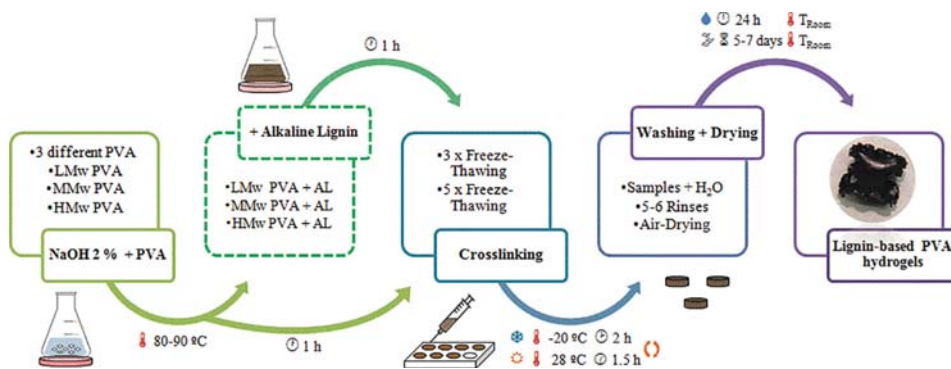


Fig. 1. Flow-diagram of the experimental procedure for hydrogel synthesis.

weighted at certain times, removing the water remaining on the surface with filter paper, for the swelling kinetics. The swelling degree was calculated from Eq. (1) [3]:

$$\text{Swelling (\%)} = (m_{\text{swollen}} - m_{\text{dry}}) / m_{\text{dry}} \cdot 100 \quad (1)$$

in which m_{swollen} and m_{dry} are the masses of swollen and dried hydrogels, successively.

Apart from distilled water, the swelling capacity of the synthesized hydrogels was also studied in a saline solution (1% NaCl) and two solutions of pH 2.5 and 12.20 prepared by adding dilute HCl or dilute NaOH. The influence of temperature was studied by keeping the samples in the corresponding solutions inside an incubator at 40 °C. The re-swelling capacity was measured by introducing the hydrogels that were swollen and left to dry once again into water.

2.3.3. Attenuated Total Reflection – Fourier Transformed Infrared Radiation (ATR-FTIR)

In order to study and verify the interactions between the polymers, a PerkinElmer Spectrum Two FT-IR Spectrometer equipped with a Universal Attenuated Total Reflectance accessory with internal reflection diamond crystal lens was used to collect Infrared spectra of the hydrogels. The studied range was from 600 to 4000 cm^{-1} and the resolution was 8 cm^{-1} . 20 scans were recorded for each grated dry sample.

2.3.4. Scanning Electron Microscopy (SEM)

SEM analyses were carried out in order to study the morphology of the hydrogels. The samples were swollen in water for 48 h at room temperature and then frozen at -20 °C. Afterwards, they were freeze-dried in an Alpha 1–4 LD freeze drier. The images of secondary electrons were taken with a MEB JEOL 7000-F. The working conditions were 5 kV and an intensity of 0.1 nA. The samples were covered with 20 nm of Cr by sputtering technique.

2.3.5. X-Ray Diffraction (XRD)

The samples were subjected to XRD analysis grated and in dry state. X-Ray Powder diffraction tests were carried out using a Phillips X'Pert PRO automatic diffractometer operating at 40 kV and 40 mA, in theta-theta configuration. Monochromatic Cu-K α ($\lambda = 1.5418$ Å) radiation and a PIXcel solid-state detector (active length in 2θ 3.347°) were employed. The collected data ranged from 5 to 80° 2θ at room temperature. The step size was 0.026 and the time per step was 80 s. 0.04 rad soller slit and fixed 1° divergence slit giving a constant volume of sample illumination were employed.

2.3.6. Differential Scanning Calorimetry (DSC)

DSC analyses were done on a Mettler Toledo DSC 822 (Mettler Toledo, Spain). Dry grated samples of between 3 and 5 mg were subjected to a heating ramp from -25 °C to 225 °C at a rate of 10 °C/min under nitrogen atmosphere to avoid oxidative reactions inside aluminium pans. After the first heating step, cooling and second heating stages were also performed. The glass transition temperature (T_g), was considered as the inflection point of the specific heat increment during the heating scans. The calibration was performed with indium standard. The degree of crystallinity (χ_c) was obtained from the enthalpy evolved during crystallization using Eq. (2) [11]:

$$\chi_c = \Delta H_m / [\Delta H_0 \cdot (1 - m_{\text{filler}})] \cdot 100 \quad (2)$$

where ΔH_m , is the apparent enthalpy for melting, ΔH_0 is the melting enthalpy of 100% crystalline PVA (average value: 161.6 J/g) and $(1 - m_{\text{filler}})$ is the weight percentage of PVA in the hydrogels [11].

2.3.7. Thermogravimetric Analysis (TGA)

TGA analyses were done on a TGA/SDTA 851 Mettler Toledo (Mettler Toledo, Spain) instrument. Dry grated samples of around 7 mg were subjected to a heating ramp of 25 °C/min from room temperature

up to 800 °C under a nitrogen atmosphere to avoid thermo-oxidative reactions.

2.3.8. Compression studies

Uniaxial compression tests were performed on the hydrogels in order to assess their mechanical strength. A compression gear was set up on an Instron 5967 machine using a 500 N load cell with a crosshead speed of 2 mm/min. Square samples of around 5 × 5 mm were cut from the initial hydrogels, which were left to swell during 48 h at room temperature. The swollen samples were compressed up to the 80% of their initial thickness. The swollen modulus, G_e , of each sample was calculated automatically by employing Eq. (3) [12,13].

$$\sigma = F/A = G_e \cdot (\lambda - 1/\lambda^2) \quad (3)$$

where F is the force, A is the original cross sectional area of the swollen hydrogel, and $\lambda = L/L_0$ where L_0 and L are the thicknesses of the samples before and after compression, respectively.

2.3.9. Methylene blue adsorption tests

The uptake of methylene blue (MB) was investigated as follows: a solution of MB was prepared at a concentration of 1 mg/L. All batch adsorption experiments were statically performed at room temperature for 24 h. The adsorption performance was calculated by Eq. (4) after the concentrations of the initial and final dissolutions were determined [14]. For this aim, a calibration curve was designed by employing several solutions of known concentrations (5–0.25 mg/L) of MB and their absorbance measured at 665 nm by a V-630 UV-Jasco spectrophotometer.

$$Q_e \text{ (mg}_{\text{MB}}/\text{g}_{\text{HG}})} = (C_0 - C_{\text{eq}}) / m \cdot V \quad (4)$$

where C_0 is the initial dye concentration, C_{eq} is the dye concentration at equilibrium, V is the total volume of dye employed for each sample and m is the dry weight of the hydrogel. The percentage of removal was also calculated by means of Eq. (5):

$$P \text{ (\%)} = (C_0 - C_{\text{eq}}) / C_0 \cdot 100 \quad (5)$$

where P is the equilibrium adsorption rate of the hydrogel and the rest of variables are the same as the ones defined for Eq. (4) [14]. Desorption studies were also performed by immersing the dyed hydrogels into a 0.1 M HCl solution for 24 h. The dye release was quantified by spectrophotometry, as done for the adsorption study [14,15].

3. Results and discussion

3.1. Crosslinking

According to previous studies, the selected composition enabled the crosslinking between alkaline lignin and medium molecular weight PVA (MMw PVA) via both 3 and 5 cycles of freeze-thawing [10]. In this case, however, the cycles were shortened, but both MMw and high molecular weight PVA (HMw PVA) still led to a successful crosslinking with lignin. Nevertheless, the samples formed with low molecular weight PVA (LMw PVA) did not result in a proper crosslinking despite having a good visual aspect. A similar result was reported by Wu et al. [7], who tried to crosslink a solution of 10% alkaline lignin with different amounts of PVA (47,000 g/mol) adding epichlorohydrin. This might have happened due to the scarce reactive sites in PVA for such amount of lignin despite adding a crosslinker to favour the formation of the hydrogel. For this reason, LMw PVA samples were discarded for further studies. Nevertheless, LMw PVA could be used in the future for hydrogel formation but varying the PVA content and the lignin content. Wu et al. [7] did also relate the reagent concentration to the crosslinking degree. Moreover, the hydrolysis degree of the PVA might have had something to do with the crosslinking. The hydrolysis degree is related to the number of acetate groups in the PVA molecule, since PVA is synthesized from the hydrolysis of pre-polymerized

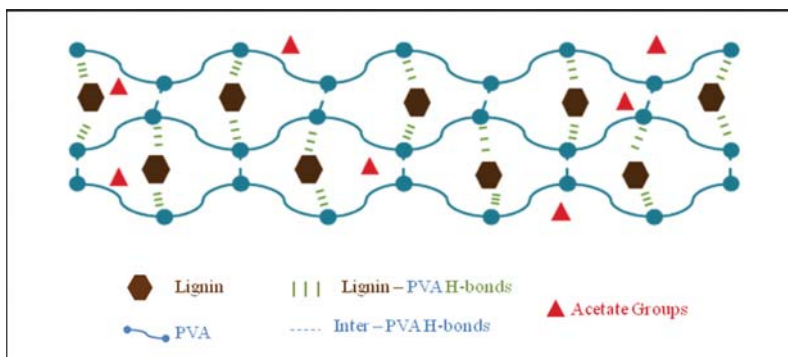


Fig. 2. Possible crosslinking scheme between PVA and lignin.

polyvinyl acetate [16,17]. Thus, a high hydrolysis degree means there will be a lower number of acetate groups in the PVA, and these groups can interfere on its chemical properties, solubility and the capacity of crystallization [17]. Moreover, the presence of acetate groups weakens both intra- and intermolecular hydrogen bonding interactions between nearby hydroxyl groups. In solution, as the degree of hydrolysis increases, the PVA interchain separation distance decreases [17]. Therefore, the non-successful crosslinking could be attributed to the lower degree of hydrolysis that LMw PVA had (87–89%) in comparison to MMw and HMw PVA (99+%), although a direct correlation is often difficult to determine [18] and might be more related to the molecular weight and concentration of PVA [7].

At first sight, comparing these hydrogels with the ones in the previous work [10], they seemed more brittle since it was more complicated to take them out of the moulds. Therefore, it can be concluded that the time as well as the number of the freeze-thawing cycles affects the consistence of the formed hydrogel [19], which would be associated to the crosslinking degree. A possible scheme of the interactions through the hydrogel matrix is proposed in Fig. 2.

3.2. Lignin waste

For the samples with HMw PVA (69.5 and 49.5% for samples 3HL and 5HL, subsequently) the lignin waste during the washing stage was lower than the one for MMw PVA samples (77.8 and 57% for the samples 3ML and 5ML, subsequently). The former could be related to the number of reactive sites in the PVA, i.e. longer polymer chains had more entanglements with lignin. According to Hennink et al. [19], the molecular weight of PVA affects the properties of the gel formed. In addition, the number of cycles also affected the lignin waste, since the hydrogels formed via 3 freeze-thawing cycles had a higher lignin waste than the ones formed via 5 cycles. This fact could mean that as the number of cycles was increased, more entanglements were formed between the elements in the blend [19,20].

3.3. Swelling capacity

As displayed in Fig. 3A, the swelling capacity was significantly higher for the hydrogels synthesized via 5 freeze-thawing cycles (890 and 790% for HMw and MMw PVA, subsequently) than for the ones made via 3 cycles (380 and 360% for HMw and MMw PVA, respectively). Moreover, for the hydrogels with the highest molecular weight PVA the swelling capacity was also the highest ($\approx 900\%$). Other authors also reported this behavior for higher molecular weight lignin-PVA hydrogels [7]. This would again enhance the previous statement about the influence of parameters such as the molecular weight of the employed PVA and the number of cycles [19]. As cycles and the molecular weight of PVA are increased, the increment on the entanglements with

lignin would permit the creation of more pores and, thus, higher water absorption ability. Wu et al. [7] also considered that an optimal amount of lignin would maintain the PVA network more relaxed, which would lead to higher water absorption. It is also worth to mention that the neat PVA hydrogels presented a very low swelling ability (200–300%), so this would confirm the fact that lignin enhances the pore size and, therefore, the water retention inside the network [4,7,21]. In addition, neat MMw PVA hydrogels presented a higher swelling rate than the ones synthesized from HMw PVA and this rate was kept higher for the ones with 5 cycles.

In comparison with the previously synthesized samples [10], which were synthesized from longer freeze-thawing periods, these hydrogels presented slightly lower swelling values (970% Vs. 890–790% for the previous and the current hydrogels, respectively). However, neat PVA samples were capable of swelling slightly more than in the previous work.

3.3.1. Influence of the pH on the swelling capacity

As smart materials are becoming of great interest, it is important to study the stimuli responsiveness (pH, temperature...) of the synthesized hydrogels [22]. Twin samples of the hydrogel 3HL were swollen into two solutions with different pH-s (2.5 and 12.20). In these experiments, it was seen that the basic medium improved the swelling capacity (see Fig. 3B). This behavior might have been observed due to the influence of soda in the expansion of crosslinked chains by electrostatic repulsions in the polymeric network [21]. On the other hand, the acidic medium hindered the swelling ability of the hydrogels. This could be attributed to protonation of the carboxylate anions, which convert $-\text{COO}^-$ groups to $-\text{COOH}$, eliminating the main anion-anion repulsive forces and decreasing at the same time the swelling values [23,24]. When pH is increased, H-bonding and the negative effect of H^+ on electrostatic repulsions are gradually weakened because many $-\text{COOH}$ groups are converted to $-\text{COO}^-$, contrary to what happened for low pH-s [24].

3.3.2. Influence of the temperature and NaCl on the swelling capacity

As aforementioned, temperature is also an external stimulus to which hydrogels are usually responsive. In addition, the swelling capacity of the hydrogels is significantly influenced by the charge valences and the salinity degree of the medium, and this capacity determines the suitability of the hydrogels to be used as water release systems in agriculture [24]. Therefore, in order to evaluate the effect of the temperature and the presence of a salt on the swelling capacity of the hydrogels, 3 samples cut into 4 of the series 3ML, 5ML and 5HL (12 samples in total, 4 per series) were submerged into different solutions. Half of them were put into 1% (w/w) NaCl solutions and the other half into distilled water. At the same time, two samples per series (one in saline media and another one in distilled water) were left to swell at

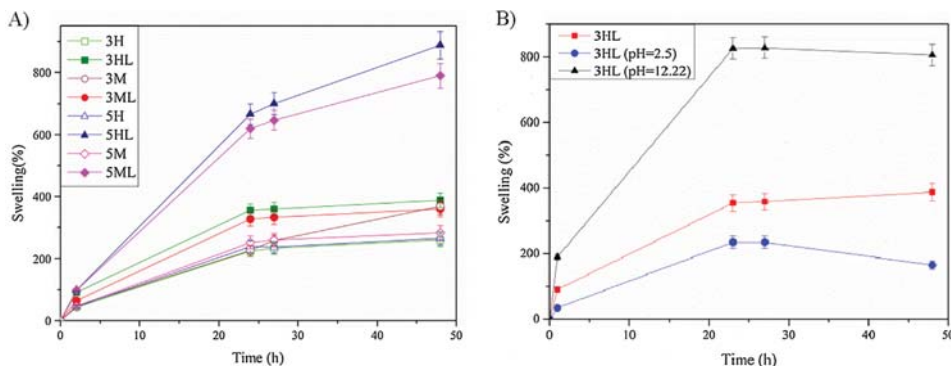


Fig. 3. Swelling performance of the hydrogels during the first 48 h (A) into distilled water (B) into solutions with different pHs.

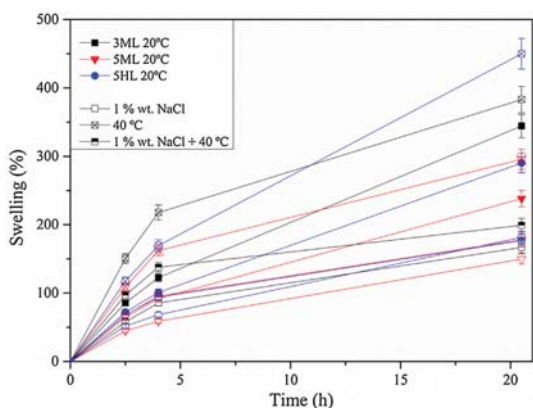


Fig. 4. Swelling performance of the hydrogels 3ML, 5ML and 5HL at 4 different mediums.

room temperature, and the other two were subjected to temperature (40 °C).

As shown in Fig. 4 temperature enhanced the swelling capacity in all cases whereas the saline medium hindered it. In fact, it could be observed that the saline medium at room temperature drastically affected the swelling abilities of all the samples since it decreased a 50, 40 and 40% for 3ML, 5ML and 5HL series, respectively. The warm saline medium also affected negatively the swelling capacity of the samples, since they swelled a 40, 25 and 40% for 3ML, 3HL and 5HL series, subsequently. At 40 °C the swelling was promoted and an increment of a 10, 25 and 55% was observed for 3ML, 5ML and 5HL series, respectively. The latest was also observed by Chang et al. [25], who saw that for the increasing salt concentration the swelling capacity kept decreasing due to the decline of anion-anion electrostatic repulsions caused by the charge screening effect of cations. The same was also reported by Tanan et al. [24], who stated that the type of salt has a strong influence on the swelling ratio due to the difference on the radiiuses and charges of the cations. According to Batista et al. [26] an increase in temperature might improve the swelling ability because of environmental entropy and the improved separation of the polymeric chains. In this case, comparing to the control samples, the ones subjected to temperature were the only ones presenting an improvement on the swelling capacity. Even the samples with the combination of NaCl and temperature had swelling ratios below the ones for control samples. So, it could be said that the effect of the saline solution was greater than the one of temperature.

3.3.3. Re-swelling capacity

A re-swelling test was also performed in order to study the reusability of the hydrogels or, in other words, to see if subsequent swelling stages would be prejudicial to their initial swelling ability. The re-swelling of the samples is shown in Fig. 5. In general, a slight decline around 7% was observed when comparing the swelling ability in the first and second tests. These results were in accordance with those reported by Tanan et al. [24], whose samples were subjected to five swelling and de-swelling cycles. These authors reported that the synthesized semi-IPN hydrogels, which also contained PVA, suffered a gradual loss in their swelling capacity when increasing the cycles. This behavior was attributed to the breakage of physical crosslinking points within the network during the repeating process of swelling-de-swelling, which could also have happened within the PVA-lignin hydrogels. These breakages could have damaged the polymeric structure, diminishing the ability to retain and absorb water at equilibrium [24]. However, the samples in this work were still capable of absorbing considerable amounts of water. Nevertheless, these hydrogels cannot be considered as reusable materials with the results of just one re-swelling test. Therefore, as reusability is an important feature nowadays, future work is needed and at least 5 re-swelling cycles should be performed.

3.4. Attenuated Total Reflection – Fourier Transformed Infrared Radiation (ATR-FTIR)

The hydrogels were analyzed by FTIR technique and their spectra are shown in Fig. S.1 (supplementary data). Both HMw and MMw PVA

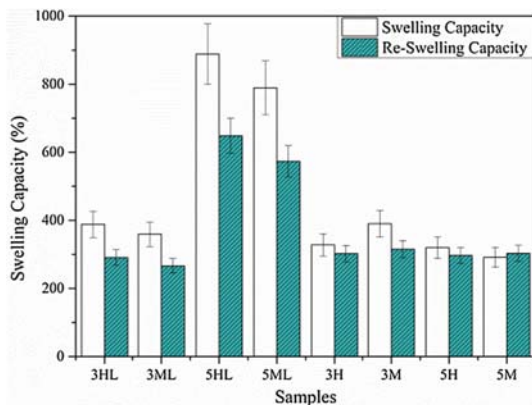


Fig. 5. Re-swelling capacity of the hydrogels.

presented almost identical spectra although HMW PVA displayed more noticeable peaks at 2920 and 2855 cm^{-1} , which could be related to the difference on their molecular weight. Nevertheless, the intensity of the bands between 1750 and 1735 cm^{-1} was very weak for both of them, meaning that few acetate groups were present in the polymer chain due to their high hydrolysis degree [17]. The samples of PVA with and without lignin presented similar spectra, except for the peaks at 1600, 1515 and 1270 cm^{-1} that PVA-lignin hydrogels showed. These three new bands confirmed the incorporation of lignin into the structure of PVA, and the shift of many other bands, such as the ones around 1720 and 1565 cm^{-1} , confirmed the interactions between the components [11]. The main spectra were similar to the one presented by commercial PVA, whose main peaks and their corresponding attributions are displayed in Table S.1 (supplementary data). The characteristic peaks of commercial alkaline lignin are shown in Table S.2 (supplementary data). It was seen that in spite of having different number of freeze-thawing cycles, the hydrogels did not present any difference on their functional groups. The FTIR results are similar to the ones reported in the previous work [10].

3.5. Scanning Electron Microscopy (SEM)

The SEM images of the samples at 2500 \times magnification are presented in Fig. 6, and 250 \times magnification in Fig. S.2 (supplementary data). The microstructures of the hydrogels exhibited three dimensionally interconnected porous networks. The freeze-thawing process is responsible for these porous structures as the ice crystals formed inside the hydrogels during the freezing stage melt during the thawing, leaving the porous structure in the samples [27].

The neat PVA samples presented a more homogeneously distributed porous structure, with bigger pores as the molecular weight of the polymer was higher and the number of cycles lower. As a result, MMW PVA hydrogels had a greater swelling capacity than the HMW ones due to the increase in the contact surface with water. Wang et al. [27] reported that neat PVA hydrogels presented high degrees of crosslinking, which were achieved due to the massive hydrogen bonding during the freeze-thawing process. This would explain the morphology of the PVA samples.

When lignin was added, the pore size distribution was more heterogeneous, leading to the creation of many macropores, since it is believed to act as a nucleation agent [16]. Bian et al. [28] reported that lignin nanoparticles acted as spacers and led, in their case, to a highly porous PVA/cellulose nanofibril structure. The behavior of the

incorporated lignin as a spacer, could explain the formation of thinner walls between the micro voids, which were significantly helpful to the water-retention ability of the hydrogels due to the higher contact surface with it and, thus, its diffusion [21,28]. In this case, the hydrogel with 5 freeze-thawing cycles and HMW PVA was the one leading to the highest water retention (890%).

3.6. X-Ray Diffraction (XRD)

The XRD patterns of raw PVA, commercial alkaline lignin and the hydrogels are displayed in Fig. S.3 (supplementary data). PVA showed the typical semicrystalline structure since it presented an intense signal at around $2\theta = 19.77^\circ$, which corresponded to the (1 0 1) lattice plane and a shoulder around 22.78° , corresponding to the (2 0 1) plane [29]. Two other weak peaks could also be detected at 11.5° and 40.8° . As reported by Ciolacu et al. [4], lignin usually displays an amorphous behaviour, which had a broad peak at 19° . As previously reported [10], the combination between the aforementioned polymers led to the formation of hydrogels still with a semicrystalline structure. The slight widening of the strong signal at 19.77° suggested that there was little change on the crystallinity degree of the samples, which was also supported by the results obtained by DSC analyses.

3.7. Differential Scanning Calorimetry (DSC)

In order to study the thermal properties of the synthesized hydrogels, DSC analyses were carried out. Temperatures of crystallization, melting and glass transitions are displayed in Table 1 (T_c , T_m and T_g), as well as melting and crystallization enthalpies (ΔH_m and ΔH_c). These parameters were recorded during the first heating, cooling and the second heating stages and the crystallization index χ_c was calculated from these data. The DSC curves for the cooling and second heating stages are presented in Fig. S.4 (supplementary data).

As seen in the previous work [10], after removing the thermal history of the samples with a first heating stage, a single T_g appeared in all the samples, which indicated the good blend miscibility [16]. This could also be intuited from the SEM micrographs, in which no lignin agglomerations were observed.

For all the samples, the T_g values were significantly higher during the first heating scan than in the second one. This usually happens due to the reduction of crystalline regions formed during the cooling stage, which at the same time enables the chain mobility at lower temperatures. The hydroxyl groups in neat PVA hydrogels tend to be highly

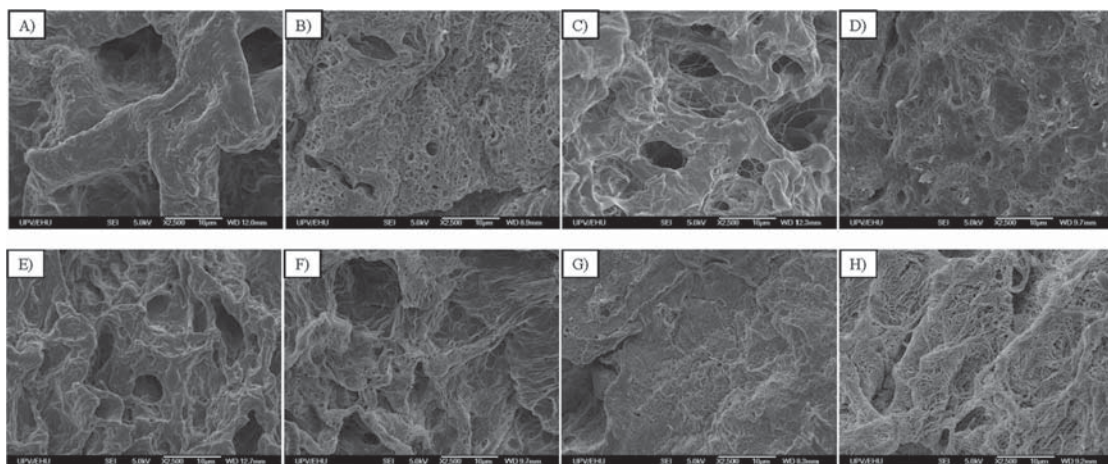


Fig. 6. SEM micrographs of the samples 3H, 3HL, 3 M, 3ML, 5H, 5HL, 5 M and 5ML at x2500 (A–H) magnification.

Table 1
Summarized results for the analyzed parameters by DSC and calculations.

Sample	1st Heating Scan						Cooling Scan			2nd Heating Scan					
	T _g (°C)	T _m (°C)	ΔH _m (W·°C/g)	ΔH _m (J/g)	m _{filler} (%)	χ _c (%)	T _c (°C)	ΔH _c (W·°C/g)	ΔH _c (J/g)	T _g (°C)	T _m (°C)	ΔH _m (W·°C/g)	ΔH _m (J/g)	m _{filler} (%)	χ _c (%)
3H	106	236	17	51	0	31	204	17	52	78	236	14	43	0	27
3HL	107	232	13	38	0.30	34	199	13	39	79	2312	9	27	0.30	24
3M	97	237	16	48	0	30	207	18	53	88	235	15	44	0	27
3ML	116	233	12	35	0.20	27	201	14	42	83	233	10	30	0.20	23
5H	111	236	18	54	0	33	204	17	52	78	234	14	41	0	25
5HL	119	232	12	36	0.38	37	197	12	35	93	230	10	29	0.38	29
5M	112	235	15	45	0	28	207	18	55	80	236	13	38	0	24
5ML	101	232	13	38	0.36	37	199	12	38	83	232	10	30	0.36	30

T_c: Crystallization temperature; T_g: Glass transition temperature; ΔH_m: Melting enthalpy; χ_c: Crystallinity degree; ΔH_c: Crystallization enthalpy; T_m: Melting temperature; m_{filler}: filler mass percentage.

interconnected by hydrogen bonding, leading to high glass transition temperatures (T_g) [30]. During the first heating scan, the T_g values for neat PVA samples with 5 freeze-thawing cycles (111 and 112 °C, for 5H and 5 M samples, subsequently) was slightly higher than for the ones with 3 cycles (106 and 97 °C, for 3H and 3 M, subsequently). However, during the second scan, the T_g values were similar. Therefore, it was concluded that the number of cycles could influence the glass transition temperature although once it had been melted the cycles did not affect. Nevertheless, the molecular weight of PVA influenced the T_g value, despite the difference being of around 3 °C.

When lignin was added, the registered T_g were, in general, higher than those for neat PVA samples since the introduction of other functional groups may support the bonding and enhance T_g values [30]. The same behaviour was observed previously, and it was attributed to the restriction on the chain mobility that lignin could have provoked due to the hydrogen bonds between the components [10,11]. The most notable difference was observed in 3ML sample, in which the temperature raised around 19 °C. The highest T_g was registered for the sample 5HL. In this case, the cycles and the molecular weight of PVA chains could have led to a higher packaging and, therefore, to this increase in T_g.

Regarding the melting temperature, no significant change was observed between both heating scans. In addition, the molecular weight of PVA did not affect the T_m. However, a decrease on the melting enthalpy was noticed when lignin was incorporated. As reported by He et al. [11], this could be due to the disruption that lignin causes on the crystalline regions that PVA chains form, breaking existing intra- and intermolecular hydrogen bondages in the matrix and creating new ones between both polymers. The melting enthalpies were slightly lower on the second heating stage as less crystalline regions were formed. This was also confirmed by the crystallization temperatures and enthalpies, which were as well reduced with the addition of lignin (see Table 1). Once again, the molecular weight of PVA did not alter the T_c.

The crystallization indexes calculated from the reported enthalpies suggested that there was no significant difference on the crystalline regions of the samples. Besides, according to the calculations, the crystallinity degree of the lignin-PVA hydrogels seemed to be higher. This behaviour was also reported by He et al. [11], who clarified that large contents (> 5% wt.) of lignin nano-particles formed crystalline regions due to an increased interface interaction via hydrogen bonding between the abundant hydroxyl groups on LNP and PVA. This would support the results for χ_c in Table 1, which decreased during the second heating stage due to the short time for crystallization.

3.8. Thermogravimetric Analysis (TGA)

TGA was performed for a rapid evaluation of the thermal stability of the samples and in order to obtain the degradation temperatures of their forming polymers. TG and DTG curves of neat PVA hydrogels and lignin-PVA hydrogels are shown in Fig. 7A and B. As expected, all the

neat PVA samples presented similar degradation profiles, also alike the ones in the previous work [10]. Four main weight loss stages were observed: the first one at around 150 °C, the second one close to 250 °C, the third and maximum degradation stage at 375 °C and the fourth around 440 °C. The first step was related to physically weak and chemically strong bound water evaporation [24], and despite the difference on the molecular weight, no variance was observed in the temperature. The second step was attributed to the initial degradation of PVA, which for the samples with lower molecular weight started some degrees earlier. The maximum degradation stage happened at the same temperature for all the samples, but a higher weight loss was observed for the MMw PVA hydrogels. This was related to the depolymerization of the acetylated and deacetylated units of the polymer, and finally, the last stage, corresponding to the thermal degradation of some by-products generated by PVA, was common for all. However, the loss was slightly more notable for the samples with HMw PVA. The registered final residue in all samples was lower than 3% of the initial weight.

When lignin was added, four main degradation steps were also observed. The first one, which was detected around 150 °C, was attributed to moisture evaporation and, as in the case of neat PVA hydrogels, no difference was noticed as the molecular weight of the polymer matrix was varied. Then, an overlapping of the second and third stages was seen. The second one was detected at around 280 °C for the samples with MMw PVA and close to 290 °C for the samples with HMw PVA, which was higher than that reported for neat PVA hydrogels. The shift of the onset temperature to higher values could be attributed to the thermal stability of lignin [31]. It was seen that having a higher molecular weight PVA had greater influence on the onset temperature than having different freeze-thawing cycles. The third and main degradation step was found at 330 °C for every sample, which was lower than the one reported by other authors for lignin-containing hydrogels [31,32]. Even though, this fact could be related to the lack of additional components in the hydrogels such as crosslinkers or reinforcing fibres, which could have led to the formation of weaker lignin-PVA linkages and permitted a more facile degradation. After this stage, there was still around a 30% of the initial samples left. The fourth weight loss was observed at 425 °C and no clear variation was detected as the molecular weight of the samples changed. However, there was a significant increase on the residue with the addition of lignin, being the sample with highest molecular weight and greater number of cycles (5HL) the one leaving the highest residual content (17%). The sample with the least residual weight (12.5%) was the one with the lowest molecular weight and fewer cycles (3ML). Thus, the addition of lignin led to a higher final residue, as well as the increase on the number of cycles and on the molecular weight of the employed matrix polymer. In general, it can be said that the variation on the molecular weight PVA and the freeze-thawing cycles do not affect the thermal stability of the samples as strongly as the addition of lignin does.

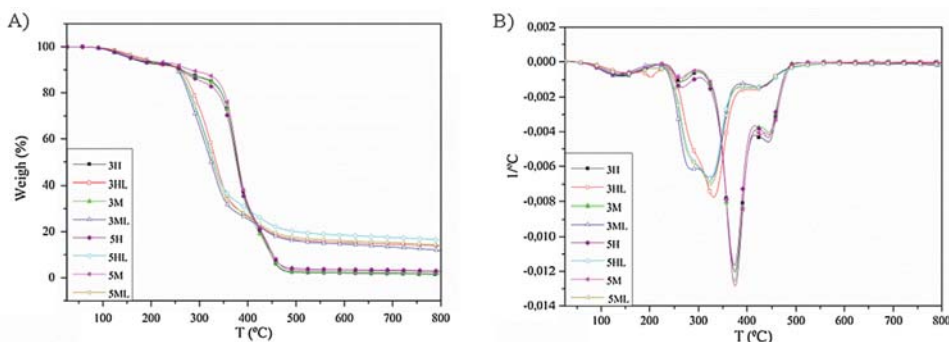


Fig. 7. (A) TG and (B) DTG curves of the hydrogels.

3.9. Compression studies

The compression behaviour of the samples was analyzed up to the 80% of their initial thickness and the compression modulus for each sample was calculated from their stress-strain curves. The calculated data is displayed in Table 2. At the maximum deformation, all the samples presented good ability of recovery, since none of them was broken and kept a total integrity. However, as expected, there were some differences among the calculated modulus.

For the samples without lignin, Young's modulus ranged from 18 to 28 MPa. The samples with MMw PVA presented the lowest values (18.13 and 19.85 MPa for 3 and 5 cycles, successively) compared to the ones for HMw PVA hydrogels (28.13 and 22.06 MPa for 3 and 5 cycles, respectively). It was surprising to observe such a fall in the modulus for HMw PVA hydrogels from 3 to 5 cycles, but as 5H sample also presented higher water retention (265%), it might also be possible to have a less compact structure. In the case of MMw PVA, an opposite behaviour was seen; in fact, the modulus was increased as the number of cycles increased.

When lignin was added, the 3HL sample did not present an adequate form for compress tests, so the rest of the series were studied. A clear decrease of the modulus was observed in all cases (> 50%). For instance, 5HL sample presented a modulus of 10.32 MPa, while the one for the same sample without lignin (5H) was of 22.06 MPa. This is a direct consequence of the reported great swelling capacity for 5HL (890%) comparing to the one presented by 5H (265%), which had a highly crosslinked and compact structure. As for 3ML and 5ML samples, there was also a clear drop on their modulus with respect to their twin blank hydrogels. In addition, there was a slight increase on the modulus when the number of cycles was augmented (8.77 MPa for 3ML and 9.64 MPa for 5ML), which would be in agreement with the reported trend for neat MMw PVA hydrogels. However, no clear correlation could be done between the swelling ability and the modulus, since 5ML presented higher water retention ability and modulus than the ones shown by 3ML sample. Nevertheless, it was clearly seen that lignin provoked a significant drop on the compression modulus of all the samples, regardless of which the molecular weight of PVA was. This

Table 2 Results for the compression tests of the samples.

Sample	Compression Modulus (MPa)	Standard Deviation (MPa)
3M	18.13	4.23
3ML	8.77	2.27
3H	28.13	4.4
5M	19.85	2.53
5ML	9.64	4.56
5H	22.06	3.29
5HL	10.32	3.05

behaviour was also seen by Chen et al. [33] on their PAM hydrogels with high lignin contents. Wu et al. [7] also reported a dominant elastic behaviour on their lignin-PVA-epichlorohydrin samples.

Comparing the synthesized hydrogels with the ones in the previous work [10], it can be confirmed that, as the modulus decreases up to 50%, the time of the cycles also has a great impact on the compression behaviour of the final hydrogels.

3.10. Methylene blue adsorption tests

Many authors have previously reported the success of lignin-hydrogels in dye removal [5,7]. Lignin-based hydrogels present large negative charges on their surface due to the numerous carboxylic acid groups and thanks to the π-π hydrophobic interactions, these hydrogels can trap positively charged dyes, i.e. cationic dyes [7]. For this reason, the adsorption of MB was evaluated. This substance is commonly used for cotton, wood and silk dyeing and it has been proven to be very harmful for human and animals [5].

The uptake of MB on the first 24 h was evaluated by spectrophotometry. Although the yield values were not as high as the ones reported by other authors [5,7], the removal values were even higher than the ones reported by them. Fig. 8A shows the removal and yield values for the samples 5HL, 5H and 3ML. It was observed that 5HL (0.012 mg MB/g hydrogel) had a lower yield than that calculated for 3ML (0.014 mg MB/g hydrogel) but the percentage of removal was greater (71.6% for 5HL and 69.1% for 3ML). For the hydrogel without lignin (5H), the yield was 0.002 mg MB/g hydrogel and the removal was of 34.8%. These values demonstrate that lignin enhances the

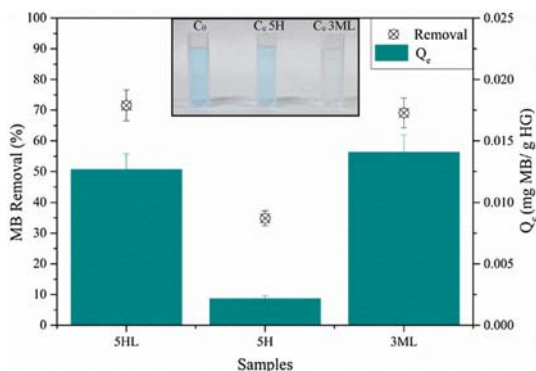


Fig. 8. (A) MB adsorption performance and removal of 5HL, 5H and 3ML samples (B) real appearance of the initial MB solution and equilibrium concentrations of 5H and 3ML samples after 24 h.

potential of these hydrogels as cationic dye adsorbents, which can also be appreciated in Fig. 8B, where the visual appearance of the initial concentration and equilibrium concentration for the samples 5H and 3ML are shown.

3.11. Complementary swelling studies

3.11.1. Influence of the Lignin Content

As shown in Section 3.2, the lignin waste during the washing stage was quite significant in all cases. In order to optimize the lignin content of the hydrogels to save lignin, an estimation of the composition of the hydrogels after washing was done, taking into account the lost lignin. In this way, no excessive lignin amount would be added, just the necessary to obtain the "same" hydrogels.

After the corresponding calculations had been done, the estimated "reduced" amount of lignin was added for each hydrogel formulation (3HL.R, 3ML.R, 5HL.R and 5ML.R). The procedure was exactly as the one for the previous hydrogels.

It was observed, that for all the synthesized hydrogels, the lignin waste was still notable. In fact, the accounted minimum lignin waste was of 37.5%, in the case of 3ML.R sample. It is true that this percentage was significantly reduced since the initial lignin waste of the same sample was of 77.8%. Nevertheless, for the three other samples (3HL.R, 5HL.R and 5ML.R) the lost lignin was of around 50%, which was still a high amount.

With regard to the swelling ability, for the samples synthesized from 5 freeze-thawing cycles, a great drop was noticed (over a 50% of their initial ability), while for the 3-times-freeze-thawed samples, just a slight variation of their swelling capacities was seen. However, these samples did not show as high swelling rates as at the beginning. This might be related to the amount of reactive sites of lignin that are initially introduced in the blend, which promote the crosslinking reactions between the PVA chains and lignin. In other words, if less reactive sites are introduced, there is a lower possibility for them to interact with the PVA chains, since no additional reagent is enhancing the reaction. Thus, the non-reacted lignin molecules get removed from the hydrogel together with NaOH as the washing stage is performed. Therefore, it can be concluded, that the initial lignin amount, the washing stage and the loss of lignin have an important effect on the subsequent swelling capacity of the hydrogel. Wu et al. [7] studied the effect of the lignin concentration on the swelling capacity of their hydrogels. These authors observed that, for the same concentration of PVA, as the concentration of lignin increased, the swelling ratio was enhanced until a maximum value, from which an increase in the lignin concentration had a negative influence on the swelling ratio [7]. In addition, they concluded that as lignin has good compatibility with PVA through hydrogen bonding, more lignin could be used to fabricate hydrogels with higher swelling ratios [7]. This might mean that for the hydrogels in this work, a reduction of the amount of PVA could have a higher impact on the swelling capacity rather than the lignin concentration. Nevertheless, it is important to bear in mind that these authors did also incorporate epichlorohydrin as a crosslinker [7].

3.11.2. Influence of the lignin type

After studying several influent factors on the swelling behaviour of the hydrogels, another variable was decided to explore. As the structure of the lignin depends on its source and extraction method, the synthesis of organosolv-lignin-based hydrogels was considered. Organosolv lignin is usually more environmentally friendly than alkaline lignin, which in this case was confirmed to be sulphur-containing kraft lignin. Therefore, the same initial amount of reagents was taken, this time with commercial organosolv lignin and also both MMw and HMw PVA, and the same experimental method was followed. The synthesized samples were then named 3MO, 3HO, 5MO and 5HO. The molecular weight distributions of both alkaline and organosolv lignins are shown in Table S.3 (supplementary data).

During the washing stage of these hydrogels, the waste of large amounts of lignin was also observed. None of the samples lost less than 70% of the organosolv lignin added initially, which was almost in all cases higher than that for the alkaline lignin. This could be directly related to the variation on total reactive sites that the lignins could have, as well as with their molecular weight. In fact, organosolv lignin presented an apparent weight average molar mass of 33,000 g/mol, with a polydispersity index of 29, while for the alkaline lignin it was of around 9300 g/mol, with a polydispersity index lower than 7.

As for the swelling ability, all the samples presented a lower water retention capacity than that shown with alkaline lignin. The maximum swelling rate was observed for the 5MO sample (352%), followed by the one for 5HO sample (350%). 3MO and 3HO samples presented a swelling capacity of 284 and 260%, respectively. This high drop on the swelling capacity demonstrates that the lignin type, apart from the molecular weight of PVA, has a strong influence on the final properties of the hydrogel, especially on the water retention rate. This could be related to the heterogeneity of the employed organosolv lignin, whose heaviest molecules might not have been able to interact with PVA, letting the smallest molecules attach to the PVA chains and, thus, leading to a lower swelling ability.

This fact was also confirmed by Wu et al. [7], who reported very different swelling capacities for the hydrogels synthesized employing three types of lignin.

4. Conclusions

Several hydrogels were successfully synthesized from medium and high molecular weight PVA and alkali lignin. It was observed that LMw PVA did not enable a good crosslinking with lignin, so it was concluded that the Mw of PVA is a key factor when synthesizing hydrogels. Apart from increasing the Mw of PVA, as the number of cycles was increased, the crosslinking of the hydrogels was also promoted and the swelling capacity of the obtained hydrogels was higher. When lignin was incorporated, the water absorption ability was greatly improved (up to 890%), and by increasing the number of cycles, the lignin waste was reduced probably due to the increment on the formed interactions and the generated porous microstructure. The hydrogels were pH and temperature responsive since they presented higher swelling capacities at high pH values and higher temperatures. Moreover, although further studies are needed, the samples could be reusable materials since they were able to swell and de-swell more than once. The thermal properties were gently influenced by the molecular weight of the polymer. The compression modulus was greater for the highest molecular weight samples; however, when lignin was incorporated it was drastically lowered. In spite of this drop, the hydrogels presented complete integrity after compressing them to the 80% of their initial thickness. Moreover, the lignin hydrogels presented improved MB adsorption capacity, making them interesting to be employed in this field.

It was observed that the twin hydrogels with reduced amounts of lignin had considerably lower swelling capacities. Therefore, the initial lignin content and the washing stage could be vital for ensuring high swelling abilities. The lignin type did also affect the swelling capacity since organosolv lignin did not enable such high water absorption rates.

In conclusion, this study shows that the molecular weight of the matrix polymer, as well as the crosslinking method and the lignin type directly affect the final properties of the hydrogels.

CRRediT authorship contribution statement

Amaia Morales: Investigation, Validation, Data curation, Formal analysis, Writing - original draft. **Jalel Labidi:** Funding acquisition, Methodology, Supervision, Writing - review & editing. **Patricia Gullón:** Visualization, Formal analysis, Writing - review & editing.

Declaration of Competing Interest

The authors declare that they have no known competing financial interests or personal relationships that could have appeared to influence the work reported in this paper.

Acknowledgements

The authors would like to acknowledge the financial support of the Department of Education of the Basque Government (IT1008-16). A. Morales would like to thank the University of the Basque Country (Training of Researcher Staff, PIF17/207). P. Gullón would like to express her gratitude to MINECO for financial support (Grant reference IJCI-2015-25304). The authors thank for technical and human support provided by SGiker (UPV/EHU/ERDF, EU).

Appendix A. Supplementary material

Supplementary data to this article can be found online at <https://doi.org/10.1016/j.eurpolymj.2020.109631>.

References

- P. Azadi, O.R. Inderwildi, R. Farnood, D.A. King, Liquid fuels, hydrogen and chemicals from lignin: a critical review, *Renew. Sustain. Energy Rev.* 21 (2013) 506–523, <https://doi.org/10.1016/j.rser.2012.12.022>.
- M. Mahinroosta, Z. Jomeh Farsangi, A. Allahverdi, Z. Shakoori, Hydrogels as intelligent materials: A brief review of synthesis, properties and applications, *Mater. Today Chem.* 8 (2018) 42–55, <https://doi.org/10.1016/j.mtchem.2018.02.004>.
- M.R. Guilherme, F.A. Aouada, A.R. Fajardo, A.F. Martins, A.T. Paulino, M.F.T. Davi, A.F. Rubira, E.C. Muniz, Superabsorbent hydrogels based on polysaccharides for application in agriculture as soil conditioner and nutrient carrier: A review, *Eur. Polym. J.* 72 (2015) 365–385, <https://doi.org/10.1016/j.eurpolymj.2015.04.017>.
- D. Ciolacu, G. Cazacu, New Green Hydrogels Based on Lignin, *J. Nanosci. Nanotechnol.* 18 (2018) 2811–2822, <https://doi.org/10.1166/jnn.2018.14290>.
- J. Domínguez-Robles, M.S. Peresin, T. Tamminen, A. Rodríguez, E. Larrañeta, A.S. Jääskeläinen, Lignin-based hydrogels with “super-swelling” capacities for dye removal, *Int. J. Biol. Macromol.* 115 (2018) 1249–1259, <https://doi.org/10.1016/j.ijbiomac.2018.04.044>.
- S. Park, S.H. Kim, J.H. Kim, H. Yu, H.J. Kim, Y.H. Yang, H. Kim, Y.H. Kim, S.H. Ha, S.H. Lee, Application of cellulose/lignin hydrogel beads as novel supports for immobilizing lipase, *J. Mol. Catal. B Enzym.* 119 (2015) 33–39, <https://doi.org/10.1016/j.molcatb.2015.05.014>.
- L. Wu, S. Huang, J. Zheng, Z. Qiu, X. Lin, Y. Qin, Synthesis and characterization of biomass lignin-based PVA super-absorbent hydrogel, *Int. J. Biol. Macromol.* 140 (2019) 538–545, <https://doi.org/10.1016/j.ijbiomac.2019.08.142>.
- A. Oryan, A. Kamali, A. Moshiri, H. Baharvand, H. Daemi, Chemical crosslinking of biopolymeric scaffolds: Current knowledge and future directions of crosslinked engineered bone scaffolds, *Int. J. Biol. Macromol.* 107 (2018) 678–688, <https://doi.org/10.1016/j.ijbiomac.2017.08.184>.
- S. Huang, S. Shuyi, H. Gan, W. Linjun, C. Lin, X. Danyuan, H. Zhou, X. Lin, Y. Qin, Facile fabrication and characterization of highly stretchable lignin-based hydroxyethyl cellulose self-healing hydrogel, *Carbohydr. Polym.* 223 (2019), <https://doi.org/10.1016/j.carbpol.2019.115080>.
- A. Morales, J. Labidi, P. Gullón, Assessment of green approaches for the synthesis of physically crosslinked lignin hydrogels, *J. Ind. Eng. Chem.* 81 (2020) 475–487, <https://doi.org/10.1016/j.jiec.2019.09.037>.
- X. He, F. Luzi, X. Hao, W. Yang, L. Torre, Z. Xiao, Y. Xie, D. Puglia, Thermal, antioxidant and swelling behaviour of transparent polyvinyl (alcohol) films in presence of hydrophobic citric acid-modified lignin nanoparticles, *Int. J. Biol. Macromol.* 127 (2019) 665–676, <https://doi.org/10.1016/j.ijbiomac.2019.01.202>.
- M.N. Collins, C. Birkinshaw, Physical properties of crosslinked hyaluronic acid hydrogels, *J. Mater. Sci. Mater. Med.* 19 (2008) 3335–3343, <https://doi.org/10.1007/s10856-008-3476-4>.
- S.A. Bencherif, A. Srinivasan, F. Horkay, J.O. Hollinger, K. Matyjaszewski, N.R. Washburn, Influence of the degree of methacrylation on hyaluronic acid hydrogels properties, *Biomaterials* 29 (2008) 1739–1749, <https://doi.org/10.1016/j.biomaterials.2007.11.047>.
- Z. Zeng, M. Xie, Q. Zhang, Y. Kang, X. Guo, H. Xiao, Y. Peng, J. Luo, Chitosan/organic rectorite composite for the magnetic uptake of methylene blue and methyl orange, *Carbohydr. Polym.* 123 (2015) 89–98, <https://doi.org/10.1016/j.carbpol.2015.01.021>.
- A. Labidi, A.M. Salaberria, S.C.M. Fernandes, J. Labidi, M. Abderrabba, Functional chitosan derivative and chitin as decolorization materials for methylene blue and methyl orange from aqueous solution, *Materials (Basel)* 12 (2019), <https://doi.org/10.3390/ma12030361>.
- W. Yang, E. Fortunati, F. Bertoglio, J.S. Owczarek, G. Bruni, M. Kozanecki, J.M. Kenny, L. Torre, L. Visai, D. Puglia, Polyvinyl alcohol/chitosan hydrogels with enhanced antioxidant and antibacterial properties induced by lignin nanoparticles, *Carbohydr. Polym.* 181 (2018) 275–284, <https://doi.org/10.1016/j.carbpol.2017.10.084>.
- W.E. Hennink, C.F. van Nostrum, Novel crosslinking methods to design hydrogels, *Adv. Drug Deliv. Rev.* 64 (2012) 223–236, <https://doi.org/10.1016/j.addr.2012.09.009>.
- K. Varaprasad, G.M. Raghavendra, T. Jayaramudu, M.M. Yallapu, R. Sadiku, A mini review on hydrogels classification and recent developments in miscellaneous applications, *Mater. Sci. Eng. C* 79 (2017) 958–971, <https://doi.org/10.1016/j.msec.2017.05.096>.
- N. Thombare, S. Mishra, M.Z. Siddiqui, U. Jha, D. Singh, G.R. Mahajan, Design and development of guar gum based novel, superabsorbent and moisture retaining hydrogels for agricultural applications, *Carbohydr. Polym.* 185 (2018) 169–178, <https://doi.org/10.1016/j.carbpol.2018.01.018>.
- Y. Meng, J. Lu, Y. Cheng, Q. Li, H. Wang, Lignin-based hydrogels: A review of preparation, properties, and application, *Int. J. Biol. Macromol.* 135 (2019) 1006–1019, <https://doi.org/10.1016/j.ijbiomac.2019.05.198>.
- W. Farhat, R. Venditti, N. Mignard, M. Taha, F. Becquart, A. Ayoub, Polysaccharides and lignin based hydrogels with potential pharmaceutical use as a drug delivery system produced by a reactive extrusion process, *Int. J. Biol. Macromol.* 104 (2017) 564–575, <https://doi.org/10.1016/j.ijbiomac.2017.06.037>.
- W. Tanan, J. Panichpakdee, S. Saengsuwan, Novel biodegradable hydrogel based on natural polymers: Synthesis, characterization, swelling/reswelling and biodegradability, *Eur. Polym. J.* 112 (2018) 678–687, <https://doi.org/10.1016/j.eurpolymj.2018.10.033>.
- C. Chang, B. Duan, J. Cai, L. Zhang, Superabsorbent hydrogels based on cellulose for smart swelling and controllable delivery, *Eur. Polym. J.* 46 (2010) 92–100, <https://doi.org/10.1016/j.eurpolymj.2009.04.033>.
- R.A. Batista, P.J.P. Espitia, J. de S.S. Quintans, M.M. Freitas, M.Á. Cerqueira, J.A. Teixeira, J.C. Cardoso, Hydrogel as an alternative structure for food packaging systems, *Carbohydr. Polym.* 205 (2019) 106–116, <https://doi.org/10.1016/j.carbpol.2018.10.006>.
- L.Y. Wang, M.J. Wang, Removal of heavy metal ions by poly(vinyl alcohol) and carboxymethyl cellulose composite hydrogels prepared by a freeze-thaw method, *ACS Sustain. Chem. Eng.* 4 (2016) 2830–2837, <https://doi.org/10.1021/acsuschemeng.6b00336>.
- H. Bian, L. Wei, C. Lin, Q. Ma, H. Dai, J.Y. Zhu, Lignin-containing cellulose nanofibril-reinforced polyvinyl alcohol hydrogels, *ACS Sustain. Chem. Eng.* 6 (2018) 4821–4828, <https://doi.org/10.1021/acsuschemeng.7b04172>.
- X.-Q. Hu, D.-Z. Ye, J.-B. Tang, L.-J. Zhang, X. Zhang, From waste to functional additives: thermal stabilization and toughening of PVA with lignin, *RSC Adv.* 6 (2016) 13797–13802, <https://doi.org/10.1039/C5RA26385A>.
- O.W. Guirguis, M.T.H. Moselhey, Thermal and structural studies of poly (vinyl alcohol) and hydroxypropyl cellulose blends, *Nat. Sci.* 04 (2012) 57–67, <https://doi.org/10.4236/ns.2012.41009>.
- H. Bian, L. Jiao, R. Wang, X. Wang, W. Zhu, H. Dai, Lignin nanoparticles as nano-spacers for tuning the viscoelasticity of cellulose nanofibril reinforced polyvinyl alcohol-borax hydrogel, *Eur. Polym. J.* 107 (2018) 267–274, <https://doi.org/10.1016/j.eurpolymj.2018.08.028>.
- I.E. Raschip, G.E. Hitruc, C. Vasile, M.C. Popescu, Effect of the lignin type on the morphology and thermal properties of the xanthan/lignin hydrogels, *Int. J. Biol. Macromol.* 54 (2013) 230–237, <https://doi.org/10.1016/j.ijbiomac.2012.12.036>.
- Y. Chen, K. Zheng, L. Niu, Y. Zhang, Y. Liu, C. Wang, F. Chu, Highly mechanical properties nanocomposite hydrogels with biorenewable lignin nanoparticles, *Int. J. Biol. Macromol.* 128 (2019) 414–420, <https://doi.org/10.1016/j.ijbiomac.2019.01.099>.

Effect of the formulation parameters on the absorption capacity of smart lignin-hydrogels

Amaia Morales, Jalel Labidi*, Patricia Gullón

Chemical and Environmental Engineering Department, University of the Basque Country UPV/EHU, Plaza Europa 1, 20018, San Sebastián, Spain

Supplementary data

Figure S.1: FTIR spectra of the hydrogels, commercial alkaline lignin and MMw/HMw PVA.

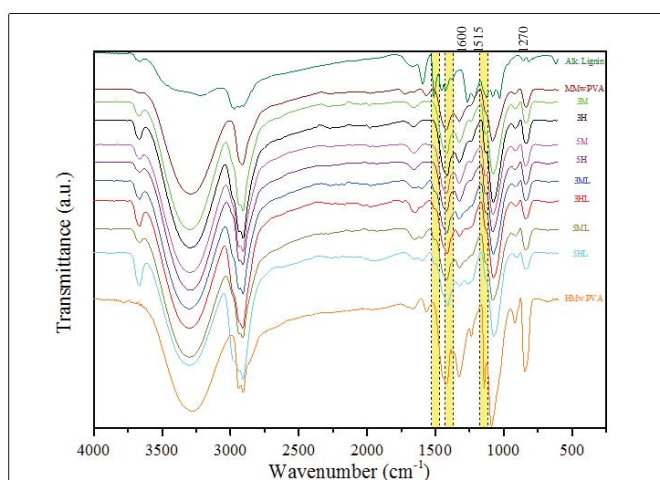


Figure S.2: SEM micrographs of the samples 3H, 3HL, 3M, 3ML, 5H, 5HL, 5M and 5ML at x250 (A–H) magnification.

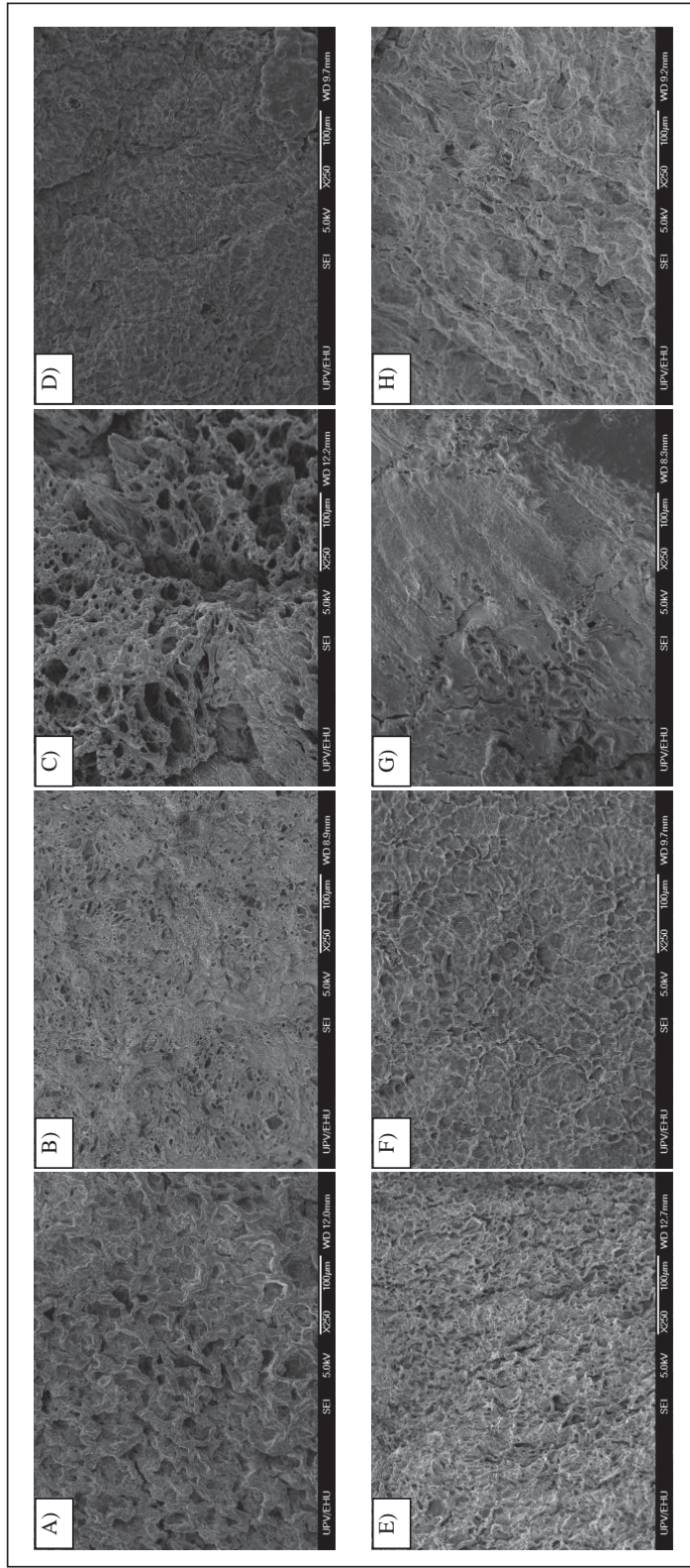


Figure S.3: XRD diffractograms of the hydrogels.

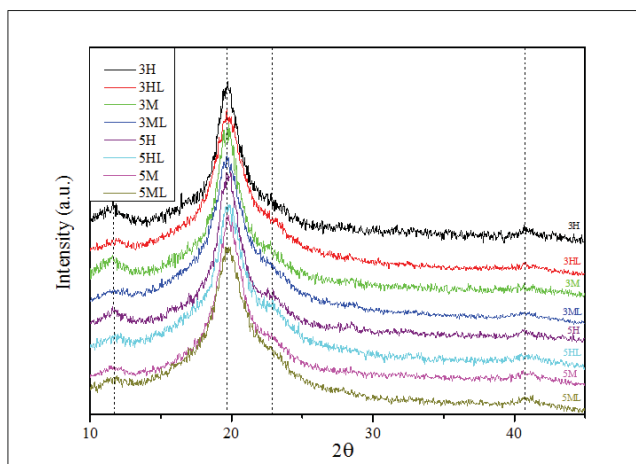


Figure S.4: DSC thermograms of the first cooling stage and second heating stage of the hydrogels.

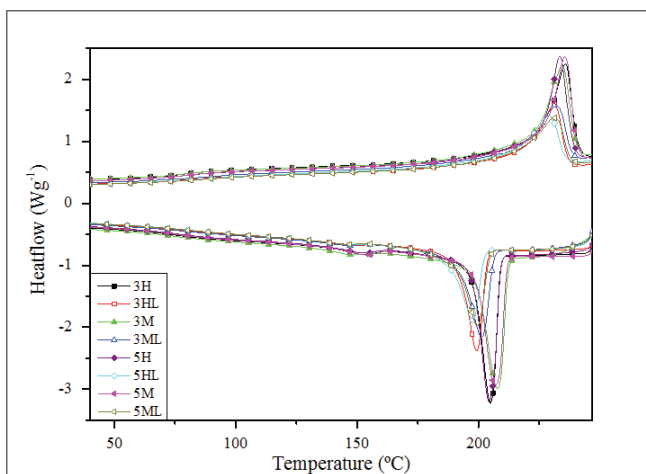


Table S.1: Characteristic FTIR peaks of PVA.

Wavenumber (cm ⁻¹)	Assignment
3300	-OH stretch vibration
2920	Alkyl asymmetric C-H stretch vibration
2855	Symmetric C-H stretch vibration
1720	Ester C=O stretch vibration
1660	Residual C=O stretch vibration
1560	C=C stretch vibration
1425	CH ₂ bending vibration
1325	O-H deformation vibration
1100	C-C stretching vibration
840	C-C and C-O stretching vibration

Table S.2: Characteristic FTIR peaks of alkaline lignin.

Wavenumber (cm ⁻¹)	Assignment
3215	-OH stretch vibration
2947	Alkyl asymmetric vibration
2913	Aromatic C-H stretching vibration
1679	C=O ester bonds
1597	C=C stretch vibration
1513	C=C aromatic vibrations
1456	C-H bonds of the methyl groups
1429	C-H bonds of the methyl groups
1269	Guaiacyl units
1100	C-C bonds
1030	C-O stretching vibration
865	C-C stretching vibration
821	aromatic -CH out of plane vibration
618	C-S bonds

Table S.3: Molecular weight distribution of alkaline and organosolv lignins.

Type of Lignin	Mw (Da)	Percentage (%)	Average Mw (Da)	Mw/Mn
Alkaline	10,424	89.2	9,333	6.8
	345	10.0		
	155	0.8		
Organosolv	82,538	37.9	32,933	29.3
	9,393	7.9		
	3,731	18.4		
	1,004	18.8		
	353	14.9		
	152	2.1		

Publication IV

Impact of the lignin type and source on the characteristics of physical lignin hydrogels

A. Morales, J. Labidi, P. Gullón

IV

Permission is not required for this non-commercial use.
baimena eskatzea.
<http://10.1016/j.susmat.2021.e00369>
2214-9937/© 2021 The Authors. Published by Elsevier B.V.
Sustain. Mater. Technol. 31 (2021) e00369



Impact of the lignin type and source on the characteristics of physical lignin hydrogels

Amaia Morales^a, Jalel Labidi^{a,*}, Patricia Gullón^b

^a Chemical and Environmental Engineering Department, University of the Basque Country UPV/EHU, Plaza Europa 1, 20018 San Sebastián, Spain

^b Centro de Apoio Científico e Tecnolóxico á Investigación, Universidade de Vigo, Technology Park of Galicia- Tecnopole, CTC Building, 32901, San Cibrao das Viñas, Ourense, Spain

ARTICLE INFO

Keywords:

Lignin
Poly (vinyl alcohol)
Almond shells
Walnut shells
Physical hydrogels

ABSTRACT

Multiple natural polymers have been investigated for the synthesis of hydrogels to the present date, but lignin has demonstrated to be a promising one for this purpose for the multiple advantages it offers. Lignin can be isolated from lignocellulosic material such as nut shells, which are usually undervalued wastes, and would be a great step forward on circular economy. Thus, in the present work, lignin was extracted from almond and walnut shells following a single-step (delignification) and double-step (autohydrolysis and delignification) biorefinery scheme. After the chemical composition and structures of these lignins were determined, hydrogels were synthesized combining them with poly (vinyl alcohol) by the means of freeze-thawing cycles so as to study the influence of the different lignins on their final properties. Additionally, the last thawing cycle of the synthesis process was lengthened in order to confirm previous assumptions about its effect on the characteristics of the synthesized materials. The obtained results showed significant variation between the 8 lignin samples, especially in their purity, molecular weights and total phenolic contents. The variation on the lignins led to several hydrogel morphologies, which directly affected their properties, primarily their swelling capacity, glass transition temperatures and compression strengths. It was also demonstrated the great effect that the duration of the last thawing had on the morphology and, hence, on the characteristics of the obtained materials. The synthesized samples were successfully employed as dye adsorbents and the evaluation of their antifungal activity showed positive results in some of the samples, which could be applied for food packaging.

1. Introduction

Synthetic polymer-based items like hydrogels have completely stirred up our everyday lives. These materials are comprised by tridimensionally entangled polymeric chains that exhibit high water retention capacity due to the multiple hydrophilic groups they contain [1]. In addition to their great swelling properties, their internal structure together with their mechanical properties have made them gain considerable attention in the last years [2]. Hydrogels can be arranged according to the types of crosslinks that their polymeric chains present, which can be physical or chemical [2]. The chemical ones often demand the presence of toxic and costly crosslinking reagents whereas the physical ones do not. Thus, physical crosslinking makes the synthesis process greener and more economical [3]. Hydrogels can be presented in many substrates and forms, which, together with the aforementioned features, make them useful in a wide range of applications such as

agriculture and environment, personal hygiene or biomedicine, among others [1].

The beginning of the 21st century has been marked by a significant economic boost coupled with high plastic pollution which have led to several irrecoverable environmental concerns. In this context, the possibility of introducing biodegradable and renewable polymers to produce new materials such as hydrogels is nowadays one of the principal goals of research. Biopolymers, which are polymers coming from plants, animals and microorganisms, seem to be the solution to the stated problem since, apart from helping to face ecological problems [4], they would also contribute to sustainability and circular economy [5].

Biopolymers and other co-products (e.g. biofuels and biochemicals) can be extracted from biomass through biorefinery processes [6]. Lignocellulosic biomass, for instance, has emerged as a potential, renewable and available source of biopolymers and biochemicals. This type of biomass involves forestry, urban and alimentary residues [7].

* Corresponding author.

E-mail address: jalel.labidi@ehu.es (J. Labidi).

<https://doi.org/10.1016/j.susmat.2021.e00369>

Received 5 July 2021; Received in revised form 14 September 2021; Accepted 26 November 2021

Available online 29 November 2021

2214-9937/© 2021 The Authors.

Published by Elsevier B.V. This is an open access article under the CC BY-NC-ND license

(<http://creativecommons.org/licenses/by-nc-nd/4.0/>).

The main constituents of lignocellulosic biomass are cellulose, hemicelluloses and lignin, which can be employed as backbones on the formulation of hydrogels and other materials.

Among these natural polymers, lignin is the most bountiful aromatic one on Earth [8]. Its amorphous and complex structure is principally constituted by a random combination of three kinds of phenyl propane monomers (coniferyl, *p*-coumaryl and sinapyl alcohols) connected through several stable linkages [8]. The isolation method influences the properties of the extracted lignin such as its reactivity. The typical lignin extraction methods include Kraft, sulphite, alkaline and organosolv delignifications [9]. Lignin is commonly obtained as a by-product of pulp and paper industries; nevertheless, a small percentage of the entire quantity (<2%) of lignin generated every year has an added-value [8]. Hence, employing it for the synthesis of hydrogels, for instance, would contribute to cover the urgent need of safe and greener alternative materials.

Almond and walnut shells are an abundant waste all over the world. The low percentage of edible kernel in both nuts leads to an enormous production of shells with no recognized industrial or commercial application [7,10]. However, these shells belong to the lignocellulosic biomass and are very rich in lignin and other biopolymers. Therefore, these residues could be further valorised through a biorefinery strategy so as to use them as input feedstocks for the production of added-value materials [7,10].

In the last years, several researchers have described the synthesis of hydrogels with lignin from different sources and with different extraction methods [11,12]. Nonetheless, a great part of the published works reports the production of chemically crosslinked hydrogels, generally involving the use of toxic crosslinkers as well as the need of removing the residual part of it [3].

In this light, the objective of the present study was to analyse the influence of the type of lignin and its features on the final characteristics of physically crosslinked lignin-hydrogels. For this aim, lignin was extracted through alkaline and organosolv delignifications from walnut and almond shells (with and without prior hydrothermal pretreatment) [7,10] and hydrogels were formulated combining lignin and poly (vinyl alcohol) following the synthesis route reported previously [13]. In addition, hydrogels were also synthesized through a variation of the initial synthesis route, which consisted in lengthening the last thawing stage. In this way, the properties of these hydrogels were compared to the other ones, highlighting the most significant differences. The isolated lignins were characterised via purity, Py-GC/MS, HPSEC, FTIR, XRD, TGA and TPC analysis. The lignin waste and swelling capacity of all the synthesized hydrogels were measured and they were further characterised by FTIR, SEM, DSC and compression tests. Finally, the adsorption capacity of the hydrogels was evaluated by employing methylene blue as water pollutant, and their antifungal capacity against *Aspergillus niger* was also studied so as to explore their applicability in food packaging, for example.

2. Materials and methods

2.1. Materials

Almond shells (AS) were supplied by local farmers (Marcona variety) and walnut shells (WNS) were kindly supplied by Olagi cider house (Altzaga, Gipuzkoa). The shells were milled and sieved (particle size between 2 and 1 mm) and stored in a dark and dry place at room temperature until use.

Poly (vinyl alcohol) ($M_w = 83,000\text{--}124,000$ g/mol, 99 + % hydrolyzed), phosphate buffer saline (PBS) tablets, trypan blue solution and methylene blue powder were purchased from Sigma Aldrich. Sodium hydroxide (NaOH, analysis grade, $\geq 98\%$, pellets) was supplied by PanReac Química SLU. Potato dextrose agar (PDA) was acquired from Scharlab S.L. and DMSO from Fisher Scientific S.L. All reagents were employed as supplied.

2.2. Lignin extraction

The operational conditions were chosen in accordance to prior knowledge [7,10]. The alkaline and organosolv delignification stages were carried out twice for each type of shells: the first one without a prior hydrothermal treatment and the second one with a prior hydrothermal treatment (autohydrolysis). Table 1 summarizes the conditions employed for each lignin extraction.

2.3. Hydrogel synthesis

Lignin-hydrogels were synthesized according to a previous work [13]. The concentrations of the blends (9.87 w.% PVA and 9.12 w.% lignin) were also determined on the basis of previous studies. Briefly, the corresponding amount of PVA (5.92 g) was added to 60 mL of a 2% (w/w) NaOH aqueous solution and it was magnetically stirred and heated to 90 °C. Once the PVA was dissolved, lignin (5.47 g) was added while stirring until complete dissolution. The blends were poured into silicon moulds. The internal bubbles were eliminated by ultrasounds and the remaining superficial air bubbles were then poked manually.

The blends were frozen for 2.5 h at -20 °C and they were then thawed at 28 °C for 1.5 h. This cycle was repeated five times, leaving the samples freezing overnight during the second and fifth cycles. Afterwards, the hydrogels were washed as it was done previously [13] in order to remove the residual lignin and NaOH. Finally, the hydrogels were dried at room temperature.

Based on prior experiments (data not shown), it was thought that the duration of the last thawing step could alter the features of the synthesized hydrogels. For this reason, hydrogels with a longer 5th thawing stage (24 h inside the heater) were also prepared. These samples were tagged as LC samples (long cycle) and the previous ones as SC (short cycle).

2.4. Characterization methods

The characterization methods and equipments used in this work both for the extracted lignins and the synthesized hydrogels are described in Table 2.

2.5. Methylene blue adsorption tests

The removal of methylene blue (MB) was investigated according to a

Table 1
Operational conditions for each of the extracted lignins.

Abbreviation	Description	Autohydrolysis	Delignification
AAL	AS alkaline lignin	–	121 °C, 90 min, 7.5 w.% NaOH, LSR 6:1
AOL	AS organosolv lignin	–	200 °C, 90 min, 70/30 (v/v) EtOH/H ₂ O, LSR 6:1
WAL	WNS alkaline lignin	–	121 °C, 90 min, 7.5 w.% NaOH, LSR 6:1
WOL	WNS organosolv lignin	–	200 °C, 90 min, 70/30 (v/v) EtOH/H ₂ O, LSR 6:1
AAAL	Autohydrolysed AS alkaline lignin	179 °C (isothermal), 23 min, LSR 8:1	121 °C, 90 min, 7.5 w.% NaOH, LSR 6:1
AAOL	Autohydrolysed AS organosolv lignin	179 °C (isothermal), 23 min, LSR 8:1	200 °C, 90 min, 70/30 (v/v) EtOH/H ₂ O, LSR 6:1
AWAL	Autohydrolysed WNS alkaline lignin	200 °C (non-isothermal), LSR 8:1	121 °C, 90 min, 7.5 w.% NaOH, LSR 6:1
AWOL	Autohydrolysed WNS organosolv lignin	200 °C (non-isothermal), LSR 8:1	200 °C, 90 min, 70/30 (v/v) EtOH/H ₂ O, LSR 6:1

Table 2
Characterization methods and equipments for the extracted lignins and synthesized hydrogels.

Analysis	Sample	Equipment	Reference
Purity	Lignin	HPLC-RI/PDA (Jasco LC-Net II/ADC, 300 × 7.8 mm Aminex HPX-87H column)	[21]
Acid soluble lignin	Lignin	UV-Vis spectrophotometer (Jasco V-630, JASCO)	[18]
Composition	Lignin	Py-GC/MS (Py: 5150 Pyroprobe, GC: Agilent 6890, MS: Agilent 5973)	[21]
Average molecular weight	Lignin	GPC (JASCO LC-NetII/ADC, detector: RI-2031Plus, Two Polar Gel-M columns: 300 mm × 7.5 mm)	[18]
Total phenolic content (TPC)	Lignin	UV-Vis spectrophotometer (Jasco V-630, JASCO)	[18]
Thermal degradation	Lignin	TGA/DTG (TGA/SDTA RSI analyser 851 Mettler Toledo)	[13]
Crystallinity	Lignin	XRD (Phillips XPert Pro Automatic multipurpose diffractometer)	[13]
Chemical structure	Lignin	ATR-FTIR (PerkinElmer Spectrum Two FTIR Spectrometer)	[22]
Lignin Waste	Hydrogels	UV-Vis spectrophotometer (Jasco V-630, JASCO)	[13]
Swelling	Hydrogels	$Swelling (\%) = \frac{m_{swollen} - m_{dry}}{m_{dry}} \times 100$	[13]
Morphology	Hydrogels	SEM (Hitachi S-4800, 5 kV, 20 nm Au covering)	[56]
Glass transition temperature	Hydrogels	DSC (Mettler Toledo DSC 822)	[13]
Compression tests	Hydrogels	Mechanical test machine (Instron 5967, 500 N load cell)	[13]

previous study [13]. In brief, first, multiple solutions of certain concentrations (5–0.25 mg/L) of MB were prepared. Then, their absorbance was measured at 665 nm by a V-730 UV-Jasco spectrophotometer, and relating each concentration with its corresponding absorbance a calibration curve was designed. For the adsorption experiments, a solution containing 1 mg/L of MB was prepared, and around 0.5 g of dry samples were introduced in 15 mL of this solution, keeping them at room temperature and static regimen for 24 h. The percentage of MB removal was also calculated by means of Eq. (1) after the concentrations of the initial and final dissolutions were determined by the calibration curve:

$$P(\%) = \frac{C_0 - C_{eq}}{C_0} \times 100 \quad (1)$$

where P is the equilibrium adsorption rate of the hydrogel, C_0 is the initial dye concentration, C_{eq} is the dye concentration at equilibrium.

The adsorption performance was similarly calculated by Eq. (2).

$$Q_e \left(\frac{mg_{MB}}{g_{HG}} \right) = \frac{C_0 - C_{eq,V}}{m} \quad (2)$$

where V is the total volume of dye employed for each sample and m is the dry weight of the hydrogel and the rest of the variables are the same as the ones defined for Eq. (1) [13].

2.6. Antifungal studies

The antifungal activity of the extracted lignins and hydrogels was measured according to the methods previously reported by Salaberria et al. (2017) and Da Silva et al. (2018) with slight modifications [14,15]. Briefly, after culturing the mould fungus *Aspergillus niger* (CBS 554.65) on Petri dishes covered with PDA for 7 days at $25 \text{ }^\circ\text{C} \pm 1.5 \text{ }^\circ\text{C}$ in a climatic chamber, some spores were diluted in a PBS dissolution and its concentration was adjusted to around 1.21×10^6 spores/ml using an automatic cell counter for the measurements (Cellometer® Mini, Nexcelom Bioscience LLC). Then, the procedure was varied according to the type of sample.

The lignins were firstly dissolved in DMSO (around 75–100 mg/mL) and then, 40 μL of the sample dissolution was poured on a Petri dish covered with PDA and the fungal strain was sprayed around. The blank was performed with DMSO [15].

In the case of the hydrogels, square portions (approximately 1 cm × 1 cm) of each sample were introduced into the PDA covered Petri dishes after having inoculated them with fungal strain. The blank was performed using neat PVA hydrogel portions.

All the tests were done by duplicate. After 7 days of incubation at $25 \text{ }^\circ\text{C} \pm 1.5 \text{ }^\circ\text{C}$, the lignins were evaluated visually using a numerical scale reported by da Silva et al. (2018) in accordance with ISO 846, whereas the hydrogels were extracted from the agar and washed with 1 mL of PBS in order to collect the spore solution into an Eppendorf. Afterwards, these solutions were tinged blue with 5 μL trypan blue solution and after shaking them, their spore concentration was determined with the abovementioned cell counter [14]. The fungal growth inhibition (FGI) of the samples were calculated through the equation given by Salaberria et al. (2017) [14].

3. Results and discussion

3.1. Lignin characterization

3.1.1. Purity

So as to analyze the selectivity of the lignin extraction processes, the purity of the lignin samples together with the amount of impurities that had precipitated with them was determined by quantitative acid hydrolysis. The measured purities for the obtained lignins were calculated taking the Klason lignin and acid soluble lignin (ASL) into account.

As shown in Table 3, the purity results were, in general, higher for organosolv lignins than for alkaline ones. These results are related to the selectivity of organosolv extractions [16]. It was also observed that the organosolv lignins without autohydrolysis (AOL and WOL) had purities over 90%, whereas the ones for alkaline lignins were lower than 59%. However, after autohydrolysis, the purities for the latest increased up to 88–95% while for the organosolv ones this increment was just of a 3–5%. Therefore, it can be said that autohydrolysis greatly improves the purity of the extracted lignins, especially in alkaline processes, because of the effective prior elimination of hemicelluloses, which are the main impurities after lignin extraction as demonstrated by Dávila et al. (2017). The obtained results are consistent with those reported previously [7,10].

3.1.2. Composition of the lignins

Pyrolysis-Gas Chromatography/Mass Spectrometry (Py-GC/MS) analyses were performed in order to study the composition of the eight different lignins. The resulting pyrograms are shown in Fig. 1. The numbered peaks correspond to lignin-derived phenolic compounds with

Table 3
Summary of the purity, GPC, TPC and TGA results for the isolated lignins.

Lignin sample	Purity (%)	M_w^a (g/mol)	M_n^b (g/mol)	M_w/M_n^c	TPC (% GAE ^d)	T_{max}^e ($^\circ\text{C}$)
AAL	58.2	4770	1109	4.3	13.8	307
AOL	90.4	8301	1072	7.8	15.6	389
WAL	49.4	4761	1054	4.5	10.6	295
WOL	92.7	6371	1246	5.1	16.5	388
AAAL	88.2	12,793	1528	8.4	33.1	355
AAOL	95.2	9020	1520	5.9	26.2	357
AWAL	95.7	16,670	1604	10.4	33.8	354
AWOL	95.2	7644	1359	5.6	27.2	365

^a M_w : weight average molecular weight.

^b M_n : number average molecular weight.

^c M_w/M_n : polydispersity index.

^d % GAE: percentage of gallic acid equivalents.

^e T_{max} : maximum degradation temperature from TG/DTGA curves.

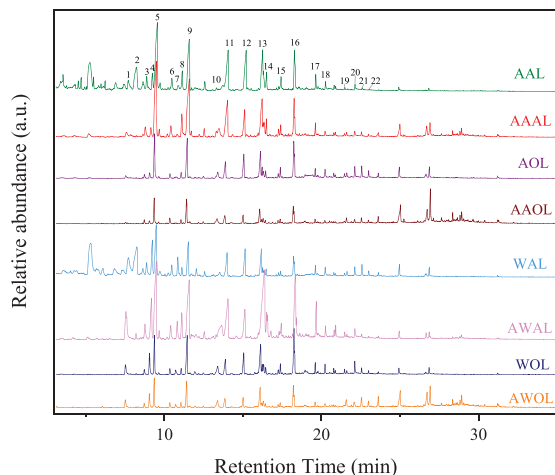


Fig. 1. Pyrograms of the extracted lignins.

larger area than 1% in at least one of the lignin samples, and their identification is displayed in Supplementary data. The untagged peaks at early times (3–7 min) mainly corresponded to degradation compounds from impurities. Furfural, for instance, was one of these compounds coming from carbohydrates and it appeared at minute 5 [10]. These impurities were especially visible in AAL and WAL samples, which also presented the lowest purity values in Table 3. From minute 23 on, the majority of the compounds with large areas were fatty acids, which are characteristic of nuts [17]. Thus, the identified compounds were detected in the range of 7–23 min and they were grouped based on the origin of their aromatic structure (*p*-hydroxyphenyl (H), guaiacol (G) and syringol (S)) [7,10].

Among the identified compounds, guaiacol (peak #5), 4-methylguaiacol (peak #9), syringol (peak #13) and 4-methylsyringol (peak #16) were the most abundant ones in all the lignin samples, constituting the 15%, 13.7%, 11.8% and 10.8% of the tagged compounds, subsequently. 4-ethylguaiacol and 4-vinylguaiacol (peaks #11 and #12, respectively) were also present in large amounts in all the samples. The compounds coming from the *p*-hydroxyphenyl unit such as phenol, *p*-cresol and *p*-ethylphenol seemed to be more abundant in WNS lignins (peaks #1, #3 and #4).

Regarding the estimated S/G ratios, all the samples presented more G units except for WOL and AWOL samples. This means that almost all the S/G ratios were below 1. However, an increase of this ratio was observed for the samples from the double-step process, which will be further studied so as to find a consistent explanation. However, these values are quite different to the ones reported previously for AS and WNS lignins [7,10], which could be related to any possible modification on the composition of the feedstock or in the extraction process.

3.1.3. Average molecular weight analysis

From the GPC analyses, based on the molecular weight distributions of the lignin samples, their number-average (M_n) and weight average (M_w) molecular weights were determined and their polydispersity indexes (M_w/M_n) were estimated. These values are displayed in Table 3.

The lignins after autohydrolysis presented higher weight and number average molecular weights in all cases. In addition, the organosolv lignins without autohydrolysis presented higher M_w than the alkaline ones, whereas for the lignins with autohydrolysis, the opposite behaviour was observed. A similar trend was perceived for the polydispersity indexes. It should also be noticed that the M_w for all the organosolv lignins was very alike, whereas for the alkaline lignins this difference was huge.

However, and looking at the purity percentages and previous works [18], these results make us believe that the analysed lignin fractions for AAL and WAL were not representative of the whole lignin samples; in other words, there were probably bigger chains than 0.40 μm (which is the pore size of the used filter) that were excluded from the analysis. These would explain such enormous difference in M_w reported for alkaline lignins with and without autohydrolysis.

Some authors also reported small variations on the molecular weights of organosolv lignins from solids with and without an autohydrolysis process [19,20]. In addition, they reported that autohydrolysis permitted the obtaining of lower polydispersity indexes for organosolv lignins [19,20], as happened in the present work.

Although it is hard to find previous research on the comparison of alkaline delignification treatments with and without a prior hydrothermal treatment, the results for alkaline lignins in Table 3 are aligned with those reported in literature [10,16,21].

3.1.4. Total phenolic content (TPC)

The phenolic hydroxyl groups in the structure of lignins are usually related to its antioxidant capacity as well as to its suitability for the synthesis of new materials [22]. Therefore, it is important to study the TPC of the lignin samples. Looking at the results, it was observed that the values for the lignin samples coming from the direct delignification of the raw material (AAL, AOL, WAL and WOL) were considerably lower than those reported for the ones coming from the two-step process (AAAL, AAOL, AWAL and AWOL), which could be related to their purities [22]. It was also appreciated that AAL and WAL presented slightly lower TPC values than AOL and WOL, and they were aligned with the results obtained by García et al. (2012, 2017) and Sequeiros et al. (2014) for soda lignin [23–25]. Nevertheless, the TPC of organosolv lignins (AOL and WOL) were significantly lower than those reported by other authors [23,24,26]. As commented, the lignin samples obtained after a prior autohydrolysis process, presented significantly greater percentages of GAE (26.2–33.8% GAE). A comparable behaviour was reported by Dávila et al. (2019) for alkaline lignin extracted from pre-treated and non-treated vine shoots [22], suggesting that a prior hydrothermal treatment can be crucial to obtain high total phenolic contents in lignin. In this case, alkaline lignin samples (AAAL and AWAL) presented higher TPC values than the ones obtained for organosolv lignins. These results are in agreement with the ones reported previously for almond shells [10]. Other authors purified lignins coming from the direct delignification of the feedstock with an acid hydrolysis; nonetheless, they reported much lower GAE percentages in the purified samples than in the original ones [23,24,27]. This fact also supports the idea of subjecting the raw material to a hydrothermal pre-treatment if high TPC values want to be achieved.

3.1.5. Thermal degradation analysis (TGA)

The thermal stability of lignins is also an important characteristic to take into account, especially for their use in the production of composite materials. Thus, the thermal degradation of the extracted lignins was studied. The TGA curves are shown in Supplementary data. The maximum degradation temperatures of the samples are displayed in Table 3. All the samples had a common initial degradation step below 100 °C, corresponding to moisture evaporation. The second degradation step was the maximum degradation stage for all the samples. However, the temperatures differed depending on the lignin extraction. In fact, for the alkaline lignins obtained through a single-step process (AAL and WAL), the maximum degradation happened around 300 °C, whereas for the organosolv lignins this temperature was significantly higher (≈ 390 °C). This could be ascribed to their high amount of impurities as well as to the fractions with low molecular weight [21,28], as reported in Section 3.1.3. The lignins coming from the double-step processes presented similar maximum degradation temperatures (354–365 °C), which were within the ones reported for single-step process lignins and were in accordance with previous results [10]. In this temperature

range, the scission of β -O-4 ether bondages tend to occur, followed by the division of C—C linkages and aromatic rings [28].

A third degradation stage was observed around 420 °C, although this temperature was again lower for AAL and WAL (\approx 390 °C) samples and higher for AOL and WOL samples (\approx 470 °C). The latest then presented a constant weight loss until 37% of their initial weight. The rest of the samples presented a fourth degradation step around 700 °C, leading to a final residue between 20 and 29% of their initial weight. This last stage could be related to the demethoxylation or condensation reactions of the volatile products of lignin [28], and the amounts of residue were aligned with those reported previously [10].

3.1.6. Crystallinity

The XRD patterns of the lignin samples are depicted in Fig. 2. As shown, all the organosolv lignins and the alkaline ones coming from the double-step processes (AAAL and AWAL), presented the typical broad signal around $2\theta = 22^\circ$, representing its amorphous structure [29]. AAL and WAL samples presented narrower peaks at the same diffraction angle. Moreover, they also presented sharp signals at 11, 12, 19, 25 and 31° , which are more characteristic of the crystalline domains of cellulose [30,31] and hemicelluloses [32]. Therefore, an important presence of impurities in these lignins was again confirmed by XRD analysis, leading to a modification on the ordered domains.

3.1.7. Chemical structure

The main functional groups of the isolated lignins were determined by FTIR technique (Figure 3). Although all the recorded spectra presented the typical lignin bands [7,22,26], the intensities of some of them changed from sample to sample. Some of these variations were observed in the range 2827 – 2998 cm^{-1} , which corresponded to the C—H (CH_3 , CH_2 and CH) stretching vibration of lignin and polysaccharides [19], and were more notable for alkaline lignin samples, probably due to the lower elimination of sugars during the autohydrolysis step. Before the footprint range, at 1650 cm^{-1} , a peak corresponding to conjugated C=O stretching vibration [19] was detected for the single-step lignins, but it disappeared after the autohydrolysis step. Although some authors have previously related this band to alkaline processes [33], it may be attributed to the presence of impurities in AAL, WAL, AOL and WOL lignins. On the footprint range (1500 – 600 cm^{-1}) the main changes were seen on the intensity of the bands. AAL and WAL samples, for instance, presented a clear decrease on the intensity of the bands ascribed to the condensed syringil or guaiacyl unit breathing (1325 cm^{-1}) [34,35] and

aromatic methyl ethers of lignin (1215 cm^{-1}) [19]. Conversely, the peaks at 1157 , 1080 , 975 and 896 cm^{-1} , corresponding to C—O stretching vibration in ester groups [34,35], C—O deformation in secondary alcohol and aliphatic ethers, —HC—CH out-of-plane and C—H deformation vibrations [35], subsequently, got intensified in the aforementioned samples. The remaining bands were similar for all the lignin samples, confirming the existence of syringyl and guaiacyl units in all the lignins, although their ratios were different, as demonstrated in Section 3.1.2.

3.2. Hydrogel characterization

3.2.1. Lignin waste

The lignin waste of the samples was analysed so as to determine their final lignin content. The results are shown in Table 4. For the samples made from alkaline lignin, the ones containing lignins from the single-step processes (AA and WA) presented higher lignin wastes than the ones containing lignins coming from double-step processes (AAA and AWA). A similar trend was observed for organosolv lignins from WNS (WO and AWO), whereas for the ones coming from AS (AO and AAO) the reported behaviour was the opposite. This might be related to the polydispersity of the lignins, since except for AOL and AAOL, the polydispersity of the rest of the lignins increased from single to double-step lignins. This fact suggests that highest molecular weight lignin chains might have been able to interact with the PVA matrix, whereas lowest molecular weight fractions were eliminated. However, further studies should be done in order to verify this statement. Moreover, lower waste percentages were accounted for AS lignins than for WNS lignins in the case of the single-step lignins (56.2 – 66.5% vs. 60.0 – 68.5%), while for the double-step lignins the contrary was appreciated (44.2 – 59.9% vs. 59.6 – 71.1%). These values are in great accordance with those reported previously [13]. It should also be noted that among the single-step lignin containing samples the ones with alkaline lignin showed greater lignin wastes than the ones containing organosolv lignin, whereas the samples with double-step lignins exhibited the inverse trend.

In addition, the samples with a long last thawing step, in general, presented lower lignin waste values, suggesting that the lengthening of the last cycle may have enhanced the interactions between the PVA and the lignin. Furthermore, the samples with single-step alkaline WNS lignin (WA) showed a significant reduction on their lignin waste. On the contrary, the samples with double-step alkaline WNS lignin (AWA) presented much greater lignin waste values than those reported before. It can also be said that, except for AWA sample, all the alkaline lignin containing hydrogels lost less lignin than the ones containing organosolv lignin.

3.2.2. Swelling

As the swelling capacity of the hydrogels is determining for assessing their applications, this property was measured for all the samples and it is displayed in Fig. 4.

The samples with short last thawing cycle presented swelling values between 336 and 505%, which corresponded to AWO and WA samples, respectively. Moreover, the samples containing alkaline lignin showed in all cases higher swelling capacities, which is in accordance with the data reported previously [13], which could be related to the attachment of the fractions with highest molecular weights to the matrix. Comparing the aforementioned samples with the ones with a long last thawing stage, a huge enhancement of this property was clearly seen. The most significant improvement (80% more regarding its prior swelling ability) was seen on AWO sample, which was the one that had previously presented the lowest swelling capacity. On the contrary, the sample that exhibited the slightest enhancement was AWA, whose swelling ability was just improved about 22%. Agudelo et al. (2018) studied the influence of various synthesis parameters such as the time of the freeze-thawing cycles on the swelling capacity of neat PVA hydrogels [36]. According to their work, the excessive lengthening of the thawing cycles

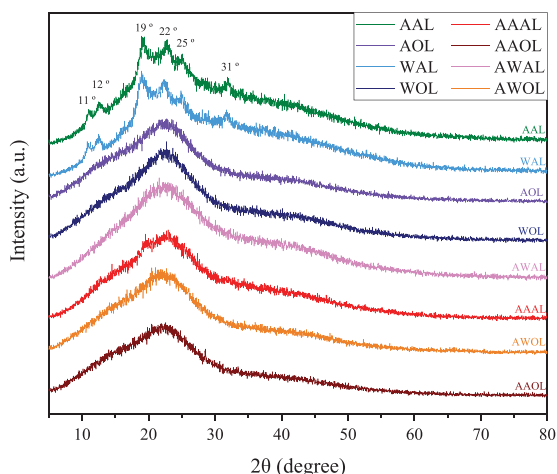


Fig. 2. XRD patterns of the extracted lignins.

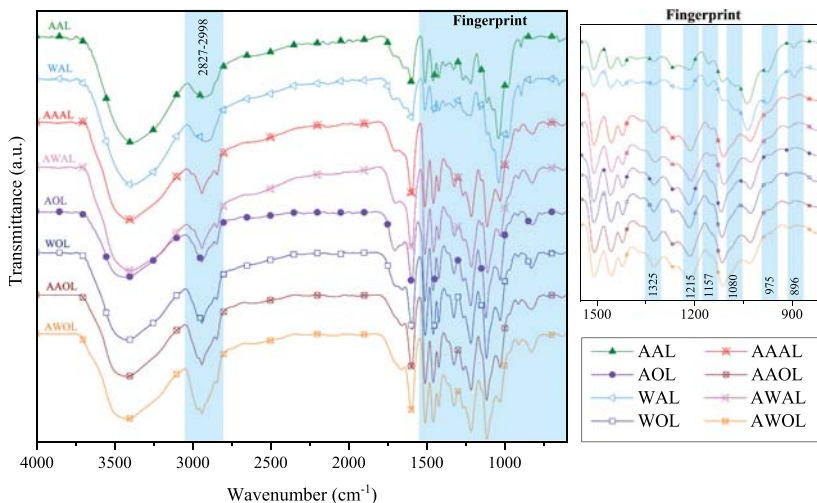


Fig. 3. FTIR spectra of the extracted lignins.

Table 4

Lignin waste (%) of the analysed short (SC) and long (LC) last thawing step samples.

Sample	SC (%)	LC (%)
AA	66.5 ± 2.9	48.5 ± 3.0
AO	56.2 ± 2.4	53.9 ± 3.4
WA	68.5 ± 0.7	26.0 ± 6.4
WO	60.0 ± 1.8	53.9 ± 2.1
AAA	59.6 ± 2.8	36.3 ± 2.0
AAO	71.1 ± 3.0	48.1 ± 3.3
AWA	44.2 ± 1.6	74.3 ± 3.7
AWO	59.9 ± 4.0	51.7 ± 2.2

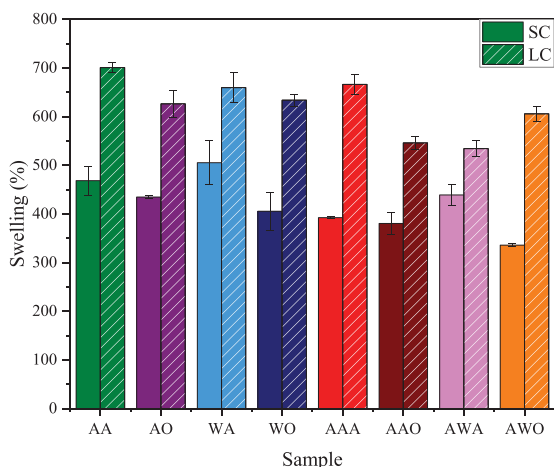


Fig. 4. Swelling capacity of the synthesized hydrogels with short (SC) and long (LC) last thawing steps.

leads to the dissolution of the formed crystallites, which reduces of their quantity and size and, hence, also the crosslinking density and the swelling capacity of the hydrogel [36]. Thus, as in the present work the

lengthened thawing step was the last one, the molten crystallites might have evaporated, reducing the crosslinking density of the samples and resulting in a notable enhancement of their swelling capacity. Nevertheless, this phenomenon should be further investigated in order to find a more reliable explanation.

It should also be mentioned that the samples containing lignins coming from single-step processes, presented higher swelling capacities than the ones coming from the double-step processes, probably due to the interactions of their impurities with the polymeric matrix. Although Wu et al. (2019) related the swelling properties to the content of phenolic hydroxyl groups and to the molecular weight of the employed lignins, their hypothesis would not explain the behaviour of the hydrogels in this work [12]. In fact, the samples containing lignin with the lowest total phenolic contents and lowest average molecular weights (AA and WA) presented the highest swelling capacities. However, this might support the previous statement about the non-representative average molecular weights determined for these lignins (Section 3.1.3) and also the one about the interactions with non-lignin components (Section 3.2.1), since these samples presented high lignin wastes.

3.2.3. Morphology

The morphology of the synthesized hydrogels was studied by Scanning Electron Microscopy (SEM). The corresponding micrographs for the samples containing AS lignins at 500× and 5000× magnifications are shown in Fig. 5 and the ones for WNS lignin samples in Supplementary data.

At first sight, it was seen that all the hydrogels presented different appearances. Although all the samples presented porous structures at different levels, their distribution, size and density was distinct. In fact, all the samples that corresponded to hydrogels containing lignins from single-step processes were quite similar and presented a highly porous honeycomb structure, as expected for lignin containing PVA hydrogels [13,37–39]. Their pore sizes and distributions were quite homogeneous, but the walls between the micro voids were smoother and more brittle in the case of AA and WA samples than in AO and WO samples, which presented thicker walls. These structures were responsible for their high water absorption capacities [40] and could have been created due to the interactions of PVA with the highest molecular weight lignin fractions.

When lignins from the double-step processes were employed, the synthesized hydrogels displayed much denser and continuous structures with hardly recognizable pores, which may be related to a higher

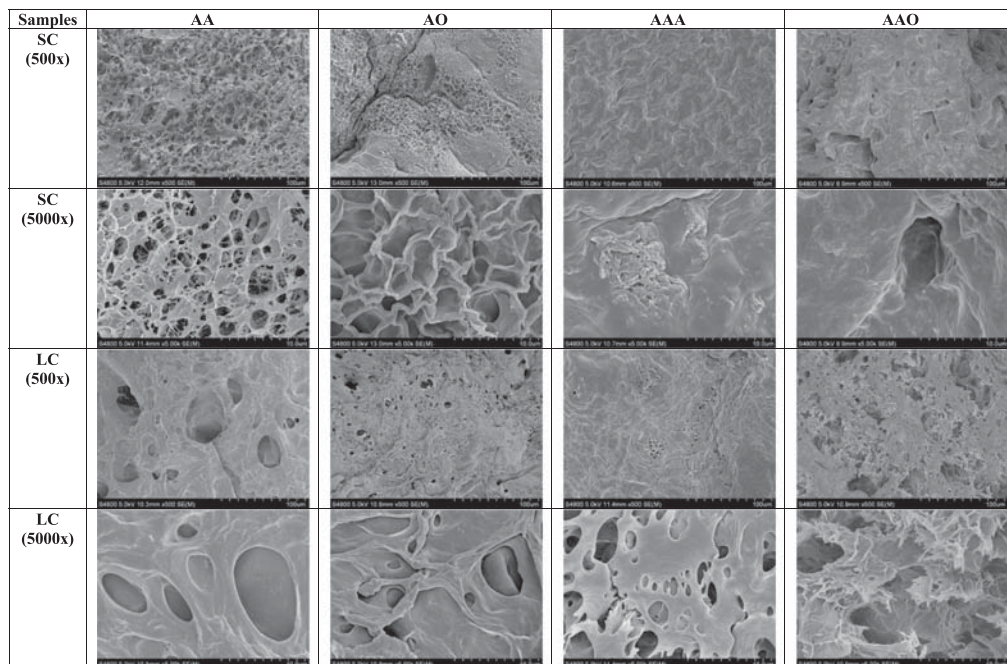


Fig. 5. SEM micrographs of the hydrogels containing AS lignins at 500× and 5000× magnifications.

crosslinking density with these lignins due to their higher contents in phenolic hydroxyl groups [12]. Rachip et al. (2013) also reported variable hydrogel morphologies according to the —OH and —COOH groups in lignin [41]. These microstructures would explain the drop on the swelling ability of the present samples compared to the aforementioned ones.

It was also appreciated that when the last thawing step was lengthened, there was an evident creation of macro pores in all cases. As aforementioned, this might be ascribed to the evaporation of molten crystallites during the last step of the synthesis, which permitted the formation of these structures and improved the swelling performance of all the hydrogels, regardless of their origin or extraction type.

Although the influence of the number of cycles has been previously studied by many authors for freeze-thawed PVA hydrogels [13,36,40,42,43], the duration of last thawing step has not been investigated. So, the present study could pave the way to new synthesis routes since it offers a simple way of enhancing the swelling capacity of the samples.

3.2.4. Glass transition temperature

The glass transition temperature (T_g) is an important characteristic of polymeric materials since it determines their applicability. Thus, the synthesized hydrogels were subjected to Differential Scanning Calorimetry (DSC) analyses and the results are presented in Table 5.

The samples containing alkaline lignins presented higher T_g values ranging from 72 to 91 °C whereas the ones containing organosolv lignins showed lower T_g values (69–86 °C). The highest T_g values were found for AA and AAA samples (≈ 91 °C), which might be because the impurities could have acted as bridges between the PVA and the lignin chains, enhancing their interactions and hindering the relaxation and arrangement of the chains [41,44]. On the contrary, although WA sample contained lignin with a higher amount of impurities, part of the latest might have dissolved in the aqueous phase, being washed out during the washing step and, hence, being unable to enhance the interactions

Table 5

Glass transition temperatures (T_g) and compression modules of the synthesized hydrogels after short (SC) and long (LC) last thawing steps.

Sample	T_g (°C)		Compression module (MPa)		MB removal (%)	
	SC	LC	SC	LC	SC	LC
AA	91.0	77.3	16.3 ± 1.8	10.8 ± 3.2	79.5 ± 3.6	81.3 ± 1.8
AO	73.0	66.6	5.0 ± 1.9	2.1 ± 0.7	90.3 ± 0.6	83.4 ± 2.8
WA	79.0	64.0	14.9 ± 1.9	13.6 ± 0.8	75.3 ± 3.7	82.3 ± 3.0
WO	69.7	77.7	6.0 ± 1.0	2.0 ± 0.8	89.6 ± 1.0	86.9 ± 4.4
AAA	91.1	66.6	13.1 ± 0.8	7.5 ± 2.7	86.6 ± 3.2	93.3 ± 1.1
AAO	85.8	82.8	2.1 ± 1.0	2.0 ± 0.8	90.1 ± 2.2	87.1 ± 6.7
AWA	72.1	66.4	6.6 ± 2.9	6.4 ± 1.3	87.9 ± 3.6	86.9 ± 5.5
AWO	70.8	92.2	5.4 ± 2.8	2.88 ± 1.2	93.0 ± 0.6	88.6 ± 1.9

between PVA and lignin. Therefore, in this case, the T_g value was lower.

Except for AWA sample, the hydrogels containing double-step lignins presented higher T_g values than the ones with single-step lignins, which also matched with the previously reported drop on their swelling capacity due to a higher crosslinking degree between lignin and PVA. However, this could also be attributed to the increment on the average molecular weights of the lignins as well as to their total phenolic content. These two factors affect the total —OH groups of lignin, which although according to Raschip et al. (2013) seemed to decrease the T_g of pure lignin, they could have enhanced the hydrogen bonding with the matrix polymer, making its chains flow at higher temperatures [41].

When the last thawing step was lengthened, all the T_g values dropped except for WO and AWO samples. This might have occurred due to an increment on the interactions between lignin and PVA after water evaporation due to the rearrangement of WO and AWO chains, which presented low average molecular weights and the lowest polydispersities. Thus, the resulting hydrogels were more thermally stable. Nevertheless, to the best of our knowledge there is no literature that supports and explains this fact.

3.2.5. Compression tests

The mechanical performance of the hydrogels was studied compressing them up to the 80% of their initial thickness. From the obtained stress-strain diagrams, the compression modules were calculated, as displayed in Table 5. As in the previous work, at the end of the tests none of the tested hydrogels was fractured and showed excellent recoverability. Nevertheless, the samples containing alkaline lignin from the single-step processes were slightly damaged due to their heterogeneous appearance.

The aforementioned samples (AA and WA) were the ones presenting the highest compression modules (14.8 and 16.3 MPa, respectively) although they were also the ones with the highest swelling ability, which might be related to the formed honeycomb structures due to the interactions of the matrix with lignin and its impurities, as shown in Section 3.2.3. In spite of their analogous morphology, the samples containing single-step organosolv lignins (AO and WO) presented much lower compression modules (4.95 and 6.01 MPa, respectively). A similar behaviour was observed for the samples composed of double-step lignins: the ones with alkaline lignin presented higher compression modules (6.63–13.07 MPa) than the organosolv ones (2.05–5.4 MPa).

The modules of all the samples presented a slight drop when increasing the duration of the last thawing step, probably due to the creation of the macro pores, as aforementioned. This trend was also aligned to the one observed for T_g values. All the estimated modules were in great accordance with previous results [13], and were higher than those reported by other authors for lignin-based hydrogels [1,45].

3.3. Methylene blue adsorption studies

So as to study the applicability of the designed hydrogels as dye adsorbents, methylene blue (MB) adsorption tests were performed following the procedure described before [13]. It is known that thanks to interactions of the multiple negative charges on the surface of lignin-hydrogels, these materials are able to capture positively charged compounds such as cationic dyes [12,13], which are also employed in many medical applications [46].

As displayed in Table 5, it was demonstrated that the synthesized samples presented great potential for MB adsorption for the tested solution, being the lowest removal value 75% and the highest 93% of the pollutant, which exceeded in both cases previous results [13]. In general, the samples containing double-step lignins were able to trap larger quantities of dye, and the alkaline lignin-based hydrogels removed slightly lower values of MB than the organosolv-based ones, which is also in line with the trend reported for the TPC of the lignins. Dominguez-Robles et al. (2018) also reported lower MB adsorption values for their samples containing soda lignin than for the ones with organosolv lignin, which could be related with the values they reported for the phenolic hydroxyl groups in these lignins [11]. In contrast, when the last thawing cycle was lengthened, the MB adsorption capacity of the samples containing alkaline lignins was enhanced whereas the MB removal of organosolv lignin-based hydrogels got slightly reduced. This fact suggested that although the last thawing cycle intensified the porosity of the samples, the availability of the negative charges on the surface was altered; nevertheless, this statement cannot be demonstrated.

In spite of the removal values being very high, it is true that the yield of the adsorption tests was much lower than in other studies. Whereas values from 2 to 200 mg dye/g hydrogel have been previously reported for lignin hydrogels [11,47–49], in this work none of the synthesized hydrogels surpassed 0.1 mg dye/g hydrogel. Furthermore, in recent years biochars have been used for the removal of these dyes, which far exceed the yields reported in this work [11,50]. Thus, the present hydrogels could be used for diluted MB environments, and modifications could be studied together with the combination with other compounds in order to enhance the adsorption yields.

3.4. Antifungal tests

The urgent need of searching for alternative eco-friendly materials has also swayed the food-packaging sector. In this context, bio-based hydrogels have emerged as potential adsorbents for these systems [51]. However, these materials should extend the shelf-life of the packaged products, which involves hindering the growth of microorganisms and fungi on them [51,52]. Thus, the antifungal properties against *Aspergillus niger* (brown-rot fungi), one of the most common fungi in food spoilage, were studied for all the synthesized hydrogels.

First of all, a visual evaluation of lignin's antifungal capacity was performed (see Supplementary data). Although mainly white-rot fungi are able to depolymerise lignin [53], some authors have also seen that brown-rot fungi are also capable to be lignin degraders. Nevertheless, in this case the tested fungi did not seem to have such ability. In spite of the growth of fungi the agar surface of all the samples, the deposited lignin drops could be clearly observed after the period of the test. This showed the antifungal ability of lignin, as also demonstrated by other authors before. Among the studied samples, the alkaline ones seemed to be able to inhibit more effectively the fungal growth than the organosolv ones, leading to a growth intensity of 3 ($GI = 3$), whereas most of the rest of the samples presented greater intensities ($GI \approx 4$), according to ISO 846 [15].

On the other hand, the same test was performed to the hydrogels. In all cases, the whole hydrogel portion was visible after the test (see Supplementary data). At first sight, the samples with alkaline WNS lignins (WA and AWA) as well as the samples containing organosolv AS lignins (AO and AWO) seemed to hinder the fungal development more than the samples containing other lignins. Moreover, there was almost no appreciable fungal growth on the top surface of the samples. In this case, the growth intensity would be between 3 and 4 for every sample [15].

The samples were washed with PBS and the surrounding spores were quantified as aforementioned. From the estimated FGI values (Fig. 6), it was seen that among the studied samples, the ones presenting the lowest fungal activity were WO and AAO (58 and 56.5% FGI, respectively), and the one presenting the highest growth was surprisingly AWA (almost 40% more than the control sample). It was observed that the samples containing single-step AS lignins presented lower FGI values than the ones with double-step AS lignins. Conversely, the samples containing double-step WNS lignins presented worse antifungal activity than the ones with single-step WNS lignins. Although the estimated values were approximate, these results helped making an idea of the antifungal properties that the synthesized samples presented. It is also worth to mention that none of the studied samples lost weight during the

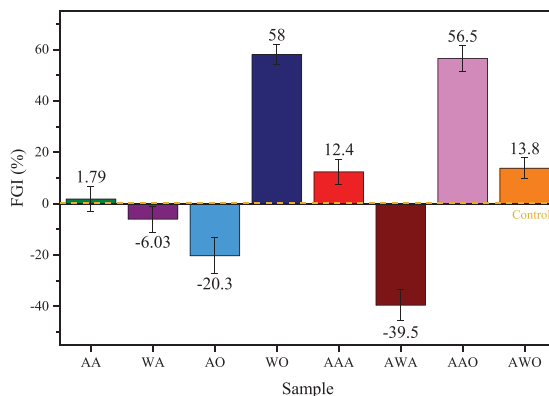


Fig. 6. Fungal growth inhibition (FGI, %) of the samples with respect to the control hydrogels ($y = 0$).

antifungal test, which supports their effectiveness against *A. niger*.

Several authors have reported similar FGI values for other materials for food packaging applications. For instance, Salaberria et al. (2017) reported 52–62% of inhibition for PLA films containing functionalized chitin nanocrystals [14]. In the study of Fernandez-Marin et al. (2021), these values were between 72 and 86% for their chitosan/ β -chitin nanofibers nanocomposites due to the incorporation of diterpenated *Origanum majorana* L. essential oil [54]. Conversely, Dey et al. (2021) reported values between 51 and 56% for neat PVA films, which were negatively affected by the addition of cellulose nanocrystals and chitosan nanoparticles [55]. Thus, taking these data into account, it can be concluded that the results reported for WO and AAO hydrogels were in total agreement with the ones reported by other authors and could be employed in food packaging.

4. Conclusions

In this study, alkaline and organosolv lignins were extracted from almond and walnut shells through two different biorefinery strategies and successfully employed for the synthesis of lignin-based physical hydrogels. The characterization of the extracted lignins showed significant differences between the lignin samples, especially on their composition, average molecular weights and total phenolic contents. As expected, the autohydrolysis enhanced the purity of the lignins, especially in the case of alkaline ones, and it also promoted the extraction of lignins with higher average molecular weights. These changes altered the morphology of the produced hydrogels and, hence, their properties such as their swelling capacity, glass transition temperatures and compression modules. In fact, hydrogels containing lignins from the single-step process resulted into a more honeycomb porous structure and, thus, a higher water absorption capacity. In addition, when the last thawing step was lengthened, larger pores were created, which also led to a notable enhancement of the swelling percentage of the hydrogels. The synthesized materials showed good methylene blue removal (75–93%) and, in some cases, antifungal properties (up to 58% of FGI), demonstrating their versatility on various application fields.

Declaration of Competing Interest

The authors declare that they have no known competing financial interests or personal relationships that could have appeared to influence the work reported in this paper.

Acknowledgements

The authors would like to acknowledge the financial support of the Department of Education of the Basque Government (IT1008-16). A. Morales would like to thank the University of the Basque Country (Training of Researcher Staff, PIF17/207). P. Gullón would like to acknowledge the Grants for the recruitment of technical support staff (PTA2019-017850-I) under the State Plan for Scientific and Technical Research and Innovation 2017–2020. The authors thank SGiker (UPV/EHU/ERDF, EU) for their technical and human support.

Appendix A. Supplementary data

Supplementary data to this article can be found online at <https://doi.org/10.1016/j.susmat.2021.e00369>.

References

- [1] R.M. Kalinoski, J. Shi, Hydrogels derived from lignocellulosic compounds: evaluation of the compositional, structural, mechanical and antimicrobial properties, *Ind. Crop. Prod.* 128 (2019) 323–330, <https://doi.org/10.1016/j.indcrop.2018.11.002>.
- [2] D. Rico-García, L. Ruiz-Rubio, L. Pérez-Álvarez, S.L. Hernández-Olmos, G. L. Guerrero-Ramírez, J.L. Vilas-Vilela, Lignin-based hydrogels: synthesis and applications, *Polymers (Basel)*. 12 (2020) 1–23.
- [3] A. Oryan, A. Kamali, A. Moshiri, H. Baharvand, H. Daemi, Chemical crosslinking of biopolymeric scaffolds: current knowledge and future directions of crosslinked engineered bone scaffolds, *Int. J. Biol. Macromol.* 107 (2018) 678–688, <https://doi.org/10.1016/j.ijbiomac.2017.08.184>.
- [4] H. Nakajima, P. Dijkstra, K. Loos, The recent developments in biobased polymers toward general and engineering applications: polymers that are upgraded from biodegradable polymers, analogous to petroleum-derived polymers, and newly developed, *Polymers (Basel)*. 9 (2017) 1–26, <https://doi.org/10.3390/polym9100523>.
- [5] S. RameshKumar, P. Shaiju, K.E. O'Connor, P. Ramesh Babu, Bio-based and biodegradable polymers - state-of-the-art, challenges and emerging trends, *Curr. Opin. Green Sustain. Chem.* 21 (2020) 75–81, <https://doi.org/10.1016/j.cogsc.2019.12.005>.
- [6] A.T. Ubando, C.B. Felix, W.H. Chen, Biorefineries in circular bioeconomy: a comprehensive review, *Bioresour. Technol.* 299 (2020), <https://doi.org/10.1016/j.biortech.2019.122585>.
- [7] A. Morales, J. Labidi, P. Gullón, Hydrothermal treatments of walnut shells: a potential pretreatment for subsequent product obtaining, *Sci. Total Environ.* 764 (2021), 142800, <https://doi.org/10.1016/j.scitotenv.2020.142800>.
- [8] G. Dragone, A.A.J. Kersemakers, J.L.S.P. Driessen, C.K. Yamakawa, L.P. Brumano, S.I. Mussatto, Innovation and strategic orientations for the development of advanced biorefineries, *Bioresour. Technol.* 302 (2020), 122847, <https://doi.org/10.1016/j.biortech.2020.122847>.
- [9] J.J. Liao, N.H.A. Latif, D. Trache, N. Brosse, M.H. Hussin, Current advancement on the isolation, characterization and application of lignin, *Int. J. Biol. Macromol.* 162 (2020) 985–1024, <https://doi.org/10.1016/j.ijbiomac.2020.06.168>.
- [10] A. Morales, F. Hernández-Ramos, L. Sillero, R. Fernández-Marin, I. Dávila, P. Gullón, X. Erdocia, J. Labidi, Multiproduct biorefinery based on almond shells: impact of the delignification stage on the manufacture of valuable products, *Bioresour. Technol.* 315 (2020), <https://doi.org/10.1016/j.biortech.2020.123896>.
- [11] J. Domínguez-Robles, M.S. Peresin, T. Tamminen, A. Rodriguez, E. Larrañeta, A. S. Jaaskeläinen, Lignin-based hydrogels with "super-swelling" capacities for dye removal, *Int. J. Biol. Macromol.* 115 (2018) 1249–1259, <https://doi.org/10.1016/j.ijbiomac.2018.04.044>.
- [12] L. Wu, S. Huang, J. Zheng, Z. Qiu, X. Lin, Y. Qin, Synthesis and characterization of biomass lignin-based PVA super-absorbent hydrogel, *Int. J. Biol. Macromol.* 140 (2019) 538–545, <https://doi.org/10.1016/j.ijbiomac.2019.08.142>.
- [13] A. Morales, J. Labidi, P. Gullón, Effect of the formulation parameters on the absorption capacity of smart lignin-hydrogels, *Eur. Polym. J.* 129 (2020), 109631, <https://doi.org/10.1016/j.eurpolymj.2020.109631>.
- [14] A.M. Salaberria, R.H. Diaz, M.A. Andrés, S.C.M. Fernandes, J. Labidi, The antifungal activity of functionalized chitin nanocrystals in poly (Lactid acid) films, *Materials (Basel)*. 10 (2017) 1–16, <https://doi.org/10.3390/ma10050546>.
- [15] D.T. Da Silva, R. Herrera, B.M. Heinzmann, J. Calvo, J. Labidi, Nectandra grandiflora by-products obtained by alternative extraction methods as a source of phytochemicals with antioxidant and antifungal properties, *Molecules*. 23 (2018) 1–16, <https://doi.org/10.3390/molecules23020372>.
- [16] J. Fernández-Rodríguez, X. Erdocia, C. Sánchez, M. González Alriols, J. Labidi, Lignin depolymerization for phenolic monomers production by sustainable processes, *J. Energy Chem.* 26 (2017) 622–631, <https://doi.org/10.1016/j.jechem.2017.02.007>.
- [17] C.S.G.P. Queirós, S. Cardoso, A. Lourenço, J. Ferreira, I. Miranda, M.J.V. Lourenço, H. Pereira, Characterization of walnut, almond, and pine nut shells regarding chemical composition and extract composition, *Biomass Convers. Biorefin.* 10 (2020) 175–188, <https://doi.org/10.1007/s13399-019-00424-2>.
- [18] A. Morales, B. Gullón, I. Dávila, G. Eibes, J. Labidi, P. Gullón, Optimization of alkaline pretreatment for the co-production of biopolymer lignin and bioethanol from chestnut shells following a biorefinery approach, *Ind. Crop. Prod.* 124 (2018), <https://doi.org/10.1016/j.indcrop.2018.08.032>.
- [19] J. Li, P. Feng, H. Xiu, J. Li, X. Yang, F. Ma, X. Li, X. Zhang, E. Kozliak, Y. Ji, Morphological changes of lignin during separation of wheat straw components by the hydrothermal-ethanol method, *Bioresour. Technol.* 294 (2019), <https://doi.org/10.1016/j.biortech.2019.122157>.
- [20] M.Q. Zhu, J.L. Wen, Y.Q. Su, Q. Wei, R.C. Sun, Effect of structural changes of lignin during the autohydrolysis and organosolv pretreatment on *Eucommia ulmoides* Oliver for an effective enzymatic hydrolysis, *Bioresour. Technol.* 185 (2015) 378–385, <https://doi.org/10.1016/j.biortech.2015.02.061>.
- [21] I. Dávila, P. Gullón, M.A. Andrés, J. Labidi, Coproduction of lignin and glucose from vine shoots by eco-friendly strategies: toward the development of an integrated biorefinery, *Bioresour. Technol.* 244 (2017) 328–337, <https://doi.org/10.1016/j.biortech.2017.07.104>.
- [22] I. Dávila, B. Gullón, J. Labidi, P. Gullón, Multiproduct biorefinery from vine shoots: bio-ethanol and lignin production, *Renew. Energy* 142 (2019) 612–623.
- [23] A. García, M. González Alriols, G. Spigno, J. Labidi, Lignin as natural radical scavenger. Effect of the obtaining and purification processes on the antioxidant behaviour of lignin, *Biochem. Eng. J.* 67 (2012) 173–185, <https://doi.org/10.1016/j.bej.2012.06.013>.
- [24] A. García, G. Spigno, J. Labidi, Antioxidant and biocide behaviour of lignin fractions from apple tree pruning residues, *Ind. Crop. Prod.* 104 (2017) 242–252, <https://doi.org/10.1016/j.indcrop.2017.04.063>.
- [25] A. Sequeiros, D.A. Gatto, J. Labidi, L. Serrano, Different extraction methods to obtain lignin from almond shell, *J. Biobased Mater. Bioenergy*. 8 (2014) 370–376, <https://doi.org/10.1166/jbmb.2014.1443>.

- [26] S. De, S. Mishra, E. Poonguzhali, M. Rajesh, K. Tamilarasan, Fractionation and characterization of lignin from waste rice straw: biomass surface chemical composition analysis, *Int. J. Biol. Macromol.* 145 (2020) 795–803, <https://doi.org/10.1016/j.ijbiomac.2019.10.068>.
- [27] I. Gómez-Cruz, M. del Mar Contreras, I. Romero, E. Castro, A biorefinery approach to obtain antioxidants, lignin and sugars from exhausted olive pomace, *J. Ind. Eng. Chem.* 96 (2021) 356–363, <https://doi.org/10.1016/j.jiec.2021.01.042>.
- [28] C. Xu, F. Liu, M.A. Alam, H. Chen, Y. Zhang, C. Liang, H. Xu, S. Huang, J. Xu, Z. Wang, Comparative study on the properties of lignin isolated from different pretreated sugarcane bagasse and its inhibitory effects on enzymatic hydrolysis, *Int. J. Biol. Macromol.* 146 (2020) 132–140, <https://doi.org/10.1016/j.ijbiomac.2019.12.270>.
- [29] A. Goudarzi, L.-T. Lin, F.K. Ko, X-ray diffraction analysis of Kraft Lignins and lignin-derived carbon nanofibers, *J. Nanotechnol. Eng. Med.* 5 (2014), 021006, <https://doi.org/10.1115/1.4028300>.
- [30] S. Kumar, Y.S. Negi, J.S. Upadhyaya, Studies on characterization of corn cob based nanoparticles, *Adv. Mater. Lett.* 1 (2010) 246–253, <https://doi.org/10.5185/amlett.2010.9164>.
- [31] A.C.F. Louis, S. Venkatachalam, Energy efficient process for valorization of corn cob as a source for nanocrystalline cellulose and hemicellulose production, *Int. J. Biol. Macromol.* 163 (2020) 260–269, <https://doi.org/10.1016/j.ijbiomac.2020.06.276>.
- [32] M.K. Haider, A. Ullah, M.N. Sarwar, Y. Saito, L. Sun, S. Park, I.S. Kim, Lignin-mediated in-situ synthesis of CuO nanoparticles on cellulose nanofibers: a potential wound dressing material, *Int. J. Biol. Macromol.* 173 (2021) 315–326, <https://doi.org/10.1016/j.ijbiomac.2021.01.050>.
- [33] M. Braham, N. Boussetta, N. Grimi, E. Vorobiev, I. Zieger-Devin, N. Brosse, Pretreatment optimization from rapeseed straw and lignin characterization, *Ind. Crop. Prod.* 95 (2017) 643–650, <https://doi.org/10.1016/j.indcrop.2016.11.033>.
- [34] X. Yang, Y. Zhao, H. Mussana, M. Tessema, L. Liu, Characteristics of cotton fabric modified with chitosan (CS)/cellulose nanocrystal (CNC) nanocomposites, *Mater. Lett.* 211 (2018) 300–303, <https://doi.org/10.1016/j.matlet.2017.09.075>.
- [35] L. Chen, X. Wang, H. Yang, Q. Lu, D. Li, Q. Yang, H. Chen, Study on pyrolysis behaviors of non-woody lignins with TG-FTIR and Py-GC/MS, *J. Anal. Appl. Pyrolysis* 113 (2015) 499–507, <https://doi.org/10.1016/j.jaap.2015.03.018>.
- [36] J.I. Daza Agudelo, J.M. Badano, I. Rintoul, Kinetics and thermodynamics of swelling and dissolution of PVA gels obtained by freeze-thaw technique, *Mater. Chem. Phys.* 216 (2018) 14–21, <https://doi.org/10.1016/j.matchemphys.2018.05.038>.
- [37] X. Han, Z. Lv, F. Ran, L. Dai, C. Li, C. Si, Green and stable piezoresistive pressure sensor based on lignin-silver hybrid nanoparticles/polyvinyl alcohol hydrogel, *Int. J. Biol. Macromol.* 176 (2021) 78–86, <https://doi.org/10.1016/j.ijbiomac.2021.02.055>.
- [38] Q. Wang, J. Guo, X. Lu, X. Ma, S. Cao, X. Pan, Y. Ni, Wearable lignin-based hydrogel electronics: a mini-review, *Int. J. Biol. Macromol.* (2021), <https://doi.org/10.1016/j.ijbiomac.2021.03.079>.
- [39] L. Sun, Z. Mo, Q. Li, D. Zheng, X. Qiu, X. Pan, Facile synthesis and performance of pH/temperature dual-response hydrogel containing lignin-based carbon dots, *Int. J. Biol. Macromol.* 175 (2021) 516–525, <https://doi.org/10.1016/j.ijbiomac.2021.02.049>.
- [40] A. Morales, J. Labidi, P. Gullón, Assessment of green approaches for the synthesis of physically crosslinked lignin hydrogels, *J. Ind. Eng. Chem.* 81 (2020) 475–487, <https://doi.org/10.1016/j.jiec.2019.09.037>.
- [41] I.E. Raschip, G.E. Hitruc, C. Vasile, M.C. Popescu, Effect of the lignin type on the morphology and thermal properties of the xanthan/lignin hydrogels, *Int. J. Biol. Macromol.* 54 (2013) 230–237, <https://doi.org/10.1016/j.ijbiomac.2012.12.036>.
- [42] A.H.A. Wahab, A.P.M. Saad, M.N. Harun, A. Syahrom, M.H. Ramlee, M.A. Sulong, M.R.A. Kadir, Developing functionally graded PVA hydrogel using simple freeze-thaw method for artificial glenoid labrum, *J. Mech. Behav. Biomed. Mater.* 91 (2019) 406–415, <https://doi.org/10.1016/j.jmbmb.2018.12.033>.
- [43] S. Butylina, S. Geng, K. Oksman, Properties of as-prepared and freeze-dried hydrogels made from poly(vinyl alcohol) and cellulose nanocrystals using freeze-thaw technique, *Eur. Polym. J.* 81 (2016) 386–396, <https://doi.org/10.1016/j.eurpolymj.2016.06.028>.
- [44] X.-Q. Hu, D.-Z. Ye, J.-B. Tang, L.-J. Zhang, X. Zhang, From waste to functional additives: thermal stabilization and toughening of PVA with lignin, *RSC Adv.* 6 (2016) 13797–13802, <https://doi.org/10.1039/C5RA26385A>.
- [45] Y. Chen, K. Zheng, L. Niu, Y. Zhang, Y. Liu, C. Wang, F. Chu, Highly mechanical properties nanocomposite hydrogels with biorenewable lignin nanoparticles, *Int. J. Biol. Macromol.* 128 (2019) 414–420, <https://doi.org/10.1016/j.ijbiomac.2019.01.099>.
- [46] A.B. Albadarin, M.N. Collins, M. Naushad, S. Shirazian, G. Walker, C. Mangwandi, Activated lignin-chitosan extruded blends for efficient adsorption of methylene blue, *Chem. Eng. J.* 307 (2017) 264–272, <https://doi.org/10.1016/j.cej.2016.08.089>.
- [47] H. Qian, J. Wang, L. Yan, Synthesis of lignin-poly(N-methylaniline)-reduced graphene oxide hydrogel for organic dye and lead ions removal, *J. Biosour. Bioprod.* 5 (2020) 204–210, <https://doi.org/10.1016/j.jobab.2020.07.006>.
- [48] L. Wu, S. Huang, J. Zheng, Z. Qiu, X. Lin, Y. Qin, Synthesis and characterization of biomass lignin-based PVA super-absorbent hydrogel, *Int. J. Biol. Macromol.* 140 (2019) 538–545, <https://doi.org/10.1016/j.ijbiomac.2019.08.142>.
- [49] Y. Meng, C. Li, X. Liu, J. Lu, Y. Cheng, L.-P. Xiao, H. Wang, Preparation of magnetic hydrogel microspheres of lignin derivate for application in water, *Sci. Total Environ.* (2019), <https://doi.org/10.1016/j.scitotenv.2019.06.278>.
- [50] X.J. Liu, M.F. Li, S.K. Singh, Manganese-modified lignin biochar as adsorbent for removal of methylene blue, *J. Mater. Res. Technol.* 12 (2021) 1434–1445, <https://doi.org/10.1016/j.jmrt.2021.03.076>.
- [51] R.A. Batista, P.J.P. Espitia, J.S.S. de Quintans, M.M. Freitas, M.Á. Cerqueira, J. A. Teixeira, J.C. Cardoso, Hydrogel as an alternative structure for food packaging systems, *Carbohydr. Polym.* 205 (2019) 106–116, <https://doi.org/10.1016/j.carbpol.2018.10.006>.
- [52] N. Nguyen Van Long, C. Joly, P. Dantigny, Active packaging with antifungal activities, *Int. J. Food Microbiol.* 220 (2016) 73–90, <https://doi.org/10.1016/j.jfoodmicro.2016.01.001>.
- [53] O.Y. Abdelaziz, D.P. Brink, J. Prothmann, K. Ravi, M. Sun, J. García-Hidalgo, M. Sandahl, C.P. Hultberg, C. Turner, G. Lidén, M.F. Gorwa-Grauslund, Biological valorization of low molecular weight lignin, *Biotechnol. Adv.* 34 (2016) 1318–1346, <https://doi.org/10.1016/j.biotechadv.2016.10.001>.
- [54] R. Fernández-Marín, M. Mujtaba, D. Cansaran-Duman, G. Ben Salha, M.Á. A. Sánchez, J. Labidi, S.C.M. Fernandes, Effect of deterpented origanum majorana L. Essential oil on the physicochemical and biological properties of chitosan/ β -chitin nanofibers nanocomposite films, *Polymers (Basel)*. 13 (2021), <https://doi.org/10.3390/polym13091507>.
- [55] D. Dey, V. Dharini, S.P. Selvam, E.R. Sadiku, M.M. Kumar, J. Jayaramudu, U. N. Gupta, Physical, antifungal, and biodegradable properties of cellulose nanocrystals and chitosan nanoparticles for food packaging application, *Mater. Today Proc.* 38 (2021) 860–869, <https://doi.org/10.1016/j.matpr.2020.04.885>.
- [56] I. Zaranzona, A.I. Puertas, M.T. Dueñas, P. Guerrero, K. de la Caba, Assessment of active chitosan films incorporated with gallic acid, *Food Hydrocoll.* 101 (2020), <https://doi.org/10.1016/j.foodhyd.2019.105486>.

Impact of the lignin type and source on the characteristics of physical lignin hydrogels

Amaia Morales^a, Jalel Labidi^{a,*}, Patricia Gullón^b

^aChemical and Environmental Engineering Department, University of the Basque Country UPV/EHU, Plaza Europa 1, 20018, San Sebastián, Spain

^bC.A.C.T.I. Laboratory, Technology Park of Galicia- Tecnopole, CTC Building, 32901, San Cibrao das Viñas, Ourense, Spain

*Corresponding author: jalel.labidi@ehu.es

Supplementary data

Table S1. Identification of the compounds detected by Py-GC/MS for the extracted lignins.

Peak #	RT (min)	Compound	Origin	AA	AO	WA	WO	AAA	AAO	AWA	AWO
1	7.5-7.7	Phenol	H	1.62	0.98	6.56	3.29	1.16		4.26	2.95
2	8.2	2-Methyliminoperhydro-1,3-oxazine	-	5.77		9.95					
3	8.7-8.9	o-cresol	H	1.53	1.04	2.42	1.22	1.80	1.14	1.66	1.21
4	9.0-9.2	p-cresol	H	1.82	1.62	5.22	5.31	1.39	0.92	4.58	4.12
5	9.3-9.5	Guaiacol	G	13.62	11.80	9.30	8.91	17.14	7.40	11.72	7.56
6	10.4	Phenol, 2,6-dimethyl-	H	1.68	1.38	1.45	1.53	1.95	1.77	1.44	1.52
7	10.7-10.8	p-Ethylphenol	H	0.74		2.40	1.66	0.54		1.71	1.43
8	11.0-11.1	3-Methylguaiacol	G	2.08	1.35	0.94	1.29	3.90	1.17	2.28	1.24
9	11.4-11.6	4-Methylguaiacol	G	9.75	12.74	5.23	10.86	15.19	8.08	10.07	7.73
10	13.3-13.5	3-Methoxycatechol	S	0.19	3.29	0.95	4.22	2.56	3.67	4.39	4.33
11	13.8-14.0	4-Ethylguaiacol	G	7.78	5.67	3.80	5.15	8.82	3.63	7.09	3.79
12	15.0-15.2	4-Vinylguaiacol	G	6.94	7.16	3.76	5.77	4.52	3.00	3.51	3.10
13	16.1-16.2	Syringol	S	7.45	9.69	3.96	10.57	8.13	5.42	16.52	7.18
14	16.3	3,4-Dimethoxyphenol	S	1.69	1.87	0.64	2.55	1.82	0.88		2.13
15	17.4	cis-Isoeugenol	G	1.12	1.70	0.34	1.60	1.19	0.85	1.35	0.84
16	18.3	4-Methylsyringol	S	4.75	12.03	2.69	13.66	5.94	6.80	9.23	7.54
17	19.6	4-Ethylsyringol	S	1.02	1.28	0.78	1.95	1.16	0.82	2.47	0.90
18	20.2-20.8	4-Vinylsyringol	S	0.23	1.92	0.24	1.72	0.62	0.73	0.87	0.96
19	21.6	Syringaldehyde	S		1.20	0.47	0.62	0.40	1.65	0.16	2.56
20	22.1	4-Allylsyringol	S	0.51	2.09	0.83	2.11	0.50	0.40	0.51	1.56
21	22.5	Acetosyringone	S	0.13	2.03	0.87	0.86	0.34	1.45	0.17	2.44
22	23.0	Homosyringic acid	S		1.07		0.42	0.15	0.64		1.30
Total S				15.96	36.48	11.43	38.67	21.62	22.47	34.31	30.90
Total G				41.29	40.44	23.37	33.57	50.78	24.14	36.02	24.26
Total H				7.39	5.02	18.05	13.00	6.84	3.84	13.65	11.23
S/G ratio				0.39	0.90	0.49	1.15	0.43	0.93	0.95	1.27

Figure S1. TGA curves of the synthesized hydrogels.

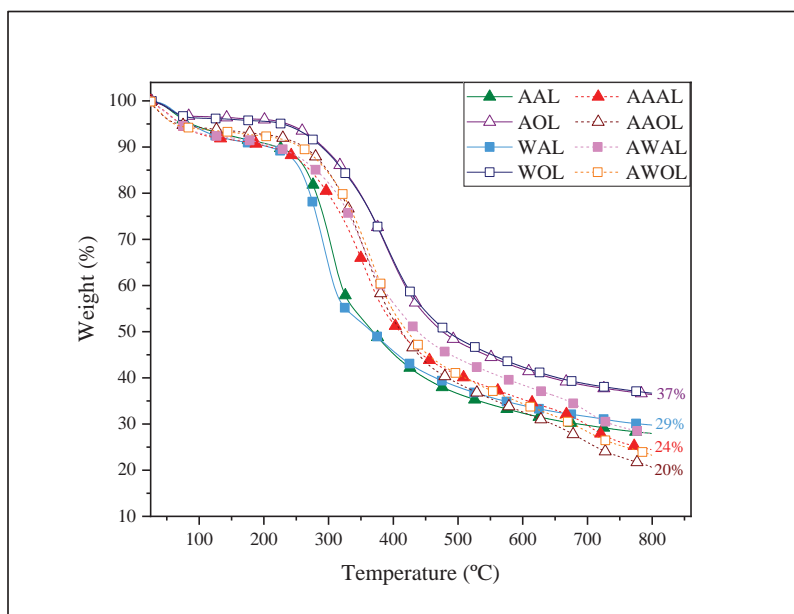


Figure S2. SEM micrographs of the hydrogels containing WNS lignins at 500x and 5000x magnifications.

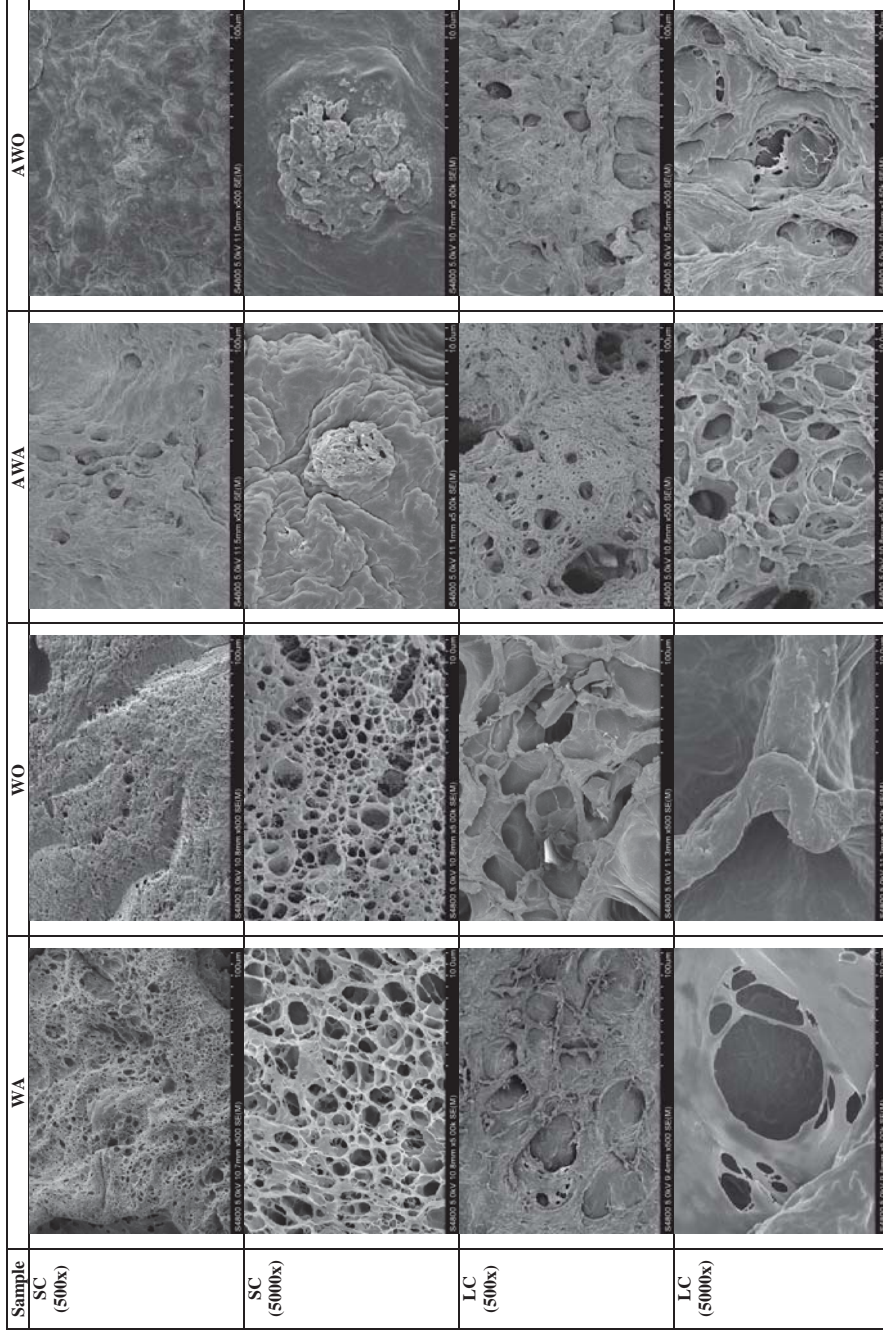
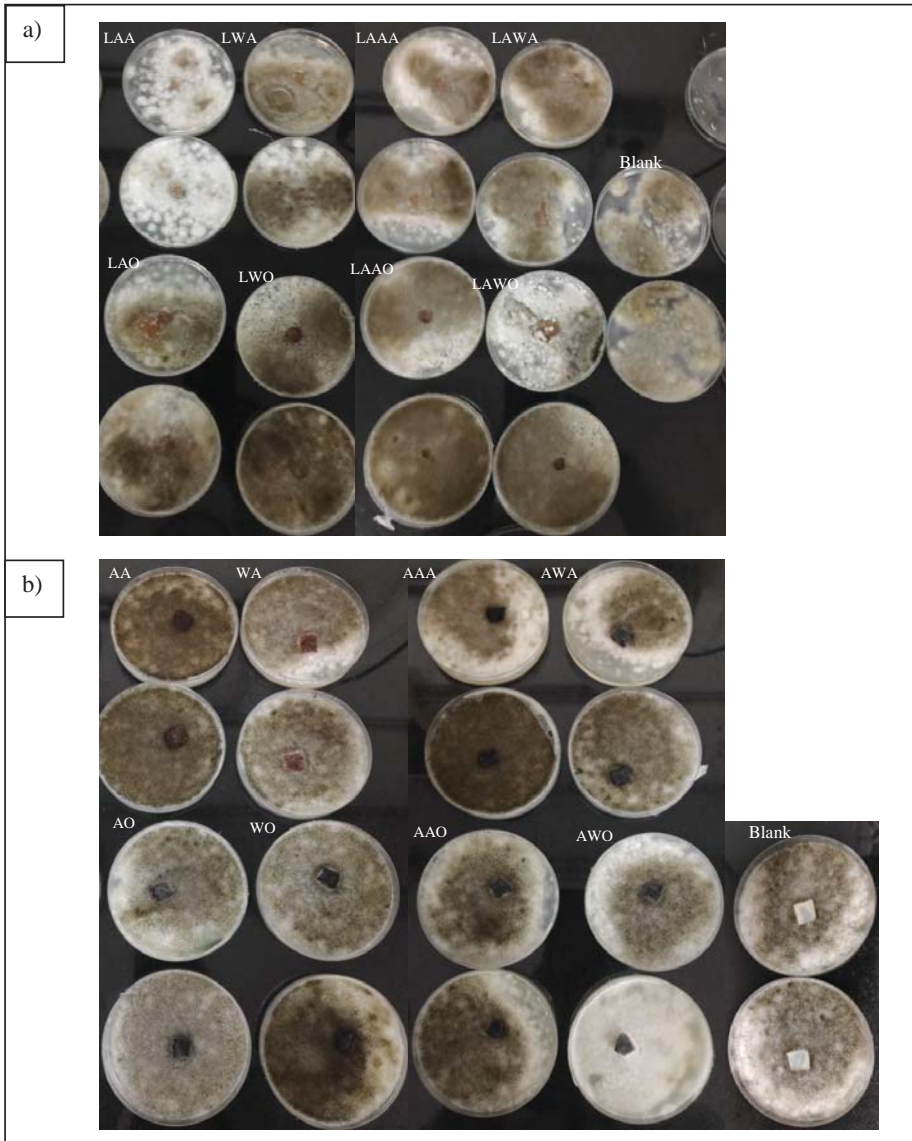


Figure S3. Images of the antifungal tests of lignins (a) and hydrogels (b).



Publication V

Influence of lignin modifications on physically crosslinked lignin hydrogels for drug delivery applications

A. Morales, J. Labidi, P. Gullón

V

Submitted to Ind. Crops. Prod.
December 2021

Influence of lignin modifications on physically crosslinked lignin hydrogels for drug delivery applications

Amaia Morales^a, Jalel Labidi^{a,*}, Patricia Gullón^b

^aChemical and Environmental Engineering Department, University of the Basque Country UPV/EHU, Plaza Europa 1, 20018, San Sebastián, Spain

^bC.A.C.T.I. Laboratory, Technology Park of Galicia- Tecnopole, CTC Building, 32901, San Cibrao das Viñas, Ourense, Spain

*Corresponding author: jalel.labidi@ehu.es

Abstract: So far, the possibility of synthesising hydrogels based on multiple biopolymers has been investigated, and among them lignin has proven to be one of the potentials for this purpose due to the multiple advantages it offers. However, because of its high molecular weight, steric hindrance and few reactive sites on its structure, it is sometimes necessary to improve its reactivity through chemical modifications. On the basis of previous results, two chemical modifications were selected in order to enhance almond, walnut and commercial alkaline and organosolv lignins' reactivity: a peroxidation reaction for alkaline ones and a hydroxymethylation for organosolv ones. Both reactions were confirmed by multiple techniques (i.e. FTIR, GPC and TGA). Hydrogels were synthesized from these lignins according to previous works. The high lignin waste of the synthesized hydrogels suggested that despite the modification of the lignins, just the highest molecular weight fractions reacted with the matrix polymer. Moreover, the swelling capacity of modified alkaline lignin-based hydrogels was negatively affected, whereas the one for organosolv lignin-based samples improved. The SEM micrographs explained the aforementioned, and the results from the DSC and compression tests were in accordance with them. Self-extracted quercetin loading and release studies suggested that these samples could be used for controlled drug delivery.

Keywords: modified lignin, peroxidation, hydroxymethylation, hydrogels, drug delivery

1. Introduction

The insatiable demand for energy and fossil resources has driven the current society to many global environmental and social concerns. In this context, lignocellulosic biomass has opened an alternative door to the production of chemicals, materials and fuels (Yoo et al., 2020). This biomass is constituted by lignin, hemicelluloses and cellulose. Although biorefineries, the sustainable combination of processes able to transform biomass into a great variety of commercial products (Dragone et al., 2020), have mostly been focused on cellulose and hemicelluloses for the production of paper and bioethanol (Kumar et al., 2020), for instance, the conversion of lignin into value-added compounds is vital for the cost-competitiveness of biorefineries (Wang et al., 2019). In fact, lignin can constitute up to 40% of woody biomass and 15% of herbal one (Tribot et al., 2019) and it has demonstrated to possess interesting properties not just in energetic terms but also for the synthesis of new bio-based materials (Iravani and Varma, 2020).

Lignins' structure is an intricate and random combination of phenylpropanoid units (i.e. coniferyl, coumaril and sinapyl alcohols), which varies according to the source and kind of plant, its culture conditions and the used lignin isolation method (Zevallos Torres et al., 2020). In addition, the lignin structure is

highly branched and has multiple functional groups including carbonyl (C=O), hydroxyl (-OH), carboxyl (-COOH) and methoxy (-CH₃O) groups (Tribot et al., 2019), which have a direct effect on its reactivity (X. Meng et al., 2019). Moreover, the reactivity of this biopolymer is usually not high enough owing to its high molecular weight, steric hindrance and few reactive sites (Chen et al., 2020; Dragone et al., 2020). Therefore, in order to overcome this drawback it is sometimes necessary to perform a chemical modification of its structure (Goliszek et al., 2021). For this aim, there are four main ways: the first one involves its depolymerization or fragmentation, the second one focuses on the creation of chemically active sites, the third one is related to the modification of the hydroxyl groups in its structure; and the last one would be through the production of graft copolymers (Figueiredo et al., 2018).

According to various studies, lignin can confer interesting properties to lignin-based composite materials such as antioxidant or antibacterial capacity (Musilová et al., 2018). This fact makes lignin attractive for the formulation of materials to be used in the biomedical field. A clear example of this is the rising trend of lignin addition into hydrogels (Rico-García et al., 2020), which are very useful materials for drug delivery

(Larrañeta et al., 2018), wound dressing (Zhang et al., 2020) and tissue engineering and regenerative medicine (Barros et al., 2016), for instance.

Recently, modified lignins have been used for the formulation of hydrogels in order to overcome some drawbacks such as agglomeration or water insolubility (Musilová et al., 2018), although many of them have been applied for pollutant adsorption (Goliszek et al., 2021; Y. Meng et al., 2019). Moreover, lignin modifications can be crucial to avoid the use of chemical crosslinking agents, promoting the synthesis of physically-crosslinked hydrogels, which are usually more environmentally friendly and economical (Oryan et al., 2018).

Previously, the influence of the source and characteristics of alkaline and organosolv nut-shell (almond and walnut) lignins was studied (Morales et al., 2021) as well as the impact of commercial ones (Morales et al., 2020a) on the characteristics of the hydrogels. Nevertheless, a great lignin waste was generally observed in all the systems as well as a lower swelling degree in organosolv lignin-containing hydrogels. Thus, the objective of this work was to modify previously employed lignins in order to enhance the aforementioned weaknesses and to observe their impact on the properties of the synthesized physical hydrogels. For this aim, alkaline lignins were fragmented via an oxidation reaction and the organosolv ones were hydroxymethylated so as to introduce new reactive sites into them. The modified lignins were characterised and the modifications were confirmed via various techniques (FTIR, GPC and ^{31}P NMR). Then, hydrogels were synthesized from modified lignins and their lignin wastes, swelling capacities, morphology, glass transition temperatures and mechanical properties were studied. In addition, the possibility of using these hydrogels as drug deliverers was studied by analysing their release kinetics of self-extracted quercetin.

2. Materials and Methods

2.1. Materials

Organosolv lignin was purchased from Chemical Point. Poly (vinyl alcohol) ($M_w = 83,000\text{-}124,000$ g/mol, 99+ % hydrolyzed), alkaline lignin and phosphate buffer saline (PBS) tablets were supplied by Sigma Aldrich. Sodium hydroxide (NaOH, analysis grade, $\geq 98\%$, pellets), hydrogen peroxide (30% w/v, for analysis), formaldehyde (37-38% w/w, stabilized with methanol, for analysis) and hydrochloric acid (37%, for analysis) were purchased from PanReac Química SLU. All reagents were employed as supplied.

Almond (AS) and walnut shell (WNS) alkaline and organosolv lignins extracted in a previous work via subsequent autohydrolysis and delignification processes were used in this work (Morales et al., 2021).

2.2. Lignin modification

Alkaline lignins from AS and WNS as well as the commercial one were subjected to a microwave assisted peroxidation reaction with hydrogen peroxide as described by Infante et al. (2007)(Infante et al., 2007). Briefly, lignin and hydrogen peroxide were introduced into a high-pressure vessel keeping a LSR of 10:1 (mL:g). After sealing the vessel, it was subjected to three irradiation cycles of 10 seconds at 1100 W with a 30 second suspension period between them. Afterwards, the vessel was cleaned with distilled water and the collected mixture was left to dry over an oven.

Organosolv lignins (from AS, WNS and the commercial one) were exposed to a hydroxymethylation reaction with formaldehyde following the procedure reported by Chen et al. (2020)(Chen et al., 2020) with slight modifications. Concisely, 0.6 g of lignin were dissolved in an aqueous NaOH solution (140 mL). Then, 0.495 mL of formaldehyde were added and the solution was heated up to 80 °C under magnetic stirring and refrigeration. The reaction was left for 3.5 hours. Afterwards, the modified lignin was precipitated with 2% hydrochloric acid, filtered, neutralized and dried.

2.3. Lignin characterisation

All the lignins were characterised employing the methods described in previous works. Their purity and composition (Dávila et al., 2017), average molecular weights and total phenolic contents (Morales et al., 2018), thermal degradation, crystallinity and chemical structure (Morales et al., 2020a) were determined. In addition, in order to confirm the chemical modification of organosolv lignins, ^{31}P -NMR was employed following the protocol described by Meng et al. (2019) (X. Meng et al., 2019).

2.4. Hydrogel synthesis

The synthesis of the hydrogels was performed based on a previously detailed method (Morales et al., 2021, 2020a). In brief, 60 mL of a 2% (w/w) NaOH aqueous solution containing 9.87 w. % PVA was prepared and heated up to 90 °C until complete dissolution of PVA. Then, 9.12 w. % of lignin was added. After the lignin was dissolved, the blends were poured into silicon moulds, eliminating the remaining internal bubbles via ultrasound and the superficial air bubbles manually.

Five freeze-thawing cycles were then performed: firstly, the blends were completely frozen (2.5 hours) at -20 °C and, then, they were thawed at 28°C (1.5 hours). During the second and last cycles, the samples were left at the freezer overnight. Finally, the hydrogels were washed into distilled water and dried at room temperature.

2.5. Hydrogel characterisation

The characterisation of the hydrogels was also done based on previous works (Morales et al., 2021, 2020a, 2020b). Their lignin waste, swelling capacity, morphology, thermal behaviours and compression modules were studied.

2.6. Drug extraction and loading-release tests

Quercetin was extracted as a drug combining the methods reported by George et al. (2019) and Jin et al. (2011) (George et al., 2019; Jin et al., 2011). Firstly, onion peels were cleaned and dried at 50 °C before being powdered. Quercetin, together with other compounds, was then extracted by microwave assisted extraction (MAE), which was based on previous experiments (data not shown) modifying the microwave power reported by Jin et al. (2011) (Jin et al., 2011). The extraction was done with a 70% ethanol/water (v/v) solution, keeping a LSR of 40:1 (v/w). Since the used equipment was not a commercial microwave oven, the employed power for intermittent 10 second irradiations was fixed at 375 W. The total reaction time was 2 minutes, leaving a 20 second interval between the irradiations. After the reaction, the solid was filtered and the liquid phase was rotary evaporated for the complete elimination of ethanol. The remaining aqueous solution was considered as quercetin extract (QE).

The concentration of the quercetin extract was determined by UV spectrophotometry. For this purpose, a calibration curve was constructed using some solutions of certain concentrations of commercial quercetin (CQE) and measuring their absorbances at 375 nm (Jin et al., 2011). The total phenolic and flavonoid contents (TPC and TFC, respectively) of QE were estimated as described by Sillero et al. (2019) (Sillero et al., 2019), although in the case of TFC the standard was done with CQE. QE was freeze-dried and analysed by FTIR and compared with the spectrum of CQE.

The loading tests were performed by introducing dry hydrogel samples into diluted QE (1 mL QE into 250 mL distilled water) solutions for 24 hours. The absorbed QE amount was calculated by the difference on the concentrations of the initial and final solutions (George et al., 2019). After the loaded hydrogels were dried, they were weighted and again immersed into PBS at 37

°C, simulating *in vitro* conditions, for 24 hours. The release kinetics was performed by measuring the concentration of QE in PBS at certain times. All release tests were done in triplicates. The obtained results were introduced into various kinetic models including zero order, first order, Korsmeyer–Peppas and Higuchi (see Equations 1-4) so as to understand the release mechanism for QE (George et al., 2020, 2019; Saidi et al., 2020).

$$F = k_0 t \quad (1)$$

$$\ln(1 - F) = -k_1 t \quad (2)$$

$$\frac{M_t}{M_\infty} = k_{kp} t^n \quad (3)$$

$$F = k_h t^{1/2} \quad (4)$$

Being F the percentage of quercetin released at time t , n the diffusion exponent and k_0 , k_1 , k_{kp} and k_h the rate constants of zero order, first order, Korsmeyer-Peppas and Higuchi kinetic models, subsequently.

3. Results and Discussion

3.1. Lignin Characterisation

As shown in Table 1 the purity of the lignins was altered after the modification reaction, especially in self-extracted lignins. This might be due to the employed reagents. As for their molecular weight, their weight average molecular weights augmented in all cases, especially in alkaline lignins. Their number average molecular weights got decreased for modified self-extracted alkaline lignins and for commercial organosolv lignin, leading to a more meaningful rise in their polydispersity index. Surprisingly, commercial organosolv lignin (COL) and its modified version (MCOL) were the most heterogeneous lignins, whereas the self-extracted native and modified organosolv lignins (AAOL, AWOL, MAAOL and MAWOL) were the most homogeneous ones. Although the peroxidation reaction was supposed to fractionate lignin, a high percentage of the chains seemed to undergo re-condensation reactions, which made the total weight average molecular weights increase. However, no certain evidence of this has been found in literature. The change on the total phenolic content suggested the degradation of aromatic rings in lignin (Infante et al., 2007; Ouyang et al., 2010). However, CAL presented the opposite trend, which could be related to the differences on the pH of the solutions. According to the results reported by Xinpeng et al. (Ouyang et al., 2010), the reaction might have yielded more degradation compounds under alkaline conditions (Figueiredo et al., 2018), but as Infante et al. (2007) had demonstrated that this could also be achieved with the non-presence of a catalyst, the present

Table 1. Summary of the purity, GPC, TPC and TGA results for the modified lignins.

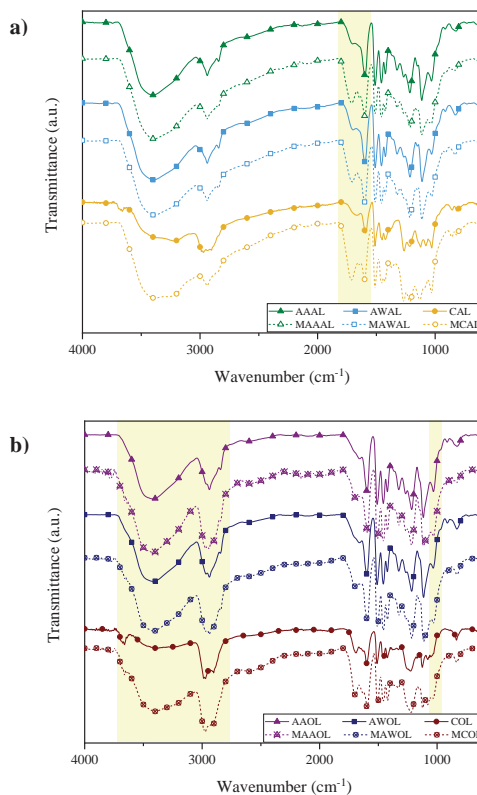
Lignin Sample	Purity (%)	M_w^a (g/mol)	M_n^b (g/mol)	M_w/M_n^c	TPC (% GAE ^d)	T_{max}^e (°C)
AAAL	88.2	12793	1528	8.4	33.1	355
AAOL	95.2	9020	1520	5.9	26.2	357
AWAL	95.7	16670	1604	10.4	33.8	354
AWOL	95.2	7644	1359	5.6	27.2	365
CAL	91.5	9333	1365	6.8	20.3	379
COL	92.5	32933	1123	29.3	19.3	343
MAAAL	85.2	17675	1348	13.1	25.3	384
MAAOL	92.3	9557	1636	5.8	20.4	383
MAWAL	84.0	19939	1369	14.6	27.6	384
MAWOL	83.6	8187	1420	5.8	23.6	383
MCAL	91.9	12141	1718	7.1	25.8	396
MCOL	96.5	32997	968	34.07	21.5	390

^a M_w : weight average molecular weight; ^b M_n : number average molecular weight; ^c M_w/M_n : polydispersity index; ^d % GAE: percentage of gallic acid equivalents; ^e T_{max} : maximum degradation temperature from TG/DTGA curves.

work was done according to the latter (Infante et al., 2007). In addition, the differences on the range 1600-1730 cm^{-1} on their FTIR spectra confirmed the reaction (see Figure 1a). In fact, the band around 1710 cm^{-1} moved to higher wavenumbers in all cases, which was attributed to the -OH oxidation of side chains, together with the weakening of the peak at 1599 cm^{-1} corresponding to aromatic C=C stretching vibration. In addition, as reported by Infante et al., the appearance of the band around 1640 cm^{-1} was also representative of the degradation of aromatic rings (Infante et al., 2007).

As for the hydroxymethylated lignins, it is known that formaldehyde may react with lignin in alkaline medium in two ways: the first one, by substituting the free ortho positions in the aromatic rings, and the second one, by reacting with the side chains containing carbonyl groups (Aini et al., 2019; Chen et al., 2020; Gilca et al., 2014). Nevertheless, if reactivity of the lignin is wanted to increase, the latter reaction should be avoided (Gilca et al., 2014). Moreover, hydroxymethyl groups can also react at free positions of other lignin units forming methylene bonds and leading to the condensation of the structure (Aini et al., 2019; Gilca et al., 2014). The variation on the distributions and average molecular weights suggested that the modification occurred (Gilca et al., 2014). Despite de fact that the change on the polydispersity of the lignins was not representative of having obtained more homogeneous modified lignins, their molecular weight distributions (Supplementary data) evoked a trend of homogenization of the highest molecular weight fractions towards the ones with lower molecular weights. This behaviour was also observed by other authors (Căpraru et al., 2012). Moreover, the increase on the number and weight average molecular weights was observed for MAAOL and MAWOL

samples, which was also reported by Capraru et al. (2012) for grass lignins.

**Figure 1.** FTIR spectra of modified and native alkaline (a) and organosolv (b) lignins.

The FTIR spectra of native and modified organosolv lignins also indicated the success of the reaction (Figure 1b)(Căpraru et al., 2012). In fact, the intensification of the -OH band (at 3400 cm^{-1}), the one corresponding to C-H (around 2930 cm^{-1}), the one

attributed to methoxyl and hydroxymethyl groups (around 2850 cm^{-1}) and the one related to the C–O stretching vibration of aliphatic C–OH and hydroxymethyl C–OH (around 1030 cm^{-1}) were a clear evidence of the introduction of hydroxymethyl groups via the modification reaction (Chen et al., 2020; Gilca et al., 2014). The appearance of a shoulder at 3660 cm^{-1} suggested the presence of free –OH groups within the modified lignin structures (Zang et al., 2015). These results were in agreement with those obtained from ^{31}P NMR analyses, in which an increase on the aliphatic hydroxyl signal between 150 and 145.4 ppm was observed for all the samples after the hydroxymethylation reaction (X. Meng et al., 2019) (Supplementary data).

The thermal stability of all the samples was altered through the modification reactions. In fact, the maximum degradation step was shifted to higher temperatures in all cases. However, in the case of alkaline lignins, another degradation step appeared between the stage corresponding to moisture evaporation (< 100 $^{\circ}\text{C}$) and the maximum degradation stage. This peak was detected around 300 $^{\circ}\text{C}$, and was attributed to the lower molecular weight fractions of lignin generated during the modification step (Dávila et al., 2017; Xu et al., 2020). It was also observed that organosolv lignins were more thermally stable and started to lose weight at higher temperatures than alkaline lignins, although their maximum degradation temperatures were slightly lower. Compared to native lignins, modified organosolv lignins presented higher thermal stability and final residue, which was also observed by Chen et al. (2020) (Chen et al., 2020). In addition, despite all the left residues being of around the 40% of the initial sample weight, modified organosolv lignins left higher residues than alkaline ones, conversely to what happened for native lignins, which may be attributed to the modification and lignin precipitation stages.

The crystallinity of the samples was almost unaltered by the modification reactions (Supplementary data). All the samples presented a wide peak around 22 $^{\circ}$, which is related to the amorphous structure of lignin (Ciolacu and Cazacu, 2018; Goudarzi et al., 2014).

3.2. Hydrogel characterization

3.2.1. Lignin waste

As in previous works, the lignin waste of the synthesized hydrogels was determined through UV spectroscopy (Table 2) (Morales et al., 2021, 2020a, 2020b). It was expected to have lower lignin wastes than in the previous works due to the higher reactivity of the modified lignins. Nevertheless, the results

proved that the hypothesis was incorrect, since the lignin waste determined for all the samples resulted to be higher than those reported previously. This change was significantly greater for the samples containing MCAL and MCOL, which presented a loss of almost 89 and 97% of their initial amount of lignin, respectively. The samples containing MAWA did also show a huge increase. The rest of the samples exhibited lower lignin waste raises, ranging from 12–14%.

Table 2. Lignin waste (%) of native and modified lignin-containing hydrogels.

Sample	Native (%)	Modified (%)
AAA	59.6 ± 2.8	73.5 ± 0.5
AAO	71.1 ± 3.0	83.4 ± 4.6
AWA	44.2 ± 1.6	71.6 ± 0.5
AWO	59.9 ± 4.0	74.0 ± 4.8
CA	67.8 ± 2.0	88.7 ± 3.4
CO	77.4 ± 1.7	96.5 ± 0.3

As the observed lignin wastes were so unexpected and so as to study the reusability of lignins in the washing solutions, it was decided to precipitate these lignins and study their molecular weights. These results are shown in Table 3. It was observed that in all cases the lost lignins had a lower weight average molecular weight than the native ones, and they were also more homogeneous, since their polydispersity indexes were lower. These results suggested that the polymeric matrix could have reacted with the highest molecular weight fractions, leading to a big elimination of the lowest molecular weight fractions.

Table 3. Average molecular weights and polydispersity indexes of the lignins recovered from the washing solutions.

Lignin Sample	M_w^a (g/mol)	M_n^b (g/mol)	M_w/M_n^c
MAAAL	10134	1317	7.7
MAAOL	7250	1592	4.5
MAWAL	10350	1643	6.3
MAWOL	6804	1569	4.5
MCAL	9710	1985	4.9
MCOL	3685	636	5.8

^a M_w : weight average molecular weight; ^b M_n : number average molecular weight; ^c M_w/M_n : polydispersity index

3.2.2. Swelling capacity

In order to determine the effect that the lignin modifications had on the properties of the synthesized hydrogels, their swelling capacity was studied. The results are depicted in Figure 2.

Comparing to previous results (Morales et al., 2021), it was observed that in the case of the alkaline lignin-containing

samples, the swelling capacity got significantly reduced when modified lignins were employed for their synthesis. These results suggest that the peroxidation of lignin performed in the present work was not an appropriate modification to obtain hydrogels with a high swelling capacity. On the other hand, when modified organosolv lignins were used, their swelling capacity was enhanced, especially in the case of the samples with MCOL (450%), which had also presented the highest lignin waste. Moreover, MAAO samples were the second ones with improved swelling capacity (410%), which also coincided with the second highest lignin waste. Similarly, MAWO samples exhibited the lightest enhancement on their swelling degree and had displayed the lowest lignin waste among the samples containing modified organosolv lignins. Thus, it could be concluded that hydroxymethylation could be a good method to enhance the swelling ability of organosolv lignin-based hydrogels.

Looking at the present results and comparing them with previous ones, it should be mentioned that although hydroxymethylation demonstrated to be effective for improving the swelling capacity of lignin-hydrogels, other variations during the synthesis process (lengthening the last thawing step, for instance) led to higher improvements on this property, without needing to modify the native lignins.

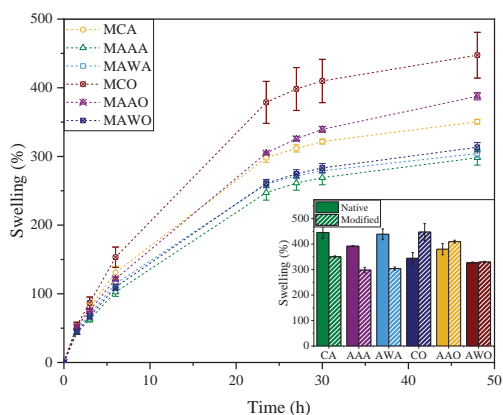


Figure 2. Swelling performance of modified lignin-based hydrogels during the first 48 h.

3.2.3. Morphology

Scanning Electron Microscopy (SEM) permitted studying the morphology of the samples. The obtained micrographs at 500x and 1500x magnifications are shown in Figure 3.

The images, in general, did not reveal highly porous structures; indeed they showed quite dense and continuous morphologies

with scarcely detectable voids. This fact was more evident in the samples containing alkaline lignins, which may be attributed to a greater crosslinking density, which would also clarify the decline on their swelling ability. For the samples containing organosolv lignins, especially for MAAO samples, the created voids were more obvious, which were probably responsible for the augment on their water absorption capacity. Hence, it is clear that the lignin modifications had direct impact on the microstructures of the synthesized hydrogels, which also clearly affected their swelling capacity.

2.1.1. Thermal behaviour

For some applications, the glass transition (T_g) and melting temperatures (T_m) of polymeric materials are determining features. Hence, these parameters together with the melting enthalpy (ΔH_m) and the crystallinity indexes (χ_c) for each sample were defined by Differential Scanning Calorimetry (DSC) and the results are displayed in Table 4. The T_g was found on the inflection point of the specific heat increment during the second heating scan, after removing the thermal memory of the samples, but the rest of the parameters were identified from the first heating scan. All the determined T_g values were in the range of 77–103 °C. These values were higher than those reported previously (Morales et al., 2021), suggesting that lignin modifications led to more compact structures in which the movement of the amorphous polymeric chains was hindered, which was also related to the obtained SEM micrographs. In addition, it was observed that the hydrogels containing modified organosolv lignins presented lower T_g values than the ones containing alkaline ones. Moreover, these results were aligned with the ones reported for the swelling capacity of the samples, being the aforementioned higher for the samples with lower T_g . Despite all the melting temperatures being similar (≈ 235 °C), they were quite close to pure the T_m of PVA hydrogels (Morales et al., 2020a, 2020b), and their melting enthalpies were also high, suggesting the existence of many crystalline regions (Yang et al., 2018). The crystallization indexes were calculated based on a well-known equation (He et al., 2019; Morales et al., 2020a), and the results suggested that a great part of the hydrogels was crystalline. In addition, the samples with higher filler contents seemed to have higher crystallinity degrees, which would be in accordance with previous results (Morales et al., 2020a) and could be due to an enhancement of interfacial interactions via hydrogen bonding between the multiple hydroxyl groups on the matrix polymer and lignin (He et al., 2019).

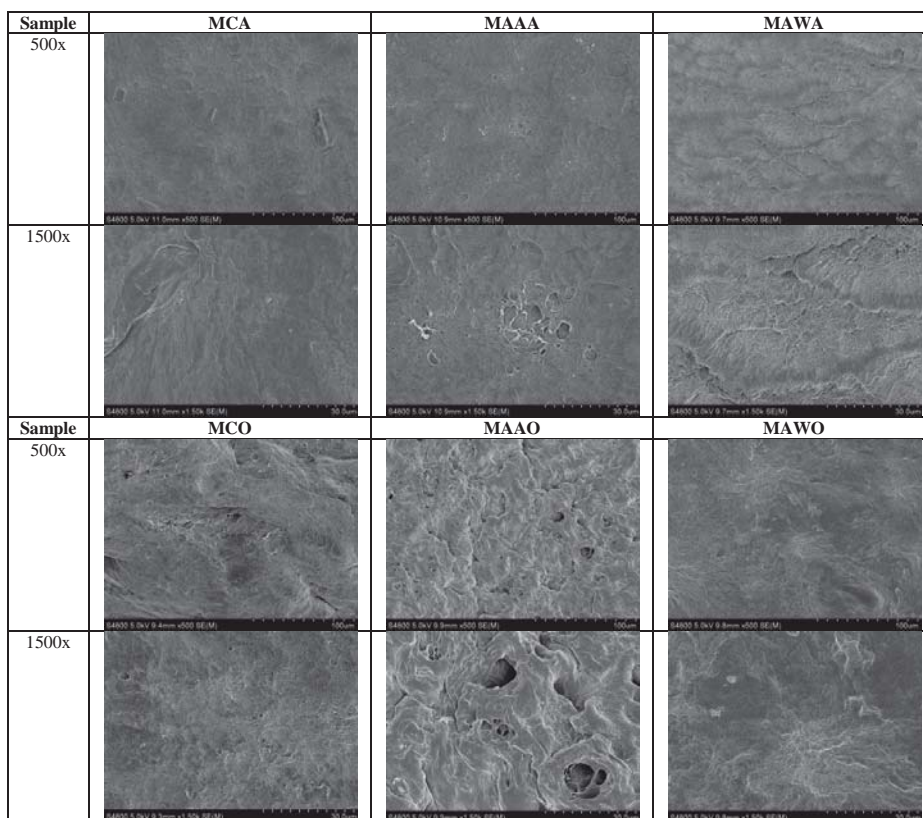


Figure 3. SEM micrographs for modified lignin-based hydrogels at 500x and 1500x magnifications.

Table 4. Summarized results for the analyzed parameters by DSC and calculations.

Sample	1 st heating scan				2 nd heating scan
	T _m (°C)	ΔH _m (J/g)	m _{filler} (%)	χ _c (%)	T _g (°C)
MAAA	235	64	25	53	103
MAAO	235	59	15	43	92
MAWA	236	62	27	52	81
MAWO	234	61	25	50	77
MCA	235	60	11	42	91
MCO	234	59	4	38	88

It was also observed that the samples containing alkaline lignin presented higher crystallinity indexes, which would explain their lower swelling abilities and higher T_g values.

2.1.2. Compression tests

The compression tests of the samples were performed in order to determine the impact that lignin modification had on their compression modulus at 80% of strain. Once again, all the tested

hydrogels were able to keep total integrity and good recoverability thanks to their elastic behaviour.

From the results in Figure 4 it was concluded that hydrogels containing alkaline lignins had greater compression modulus than those containing organosolv lignins. The latter is consistent with the results obtained for their crystallinity, since the more crystalline and compact the sample is the higher its compression modulus should be (Holloway et al., 2013). Nevertheless, this improvement of the compression modulus could also be attributed to the higher solid content (m_{filler}) on alkaline hydrogels, as explained by Queiroz et al. (2021) (Queiroz et al., 2021). Moreover, all the modulus values for the samples with alkaline lignin were in the range of 10-12 MPa, whereas the ones for hydrogels with organosolv lignin were between 4.5 and 6 MPa. Comparing to the previous work (Morales et al., 2021), an enhancement of its compression modulus was especially observed for MAWA samples, although MAAO also got slightly higher. All these values were aligned with the results reported for lignin-hydrogels by some authors (Cai et al., 2020) but they

were also higher than those obtained by others (Chen et al., 2019; Kalinoski and Shi, 2019; Queiroz et al., 2021).

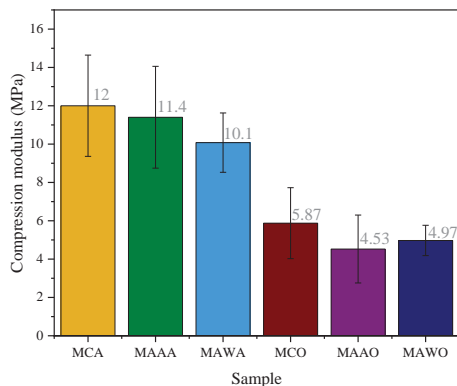


Figure 4. Compression behaviours of modified lignin-based hydrogels.

2.1.3. Drug loading and delivery tests

Quercetin (QE) is a bioflavonoid present in fruits and vegetables with interesting anti-inflammatory, antioxidant, anti-carcinogenic and anti-obesity properties (George et al., 2019; Jin et al., 2011; Lee et al., 2017). Due to the aforementioned characteristics and the current trend of preferring natural compounds rather than synthesized drugs, quercetin has recently gained great attention. This compound can be found in onion peels, which are an abundant waste all over the world. Thus, the obtaining of a flavonoid-rich extract from this waste would give an added-value to it, contributing to circular economy.

Among the extraction strategies that have been studied for QE, microwave assisted extraction (MAE) has proven to be a promising sustainable and green process (Jin et al., 2011). Therefore, QE was extracted through MAE.

2.1.3.1. Characterisation of QE extract

The solid content on the extract was determined through gravimetric analyses, drying 1 ml of the extract at 105 °C for 24 h. This measurement revealed a solid content of 18.3 ± 0.2 mg of solid/g of liquid extract. TPC and TFC analyses showed high phenolic and flavonoid contents for the extract (576.4 ± 75.4 mg GAE/g dry extract and 470.1 ± 22.5 mg CQE/g dry extract). These values for TPC were higher than those reported by other authors and the ones for TFC were similar (George et al., 2019). In addition, the characteristic peaks of CQE reported by George et al. (2019) were also present on the FTIR spectra of QE, confirming the existence of this compound in the extract (see Figure 5a)(George et al., 2019).

2.1.3.2. Drug loading tests

The drug loading tests were performed by immersing dry hydrogels into diluted QE solutions (68.4 mg quercetin/L). The objective of these tests was to analyse the capacity of these samples of absorbing and releasing this drug, not to optimize the loading-release kinetic.

According to the absorbance difference between the initial and final solutions, all the samples were capable of trapping between 26 and 34% of the drug in the initial solution (see Table 5), being this percentage higher for the hydrogels containing organosolv lignins, which had also presented the highest swelling capacities.

2.1.3.3. Drug release tests

After the loaded hydrogels had dried, they were immersed in PBS at 37 °C for drug release, simulating *in vitro* conditions. The absorbance of the release medium was performed at several times during the first 6.5 h. As the hydrogels contained lignin, and this lignin presented an absorbance peak at 330 nm, at high concentrations this peak sagged the results of the peak corresponding to QE at 375 nm. Thus, the release kinetics was performed during the first 6.5 h, while the released lignin was negligible.

From the release profiles shown in Figure 5b it was concluded that although all the samples were able to be loaded with similar drug amounts, the release capacity was completely different for each sample. In fact, with respect to the loaded amounts of drug, the released drug percentages ranged from 12 to 30%. The samples displaying the highest release drug percentage were MAWA, followed by MAAO and MAAA. The lowest release was observed for MCO samples, suggesting that despite having higher drug loading abilities, the interactions with the drug made its release difficult. Nevertheless, it should be noted that these profiles were just for the first 6.5 h, and cannot be extrapolated to longer times.

So as to determine the release kinetics, several models were applied (i.e. zero order, first order, Korsmeyer–Peppas and Higuchi) (George et al., 2020, 2019; Saidi et al., 2020). The estimated kinetic parameters for each of these models are displayed in Table 5 and the graphic representations of the four kinetic models in the Supplementary data. From the original release profile, it was inferred that the release kinetics would not fit correctly to a zero order model, which was confirmed by the determination coefficients (R^2). Among the rest of the models, Korsmeyer–Peppas model was the one fitting the best, except

for MCA sample, whose fitting did not improve either with Higuchi model.

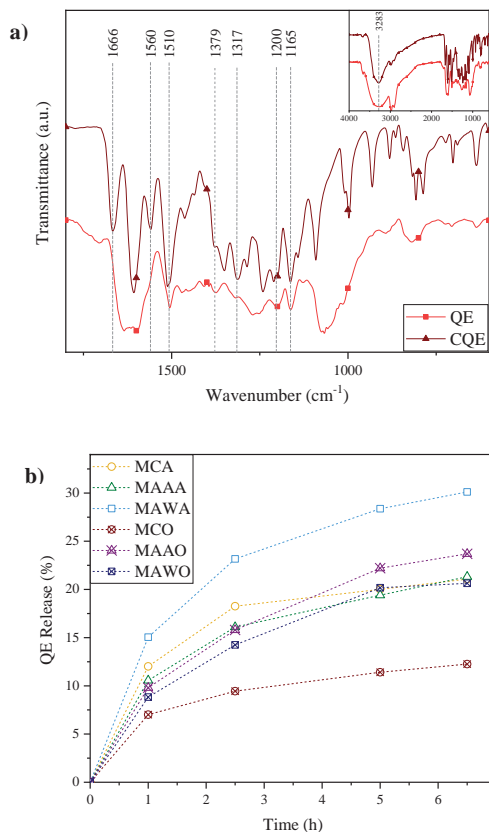


Figure 5. (a) FTIR spectra of self-extracted (QE) and commercial (CQE) quercetin extract and (b) QE release profiles of modified lignin-based hydrogels.

As indicated by Saidi et al. (2020) (Saidi et al., 2020), the release exponents (n) and the rate constants (k_{kp}) were determined from the slopes and intercepts of the plots ($\ln(QE\%)$ versus $\ln(t)$) of the experimental data. As shown in Table 5, all the estimated values for n were below 0.5. Although Fickian diffusion is usually considered when $n=0.5$ (George et al., 2020, 2019), in this case it could also be said that the QE release followed a Fickian diffusion (George et al., 2019). Thus, it could be said that the synthesized hydrogels could be used as controlled drug delivery systems.

3. Conclusions

On the basis of the results obtained for the properties of previously synthesized alkaline and organosolv lignin-based

Table 5. Kinetic parameters estimated from models for QE release from hydrogels.

Sample	Loading (%)	Zero order R^2	First order R^2	Korsmeyer–Peppas			Higuchi R^2
				R^2	n	k_{kp}	
MAAA	29.0	0.82	0.84	0.99	0.37	10.9	0.98
MAAO	31.8	0.90	0.92	0.99	0.48	9.9	0.99
MAWA	30.4	0.81	0.85	0.98	0.37	15.5	0.97
MAWO	32.0	0.88	0.90	0.99	0.47	9.0	0.99
MCA	26.0	0.73	0.75	0.93	0.29	12.6	0.93
MCO	34.5	0.77	0.79	0.99	0.30	7.1	0.96

hydrogels, two chemical modifications were performed to these lignins in order to enhance their reactivity. The peroxidation of alkaline lignin was confirmed by FTIR, but the molecular weight studies suggested that condensation reactions had also happened during the reaction, leading to fractions with higher average molecular weights. The hydroxymethylation of organosolv lignin was also confirmed by FTIR, ^{31}P NMR and GPC. Moreover, this reaction led to more thermally stable lignins, which supported the success of the reaction. The lignin waste of the synthesized hydrogels was higher than the one reported for previously synthesized samples, suggesting that despite the modification of lignins, just the highest molecular weight fractions reacted with the matrix polymer. Moreover, the swelling capacity of modified alkaline lignin-based hydrogels was negatively affected, whereas the one for organosolv lignin-based samples improved. The continuous and compact structures seen on SEM micrographs explained the aforementioned, and the results from the DSC and compression tests were in accordance with them. The drug loading and release studies suggested that these samples allowed a Fickian diffusion of QE and they could be employed as controlled drug delivery systems.

Acknowledgements

The authors would like to acknowledge the financial support of the Department of Education of the Basque Government (IT1008-16). A. Morales would like to thank the University of the Basque Country (Training of Researcher Staff, PIF17/207). P. Gullón would like to acknowledge the Grants for the recruitment of technical support staff (PTA2019-017850-I) under the State Plan for Scientific and Technical Research and Innovation 2017-2020. The authors thank SGiker (UPV/EHU/ERDF, EU) for their technical and human support.

References

Aini, N.A.M., Othman, N., Hussin, M.H., Sahakaro, K., 2019.

- Hydroxymethylation-Modified Lignin and Its Effectiveness as a Filler in Rubber Composites. *Processes* 7, 315. <https://doi.org/10.3390/pr7050315>
- Barros, A., Quraishi, S., Martins, M., Gurikov, P., Subrahmanyam, R., Smirnova, I., Duarte, A.R.C., Reis, R.L., 2016. Hybrid Alginate-Based Cryogels for Life Science Applications. *Chemie-Ingenieur-Technik* 88, 1770–1778. <https://doi.org/10.1002/cite.201600096>
- Cai, J., Zhang, X., Liu, W., Huang, J., Qiu, X., 2020. Synthesis of highly conductive hydrogel with high strength and super toughness. *Polymer (Guildf)* 202, 122643. <https://doi.org/10.1016/j.polymer.2020.122643>
- Căpraru, A.M., Ungureanu, E., Trincă, L.C., Mălutan, T., Popa, V.I., 2012. Chemical and spectral characteristics of annual plant lignins modified by hydroxymethylation reaction. *Cellul. Chem. Technol.* 46, 589–597.
- Chen, Y., Zhang, H., Zhu, Z., Fu, S., 2020. High-value utilization of hydroxymethylated lignin in polyurethane adhesives. *Int. J. Biol. Macromol.* 152, 775–785. <https://doi.org/10.1016/j.ijbiomac.2020.02.321>
- Chen, Y., Zheng, K., Niu, L., Zhang, Y., Liu, Y., Wang, C., Chu, F., 2019. Highly mechanical properties nanocomposite hydrogels with biorenewable lignin nanoparticles. *Int. J. Biol. Macromol.* 128, 414–420. <https://doi.org/10.1016/j.ijbiomac.2019.01.099>
- Ciolacu, D., Cazacu, G., 2018. New Green Hydrogels Based on Lignin. *J. Nanosci. Nanotechnol.* 18, 2811–2822. <https://doi.org/10.1166/jnn.2018.14290>
- Dávila, I., Gullón, P., Andrés, M.A., Labidi, J., 2017. Coproduction of lignin and glucose from vine shoots by eco-friendly strategies: Toward the development of an integrated biorefinery. *Bioresour. Technol.* 244, 328–337. <https://doi.org/10.1016/j.biortech.2017.07.104>
- Dragone, G., Kersemakers, A.A.J., Driessen, J.L.S.P., Yamakawa, C.K., Brumano, L.P., Mussatto, S.I., 2020. Innovation and strategic orientations for the development of advanced biorefineries. *Bioresour. Technol.* 302, 122847. <https://doi.org/10.1016/j.biortech.2020.122847>
- Figueiredo, P., Lintinen, K., Hirvonen, J.T., Kostiainen, M.A., Santos, H.A., 2018. Properties and chemical modifications of lignin: Towards lignin-based nanomaterials for biomedical applications. *Prog. Mater. Sci.* 93, 233–269. <https://doi.org/10.1016/j.pmatsci.2017.12.001>
- George, D., Begum, K.M.M.S., Maheswari, P.U., 2020. Sugarcane Bagasse (SCB) Based Pristine Cellulose Hydrogel for Delivery of Grape Pomace Polyphenol Drug. *Waste and Biomass Valorization* 11, 851–860. <https://doi.org/10.1007/s12649-018-0487-3>
- George, D., Maheswari, P.U., Begum, K.M.M.S., 2019. Synergic formulation of onion peel quercetin loaded chitosan-cellulose hydrogel with green zinc oxide nanoparticles towards controlled release, biocompatibility, antimicrobial and anticancer activity. *Int. J. Biol. Macromol.* 132, 784–794. <https://doi.org/10.1016/j.ijbiomac.2019.04.008>
- Gilca, I.A., Ghitescu, R.E., Puteil, A.C., Popa, V.I., 2014. Preparation of lignin nanoparticles by chemical modification. *Iran. Polym. J. (English Ed.)* 23, 355–363. <https://doi.org/10.1007/s13726-014-0232-0>
- Goliszek, M., Kołodyńska, D., Pylypchuk, I. V., Sevastyanova, O., Podkościelna, B., 2021. Synthesis of lignin-containing polymer hydrogels with tunable properties and their application in sorption of nickel(II) ions. *Ind. Crops Prod.* 164, 20–31. <https://doi.org/10.1016/j.indcrop.2021.113354>
- Goudarzi, A., Lin, L.-T., Ko, F.K., 2014. X-Ray Diffraction Analysis of Kraft Lignins and Lignin-Derived Carbon Nanofibers. *J. Nanotechnol. Eng. Med.* 5, 021006. <https://doi.org/10.1115/1.4028300>
- He, X., Luzi, F., Hao, X., Yang, W., Torre, L., Xiao, Z., Xie, Y., Puglia, D., 2019. Thermal, antioxidant and swelling behaviour of transparent polyvinyl (alcohol) films in presence of hydrophobic citric acid-modified lignin nanoparticles. *Int. J. Biol. Macromol.* 127, 665–676. <https://doi.org/10.1016/j.ijbiomac.2019.01.202>
- Holloway, J.L., Lowman, A.M., Palmese, G.R., 2013. The role of crystallization and phase separation in the formation of physically cross-linked PVA hydrogels. *Soft Matter* 9, 826–833. <https://doi.org/10.1039/c2sm26763b>
- Infante, M., Ysambert, F., Hernández, M., Martínez, B., Delgado, N., Bravo, B., Cáceres, A., Chávez, G., Bullón, J., 2007. Microwave assisted oxidative degradation of lignin with hydrogen peroxide and its tensoactive properties. *Rev. Tec. la Fac. Ing. Univ. del Zulia* 30, 108–117.
- Iravani, S., Varma, R.S., 2020. Greener synthesis of lignin nanoparticles and their applications. *Green Chem.* 22, 612–636. <https://doi.org/10.1039/c9gc02835h>
- Jin, E.Y., Lim, S., Kim, S. oh, Park, Y.S., Jang, J.K., Chung, M.S., Park, H., Shim, K.S., Choi, Y.J., 2011. Optimization of various extraction methods for quercetin from onion skin using response surface methodology. *Food Sci. Biotechnol.* 20, 1727–1733. <https://doi.org/10.1007/s10068-011-0238-8>
- Kalinoski, R.M., Shi, J., 2019. Hydrogels derived from lignocellulosic compounds: Evaluation of the compositional, structural, mechanical and antimicrobial properties. *Ind. Crops Prod.* 128, 323–330. <https://doi.org/10.1016/j.indcrop.2018.11.002>
- Kumar, A., Anushree, Kumar, J., Bhaskar, T., 2020. Utilization of lignin: A sustainable and eco-friendly approach. *J. Energy Inst.* 93, 235–271. <https://doi.org/10.1016/j.joei.2019.03.005>
- Larrañeta, E., Imízcoz, M., Toh, J.X., Irwin, N.J., Ripolin, A., Perminova, A., Domínguez-Robles, J., Rodríguez, A., Donnelly, R.F., 2018. Synthesis and Characterization of Lignin Hydrogels for Potential Applications as Drug Eluting Antimicrobial Coatings for Medical Materials. *ACS Sustain. Chem. Eng.* 6, 9037–9046. <https://doi.org/10.1021/acssuschemeng.8b01371>
- Lee, S.G., Parks, J.S., Kang, H.W., 2017. Quercetin, a functional

- compound of onion peel, remodels white adipocytes to brown-like adipocytes. *J. Nutr. Biochem.* 42, 62–71. <https://doi.org/10.1016/j.jnutbio.2016.12.018>
- Meng, X., Crestini, C., Ben, H., Hao, N., Pu, Y., Ragauskas, A.J., Argyropoulos, D.S., 2019. Determination of hydroxyl groups in biorefinery resources via quantitative ^{31}P NMR spectroscopy. *Nat. Protoc.* 14, 2627–2647. <https://doi.org/10.1038/s41596-019-0191-1>
- Meng, Y., Li, C., Liu, X., Lu, J., Cheng, Y., Xiao, L.-P., Wang, H., 2019. Preparation of magnetic hydrogel microspheres of lignin derivate for application in water. *Sci. Total Environ.* <https://doi.org/10.1016/j.scitotenv.2019.06.278>
- Morales, A., Gullón, B., Dávila, I., Eibes, G., Labidi, J., Gullón, P., 2018. Optimization of alkaline pretreatment for the co-production of biopolymer lignin and bioethanol from chestnut shells following a biorefinery approach. *Ind. Crops Prod.* 124. <https://doi.org/10.1016/j.indcrop.2018.08.032>
- Morales, A., Labidi, J., Gullón, P., 2021. Impact of the lignin type and source on the characteristics of physical lignin hydrogels. *Sustain. Mater. Technol.* e00369. <https://doi.org/10.1016/j.susmat.2021.e00369>
- Morales, A., Labidi, J., Gullón, P., 2020a. Effect of the formulation parameters on the absorption capacity of smart lignin-hydrogels. *Eur. Polym. J.* 129, 109631. <https://doi.org/10.1016/j.eurpolymj.2020.109631>
- Morales, A., Labidi, J., Gullón, P., 2020b. Assessment of green approaches for the synthesis of physically crosslinked lignin hydrogels. *J. Ind. Eng. Chem.* 81, 475–487. <https://doi.org/10.1016/j.jiec.2019.09.037>
- Musilová, L., Mráček, A., Kovalčík, A., Smolka, P., Minařík, A., Humpolíček, P., Vicha, R., Ponižil, P., 2018. Hyaluronan hydrogels modified by glycinated Kraft lignin: Morphology, swelling, viscoelastic properties and biocompatibility. *Carbohydr. Polym.* 181, 394–403. <https://doi.org/10.1016/j.carbpol.2017.10.048>
- Oryan, A., Kamali, A., Moshiri, A., Baharvand, H., Daemi, H., 2018. Chemical crosslinking of biopolymeric scaffolds: Current knowledge and future directions of crosslinked engineered bone scaffolds. *Int. J. Biol. Macromol.* 107, 678–688. <https://doi.org/10.1016/j.ijbiomac.2017.08.184>
- Ouyang, X., Lin, Z., Deng, Y., Yang, D., Qiu, X., 2010. Oxidative Degradation of Soda Lignin Assisted by Microwave Irradiation. *Chinese J. Chem. Eng.* 18, 695–702. [https://doi.org/10.1016/S1004-9541\(10\)60277-7](https://doi.org/10.1016/S1004-9541(10)60277-7)
- Queiroz, B.G., Ciol, H., Inada, N.M., Frollini, E., 2021. Hydrogel from all in all lignocellulosic sisal fibers macromolecular components. *Int. J. Biol. Macromol.* 181, 978–989. <https://doi.org/10.1016/j.ijbiomac.2021.04.088>
- Rico-García, D., Ruiz-Rubio, L., Pérez-Álvarez, L., Hernández-Olmos, S.L., Guerrero-Ramírez, G.L., Vilas-Vilela, J.L., 2020. Lignin-Based Hydrogels : Synthesis and Applications. *Polymers (Basel)* 12, 1–23.
- Saidi, M., Dabbaghi, A., Rahmani, S., 2020. Swelling and drug delivery kinetics of click-synthesized hydrogels based on various combinations of PEG and star-shaped PCL: influence of network parameters on swelling and release behavior. *Polym. Bull.* 77, 3989–4010. <https://doi.org/10.1007/s00289-019-02948-z>
- Sillero, L., Prado, R., Andrés, M.A., Labidi, J., 2019. Characterisation of bark of six species from mixed Atlantic forest. *Ind. Crops Prod.* 137, 276–284. <https://doi.org/10.1016/j.indcrop.2019.05.033>
- Tribot, A., Amer, G., Abdou Alio, M., de Baynast, H., Delattre, C., Pons, A., Mathias, J.D., Callois, J.M., Vial, C., Michaud, P., Dussap, C.G., 2019. Wood-lignin: Supply, extraction processes and use as bio-based material. *Eur. Polym. J.* 112, 228–240. <https://doi.org/10.1016/j.eurpolymj.2019.01.007>
- Wang, H., Pu, Y., Ragauskas, A., Yang, B., 2019. From lignin to valuable products—strategies, challenges, and prospects. *Bioresour. Technol.* 271, 449–461. <https://doi.org/10.1016/j.biortech.2018.09.072>
- Xu, C., Liu, F., Alam, M.A., Chen, H., Zhang, Y., Liang, C., Xu, H., Huang, S., Xu, J., Wang, Z., 2020. Comparative study on the properties of lignin isolated from different pretreated sugarcane bagasse and its inhibitory effects on enzymatic hydrolysis. *Int. J. Biol. Macromol.* 146, 132–140. <https://doi.org/10.1016/j.ijbiomac.2019.12.270>
- Yang, W., Fortunati, E., Bertoglio, F., Owczarek, J.S., Bruni, G., Kozanecki, M., Kenny, J.M., Torre, L., Visai, L., Puglia, D., 2018. Polyvinyl alcohol/chitosan hydrogels with enhanced antioxidant and antibacterial properties induced by lignin nanoparticles. *Carbohydr. Polym.* 181, 275–284. <https://doi.org/10.1016/j.carbpol.2017.10.084>
- Yoo, C.G., Meng, X., Pu, Y., Ragauskas, A.J., 2020. The critical role of lignin in lignocellulosic biomass conversion and recent pretreatment strategies: A comprehensive review. *Bioresour. Technol.* 301. <https://doi.org/10.1016/j.biortech.2020.122784>
- Zang, D., Liu, F., Zhang, M., Gao, Z., Wang, C., 2015. Novel superhydrophobic and superoleophilic sawdust as a selective oil sorbent for oil spill cleanup. *Chem. Eng. Res. Des.* 102, 34–41. <https://doi.org/10.1016/j.cherd.2015.06.014>
- Zevallos Torres, L.A., Lorenci Woicichowski, A., de Andrade Tanobe, V.O., Karp, S.G., Guimarães Lorenci, L.C., Faulds, C., Soccol, C.R., 2020. Lignin as a potential source of high-added value compounds: A review. *J. Clean. Prod.* 263. <https://doi.org/10.1016/j.jclepro.2020.121499>
- Zhang, Yiwen, Yuan, B., Zhang, Yuqing, Cao, Q., Yang, C., Li, Y., Zhou, J., 2020. Biomimetic lignin/poly(ionic liquids) composite hydrogel dressing with excellent mechanical strength, self-healing properties, and reusability. *Chem. Eng. J.* 400, 125984. <https://doi.org/10.1016/j.cej.2020.125984>

Influence of lignin modifications on physically crosslinked lignin hydrogels for drug delivery applications

Amaia Morales^a, Jalel Labidi^{a,*}, Patricia Gullón^b

^aChemical and Environmental Engineering Department, University of the Basque Country UPV/EHU, Plaza Europa 1, 20018, San Sebastián, Spain

^bC.A.C.T.I. Laboratory, Technology Park of Galicia- Tecnopole, CTC Building, 32901, San Cibrao das Viñas, Ourense, Spain

*Corresponding author: jalel.labidi@ehu.eus

Supplementary data

Figure S1. Molecular weight distributions of modified and native alkaline (a) and organosolv (b) lignins.

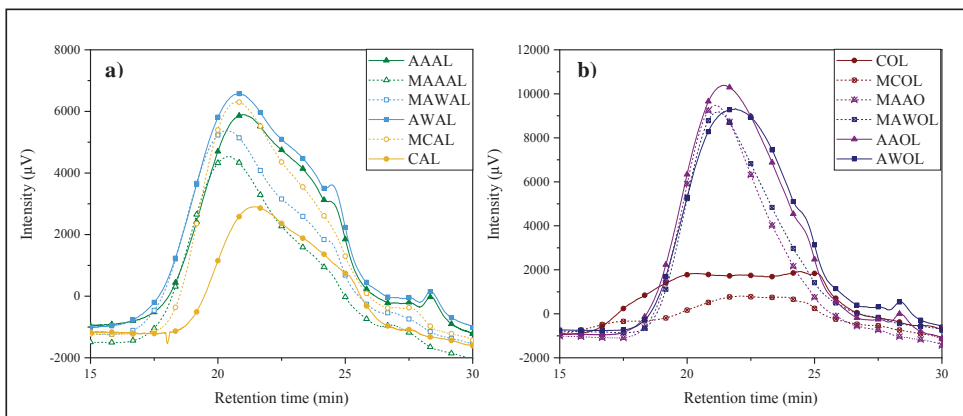


Figure S2: ³¹P NMR spectra of COL and MCOL samples.

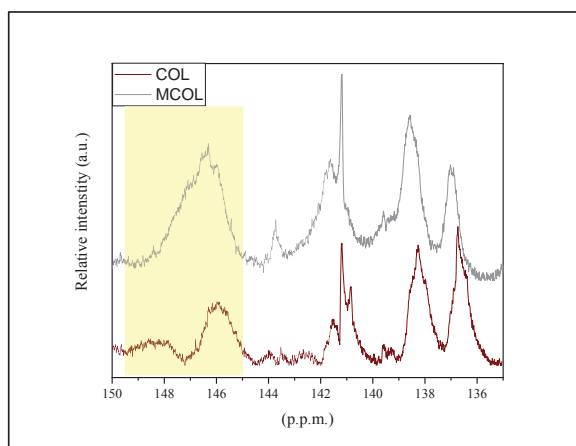


Figure S3. XRD patterns of modified and native alkaline (a) and organosolv (b) lignins.

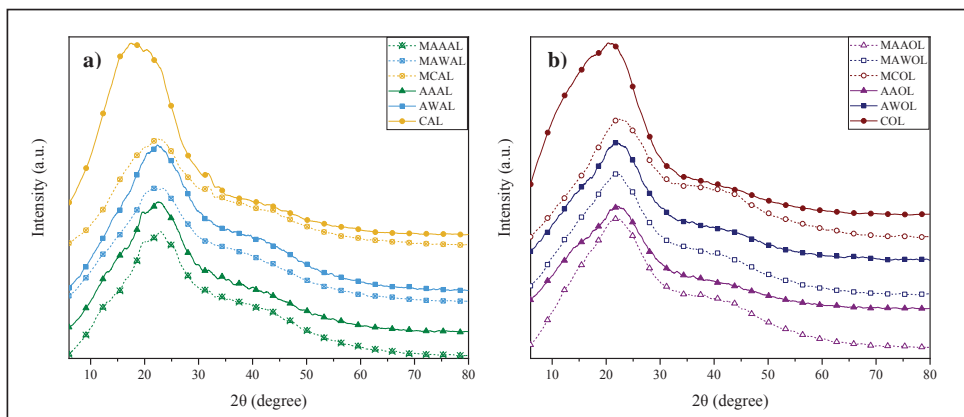
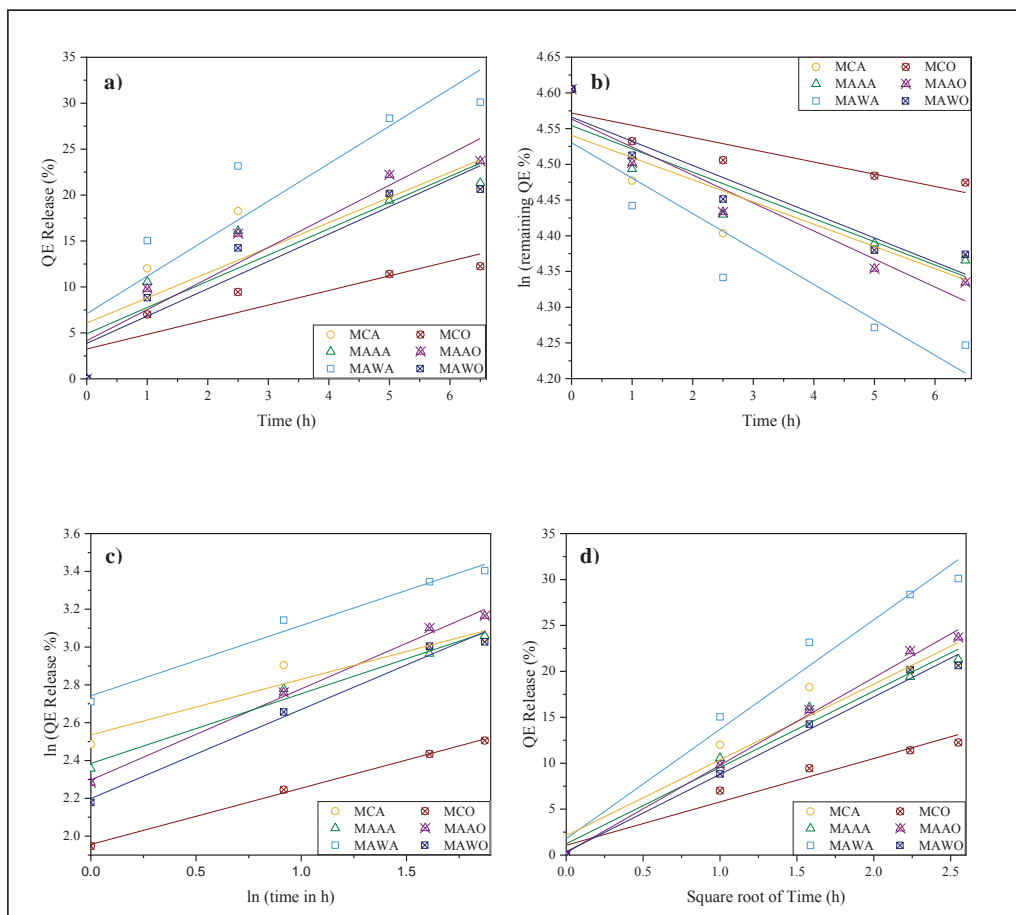
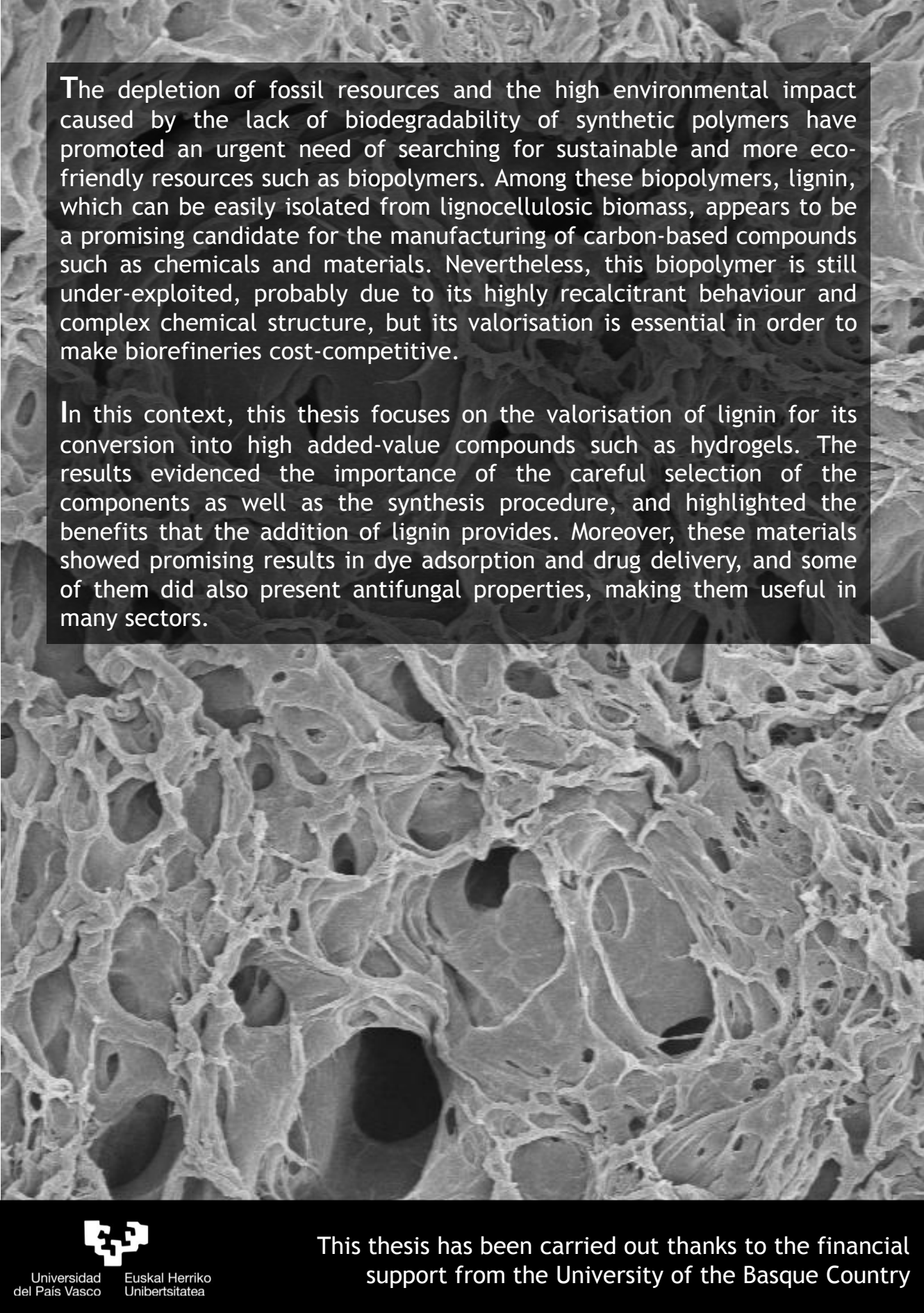


Figure S4. QE release kinetic models of zero order (a), First order (b), Korsmeyer–Peppas (c) and Higuchi models (d).





The depletion of fossil resources and the high environmental impact caused by the lack of biodegradability of synthetic polymers have promoted an urgent need of searching for sustainable and more eco-friendly resources such as biopolymers. Among these biopolymers, lignin, which can be easily isolated from lignocellulosic biomass, appears to be a promising candidate for the manufacturing of carbon-based compounds such as chemicals and materials. Nevertheless, this biopolymer is still under-exploited, probably due to its highly recalcitrant behaviour and complex chemical structure, but its valorisation is essential in order to make biorefineries cost-competitive.

In this context, this thesis focuses on the valorisation of lignin for its conversion into high added-value compounds such as hydrogels. The results evidenced the importance of the careful selection of the components as well as the synthesis procedure, and highlighted the benefits that the addition of lignin provides. Moreover, these materials showed promising results in dye adsorption and drug delivery, and some of them did also present antifungal properties, making them useful in many sectors.

